HYDROGENOLYSIS OF FURAN AND SYLVAN OVER SUPPORTED METAL CATALYSTS

By

CORNELIUS J. M. DRIESSEN

Thesis presented for the degree of

Master of Science

University of Edinburgh 1970

To my parents.

ACKNOWLEDGEMENTS

I wish to express my sincere gratitude to my supervisors, Dr. J. Newham and Dr. D. Taylor, for their helpful guidance and continual encouragement.

I also wish to thank Dr. H. Marsh, Dr. B.A.O. Randall, Mr. M. Boult, Mr. N. Rollo and Mr. J. Lyons for their technical assistance; Mr. G. Form and Mr. M. Spence for useful discussions; Mr. L.H.W. Hallett and the Newcastle upon Tyne Education Committee for providing a maintenance grant for two and a half years, and Rutherford Polytechnic for providing the facilities for this research.

In conclusion I would like to express my heartfelt gratitude to Mrs. E. Brett for the great care with which she typed the manuscript.

SUMMARY

The gas phase hydrogenations of furan and sylvan (2- methylfuran) over supported nickel and platinum catalysts were investigated in order that the kinetics of these reactions might be studied, particular emphasis being placed on the relative rates of hydrogenolysis of the two furans' C - O bonds. Information concerning the relative rates of reaction was found both by comparing the rates of furan and sylvan hydrogenations carried out at the same temperature and by analysis of simultaneous hydrogenations of the two compounds.

Hydrogenations over nickel catalysts were studied over a wide range of temperatures ($90^{\circ}C$ to $220^{\circ}C$). However, since there was not a temperature at which both furan and sylvan gave a satisfactory yield of C - O bond hydrogenolysis products, hydrogenations over these catalysts were not investigated in depth.

Supported platinum catalysts, with the exception of Pt/Al_2O_3, were found to give high yields of hydrogenolysis products for both the furans at the same reaction temperatures ($50^{\circ}C \pm 30^{\circ}C$). However, of these catalysts only platinum supported on pumice was free from strong adsorption of the products of hydrogenation, alcohols in particular, and hence reactions of the two furans over only these catalysts were subjected to detailed kinetic analysis.

Hydrogenations over all the catalysts were subject to autopoisoning. This was found not to be caused by strong adsorption of the products of the reactions but to be a time dependent phenomenon, the rate equation adopted for a furan's hydrogenation being the product of a time dependent function

(representing the decreasing activity of the catalyst) and of a function of the pressures of the reactants (representing the kinetics of the reaction with the masking effect of the poisoning removed). The rate equation takes the form :

$$\frac{dP_R}{dt} = - K_R P_R^{0.2} P_H^{1.0} \exp (- K' t^{\frac{1}{2}}) ,$$

where P_R and P_H are the furan and hydrogen pressures respectively at time t, the rate constant being K_R while K' is a constant dependent on the rate of poisoning.

Because of the difficulties encountered a large emphasis has been placed on the techniques developed to overcome them, falling into three main categories. Firstly, methods for detecting adsorption of reactants and products, secondly, methods for studying the autopoisoning and the underlying kinetics of furan hydrogenations and finally, techniques for studying the kinetics of the two simultaneous, autopoisoned, reactions, complicated by strong adsorption of both furan and sylvan. Solution of the two latter problems could only be achieved by use of a computer. All the necessary computer programs, in FORTRAN, with the exception of two subroutines, one of which was modified before being used, had to be written. The main ones are listed in the appendices. It was attempted to make the programs sufficiently flexible to enable different systems to be investigated with the minimum of difficulty.

CONTENTS

CHAPTER I

Introduction

1.1 Physical properties of furan

Any discussion of a chemical reaction involving furans must be prefaced by a resume of the physical properties of the furan molecule. These show furan to have properties associated with an aromatic compound while at the same time preserving some of the characteristics of a diene.

Fig. 1.1 The structure of the furan molecule.

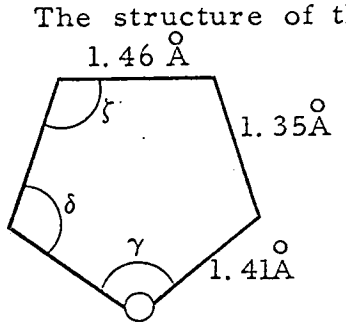

$\gamma = 107 \pm 4^{\circ}$

$\delta = 109 \pm 3^{\circ}$

$\zeta = 107 \pm 2^{\circ}$

Molecule is planar

From the structure of the furan molecule, fig. 1.1, determined by electron diffraction (refs. 1 and 2) it is clear that the structure of furan is not adequately represented by I,

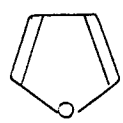

I

since the $\beta,\beta-$ C - C bond length of 1.46 Å lies between that of a normal C - C bond, 1.54 Å, and a C - C double bond, 1.33 Å, hence this bond in the furan nucleus possesses some multiple bond character. On the other hand the α,β C - C bond lengths, 1.35 Å, are larger than would be expected from I, suggesting that the α,β bonds have a fractional order lying between one and two. From the bond lengths for furanic C - O it has been estimated (ref. 2) that these bonds possess $5 \pm 5\%$ double bond character.

That furan has a high resonance energy was shown both by analysis of combustion data (refs. 2 and 3), 23 Cals./mole, and by the superior method of Kistiakowsky (ref. 4) from the heat of hydrogenation. Since this was shown to be 36.6 Cals./mole (ref. 5) the resonance energy by this method is 19.8 Cals./mole. Therefore, the molecule is usually represented in terms of a resonance hybrid of the following forms (ref. 6).

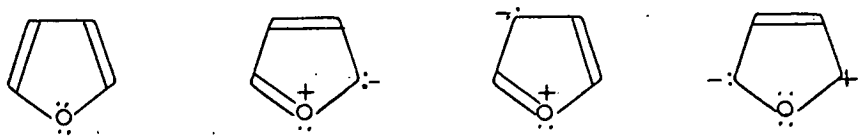

II III IV V

(where V is the excited state characteristic of a conjugated diene system).

From bond length data Schomaker and Pauling (ref. 2) estimated that forms III and IV contribute only approximately 15% to the furan resonance energy (born out by calculations using furan's dipole moment, (ref. 2). Furthermore it is thought likely that III makes a greater contribution to the resonance of furan than IV since the charge separation for III is smaller than IV (and hence it has a lower energy). This is born out by the chemical evidence that attack of the furan nucleus occurs almost exclusively at the α position suggesting that there is a higher electron density at this position.

A comparison of the Raman spectral band corresponding to the furan double bond (1485 cm.$^{-1}$) with the corresponding bands for cyclo-pentadiene (1500 cm.$^{-1}$), benzene (1580 cm.$^{-1}$) and an ethylenic double bond (1600 cm.$^{-1}$) shows the similarity between furan and cyclopentadiene. According to Trucket and Chapron (ref. 7) the shifts in the band spectra of the furan double bonds are due to oscillation of conjugated double bonds which is in agreement with the concept of an aromatic five membered ring.

From a study of the depolarization factor and the frequency values, Reïtz (ref. 8) concluded that the furan molecule was planar and diolefinic in character, the planar nature of the molecule being confirmed by electron diffraction (ref. 2) and by comparison of infrared and Raman spectra (ref. 9).

More recently the aromaticity of furan was finally confirmed by N.M.R. studies (ref. 10) of the dilution shifts of the aromatic protons in non-polar isotropic solvents.

The conclusion from the studies of the physical properties of furan is that it behaves as a conjugated diene ether stabilised by resonance energy, yet exhibiting aromatic properties.

A deeper insight into the nature of the properties of furan is provided by wave mechanical models of the ring. Interesting information as to the chemical properties of furan are found by Zurawski (ref. 11) using the Generalized Free Electron Molecular Orbital method to calculate localization energies and frontier electron populations for electrophilic, radical and nucleophilic substitutions which are given in the following table.

Table 1.1 Frontier electron populations and localization energies of furan.

position	Electrophilic substitution		Radical substitution		Nucleophilic substitution	
	A	B	A	B	A	B
3 and 4	0.2398	5.845	0.2269	5.714	0.2140	5.583
2 and 5	0.7848	3.411	0.8278	4.007	0.8708	4.603

where A is the frontier electron population and B is the localization energy in e.v.

From the chemical reactivity indices in table 1.1 it can be predicted that positions 2 and 5 are more sensitive to all the above mentioned substitutions than positions 3 and 4 which is in agreement with chemical data (ref. 12).

An interesting confirmation that the 5 and 2 positions are more susceptible to attack than the two β positions was furnished by the examination of the catalytic exchange reactions in the liquid phase of furans with D_2O over a variety of group VIII transitious metals (ref. 13) Exchange always occurred to a much greater extent at the α positions (almost exclusively over PtO_2 and $NiCl_2$).

1.2 General characteristics of catalysts used for the hydrogenation and hydrogenolysis of furans.

In 1897 Sabatier discovered that organic compounds could be catalytically hydrogenated over nickel. Since then the hydrogenation of a wide range of compounds has been accomplished over numerous catalysts, the first hydrogenation of furan, over nickel, being carried out in 1906 (ref. 14).

While such reactions are widely used in industrial processes, the petroleum and margarine industries in particular, it has been found that the heterogeneous hydrogenation of a compound can be a function of so many variables (all of which are not necessarily known) that reproducible results are often difficult to obtain. The rate, extent and direction of a hydrogenation can be influenced not only by the catalyst used but also by impurities either deliberately or inadvertantly added to the catalyst (refs. 15 and 16), the procedure by which it is prepared (ref. 17), reaction temperature (ref. 18), pressure (ref. 19), efficiency of shaking (ref. 17), batch size (ref. 20), solvent (ref. 21), acidity (ref. 22), nature of catalyst support (ref. 23), etc. Even with all these variables held constant the activity of a catalyst may still vary from batch to

batch. In other words since all of the factors which affect a heterogeneous catalytic reaction may be operative, one should not expect to reproduce exactly any procedure reported in the literature although it is possible to draw general conclusions as to the properties of different catalysts.

Certain simplifications may be made, the easiest being to carry out hydrogenations in the gas phase, hence eliminating any solvent effects and reducing problems arising from possible diffusion control of reactions. The number of variable factors may be reduced still further by the use of metal films as catalysts, however, these suffer from the drawback that they have a low surface area and hence are not practical for the study of very slow reactions.

It has been found that the interaction of an organic compound and hydrogen at the surface of a transition metal or metal oxide may lead to the cleavage of one or more of the molecule's bonds; such a cleavage is called hydrogenolysis. This process is observed during the hydrogenation of the furan nucleus of furan and its derivatives in varying degrees over all the catalysts surveyed in the literature (see the reviews on the hydrogenation of furans, refs. 17, 24, 25, 26, 27 and 28).

On hydrogenating furans it is found that the bulk of the hydrogenolysis which occurs is at the C - O bonds, though at elevated temperatures this is accompanied by simultaneous cleavage of the furanic carbon chain (the temperature at which this so called 'conjugative hydrogenolysis' begins being dependent on the catalyst and reaction pressure). Furthermore, for singly α substituted furans, VI, the C - O bond which is broken is dependent upon the nature of the substituent, R (ref. 29).

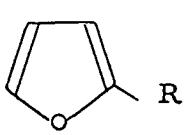

VI

For example when R = COOH or an aryl group the 1, 2 C - O bond is preferentially cleaved (ref. 29), while for R = alkyl group, the 1, 5 C - O bond is attacked, almost exclusively for R = methyl over Pt O_2 in acetic acid (ref. 29). Hence the main hydrogenolysis products of sylvan are pentan-2-ol and pentan-2-one while that for furan itself is n-butanol.

Catalysts used in the hydrogenation of furans may be divided into two classes : those which hydrogenate a furan's nucleus in preference to rupturing it, 'class A', and those which promote hydrogenolysis of the C - O bonds rather than forming the tetrahydro-derivative formed by hydrogenation of the furan ring, 'class B'.

'CLASS A' catalysts (for gas phase reactions)

Pd (refs. 30 and 31, at 150°C)
Pd-Al (ref. 32, at 275°C)
Ni (ref. 19, at 100°C and 20-80 atm.; ref. 33, 140°C; ref. 34, at 190-200°C and 60-80 atm.)
Rh (ref. 35, at 200°C)
Cu (ref. 34, at 190-200°C and 60-80 atm.)
Mo (ref. 34, at 190-200°C and 60-80 atm.)

Increasing the reaction vessel pressure leads to an increased yield of tetrahydro-derivatives for all the catalyst systems as well as increasing the rate of reaction. Hence copper would normally be in 'class B' since at atmospheric pressure it induces hydrogenolysis, though at this pressure it is only slightly reactive below 220°C. Of the above catalysts only palladium and Pd-Al are almost completely specific for ring hydrogenation over a wide range of temperatures (20°C to 275°C).

'CLASS B' catalysts (for gas phase reactions)

Pt (ref. 36, at 275°C; ref. 38, at 20-60°C)
Os (ref. 35, at 200-300°C)
Ir (ref. 35, at 200-300°C)
Ru (ref. 35, at 200-300°C)
Ni-Zu (ref. 32, at 250-300°C)
Cu-Al (ref. 37, at 250-300°C)
Ni-ZnO (ref. 37, at 250-300°C)

Decreasing the reaction temperature tends to decrease the amount of hydrogenolysis which occurs, hence finely divided osmium supported on asbestos falls into 'class A' if the reaction temperature is sufficiently low (70°C, ref. 39).

While it should be stressed that a metal's membership to the above two classes of catalysts may be dependent on temperature and/or pressure, most of the catalysts listed above belong to 'class A' (e.g. Pd) or 'class B' (e.g. Pt) respectively over widely varying reaction conditions.

1.3 Mechanisms for furan-hydrogen reactions.

Unfortunately the bulk of the research on the hydrogenation of furan and sylvan has been carried out with the aim of developing catalysts and reaction conditions that would give as high a yield as possible of the tetrahydro derivatives of these compounds since they can be easily converted to the industrially important compounds butadiene and cyclopentadiene and piperylene respectively (ref. 40). Almost none of the work has been concerned with the kinetics or the mechanisms of the hydrogenation and hydrogenolysis reactions. What little rather superficial work which has been carried out in order to gain an insight into the mechanisms is summarised in this section.

Since the hydrogenation of furan compounds yields on the one hand the corresponding tetrahydrofuran and on the other hydrogenolysis products, the possibility arises that the tetrahydrofurans act as intermediates in the cleavage of the furan nucleus. This is not unreasonable since on hydrogenating diethyl ether over platinum films (ref. 41) below 100°C cleavage of a single C - O bond occurs, ethane and ethanol being produced. Hence, in a similar manner, cyclic ethers such as the tetrahydro derivatives of furan and sylvan would be expected to form n-butanol and a mixture of n-pentanol, pentan-2-ol and pentan-2-one respectively. Formation of such products has been shown not to occur (ref. 18) over a platinum catalyst at low temperatures (<100°C) under conditions where the hydrogenation of furan and sylvan results almost solely in hydrogenolysis products.

Furthermore, at temperatures exceeding 220°C both diethyl ether and tetrahydrosylvan (refs. 42 and 18 respectively) are hydrogenated over nickel to form alkanes and carbon monoxide only while sylvan under similar conditions forms ketones. At slightly lower temperatures, 200°C, tetrahydrosylvan was found to isomerise slowly (ref. 43) to pentan-2-one over Ni/Ni-Al, the products of ring cleavage amounting to $\leq 10\%$, whereas under identical conditions they amounted to 80% for a sylvan-hydrogen reaction.

From the above evidence, confirmations of which having been reported sporadically, one may conclude that tetrahydrofurans are not intermediates in the formation of the hydrogenolysis products of the furans. Hence the hydrogenolysis of the C - O bond can take place either in the furan ring itself, in the dihydrofuran or in some adsorbed intermediate not readily formed during the hydrogenation of tetrahydrofurans.

Those engaged in research into furan-hydrogen reactions fall into two groups, those who favour the notion that a dihydrofuran, VII, is an intermediate in both the hydrogenation and hydrogenolysis of furans, 'mechanism A', and those who claim that hydrogenation and hydrogenolysis of the furan nucleus proceeds by two separate pathways ('mechanism B') having only adsorbed furans in common. Apparently no one believes that cleavage of the furanic ring may take place in an adsorbed complex other than adsorbed furan or its adsorbed tetrahydro-derivative.

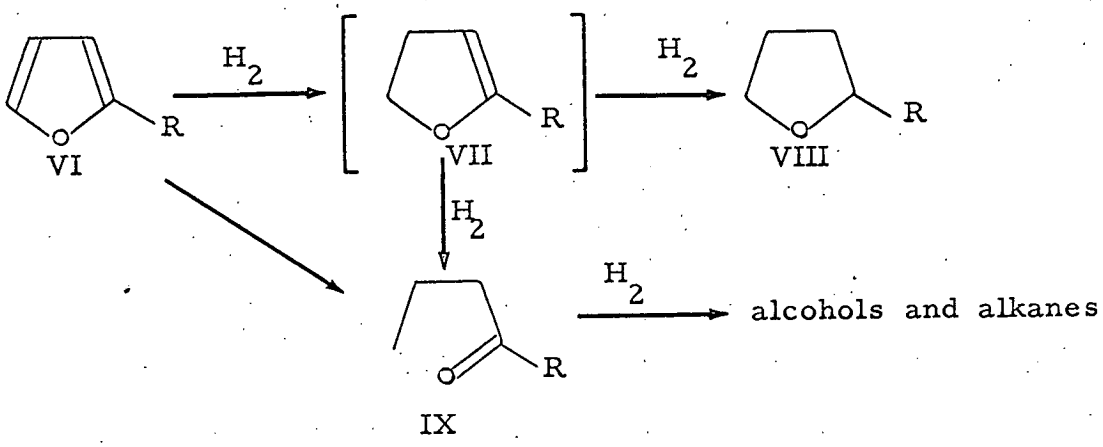

Mechanism A

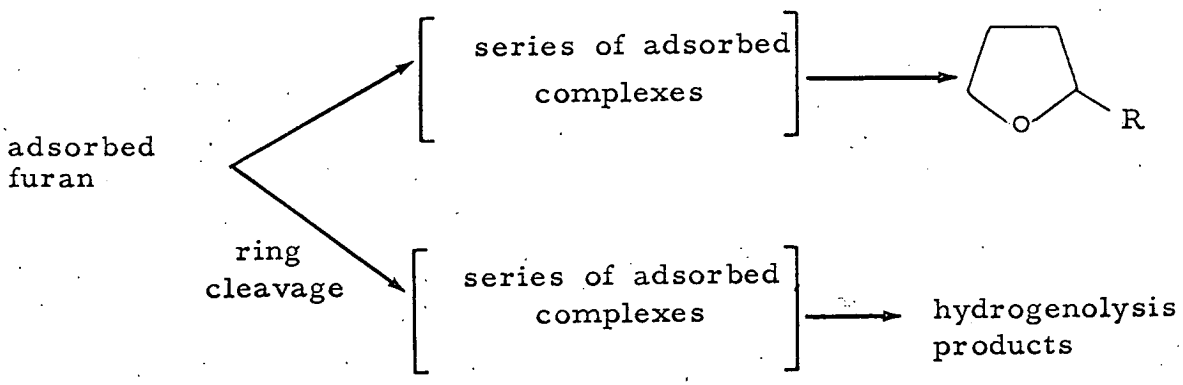

Mechanism B.

Evidence that VII (or the analagous adsorbed species) is an intermediate is only of an indirect nature since the dihydro-compound has never been detected during the hydrogenation of a furan. This is not surprising since furan has a high resonance energy (20 K. cal. mole^{-1}) and hence the activation energy required

to transform VI to VII or IX would be higher than that required to hydrogenate VII. Wilson (ref. 45) has shown that 2, 3-dihydrofuran is hydrogenated faster than furan while Swadesh et. al. have found that VII (R = CH_3) is much more easily hydrogenated than sylvan (ref. 45). The indirect evidence for 'mechanism A' comes from five main sources.

First, Topchiev (ref. 46) reported 5-hydroxypentan-2-one as a product from the partial hydrogenation of sylvan in the presence of water over nickel and palladium catalysts. No experimental details were reported but the following mechanism was suggested.

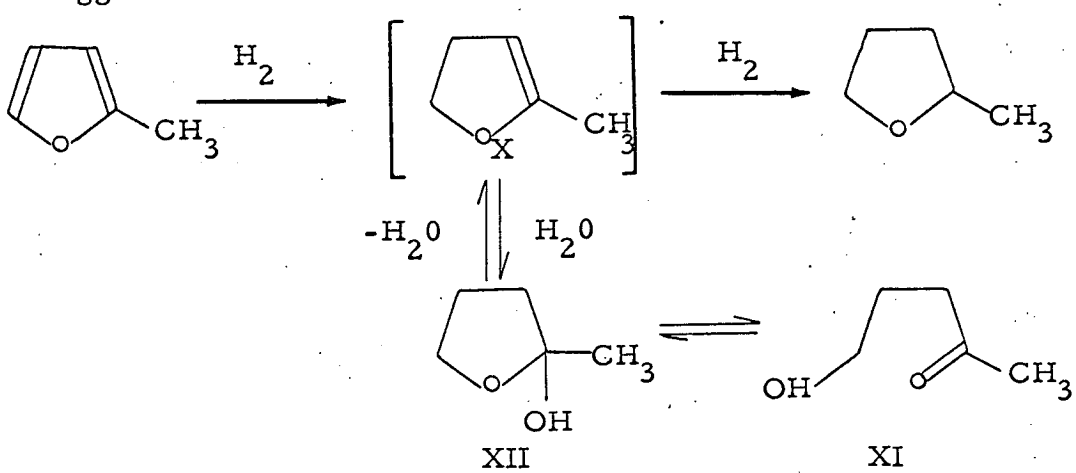

XII XI

Second, an intensive study was made of the above reaction (ref. 47) when it was established that the presence of a trace of formic acid promoted the formation of XI. If Topchiev's mechanism is valid the effect of the acid would be to catalyse the addition of water to the vinyl ether X. This promotion of hydrogenolysis by acid is a feature of many liquid phase hydrogenation reactions of furans (for example see ref. 29).

Third, on hydrogenating sylvan in acidic alcoholic media (ref. 45), 2-methyl-2-alkoxytetrahydrofuran, XIII, was formed in a similar manner to XII :

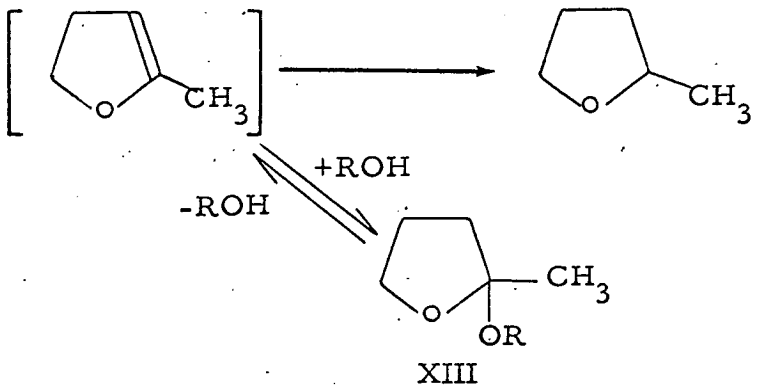

XIII

Fourth, the existence of the dihydrofuran has been used to account for a minor by-product, 2, 5-bis (trimethyleneoxy)-1, 4-dioxane, XV, obtained during the hydrogenation of furfuryl alcohol, XIV, ref. 48.

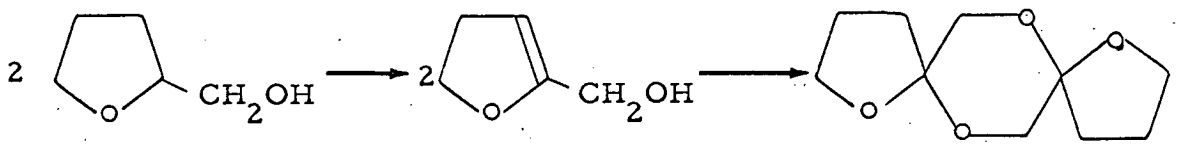

XIV XV

alternatively 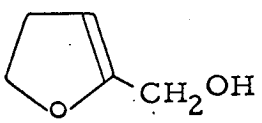 + XIV $\xrightarrow{H_2}$ XV

Fifth, on a similar basis to the above reaction the formation of spirononanes during the hydrogenation of various furyl acroleins over nickel copper and chromium catalysts has been attributed to dihydrofuran intermediates. For example (ref. 49) 1, 9-dioxa-5-spirononane, XVII, is formed in 33% yield by hydrogenating 3-(2-furyl) acrolein, XVI, over Ni/ kiezelguhr at 160°C :-

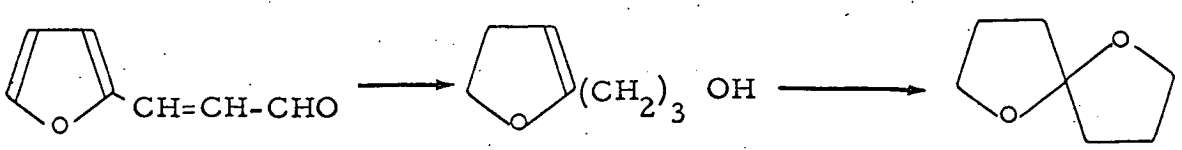

XVI XVII

The conclusion from the above five pieces of evidence is that hydrogenation of the furan nucleus proceeds in a stepwise fashion with a dihydrofuran or its adsorbed analog probably being an intermediate in the reaction. The evidence for this intermediate also being formed during the hydrogenolysis of the ring is more dubious since the hydrogenolysis reactions were probably provoked by the presence of the water and acid. Topchiev called palladium a 'specific catalyst' for the formation of XI, however, palladium is notorious for being a catalyst which causes practically no hydrogenolysis even under extreme conditions. Furthermore, spirononanes were not formed from 3-(2-furyl) acroleins over platinum (ref. 59), a catalyst noted for its ability to hydrogenolyse the furan nucleus.

The evidence for 'mechanism B' is also indirect in nature. Firstly, Bradley (ref. 38) claimed that the hydrogenation of furan does not proceed by a stepwise process since graphs of uptake of hydrogen during the conversion of furan to n-butanol over PtO_2 against time gave smooth curves. However, providing the concentration of the dihydro-intermediate on the catalyst's surface is low 'mechanism A' would give an identical result.

A second more positive piece of evidence was presented by Shuikin et. al. (ref. 49) who claim to have proved conclusively that dihydrosylvan is not an intermediate in the hydrogenolysis of sylvan since at 250-260^{o}C over Pt/C and Ni/ZnO dihydrosylvan is converted mainly to tetrahydrosylvan (only 10% and 15 to 20% respectively of pentan-2-one being formed). Under identical conditions practically no tetrahydrosylvan is formed on hydrogenating sylvan. Shuikin concludes that nuclear C - O bond hydrogenolysis occurs before the ring is hydrogenated, such a result confirming the conclusions of Balandin's multiplet theory which predicts that hydrogenation of

the first double bond in the furan ring occurs with approximately the same ease as does the hydrogenolysis of a furanic C - O bond (ref. 50).

Neither mechanism deals with the possible role of intermediate adsorbed species, probably because there is not sufficient information to provide more than the barest outline of the mechanism whereby hydrogenation is achieved. However, since on deuterating furan over rhodium under pressure (ref. 51) an almost quantitative yield of tetrahydrofuran -2, 3, 4, 5-d_4 is obtained, (hence deuteration proceeds without exchange) it is probable that the furan ring lies parallel to the catalyst surface during hydrogenation, the initial adsorbed species being an intact furan molecule bound to the catalyst's surface by overlap of the furan's π orbitals with empty metal d - orbitals (c.f. benzene, ref. 61). Furthermore, exchange reactions occur much more readily at the α positions in the furan ring (ref. 13, also note the similar behaviour of thiophene over MoS_2, ref. 52), hence the first attack on the furan nucleus during hydrogenation will occur at the 1 or the 5 positions.

The reaction mechanism will be dealt with in more detail in chapter 7.

1.4 Similarities between furan and benzene hydrogenations.

As mentioned previously furan has a high resonance energy, 20 K.cals.mole^{-1}. While this is smaller than benzene's, 36 K.cals.mole^{-1}, it is far higher than that for a typical conjugated diene, 3 K.cals.mole^{-1}, and hence it is probable that, as with benzene, ref. 53, the rate determining step is the addition of the first hydrogen atom or molecule to the ring. Comparison of the rate constants for hydrogenation of a series of furans with their benzene analogs showed the rate constants for the furans were between 1.3 to 3.8 times as great as those

for their benzene counterparts (ref. 29), while comparison of the activation energies (ref. 29) show benzene derivatives to have a slightly lower activation energy than their furanic counterparts the latter having higher frequency factors (from the Arrhenius equation). All the above data was collected from hydrogenations in acetic acid over PtO_2.

On hydrogenating alkenyl furans (for example 2-vinylfuran, ref. 54) using gentle conditions the side chain may be selectively hydrogenated. Similarly, using more violent conditons aryl furans (for example 2-benzylfuran, ref. 55, or 5-phenylfuran-2-carboxylic acid, ref. 56) may be selectively hydrogenated to their corresponding aryl tetrahydrofurans. This order of reactivity is consistent with the resonance energies of the vinyl group in vinyl furans, of furan and of benzene.

Apart from both having a high resonance energy and similar activation energies for hydrogenation reactions, furan and benzene derivatives follow the same kinetics for their reactions with hydrogen over PtO_2 in acetic acid, namely first and zero order in hydrogen and furan pressure respectively (ref. 29). Hence furan, like benzene, must be strongly adsorbed on a catalyst surface.

The deuteration of furan already referred to (over rhodium, ref. 51) shows that no exchange occurs during the hydrogenation of furan. This behaviour, which is quite unlike that observed during the deuteration of an alkene (ref. 57), is similar to the behaviour of benzene on deuteration over palladium and platinum films (ref. 53) where it has been shown that the deuteration and exchange reactions proceed by different reaction pathways and that little redistribution of deuterium occurs during deuteration.

While deuterium exchange reactions with benzene are rapid it has been shown that at -34°C benzene exchanges 200 times more slowly than cyclohexene, this divergence in rates increasing with temperature (ref. 62). Furan's exchange reactions are also much slower than alkene exchange rates (refs. 13 and 63).

Finally, it is interesting to note that it has been suggested that cyclohexene is an intermediate in the hydrogenation of benzene, evidence coming from the detection of tetrahydroxylenes during the hydrogenation of their parent xylenes over ruthenium, rhodium and nickel (ref. 60) and from the configurations of the hexahydroxylene end products (refs. 58 and 60)., As was shown in the previous section there is evidence that partially saturated furan is an intermediate in furan's hydrogenation.

All the above evidence points to the fact that furan's behaviour on hydrogenation is closely related to benzene's. The similarity of the two systems, (which is exploited in chapter 7) , is all the more important since, while a large volume of basic research has been carried out on benzene-hydrogen reactions, relatively little has been devoted to the analagous furan reactions.

CHAPTER 2

EXPERIMENTAL ASPECTS

2.1 Nomenclature for labelling experiments.

Each reaction is referred to by a code of the form

C X Y Z 2.1

Where C X refers to the X^{th} batch of supported metal salt prepared. C X Y identifies the supported metal sample prepared from the batch of supported metal salt C X and Z is the Z^{th} reaction carried out over the catalyst sample C X Y. X and Z are numbers, Y is an alphanumeric character.

For example the experiment C4C2 is the second carried out over the catalyst sample C4C, which is the third sample prepared from the batch of supported metal salt C4 (the fourth such batch to be prepared).

The type of catalyst used is clearly dictated by the number X and may be found by reference to the following table.

Table 2.1 Identification of the type of catalyst

X (see 2.1)	Type of catalyst (percentages are w.w.)
1	5% Ni/Al_2O_3
2	
3	
4	5% Ni/SiO_2
5	SiO_2
6	5% Pt/SiO_2
7	10% Pt/pumice
8	5% Pt/pumice
9	5% Pt/Al_2O_3
10	5% Pt/pumice

FIGURE 2.1

Block diagram of the apparatus

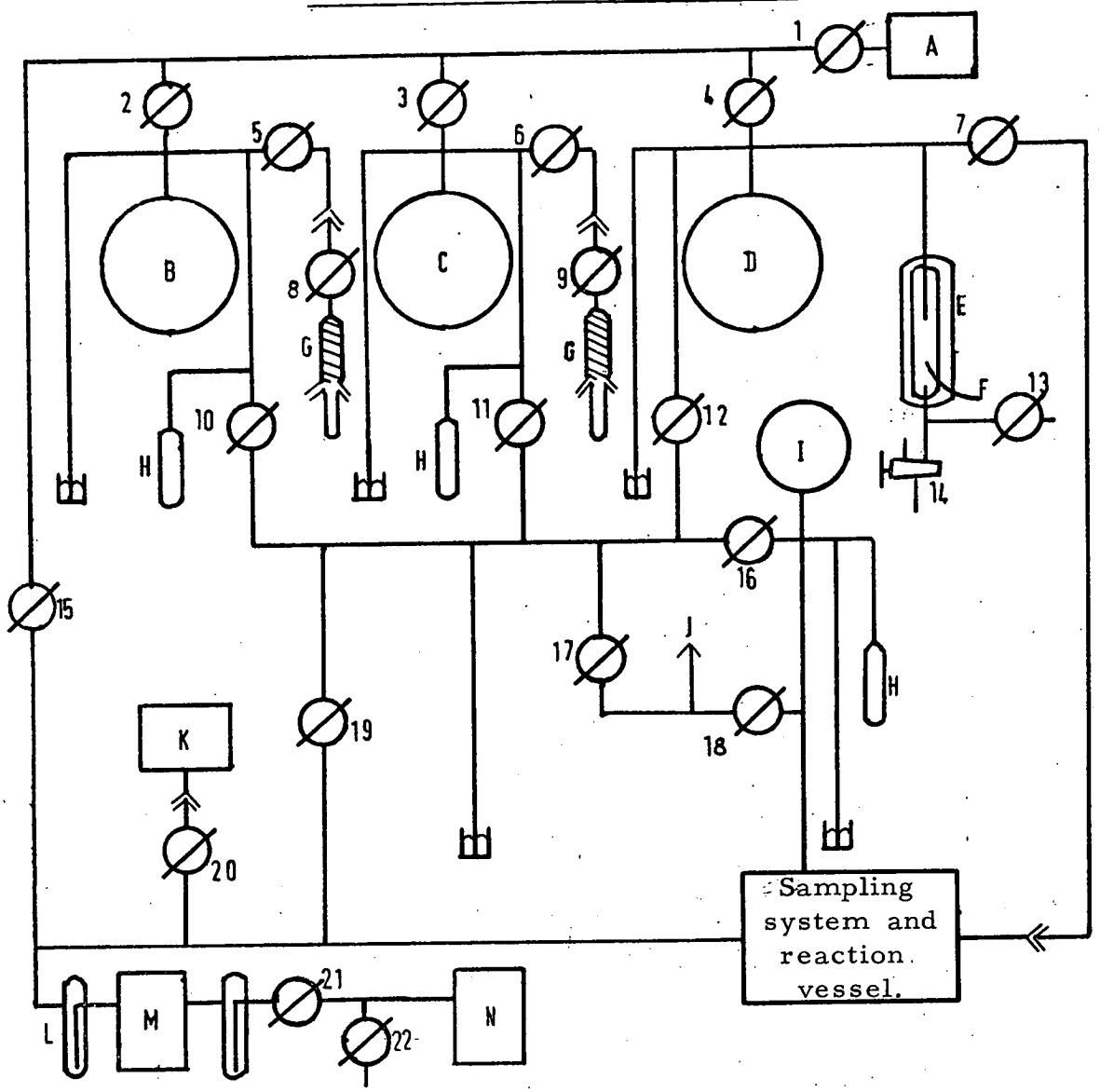

KEY

A - McLeod gauge.
B, C and D - 21. storage vessels for the reactants, B containing pure hydrogen.
E - Hydrogen purification system (see Fig. 2.2).
F - Thermocouple (chrome-alumel).
G - Reactant purification columns packed with molecular sieve.
H - Liquid air traps for freezing out reactants.
I - Mixing and storage vessel for reaction mixtures
J - Facility for sampling reaction mixtures prior to their injection into the reaction vessel.
K - Pirani gauge.
L - Liquid air trap.
M - Mercury diffusion pump.
N - Rotary piston pump.

The code letter C refers to all the reactions with the exception of the consecutive reactions, described in section 2.5.3, these being identified by CS or a CR in the place of the C, for instance, CS8C2 is the second of a series of consecutive reactions carried out over the third catalyst sample of the 8th batch of catalyst (5% Pt/pumice), table 2.1, to be prepared.

2.2 The Apparatus

The apparatus consisted of a pyrex glass vacuum rig shown diagrammatically in figure 2.1.

2.2.1 Storage of Reactants.

Three two litre vessels were used for storing reactants in their gas phases, one of which was only used for pure hydrogen, (diffused through a palladium thimble from a gas cylinder). The other two vessels had attachments in which the reactants could be frozen out in a liquid air trap to minimise decomposition and to protect the grease on associated taps.

Reaction mixtures were stored in a 750 ml. vessel which was sufficiently large to enable a reaction mixture of the same composition to be used more than once.

2.2.2 Vacuum pumps and pressure measuring systems.

A three stage glass mercury diffusion pump, in conjunction with a liquid air trap, backed up by N. G. N. Ltd., Model PD.2, three stage rotary piston pump evacuated the apparatus down to a pressure of 4×10^{-5} torr. Pressures below one torr. were measured by an Edwards High Vacuum Pirani gauge, using a G5C.2 head, whose callibration was checked using a 299.8 ml. McLeod gauge and found to be satisfactory (Graph 2.1). Higher pressures were measured using mercury manometers.

GRAPH 2.1

Check on the calibration of the Pirani gauge.

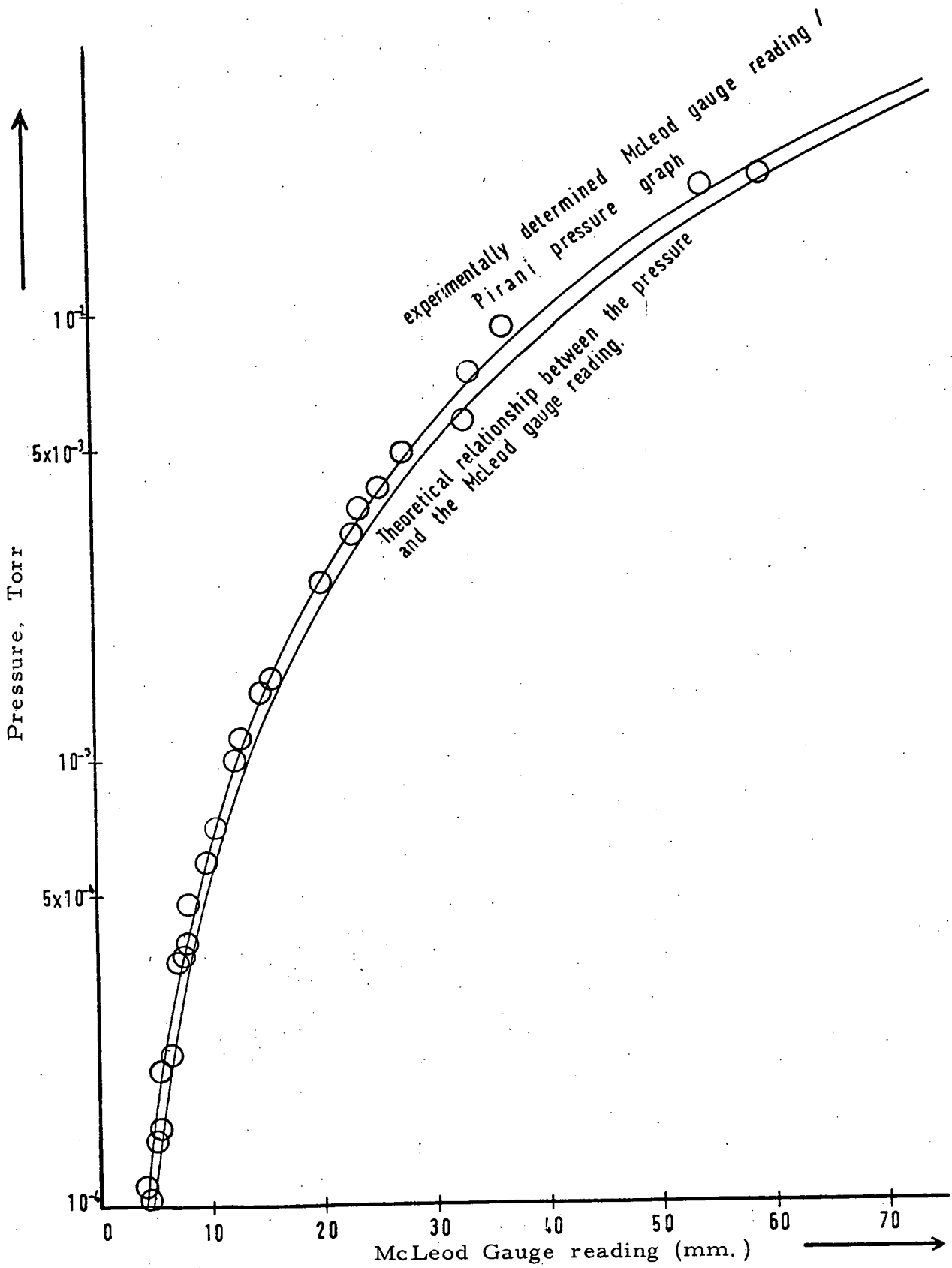

GRAPH 2.2

Calibration of the chrome-alumel thermocouple used for temperature measurements of the reaction vessel.

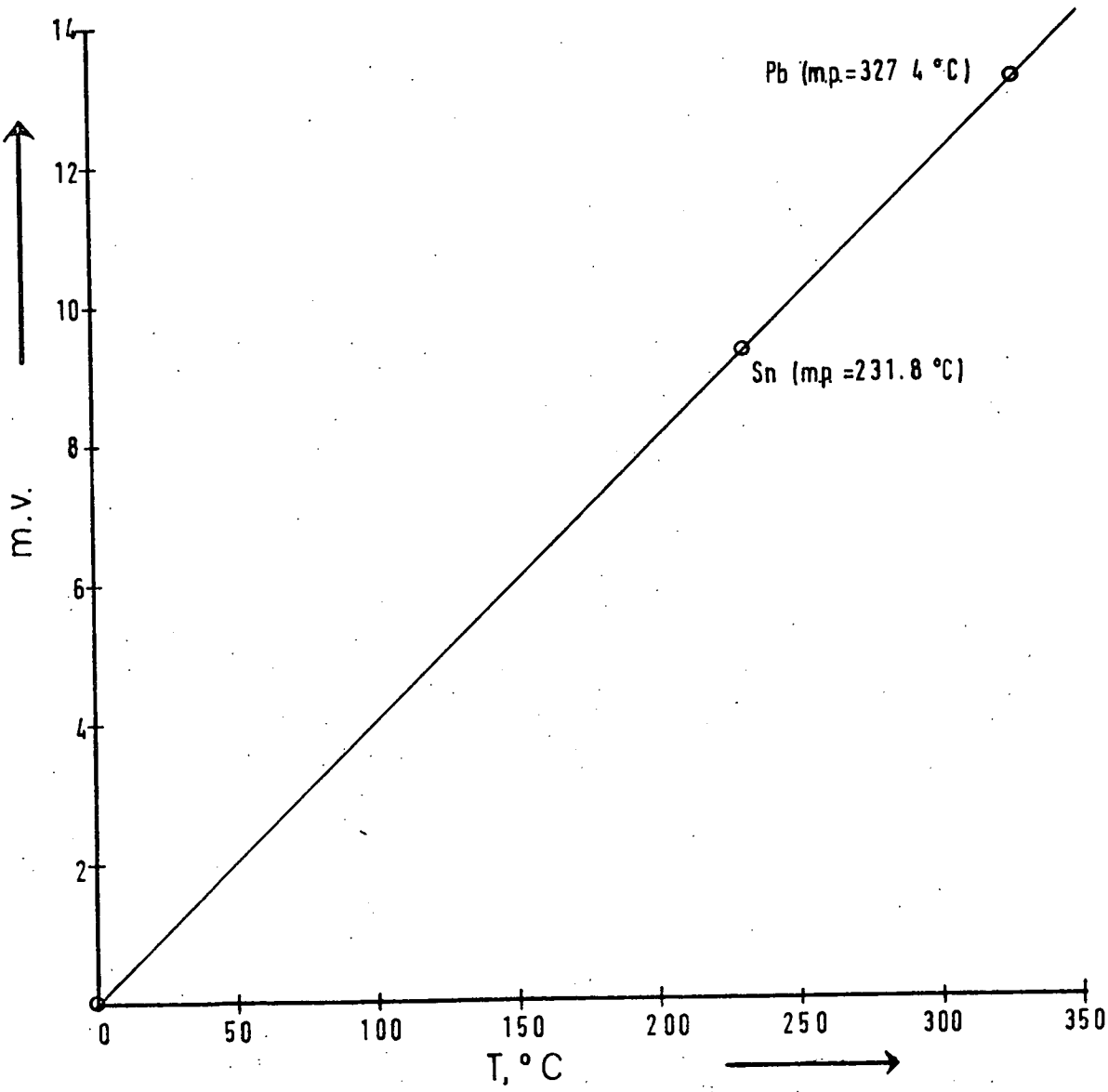

2.2.3 Furnaces, their temperature control and measurement.

Two furnaces were used, one surrounding a palladium thimble used for hydrogen purification, the other used for heating the reaction vessel. The temperature in both furnaces was measured using chrome alumel thermocouples calibrated using lead, zinc and ice baths as standards (Graph 2.2). The potentials generated by the thermocouples were measured using a Cambridge potentiometer.

The palladium thimble's furnace was built out of a pyrex tube encasing a palladium thimble. The glass tube was surrounded by layers of asbestos containing windings of Nichrome resistance wire, (resistance 10 Ω), fig. 2.2. The thermocouple was contained in a well protruding into the body of the tube. The furnace temperature was maintained at 300°C using a three ampere variable transformer set at 29.5 volts.

The furnace, an Amalgams V.T.M.1/123, surrounding the reaction vessel, fig. 2.3, was mounted horizontally and could be moved along its axis to facilitate access to the reaction vessel. The temperature measuring thermocouple was attached to the reaction vessel itself using asbestos rope while a thermistor (used to control the oven temperature) was placed in contact with the central oven coils. The thermistor formed one arm of a Whetstone bridge, and a variable resistance, which acted as the temperature selector, another. The bridge was kept in balance by means of a thyristor supplying power to the oven coils when the resistance of the thermistor was too low to maintain the bridge in balance. This reliable temperature controlling system maintained the furnace at temperatures up to 450°C to within $\pm$ 0.25°C.

FIGURE 2.2

HYDROGEN PURIFICATION SYSTEM

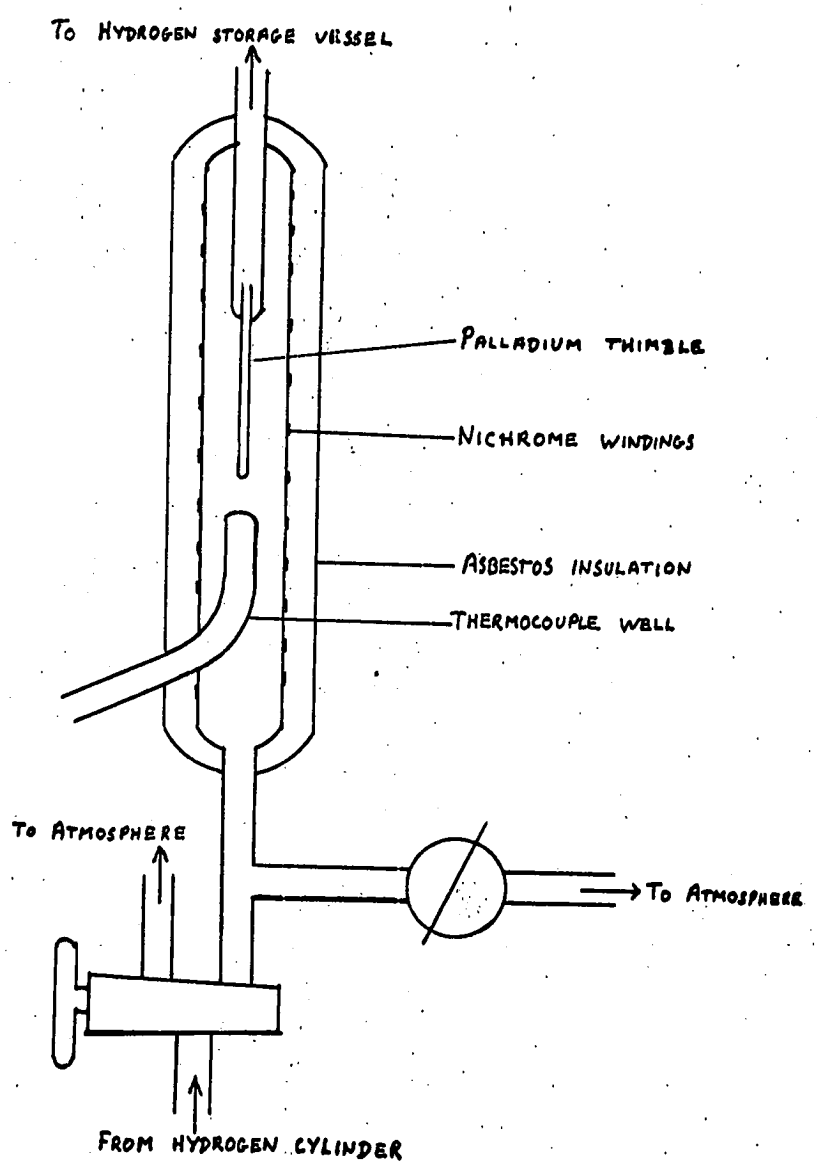

GRAPH 2.3

Temperature gradient along the reaction vessel's furnace, the reaction vessel lies between the broken lines.

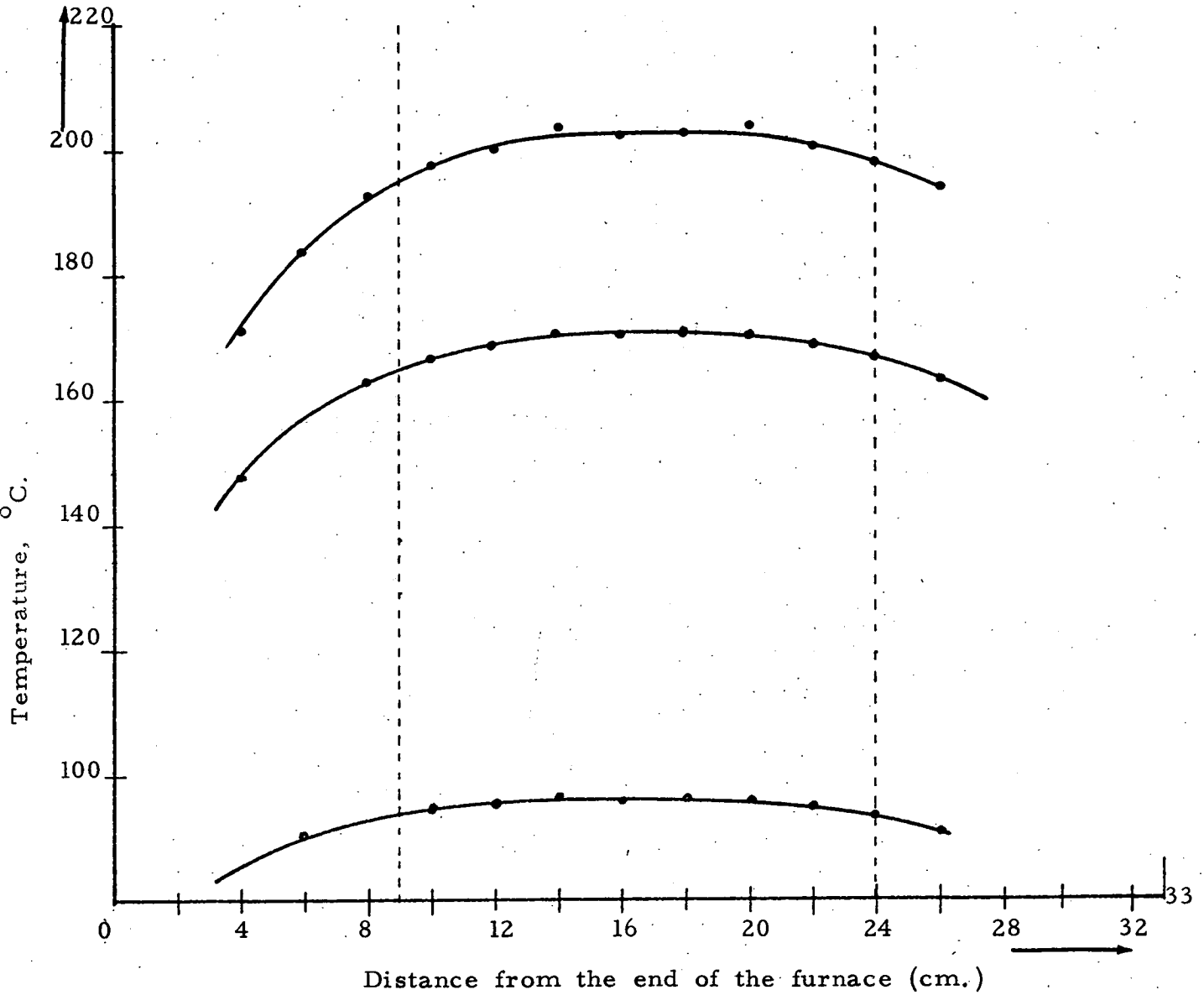

Even with one inch thick oven ends machined out of asbestos a temperature gradient existed along the oven (graph 2.3) at high temperatures. However the gradient along the reaction vessel itself was small, particularly at the low temperatures used for hydrogenations.

2.2.4 The Reaction Vessel.

A 200 ml. reaction vessel lying horizontally in the furnace was used, fig. 2.3. While a reaction vessel of the form outlined in fig. 2.3 was used for the later experiments, the one used first differed in that no ground glass joint was used at the end where samples were taken, see fig. 2.4, the reaction vessel being sealed onto the vacuum line each time a new catalyst sample was used.

To ensure that the hydrogen used in the reduction of a catalyst sample was as uncontaminated by organics as possible it was only admitted to the reaction vessel through the greaseless tap at one end of the reaction vessel (tap 5, fig. 2.3 or fig. 2.4). This tap was connected directly to the hydrogen storage vessel by a short length of nylon tubing. Reaction mixtures were admitted through the connection at the other end of the reaction vessel which was also used for taking samples of a reaction mixture and for evacuating the vessel.

Contamination of the catalysts by tap grease was minimised by applying an annulus only of Apiezon T silicon grease (Edward high vacuum Ltd.) to the ground glass joints at either end of the reaction vessel (fig. 2.3). This did not impair the vacuum holding ability of the system.

Between experiments the reaction vessel was washed first with dilute nitric acid, then thoroughly with distilled water and left to dry in an oven overnight. The catalyst samples

FIGURE 2.3

Sampling system and reaction vessel finally adopted

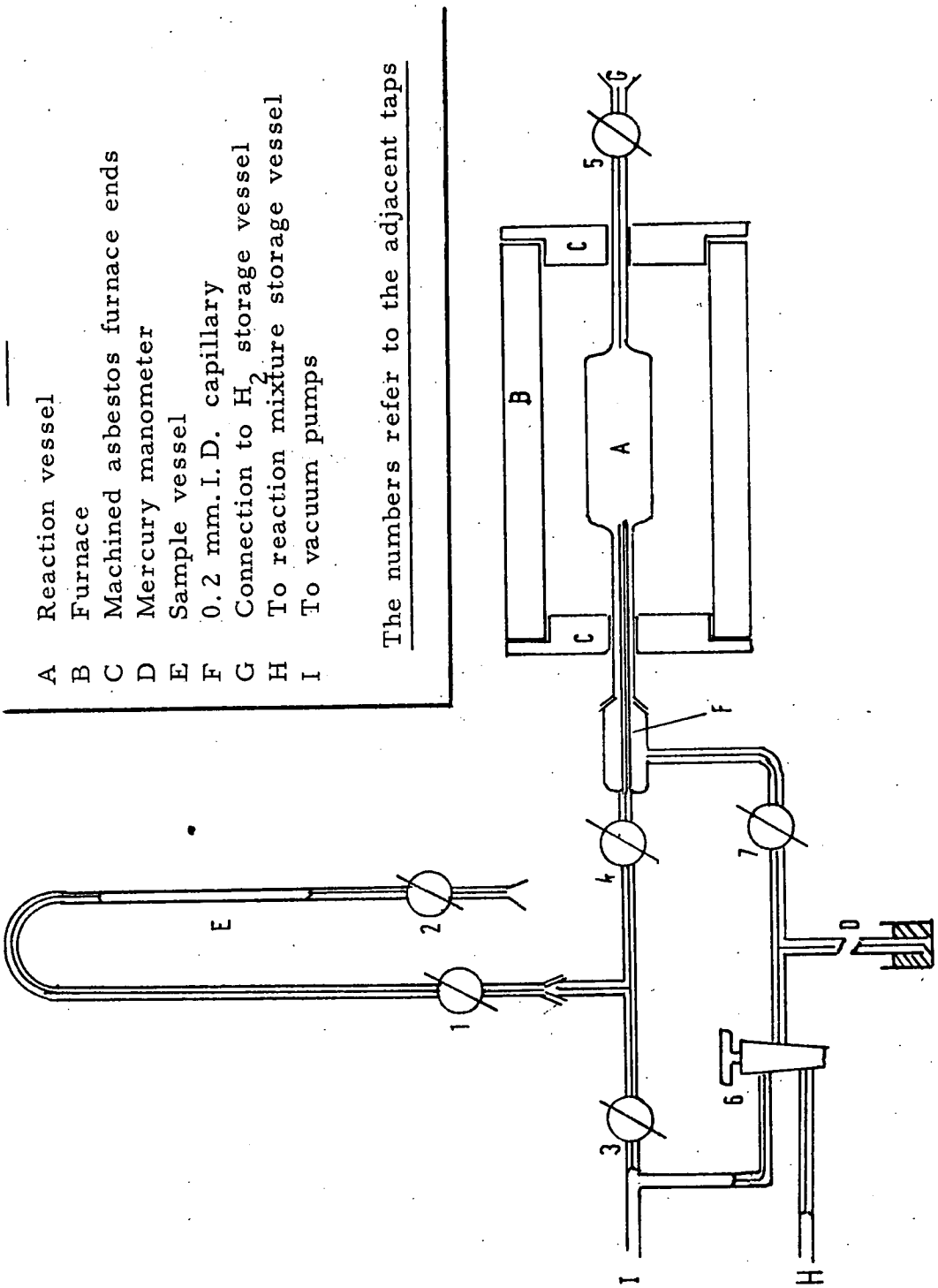

FIGURE 2.4

Sampling system and reaction vessel used originally.

KEY

A Reaction vessel containing catalyst.

B Sample vessel

C Connection to vacuum pumps

D Mercury manometer

E Connection to reaction mixture storage vessel.

F Connection to H_2 storage vessel

the number refer to the adjacent taps.

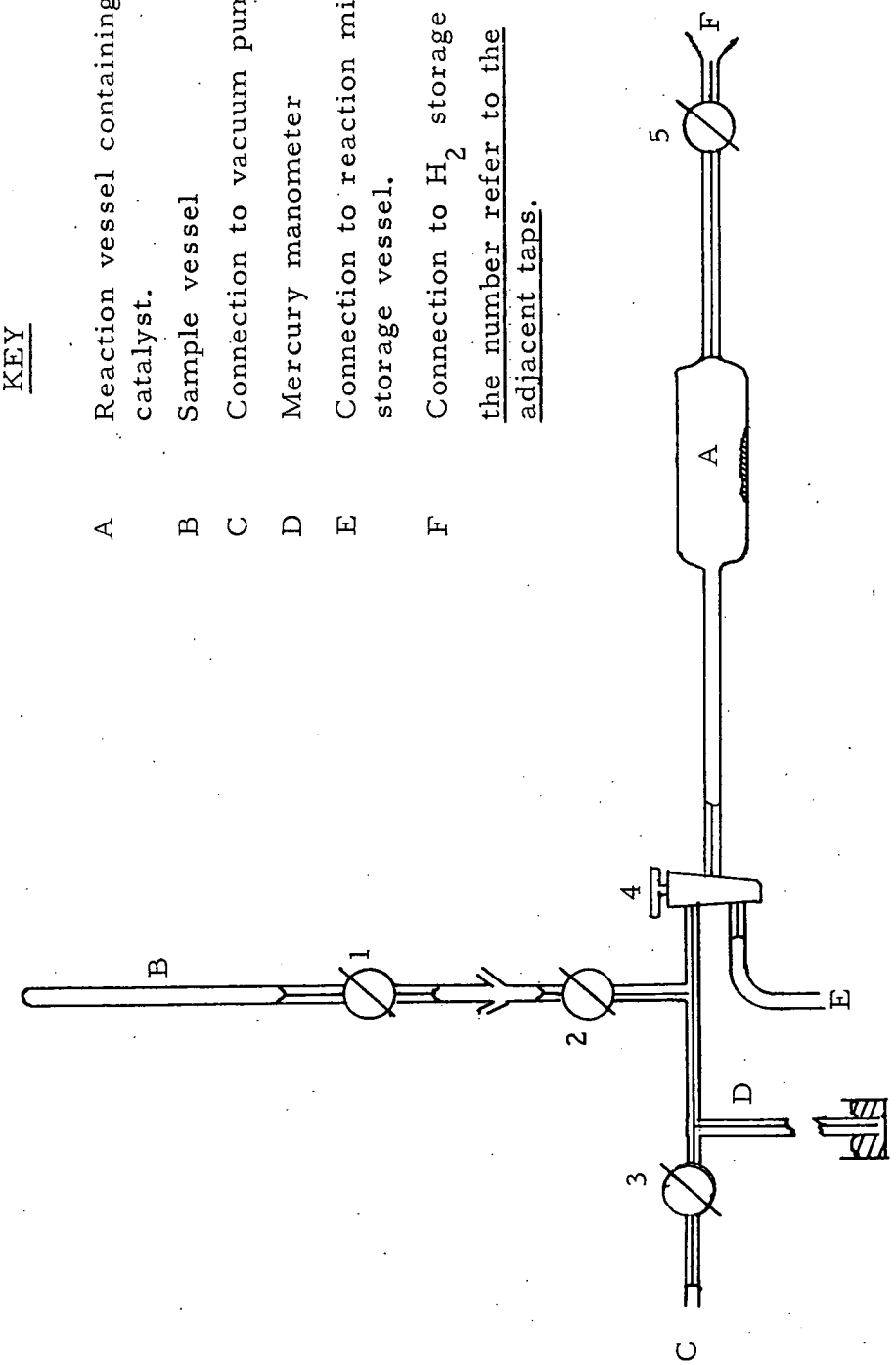

were positioned near the mid point of the reaction vessel's floor, as in fig. 2.4.

2.2.5 Sampling systems.

Two main sampling systems were used shown diagrammatically in figs. 2.4 and 2.3, the latter system being superior for two reasons. First, it ensures that, as far as is possible, a sample taken of the reaction mixture has the same composition as the reaction mixture in the immediate vicinity of the catalyst, samples being taken through an 0.2 mm. Veridia pyrex capillary projecting into the reaction vessel. Second, by changing from the system outlined in figure 2.4 to that shown by figure 2.3, the percentage pressure drop in the reaction vessel on taking a sample was reduced by almost an order of magnitude (from approximately 15% to 1.7%).

The latter improvement, which was achieved by reducing the dead space in the sampling system, was of great importance in the later experiments during which up to 14 samples were taken (e.g. run C10M1). Furthermore, it was easier to follow the kinetics of a reaction if the pressure drops caused by taking samples were reduced to a minimum.

A further advantage of the sampling system outlined in figure 2.3 is that sample tubes with capillary taps and ground glass joints at either end were used, which simplified the analysis procedure (section 2.3.3) without a detectable increase in the adsorption of reactants or their products on the tap grease.

The procedure used when sampling was basically the same for the two systems. After as much of the dead space between the sample and reaction vessels had been evacuated a sample of the reaction mixture was expanded into an evacuated sample vessel.

2.3 Chemicals

2.3.1 Reactants

Hydrogen	Hydrogen (British Oxygen Company, Laboratory grade) was purified by diffusion through a silver palladium alloy thimble, maintained at 300°C.
Furan	(B. D. H. Ltd., Laboratory Reagent grade) showed no detectable impurities on G. L. C. analysis using a flame ionisation detector. It was further purified by distillation through a column of molecular sieve, type 4A, to remove water and any dissolved gases.
Sylvan	(Fluka AG. Buchs SG.) quoted as having less than 1% impurity, born out by G. L. C. analysis which showed only a trace of furan to be present, was further purified by distillation through a column of 4A molecular sieve.
Benzene	'Analar' grade (B. D. H. Ltd.), further purified in the same manner as furan.
n-Hexene	(Koch-Light, 'Puriss'), purified as above.
tetrahydrofuran	(B. D. H. Ltd., Laboratory Reagent grade stabilised with 0.1% quinol) purified as above.
n-butanol	(B. D. H. Ltd., Laboratory Reagent grade, purity exceeding 95%) purified as above.
n-propanol	(B. D. H. Ltd., 'Analar' grade) purified as above.

Fig. 2.5

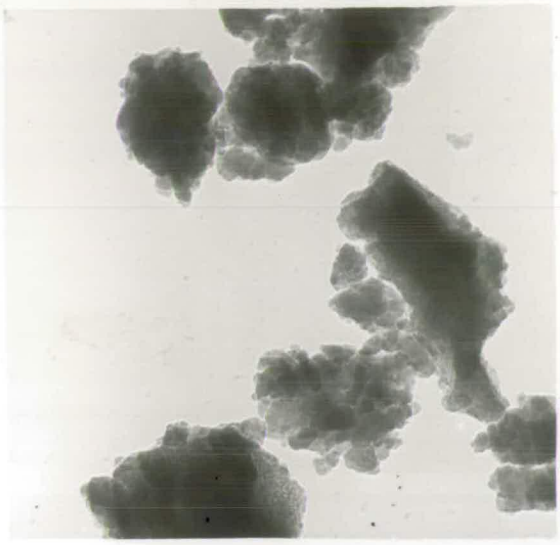

Silica [transmission], X 57,500

Fig. 2.6

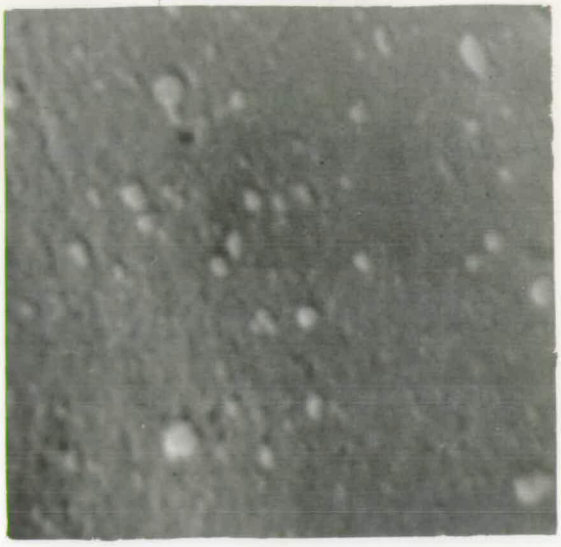

Silica [scanning] X 20,000

Fig. 2.7a

Pumice [scanning] X 500.

Figure 2.7b

Silica X20,000 (Scanning).

Figure 2.8

Pumice X60,000 (Transmission)

2.3.2 Catalyst supports

Alumina

Type 1 :- Activated alumina, 16/32's mesh (Laporte Industries Ltd., 'Type A' alumina).

Type 2 :- Prepared in the Laboratory from aluminium nitrate (section 2.4.1).

Silica

'Sorbosis M60' (Crosfield Chemicals Ltd.) The surface area quoted by the manufacturers is 500 to 600 $m.^2 g^{-1}$.

Information on the pore size and density was obtained from transmission (fig. 2.5) and scanning (fig. 2.6) electron micrographs, courtesy of Mr. Boult, of the Electron Micrographical Dept., University of Newcastle. The transmission micrographs were obtained by pulverising a silica sample to such an extent that some of the fragments, ultrasonically dispersed on a grid, were sufficiently thin to allow partial transmission of the electron beam to occur. The minimum pore density is $10^{16} g.^{-1}$ while the maximum pore diameter is approximately 10^3 Å, most pores having a diameter of 150 to 500 Å.

Pumice

'Pumice Stone', mesh 6-16 (B.D.H. Ltd.) The surface area, courtesy of Dr. H. Marsh, University of Newcastle, was 55 $m^2 g^{-1}$ ± 10%, found by the B E T method using an electrobalance. No fine pore structure was detected by electron microscopy (scanning electron micrographs taken at the University of Newcastle, figs. 2.7a and 2.7b, transmission micrographs taken by Mr. J. Lyons, Newcastle

Polytechnic, fig. 2.8). The highly convoluted nature of the pumice's surface is illustrated by fig. 2.7a, taken at low magnification (X200).

Examination of a pumice sample by Dr.B.A.O.Randall of the Geology Dept., University of Newcastle, established the pumice to be a ryalite, a type of glassy mineral of greatly varying composition, being a mixture of silicates.

2.4 Catalyst preparations.

Six types of supported catalyst were prepared :

Table 2.2 Catalysts prepared

Catalyst (all %'s are w.w.)	Code of the catalyst batch (section 2.1)
5% Ni/Al_2O_3	C1, C2 and C3
5% Ni/SiO_2	C4
5% Pt/SiO_2	C6
5% Pt/Al_2O_3	C9
5% Pt/pumice	C8, CS8, C10, CR10
10% Pt/pumice	C7

In the preparation of the above catalysts a supported metal salt was prepared first, nickel nitrate and chloroplatinic acid for the nickel and platinum catalysts respectively. Supported nickel nitrate was then converted to support nickel oxide by heating under vacuum on a sand bath or in a bath of dioctyl phthalate. Samples of supported chloroplatinic acid or nickel oxide were reduced with pure hydrogen in the reaction vessel prior to a reaction.

The first of the catalysts listed above proved unsatisfactory since a number of different methods of preparation of the Ni/Al_2O_3 (all three) led to hydrogen sulphide being produced on reduction of the supported nickel salt. This was shown by infra red spectroscopy to be caused by sulphate being present in the activated alumina sample. A peak was observed in the spectrograph at 1050 cm^{-1} as compared with the literature value (ref. 64) for the sulphate group in aluminium sulphate of 1110 cm^{-1}.

2.4.1 Catalyst supports.

The supports used in the preparation of the first three catalysts listed in table 2.2, were used as supplied by the manufacturers, section 2.3.2, while the alumina used in the preparation of the Pt/Al_2O_3 catalyst was prepared in the laboratory from aluminium nitrate and the pumice used in both pumice supported catalysts was pretreated before use.

Preparation of the alumina used for the Pt/Al_2O_3 catalyst. (ref. 65)

44g. of hydrated aluminium nitrate were dissolved in 300 mls. boiling distilled water. Excess dilute ammonium hydroxide was carefully added to the stirred boiling solution of the nitrate to precipitate the aluminium as its 'hydrated oxide'. The hot precipitate was isolated by filtration and was washed with a hot solution (10% w.w.) of ammonium nitrate followed by a thorough washing with hot distilled water. The hydrated alumina was then transferred to a crucible and heated to 750°C for five hours. On cooling the alumina was pulverised in a mortar and stored in a vacuum desicator.

Pretreatment of the pumice stone used in the preparation of the Pt/pumice catalyst.

The pumice stone supplied by B. D. H. contained some foreign organic matter, mainly wood, which was removed by thorough washing of a pumice sample with water followed by decantation. Any further organic matter was removed by heating the sample in a furnace at 500°C for three hours. The cooled pumice was washed thoroughly in hot dilute nitric acid and distilled water in turn. The large quantity of fines present were removed by decantation during the final washing of the pumice with water. Finally the pumice was dried at 150°C in an oven.

2.4.2 Preparation of supported metal salts.

Standard solutions of nickel nitrate and chloroplatinic acid were made up to prepare supported nickel and platinum catalysts respectively. A known volume of the appropriate standard solution was added to a sample of the support and evaporated to dryness over a steam bath, the mixture being stirred continuously. The last traces of moisture were removed by heating the supported metal salts in an oven at 110°C for one hour.

The supported chloroplatinic acid samples were then transferred to a vacuum desicator until required while the supported nickel nitrate samples were converted to supported nickel oxide by heating under vacuum at 300°C to 360°C for about three hours after which they were also transferred to a vacuum desicator.

The weights of chemicals used to prepare the catalysts are summarised in the following table.

Table 2.3

Type of Catalyst	Catalyst System	Weight of support	Wt. of metal, from conc. & vol. of stand. solution	Percent, w.w., Metal in Support Catalyst
Nickel/SiO_2	4	10.611g	0.5693g	5.1%
SiO_2 *	5	1.00g	0.0g	0.0%
Pt/SiO_2	6	1.880g	0.0992g	5.0%
Pt/pumice	7	0.891g	0.0992g	10%
Pt/pumice	8	7.2583g	0.3886g	5.1%
Pt/Al_2O_3	9	0.7326g	0.0397g	5.1%
Pt/pumice	10	7.5695g	0.3986	5.0%

* Used to test for possible catalytic activity of the support.

2.4.3 Reduction to supported metals.

The supported salts were reduced to supported metals in the reaction vessel in an atmosphere of hydrogen using a static system. Reductions were carried out using a two stage process :-

1. The supported salts were reduced for 45 mins. $\pm$ 15 mins. at a temperature of 400°C $\pm$ 10°C in an atmosphere of pure hydrogen at a pressure of about 300 mm. Hg. After the reduction the reaction vessel was evacuated.

2. The first stage was then repeated at the same temperature, the reaction vessel being finally pumped out and the supported metal catalyst allowed to cool under pure hydrogen.

A qualitative examination of the activity of the catalyst with respect to reduction times showed no correlation with the length of time the catalyst had been reduced.

2.5 Experimental techniques involved in carrying out a hydrogenation.

2.5.1 Preparation of the reaction mixture.

The condensible reactants, after introduction into the storage vessels, were degassed by repeated cycles of freezing in liquid air traps, followed by evacuation of the storage vessels.

In the preparation of a reaction mixture a condensible reactant is expanded from a storage vessel into the volume bounded by taps 10, 11, 12, 16 and 17, fig. 2.1, and from there into the mixing vessel I. The process is repeated until the desired reactant pressure is obtained. The former volume is then evacuated and the second reactant expanded into it, and from there into the mixing vessel, the process being repeated until all the reactants have been added, hydrogen always being the last since there is a high partial pressure of hydrogen available in its storage vessel (D, fig. 2.1).

Since all reactant pressures were measured using mercury manometers it was often found convenient to input high reactant pressures (in the required ratio of partial pressures) into the mixing vessel, the total pressure of the mixture of reactants then being reduced by a suitable factor. By this technique a greater accuracy in the relative and absolute partial pressures of reactants can be achieved, particularly for a reaction mixture in which one of the reactants

has a low partial pressure. For example, the reaction mixture for run CR10D4 was made by preparing a mixture of furan (14.1 mm. Hg) and hydrogen (468.4mm. Hg), the total pressure of the mixture then being reduced by a factor of 0.44, by partial evacuation of the mixing vessel, giving a final furan pressure of 6.2 mm. Hg.

By G L C analysis of a sample (taken using the sampling facility attached to the mixing vessel) of a reaction mixture containing two reactants detectable by an F I D detector their relative concentrations may be found accurately, see reactions C10J1, C10K1, C10L1, C10N1, C10M1, C10O1, C8G1, C10A1, C10C1.

The mixing vessel had a sufficiently large volume (750 ml). compared with the reaction vessel's volume (200 ml.) to allow more than one sample of single reaction mixture to be injected into the reaction vessel. Hence a series of reactions e.g., C6C1, C6D1, C6E1, C6E2 and C6E3, could be carried out using reaction mixtures of identical initial mole percent compositions.

2.5.2 Techniques involved in a single run.

When the reaction vessel furnace had settled down to a constant temperature the reaction vessel was evacuated and the reaction mixture admitted from the mixing vessel. The reaction was followed by observing the reaction vessel pressure and by taking samples for G. L. C. analysis by expanding the reaction mixture into an evacuated sample tube. (see section 2.1.5).

2.5.3 Techniques involved in 'consecutive run' experiments.

'Consecutive run' experiments refer specifically to two groups of experiments (CS8 and CR10 series) where a reaction is carried out over a catalyst sample, stopped after a given time by flushing the reaction vessel out with pure hydrogen and immediately injecting another reaction mixture. These experiments differ from a series of runs such as C6E1, 2 and 3 where the procedure between runs is to evacuate the reaction vessel for some minutes after which the catalyst is left in an atmosphere of pure hydrogen until next required.

The termination of a reaction in a series of consecutive runs is achieved by reducing the reaction vessel pressure to 5 cm. Hg, isolating the reaction vessel from the vacuum, admitting ≥ 350 mm. Hg of pure hydrogen, evacuating the reaction vessel to a pressure of 5 cms again, isolating from the vacuum, admitting ≥ 300 mm. Hg of pure hydrogen and evacuating down to 5 cms. Hg pressure. A new reaction mixture is immediately injected into the reaction vessel. The above process was carried out as quickly as possible since it was necessary to disturb the state of the catalyst by as little as possible between runs.

2.6 Analysis Techniques.

Analysis of gaseous samples were carried out on a gas-liquid chromatograph (Pye 'Pancromatograph') using a flame ionization detector in conjunction with a gas sampling valve. The carrier gas used was argon and ancillary equipment consisted of a digital integrator (Kent 'Cromalog 1') and a chart recorder (Honywell). The chromatograph's columns were packed glass tubing, length 9', internal diameter $\frac{1}{4}$".

KEY

A	To chromatograph
B	From carrier gas supply
C	To rotary piston vacuum pump

FIGURE 2.9

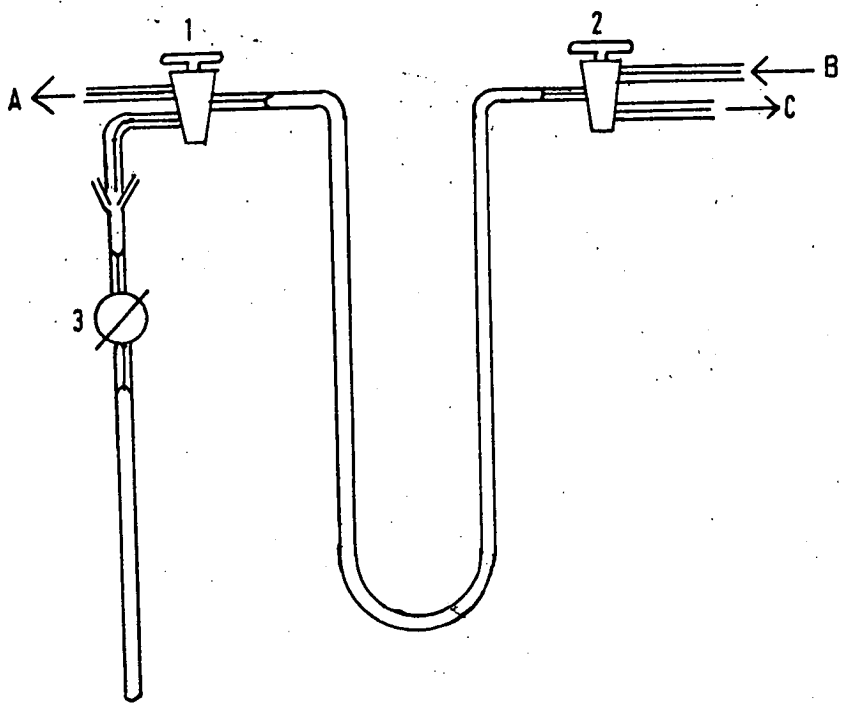

FIGURE 2.10

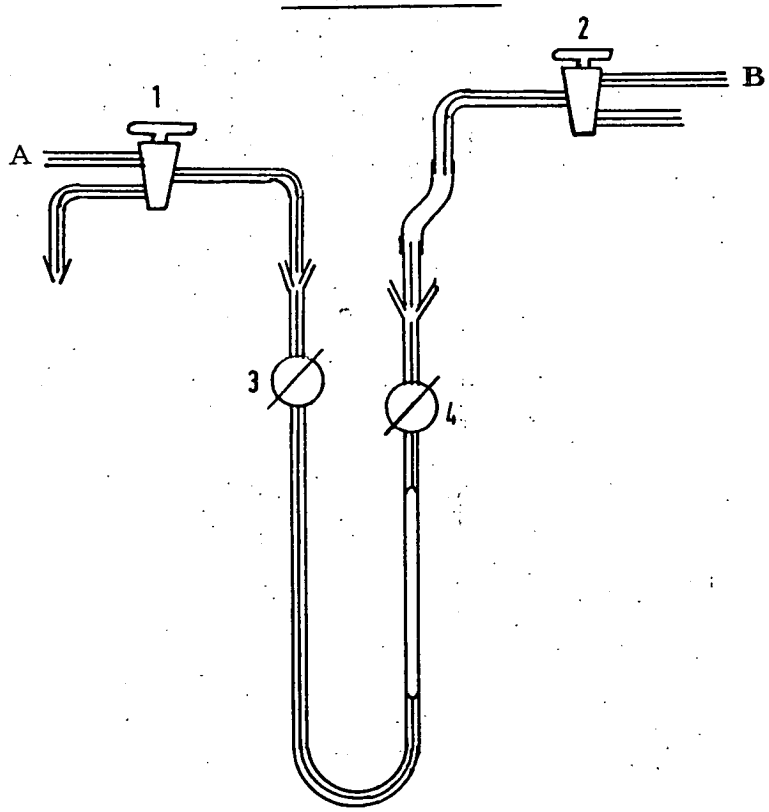

A commercial gas sampling valve (Pye 104) was tried but was found unsatisfactory at low pressures, hence pyrex glass sampling valves were made in the laboratory, the two principle ones illustrated in figs. 2.9 and 2.10. Both systems shown in the diagrams were made possible because in the 'Pancromatograph' the carrier gas enters a column through two inlets, therefore, isolation of a sampling valve from the chromatograph (by closing taps 1 and 2, figs. 2.9 and 2.10), which is essential when the sample vessels are changed, does not prevent carrier gas from flowing through the column.

The system outlined in fig. 2.10 was finally adopted since samples could be analysed more quickly without detectable loss in accuracy. (It had been feared that a system using so many greased taps and joints would be unsatisfactory).

2.6.1 Operation of the gas sampling valves.

For the sampling valve outlined in fig. 2.9, the sample vessel was immersed in liquid air while the volume from tap 3 to the rotary piston pump was evacuated. Tap 3 was then opened briefly to the vacuum to remove the uncondensible gases, hydrogen, when tap 2 was closed, the glass loop between taps 1 and 2 immersed in liquid air and the sample tube allowed to come to room temperature, (tap 3 open). After 15 mins. $\pm$ 5 mins. the glass loop was isolated now containing the detectable constituents of the sample to be analysed, and warmed to return the mixture to the gas phase. Finally taps 1 and 2 were opened simultaneously to the chromatograph hence injecting the gas sample.

In the analysis of a gaseous sample using the valve shown in fig. 2.10, the sample vessel was positioned as shown in the figure with taps 1 and 2 closed, taps 1 and

were then opened to the chromatograph and after approximately one minute, when the chromatograph's column line pressure had returned to its normal value, taps 3 and 4 were opened simultaneously, the carrier gas sweeping the sample into the chromatograph. After 30 seconds tap 1 was closed whereupon tap 2 was opened to the atmosphere (to relieve the pressure on the sample loop's ground glass connections).

2.6.2 Peak area measurement.

Since the treatment of the data obtained from chromatographical analysis will be dealt with in detail in the following chapter, suffice it to say for the time being that the data used in quantitative analyses was in the form of peak areas. These were measured either by an electronic digital integrator or, when this was not available, visually using the following relationship:

Peak area = (peak height) x (peak width at half height) 2.2

It was feasible to use equation 2.2 since all the columns used gave symmetrical peaks, showing only slight tailing.

CHAPTER 3

ANALYSIS

3.1 Theoretical Aspects

3.1.1. Choice of analytical method

Results from analysis of samples by gas-liquid chromatography were processed to yield relative molar quantities of components (c.f. ref. 66) rather than the absolute number of moles of each constituent, the ratio of the number of moles of each constituent being found relative to the number of moles of one of the constituents. This method was employed for the following reasons.

A. A higher accuracy in the standardisation procedure is possible since the actual amount of a standard mixture analysed is immaterial (the molar ratios of any two components in a sample of the standard mixture are not affected by the amount of sample analysed). Hence a source of error is eliminated.

B. For the same reasons given in A the size of the sample vessel is not of importance. The error introduced when determining the volume of the sample tube is avoided.

C. If the sampling system illustrated in fig. 2.3 is used a relative analysis technique becomes essential since the pressure in the sample loop depends both on the reaction vessel pressure and the time required to take a sample. An expression, equation 3.1, relating these three quantities was derived from Poiseuille's equation for the flow of a gas through a capillary (ref. 67), see Appendix I.

$$t = \frac{2.303\ V_1\ 8\ l\ \eta\ \log\left((P_2 + P_1) / (P_2 - P_1)\right)}{P_2\ r^4\ \pi} \qquad 3.1$$

Where V_1 is the volume in ml of the sampling system containing gas at pressure P_1 dyne cm.$^{-2}$ after taking a sample of viscosity η poise for time 6 seconds from the reaction vessel containing a reaction mixture at pressure P_2 dyne cm.$^{-2}$ through

a capillary length l cms., bore radius r cms.

For a typical reaction mixture pressure of 100 mm Hg estimates of the time taken, using equation 3.1, for the pressure in the sample loop to reach 50 mm. Hg and 90 mm. Hg were 18.5 and 49.5 secs. respectively.

Sampling times used in practice ranged from 5 to 50 seconds depending on the reaction mixture pressure and on the percent reaction. Hence samples had pressures differing widely from that of the reaction mixtures they were taken from. Inclusion of a manometer in the sampling system for pressure measurement would have increased the dead space by at least 300%. Furthermore since sample pressures were usually low a large inaccuracy in their determination would be introduced.

D. The sensitivity of the chromatograph, which was shared with other students, varied by ± 7% from day to day. However since changes in sensitivity occurred slowly they were negligible during the analysis of a single sample, data from numerous series of successive standardisations show ratios of peak areas remain constant to ± 1.4% during any one analysis. As an example the following table gives the area ratios for four standardisations using the same standard mixture together with the percentage divergences for each compound.

Table 3.1 Standardisation data for a 13% DNP/2% PEG 400/85% Phasep Pl. Column Packing using 0.5 ml of a standard mixture.

Compound	Area ratios relative to furan peak area.				Max % divergence
Furan	1.00	1.00	1.00	1.00	-
Sylvan	0.814	0.813	0.808	0.815	± 0.3%
Methylethyl ketone	0.943	0.945	0.942	0.946	± 0.2%
butan-2-ol	0.872	0.876	0.865	0.874	± 0.6%
penton-2-one	0.811	0.802	0.795	0.805	± 1.0%
penton-2-ol	0.718	0.707	0.705	0.715	± 0.9%

Hence while a method of analysis which determines absolute molar quantities would require a standardisation to be carried out at least once during the analysis of samples from a run, the method employed makes this unnecessary.

3.1.2. Relative molar quantities or molar ratios.

The area of a peak on a chromatogram is directly proportional to the number of moles of the substance producing the peak (ref. 72).

$$M_A \propto A_A \qquad 3.3$$

Where A_A is the area of a peak on a chromatogram produced by M_A moles of compound A. It follows from equation 3.3 that for compounds A and B,

$$\frac{M_A}{M_B} = C_B^A \frac{A_A}{A_B} \qquad 3.4$$

C_B^A is the proportionality constant and the ratio M_A / M_B is the relative molar quantity for compounds A and B. C_B^A will be referred to as the conversion factor for A to the base B.

To find C_B^A a standard mixture of known composition containing compounds A and B is analysed and C_B^A calculated using equation 3.5. Rearranging 3.4 :-

$$C_B^A = \frac{A_B}{A_A} \frac{M_A}{M_B} , \qquad 3.5$$

Where $\frac{M_A}{M_B}$ is the molar ratio of A and B in the mixture and A_A and A_B are the peak areas A and B produce.

For a given G L C column C_B^A values were found for all the products and reactants encountered where compound B was either furan or sylvan. Actual C_B^A values were computed from the averages of the area ratios from a series of standardisations on the same standard mixtures.

Once a G L C column has been standardised the results from the analysis of samples may be processed. The molar ratios themselves are of little use, however, they may be used to calculate the mole fraction of the detectable components in a reaction mixture, The mole fraction of the i^{th} component (M_j moles of component, present in the sample taken) of an n-component mixture is :-

$$M_i \Big/ \sum_{j=1}^{n} M_j \,, \qquad 3.6$$

but the same expression is obtained if the molar ratios discussed above are used in place of actual numbers of moles :-

$$(M_i \,/\, M_B) \Big/ \sum_{j=1}^{n} \frac{M_j}{M_B} = M_i \Big/ \sum_{j=1}^{n} M_j, \qquad 3.7$$

Hence combining equations 3.4 and 3.7, expressions for the mole fraction of the i^{th} component of an n-component mixture may be obtained in terms of peak areas :-

$$\frac{A_i}{A_B} C_B^i \Big/ \sum_{j=1}^{n} C_B^j \frac{A_j}{A_B} = M_i \Big/ \sum_{j=1}^{n} M_j \,, \qquad 3.8$$

or

$$A_i \; C_B^i \Big/ \sum_{j=1}^{n} C_B^j \, A_j = M_i \Big/ \sum_{j=1}^{n} M_j \qquad 3.9$$

Where the peak area produced by M_j moles of the j^{th} component is A_j. All areas are measured relative to the peak area A_B.

Although equation 3.9 is simpler than equation 3.8 the latter was generally used because calculation of the ratios A_j/A_B immediately shows up any gross errors in the estimation of peak areas, this is of greatest importance when peak areas are measured visually. Computer programs were written to

calculate mole fractions using equations 3.8 and 3.9, see Appendix 3.

3.1.3. Changing conversion factors based on one compound to those based on another.

A convenient property of the conversion factors C_A^B C_B^A is that it can be expressed in terms of the conversion factor C_D^A where D is a third compound. Namely for compounds A and D an expression similar to 3.5 is obtained :-

$$C_D^A = \frac{A_D \; M_A}{A_A \; M_D} \qquad 3.10$$

(A_D and M_D are the peak areas and the number of moles of compound D producing a peak respectively).

Dividing 3.5 by 3.9 gives :-

$$C_B^A \; / \; C_D^A = A_B \; M_D \; / \; A_D \; M_B \qquad 3.11$$

Comparing the R.H.S. of 3.11 with that of 3.10 clearly 3.11 may be rewritten as,

$$C_B^A \; / \; C_D^A = C_B^D \; , \qquad 3.12$$

or rearranging 3.12 ,

$$C_D^A = C_B^A \; / \; C_B^D \qquad 3.13$$

The main use of relationship 3.13 is when A has been standardised relative to compound B but not to compound D and the conversion factor C_D^A is required. This is particularly useful if it is inconvenient to carry out such a standardisation. (e.g. Methane, ethane, n-propane and n-butane were standardised directly relative to furan but relationship 3.13 was used to find their conversion factors relative to sylvan). Another minor advantage is that when two compounds are reacting simultaneously with a third compound it is useful to use a single set of conversion factors only. When furan and sylvan reacted competitively with hydrogen the results of the analyses of samples

were processed by a computer program (Appendix 3) which made use of relationship 3.13.

3.1.4. Calculation of the amount of furan and its products removed from the gas phase by adsorption without using pressure measurements.

The problem of how much of a reaction mixture is removed from the gas phase by adsorption on a catalyst is of importance since furan and hydrogen pressures are calculated from the results of analyses of samples, using the assumption that a negligible amount of adsorption occurs. Hence failure to detect adsorbed furan and/or adsorbed products could lead to distortion of the results from the treatment of the analysis data.

The simplest method of determining the extent of adsorption is to compare the observed pressure drop in the reaction vessel with pressure change predicted from the G L C analysis (see section 3.1.5.). However this method has the drawback that the accuracy of the pressure data leaves something to be desired since pressures were measured using a mercury manometer. The inaccuracies inherent in this method become particularly severe if numerous samples are taken because the sum of the pressure drops due to the taking of samples must be estimated, these pressure drops being small leads to high percentage errors. The following technique circumvents this problem by predicting directly from analysis data the molar fraction of adsorption of furan and its products to the initial amount of furan injected into the reaction vessel. No pressure data is required.

The method employed requires that the reaction mixture contains a compound which does not react and which is detectable using an FID detector on the chromatograph, n-hexane was used in runs C10A1 and C8H1.

From equation 3.4 :-

$$\frac{M_X(1)}{M_F(1)} = \frac{A_X(1)}{A_F(1)} \; C_F^X \qquad 3.14$$

Where $A_X(1)$ is the peak area produced by $M_X(1)$ moles of the inert constituent X and $A_F(1)$ is the peak area produced by $M_F(1)$ moles of furan, both in sample (1).

A similar relationship holds for any other sample, sample (2) :-

$$\frac{M_X(2)}{M_F(2)} = \frac{A_X(2)}{A_F(2)} \; C_F^X \qquad 3.15$$

Dividing 3.14 by 3.15 gives :-

$$\frac{M_F(2)}{M_F(1)} = \frac{A_X(1) \; A_F(2)}{A_F(1) \; A_X(2)} \; , \qquad 3.16$$

providing the amount of X in the gas phase remains constant.

Let $\sigma(1)$ and $\sigma(2)$ be the mole fraction of furan only of furan and detectable furan products for sample (1) and (2) respectively (i.e. hydrogen, water and the added inert compound are not involved in the expression for the mole fraction, σ, of furan in a sample). Then provided that the C_4 chain remains intact during the reaction :-

$$\sigma(1) = M_F(1) \; / \; M_F^O \qquad 3.17$$

Where M_F^O is the number of moles of furan present at the start of the reaction. For the reactions examined using this technique, the percent reaction which resulted in rupture of the C_4 chain was less than 3%. (Appendix 2 deals with a more general treatment allowing for breakage of the carbon chain).

For sample (2) the equation corresponding to 3.17 is :-

$$\frac{M_F(2)}{M_F^O} = \sigma(2) \qquad 3.18$$

Dividing 3.18 by 3.17 yields

$$\frac{\sigma(2)}{\sigma(1)} = \frac{M_F(2)}{M_F(1)} \quad , \qquad 3.19$$

and substituting areas for molar quantities using equation 3.16 in 3.19:-

$$\frac{\sigma(2)}{\sigma(1)} = \frac{A_X(1)A_F(2)}{A_F(1)A_X(2)} \qquad 3.20$$

Hence $\sigma(2)$ may be expressed in terms of observed areas only, i.e., substituting for $\sigma(1)$ in 3.20 by 3.9 and rearranging :-

$$\sigma(2) = \frac{A_X(1).\ A_F(2)}{\left(\sum_{j=1}^{n} C_f^j A_j(1) - A_X(1)\right) A_X(2)} \qquad 3.21$$

The above technique is of most use if a sample of the reaction mixture is analysed prior to its injection into the reaction vessel, namely, a sample is taken from the mixing vessel (see fig. 2.1.) In this way the amount of reactant initially adsorbed may be estimated. Furthermore $\sigma(1)$ in this case is unity, hence equation 3.20 reduces to :-

$$\sigma(2) = \frac{A_F(2).\ A_X(1)}{A_F(1).\ A_X(2)} \qquad 3.22$$

If M (2) (ads.) moles of furan and its products were adsorbed equation 3.19 would only apply to gaseous furan. Rewriting 3.19 for convenience,

$$\sigma(2) = M_F(2)(g) \ / \ M_F(1)(g) \qquad 3.23$$

($\sigma(1)$ as above is unity). But the mole fraction of gaseous furan, $\sigma^1(2)$ found by applying equation 3.8 to the results from analysis of sample (2) can also be expressed as :-

$$\sigma^{1}(2) = \frac{M_F(2)(g)}{M_F(1)(g) - M(2)(ads.)} \quad . \qquad 3.24$$

Eliminating $M_F(2)(g)$ from 3.23 and 3.24 gives

$$\sigma^{1}(2) = \frac{\sigma(2)\, M_F(1)(g)}{(\sigma(2)\, M_F(1)(g) - M(2)(ads.)} \quad . \qquad 3.25$$

Solving 3.25 for $\frac{M(2)(ads.)}{M_F(1)(g)}$. (the ratio of the adsorbed species to the initial amount of furan gives

$$\frac{M(2)(ads.)}{M_F(1)(g)} = \frac{\sigma^{1}(2) - \sigma(2)}{\sigma^{1}(2)} \quad . \qquad 3.26$$

Where $\sigma^{1}(2)$ and $\sigma(2)$ are found using equations 3.8 and 3.22 respectively. ($M_F(1)(g) = M_F(1)$ by definition).

The following table shows the results from analysis of samples from run C10A1 (X is hexane, weight of 5% Pt/pumice catalyst is 0.382 g, reaction temperature is 65°C) processed using equation 3.26 to yield fractions of adsorbed species. ($\sigma(1) = 1.00$).

TABLE 3.2 Fractions of furan adsorbed for run C10A1

Sample	$\sigma(2)$	$\sigma^{1}(2)$	Fraction of adsorbed species	Reaction time (mins.)
2C10A1	0.882	0.916	0.037 ± 0.04	16.5
3C10A1	0.818	0.865	0.047 ± 0.04	40.0
5C10A1	0.667	0.715	0.067 ± 0.05	1027.

Table 3.2 shows that little adsorption of furan and its products occurs for the Pt/pumice catalyst, appearing to increase slowly with time. It is worth pointing out that if an inert compound is included in the reaction mixture, as above, then an accurate method of following the reaction kinetics

is possible by application of equation 3.22. This method not only has the advantages associated with a relative method of analysis discussed in section 3.1.1. but also requires no standardisations to be carried out.

3.1.5. Calculation of reaction vessel pressure drops from analysis data and the initial pressures of the reactants.

Knowing the % composition of a reaction mixture (from pressure measurements during its preparation) the initial reactant pressures can readily be calculated knowing the initial total pressure in the reaction vessel.

Let the hydrogenation of a reactant k proceed by n pathways such that one molecule of R reacting by one pathway forms a single molecule of a detectable product i. Results from analyses show this to hold to all intents and purposes for the reactions examined over Pt supported catalysts.

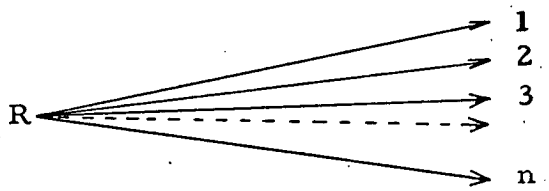

Let the fraction of R reacting to form the product i be G_i and the pressure drop associated with one mm. Hg partial pressure of R reacting to form product i only be Z_i mm. Hg. Then the total pressure drop (L) in the reaction vessel due to the reaction of one mm. Hg partial pressure of R is

$$L = \sum_{i=1}^{n} G_i \; Z_i \text{ mm. Hg} \qquad 3.27$$

but G_i may be expressed in terms of areas.

$$G_i = A_i C_i \Big/ \sum_{i=1}^{n} A_i C_i \; . \qquad 3.28$$

Then substituting 3.28 into 3.27 :-

$$L = \frac{1}{\sum_{i=1}^{n} A_i C_i} \sum_{i=1}^{n} A_i C_i Z_i \text{ mm. Hg.} \qquad 3.29$$

Hence the pressure drop ΔP_C at any % increase is

ΔP_C = L X (number of mm. Hg partial pressure of R reacted). 3.30

But the number of mm. Hg partial pressure of R reacted is the product of the initial pressure of R, P_R^O, and the fraction of R reacted. Hence using equation 3.30 becomes

$$\Delta P_C = L P_R^O \sum_{i=1}^{n} (A_i C_i / A_R C_R + \sum_{i=1}^{n} A_i C_i) \qquad 3.31$$

Substituting for L, using 3.29 into 3.31 and cancelling :-

$$\Delta P_C = P_R^O \sum_{i=1}^{n} A_i C_i Z_i / (A_R C_R + \sum_{i=1}^{n} A_i C_i) \qquad 3.32$$

Where no adsorption of reactants or products to occur

$$\Delta P_C = \Delta P_{OBS} \qquad 3.33$$

Where P_{OBS} is the pressure change in the reaction vessel observed using a mercury manometer. However for furan reacting over Pt/SiO_2 catalysts 3.33 was not found to hold (see table 4.2) hence adsorption is occuring.

Clearly there are three possible types of adsorption. Adsorption of the reactant, adsorption of products and adsorption of reactant and products.

If the reactant alone is adsorbed and if the number of mm. Hg. partial pressure of R removed from the gas phase is X then from 3.32 the pressure drop due to the reaction of the reactant is $(P_R^O - X)\frac{\Delta P_C}{P_R^O}$, i.e., if the reactant is removed from the gas phase it is the same as saying the initial reactant pressure is reduced. Inclusion of the pressure drop due to the adsorption of reactant itself gives

$$\Delta P_{OBS} = (P_R^O - X)\frac{\Delta P_C}{P_R^O} + X \qquad 3.34$$

Then from 3.34 the observed pressure drop is greater than ΔP_C for $\frac{\Delta P_C}{P_R^O}$ smaller than unity, for values of this ratio greater than unity the reverse is true. (At $\frac{\Delta P_C}{P_R^O} = 1$, 3.34 reduces to $\Delta P_{OBS} = \Delta P_C$).

This behaviour was never observed, see table 4.2.

For adsorption of the products a complex relationship between ΔP_{OBS} and ΔP_C is found to hold, see Appendix 4, but it can be shown that ΔP_C is always smaller than ΔP_{OBS}. Furthermore as the reaction proceeds to high percent reaction the difference between the two pressure drops will become smaller, tending in the limit (at 100% reaction), to the partial pressures of the adsorbed products. This behaviour was observed in practice, see table 4.2 for furan hydrogenations over Pt/SiO_2.

For adsorption of both reactant and products the relationship between $\Delta P_C - \Delta P_{OBS}$ and percent reaction will lie between the two types of adsorption already considered. It is doubtful if the adsorption of both reactants and products can be differentiated from the adsorption of products alone. However, for furan hydrogenations over Pt/SiO_2 and Pt/Al_2O_3 it is possible to show conclusively by the above techniques that adsorption of one or more of the products is occurring. (see Section 4.3.2.)

3.2 Columns used for gas liquid chromatographical analysis.

3.2.1 Column packings.

All chromatographical columns used were packed $^1/_4$" I.D., 9' long glass tubes. The column packings used consisted of a liquid stationary phase supported on Phasep Pl (60-85 mesh brick dust with an antitailing additive, supplied by Phase Separations Ltd.). The majority of runs were analysed using one of the three column packings below.

Packing A: 15% polyethylene glycol 400/ Phasep Pl.

Packing B: 4.75% β,β'-oxydipropionitrile, 6.2% dinonyl phthalate/Phasep Pl.

Packing C: 2% polyethylene glycol, 13% dinonyl phthalate/Phasep Pl.

All the percentages quoted above are on a w/w basis.

Packing A was used for the analysis of the early runs carried out over the Ni/silica catalysts. However separation of the alkane peaks and tetrahydrofuran from tetrahydrosylvan was not possible. Both problems were overcome using packing B at the cost of poor separation of n-butanol and pentan-2-ol peaks but since the next series of runs, over 5% Pt/SiO_2 catalysts, did not require these peaks to be separated (hydrogenation of sylvan produced little pentan-2-ol, $< 10\%$ of all the products).

However n-butanol and pentan-2-ol were the major products of the hydrogenations of furan and sylvan respectively over the last type of catalyst tried, Pt/Pumice, hence it was necessary to use column packing C for the analyses from simultaneous hydrogenations of furan and sylvan. This packing separated the above two alcohols at the cost of poor separation of butan-2-one from tetrahydrofuran, fortunately this was of no importance since no butan-2-one was formed over this catalyst in the range of temperatures investigated ($22^{\circ}C$ to $100^{\circ}C$).

Table 3.3 lists the retention times relative to furan of various compounds for the three column packings.

Table 3.3 Relative retention times for the three main column packings.

Compound	Relative Retention Times for Packing		
	A	B	C
Methane & ethane	0.456-0.474	0.251-0.258	0.20
n-propane		0.380	0.23
n-butane		0.342	0.272
n-pentane	-	0.505	0.408
furan	1.00	1.00	1.00
sylvan	1.30	1.86	1.71
tetrahydrofuran	1.57	2.48	2.07
tetrahydrosylvan	1.58	2.64	2.51
butan-2-one	1.77	3.37	2.09
pentan-2-one	2.46	6.2	3.69
n-hexane	-	0.864	-
n-hexene	-	0.921	-
cyclohexane	-	-	1.75
benzene	-	-	2.69
n-propanol	3.87	4.01	3.47
pentan-2-ol	5.25	9.0	5.73
n-butanol	6.67	8.78	5.16
n-pentanol	9.1	12	6.23
butan-2-ol	3.35	4.21	2.78

Table 3.4 gives a brief summary of some of the other column packings investigated and the reason they were not used.

Table 3.4 Stationary phases, supported on Phasep Pl, and the reasons why they were not used.

	Stationary Phase	Disadvantages
I	Porapak Q (unsupported)	To achieve a good separation a column temperature of 150°C (or less) is required. At these temperatures the peaks were not symmetrical and the retention time of the alcohols was too high (over an hour for n-butanol).
II	10% tetraethylene glycol diethyl ether	Sylvan and tetrahydrofuran are not separated satisfactorily (unless a temperature of 50°C or less is used when the retention times are very large).
III	3% tetraethylene glycol diethyl ether	The separation is poorer than for the 10% column, furthermore sylvan overlaps with the tetrahydrosylvan peak.
IV	20% β,β'-ODPN	Pentan-2-ol and pentan-2-one are not seperable, furthermore butan-2-ol and butan-2-one separation is poor.
V	1.5% PEG 400, 18% β,β'-ODPN	At 92°C butan-2-one and butan-2-ol come off together and tetrahydrofuran and tetrahydrosylvan separation is poor, the latter separation is worsened by reducing the temperature.

VI	3% PEG 400, 17% ODPN	Tetrahydro derivatives of the two furans are not separated satisfactorily.
VII	12% DNP, 2% PEG400, 2% ODPN	Butan-2-one and tetrahydrosylvan separation is poor.
VIII	12% DNP, 2% PEG400, 5% ODPN	Neither the separation of butan-2-one from tetrahydrosylvan nor the separation of n-butanol from pentan-2-ol is satisfactory.
IX	12% DNP, 8% ODPN, 2% PEG400	Separation of pentan-2-ol from butan-2-ol is not satisfactory.
X	11% DNP, 6.5% ODPN, 2% PEG400	As for IX.

The abbreviations used were -

PEG400 - Polyethylene glycol, average molecular weight of 400.

DNP - Dinonyl phthalate

ODPN - β,β'-Oxydipropionitrile.

3.2.2 Standardisation of the column packings.

All standardisations found conversion factors with furan as the base using equation 3.5. Mixtures of known composition were either injected into the chromatograph in the gas or liquid phase and the resultant peak areas produced on the chromatogram were either measured using an electronic integrator or visually using relationship 2.2.

To produce a gas sample approximately 0.5 microlitres of a standard mixture are injected, using a one microlitre syringe, into a small sample tube with a ground glass joint at one end. This is immediately attached to the gas sample valve at C, see figures 2.8 and 2.9, and expanded into the evacuated gas sampling valve's loop which is immersed in a liquid air bath (a rotary piston pump

connected to D, see figures 2.8 and 2.9, is used for the evacuation). After approximately ten minutes the loop is isolated and warmed to room temperature when the gas sample is injected into the chromatograph.

As can be seen from table 3.5, which compares area ratios found using gas and liquid samples of the same standard mixture, there is no significant advantage in injecting gaseous samples. Hence all later standardisations were carried out by injection of liquid samples since this technique was faster and more reliable.

Table 3.5 Average area ratios, for a standard mixture, from six gas and eight liquid samples respectively for packing A (areas measured visually).

Compound	Average area ratios using gaseous samples	Average area ratios using liquid samples
Furan	1.00	1.00
Sylvan	0.97 ± 0.04	0.97 ± 0.04
Butan-2-one	1.22 ± 0.02	1.22 ± 0.03
Pentan-2-one	1.19 ± 0.04	1.16 ± 0.02
Butan-2-ol	1.26 ± 0.09	1.24 ± 0.04
Pentan-2-ol	1.10 ± 0.06	1.13 ± 0.04

Comparison of peak area ratios where the same peak areas were measured visually and by an electronic integrator respectively show a divergence of less than 2%, see table 3.6, hence the same conversion factors were used for analysis by either techniques.

Table 3.6 Average of three peak area ratios measured visually and by an integrator respectively for packing B (liquid samples used).

Compound	Area ratios, areas measured visually	Area ratios, areas measured by an Integrator
furan	1.00	1.00
sylvan	0.90 ± 0.01	0.89 ± 0.005
tetrahydrofuran	1.06 ± 0.03	1.04 ± 0.01
tetrahydrosylvan	0.99 ± 0.01	0.98 ± 0.01
butan-2-ol	1.10 ± 0.03	1.10 ± 0.005
butan-2-one	1.08 ± 0.02	1.09 ± 0.005
pentan-2-one	1.01 ± 0.02	1.03 ± 0.02
n-butanol	0.96 ± 0.03	0.96 ± 0.01

CHAPTER 4.

HYDROGENATION OF FURAN AND SYLVAN OVER SUPPORTED METAL CATALYSTS.

4.1 Poisoning effects

Poisoning occurred over all the catalysts tried at all the reaction temperatures used (22°C to 240°C) for both furan and sylvan hydrogenations. As an illustration, Graph 4.1 shows a typical furan hydrogenation (C8A1, carried out at 46.5°C over a 5% Pt/pumice catalyst). Furthermore as the reaction temperature is increased the poisoning becomes increasingly severe, particularly for Pt/pumice catalysts, as is shown by Graph 4.2 of three furan hydrogenations carried out at three different temperatures over 5% Pt/pumice catalysts.

Attempts to regenerate catalysts, either by heating them in hydrogen or in air at 400°C followed by hydrogen at the same temperature, met with partial success at best; the latter technique restored one catalyst, C8D, once to 70% of its initial activity however failed to regenerate the same catalyst for a second time, it was also unsuccessful with other catalysts (C8E, C10A and C10B).

Poisoning will be dealt with in greater detail in section 4.5.4 and in the following chapter.

4.2 Hydrogenations over Ni/SiO_2 catalysts (C4 series).

Hydrogenations of furan over Ni/SiO_2 give product distributions dependent on the time that the catalysts have been exposed to the reaction mixture as is shown by Graph 4.3 of the product distribution against the fraction of furan reacted for run C4H1 carried out at 180°C. This graph also shows that at this temperature the major products of a furan-hydrogen reaction are tetrahydrofuran and hydrocarbons while the product

GRAPH 4.1

Furan hydrogenation C8A1 over 5% Pt/pumice at 46.4°C.

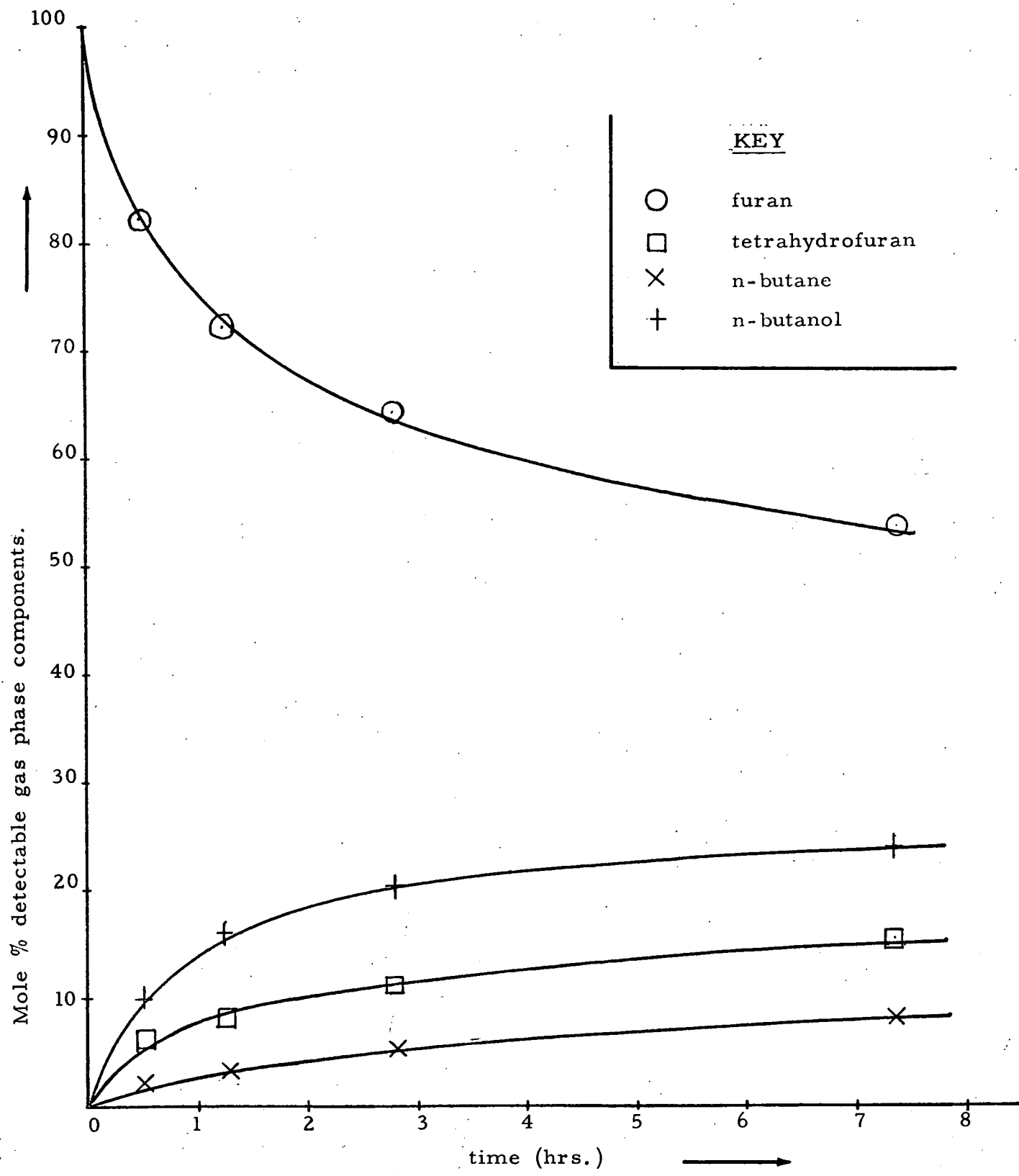

GRAPH 4.2

To show the increasingly severe poisoning with increasing reaction temperature for three furan hydrogenations over Pt/pumice.

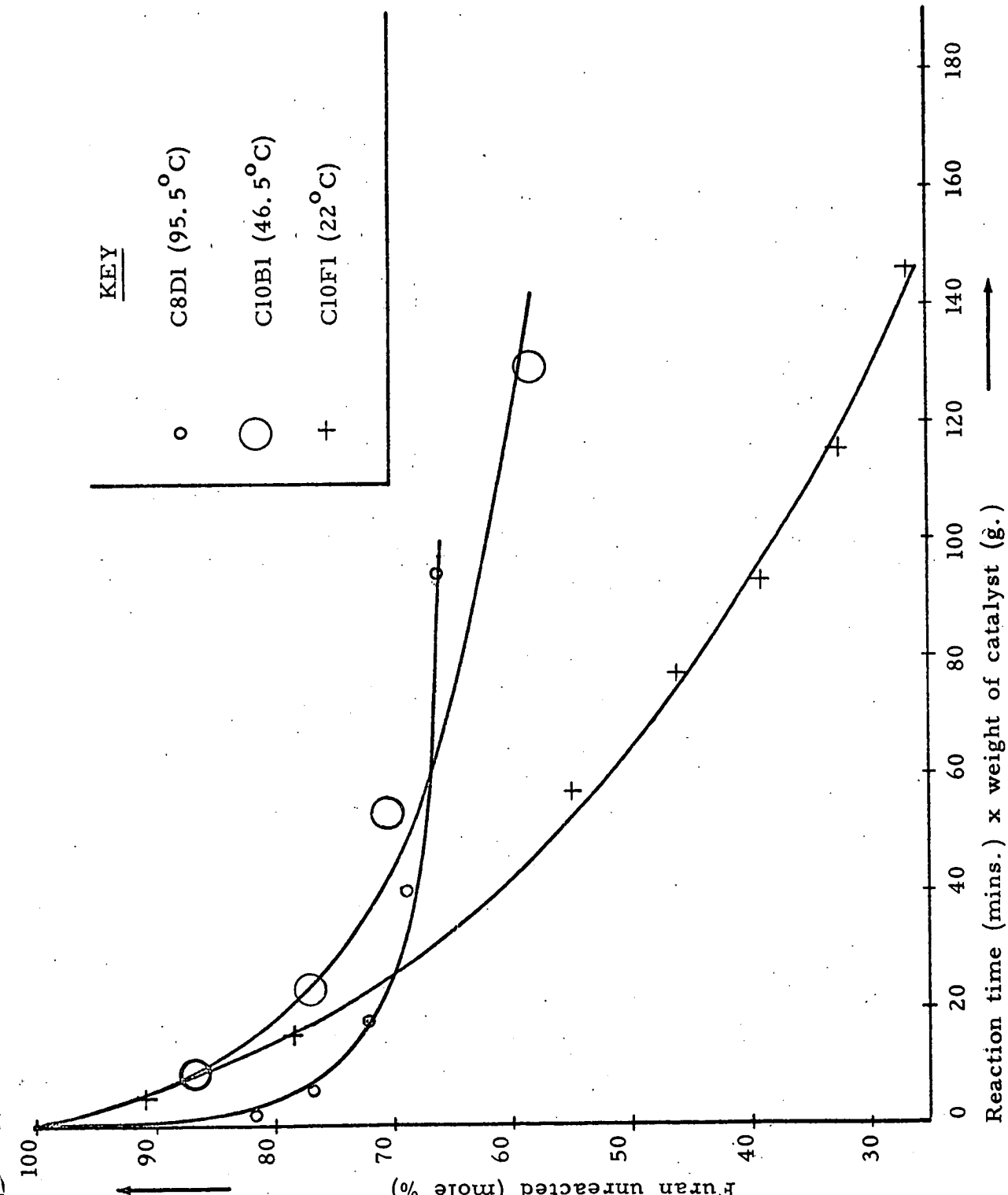

GRAPH 4.3

Product distribution for the furan hydrogenation C4H1 (over 5% Ni/SiO_2 at 180°C, initial furan and hydrogen pressures = 14.1 and 67.9 mm. Hg respectively).

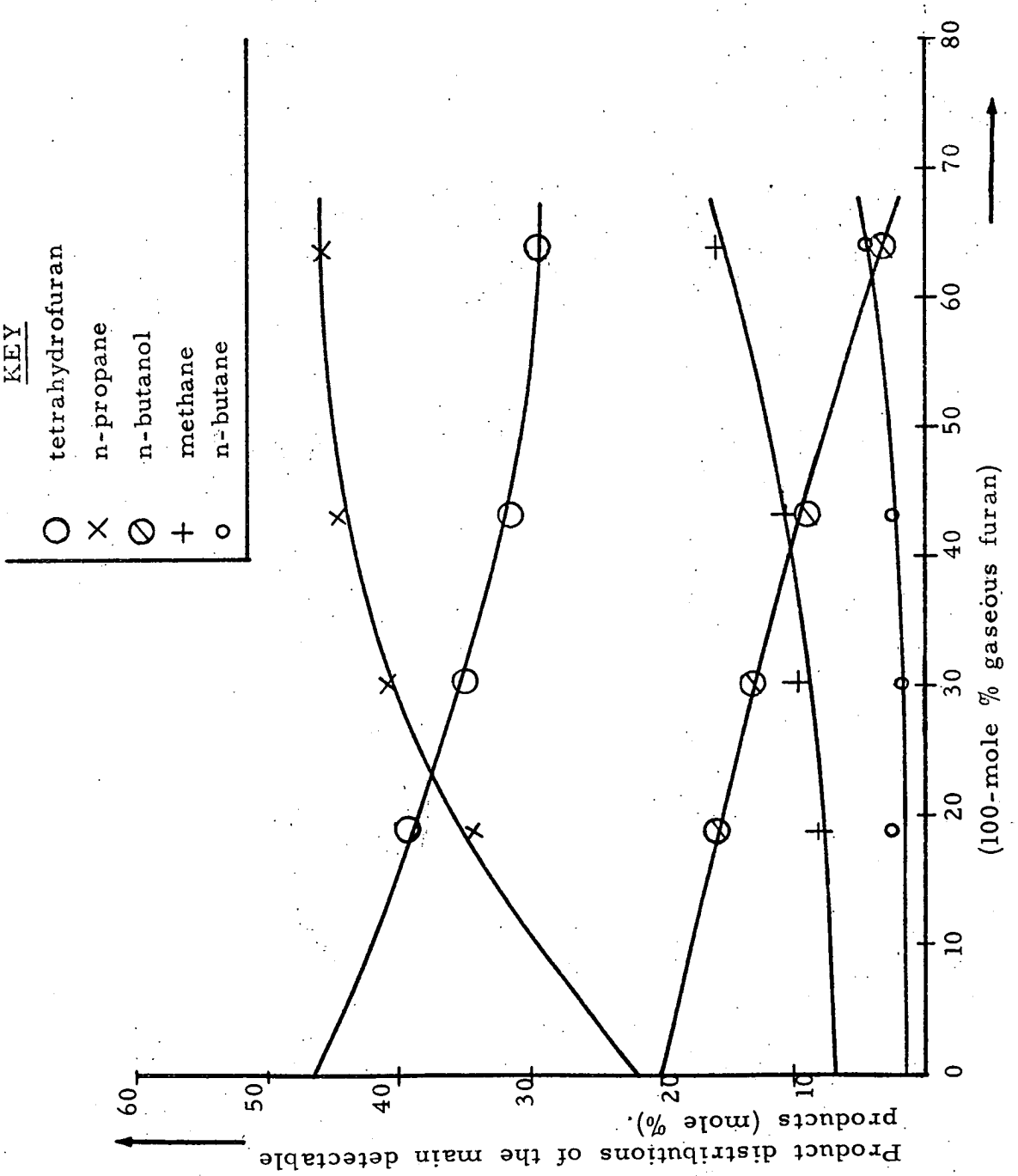

GRAPH 4.4

Product distributions for the sylvan hydrogenation C4G1 (over 5% Ni/SiO_2 at 180°C, initial sylvan and hydrogen pressures = 15.0 and 75.0 mm. Hg respectively).

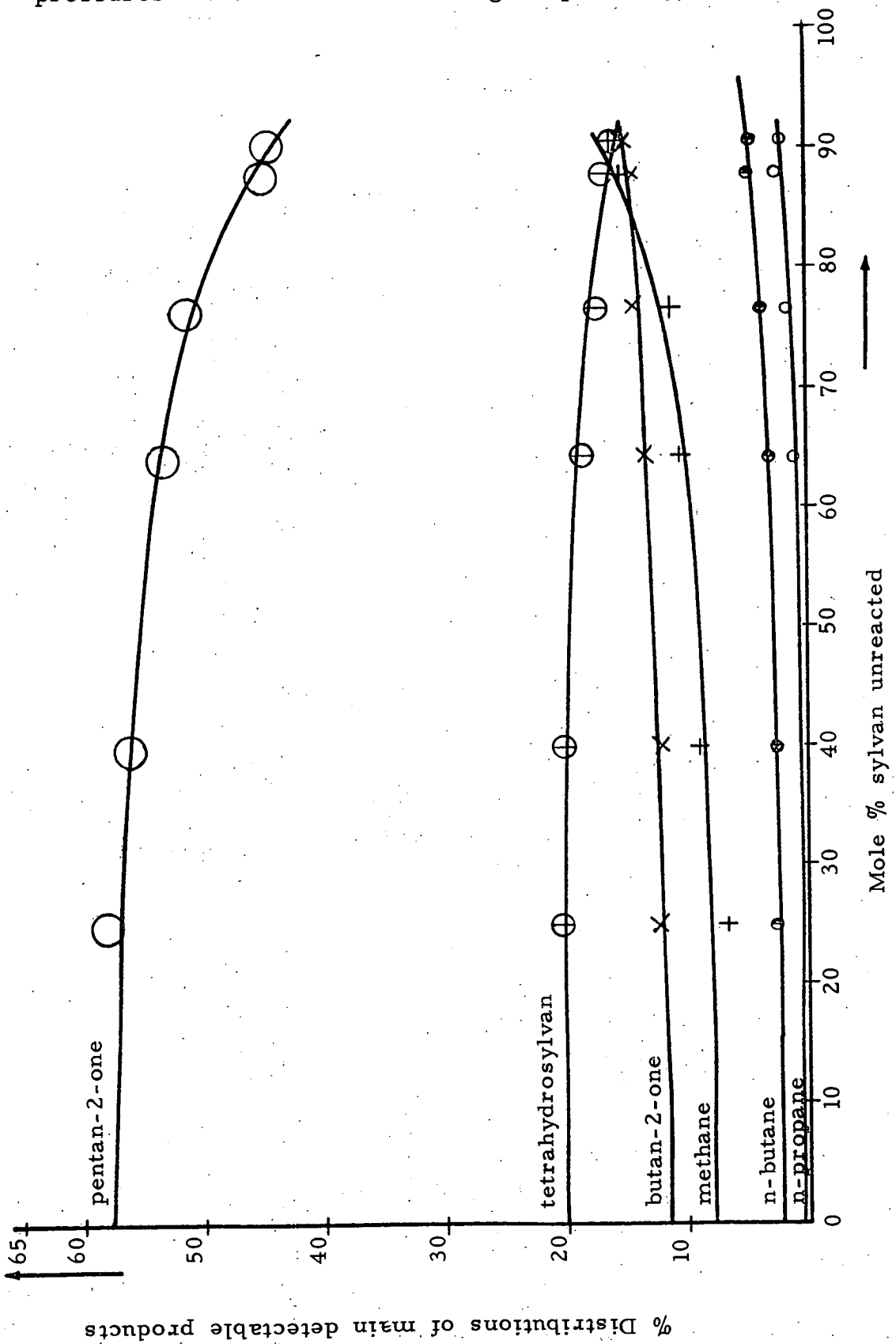

produced by hydrogenolysis of a C - O bond without rupture of the carbon chain (n-butanol) accounts for less than 20% of the products. Lowering the reaction temperature decreases the amount of n-propane and methane produced, tetrahydrofuran being the only major product.

Unlike furan, sylvan's product distributions on hydrogenation show a far smaller time dependence, see graph 4.4 for run C4G1, 180°C. Further, the product distributions show an interesting dependence on the reaction temperature, see graph 4.5 compiled from the initial product distributions for a series of sylvan reactions carried out at temperatures between 150°C and 245°C. A similar effect was observed by Wilson (ref. 18) for sylvan hydrogenations over unsupported nickel catalysts. At reaction temperatures below 160°C hydrogenation without cleavage of the ring occurs almost exclusively (85% tetrahydrosylvan is produced at 160°C, while at 190°C the main product is pentan-2-one, 65%, produced by hydrogenolysis of the 1,5 C - O bond. At temperatures exceeding 230°C the major products are n-propane and methane indicating rupture of the carbon chain.

A more detailed list of products than is given in Graphs 4.3 and 4.4 is given in table 4.1 :-

Table 4.1 Initial product distributions for furan and sylvan hydrogenations over 5% Ni/SiO_2 at 180°C.

for runs C4H1 (initial furan and hydrogen pressures = 15.0 and 75.0 mm.Hg.) and C4G1 (initial sylvan and hydrogen pressures = 14.1 and 67.9 mm. Hg.) respectively.

Product	Furan Hydrogenation	Sylvan Hydrogenation
Methane *) Ethane *)	7%	8.4%
n-propane	22%	2.6%
n-butane	1.5%	2.6%
n-pentane	< 0.4%	0.6%
tetrahydrofuran	49%	-
tetrahydrosylvan	-	19%
butan-2-one	-	12%
butan-2-ol	-	0.9%
pentan-2-one	-	52%
pentan-2-ol	-	4.5%
n-butanol	21%	-
n-propanol	-	0.3%
n-pentanol	-	0.8%

* It was not possible to separate Methane and Ethane.

Table 4.1 indicates how the 1, 5 C - O bond in sylvan is much more prone to hydrogenolysis than the 1, 2 C - O bond. This is not thought to be caused by any shielding effect the methyl group may be exerting, rather that the 1, 5 C - O bond is more liable to attack because of the presence of the methyl

GRAPH 4.5

Dependence of Sylvan's initial product distribution on hydrogenation over 5% Ni/SiO_2.

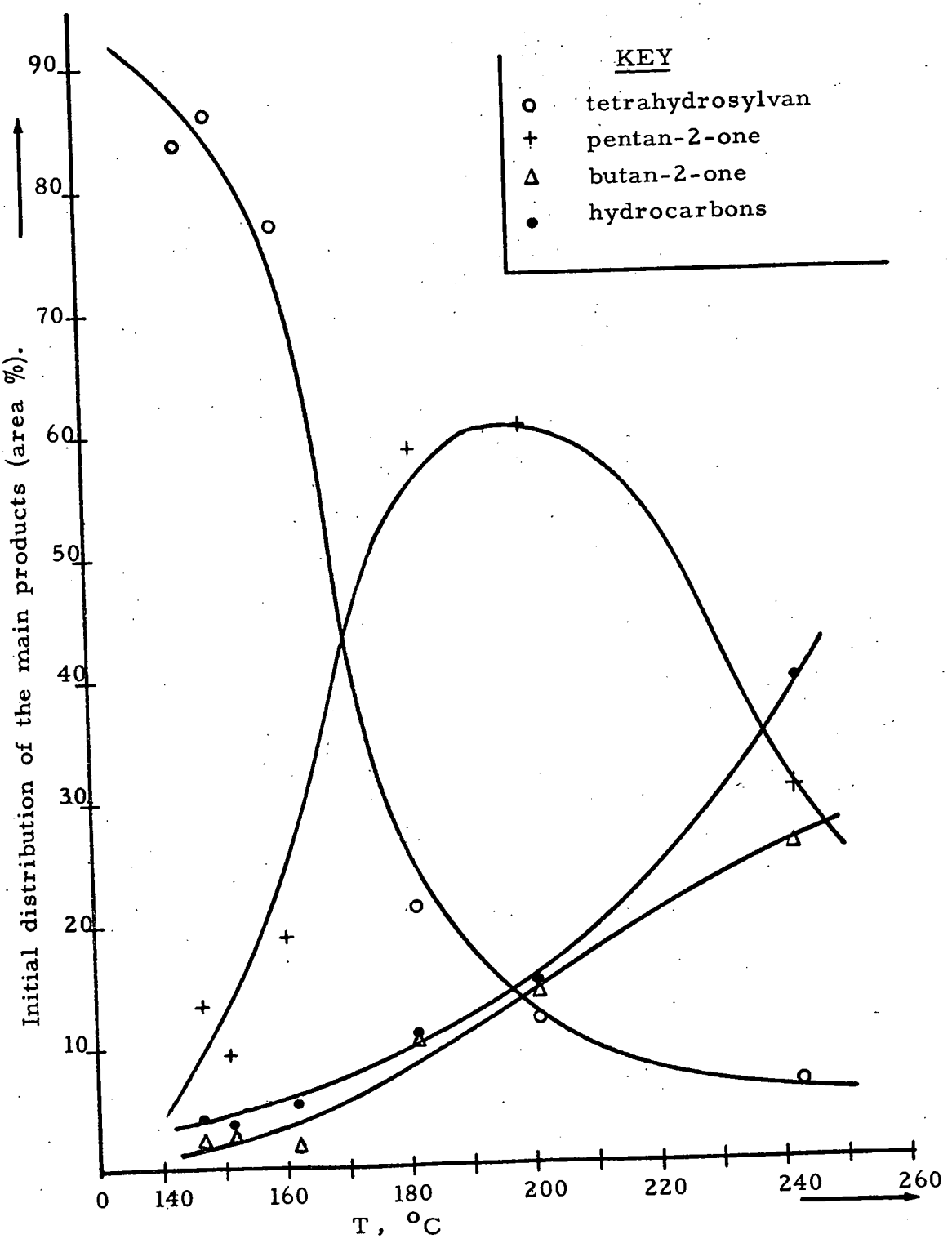

GRAPH 4.6

Comparison of the rates of reaction for furan (run C4H1) and sylvan (run C4G1) with hydrogen over Ni/SiO_2 at 180°C.

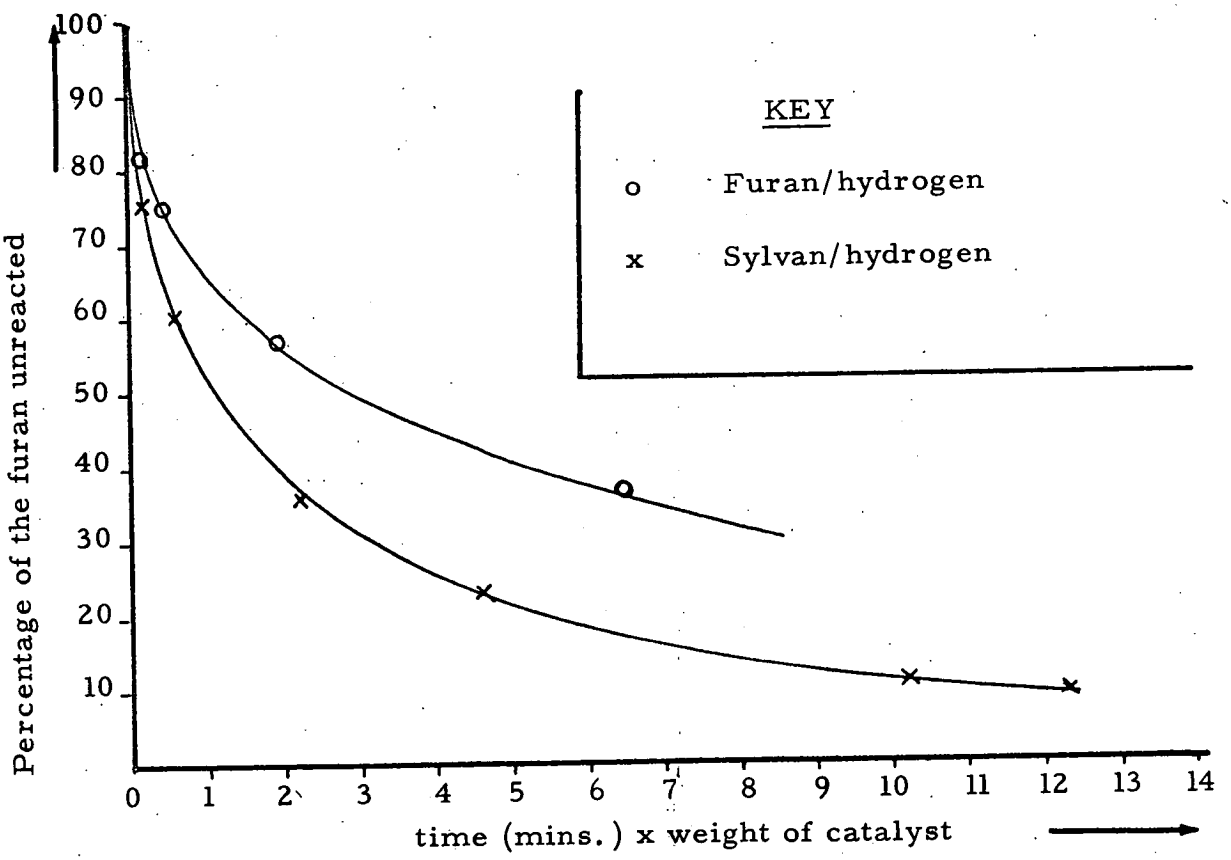

group at the 2 position for two reasons:

First, more hydrogenolysis of the furan nucleus occurs on hydrogenating sylvan than furan (72% as opposed to 51%) while a shielding effect would require the reverse to hold, unless it were accompanied by a stronger inhibition of the hydrogenation without hydrogenolysis reaction. This is ruled out by the following piece of evidence:

Second, sylvan is hydrogenated more quickly than furan at 180°C, see graph 4.6 which compares the rate of reaction for the two compounds (data from runs C4H1 and C4G1). From initial rate data for these two runs, sylvan reacts approximately 25% faster than furan. More reliable proof for the faster rate of reaction of sylvan is obtained from data at 50% reaction of furan for reaction C4F1 at 183°C where furan and sylvan were hydrogenated simultaneously, sylvan was found to react approximately 32% faster than furan. (Initial furan, sylvan and hydrogen pressures for run C4F1 were 19.9 , 20.3 and 162.4 mm. Hg respectively).

It could be argued that sylvan only appears to react more quickly than furan since it might poison the catalyst more slowly. However, poisoning should not affect the initial rates of reaction and furthermore it is reasonable to assume that the hydrogenation of the two compounds will occur at similar sites on the catalyst's surface, hence hydrogenation of a mixture of furan and sylvan would poison both reactions to about the same degree.

The catalyst was not investigated further for two reasons. First, since the product distribution obtained from hydrogenating furan was strongly time dependent, rate data analysis would be complex because a skewed time/product distribution graph suggests that two or more processes are occurring at once.

Second, it was intended to pay particular attention to the hydrogenolysis of the furan ring's C - O bonds. While this could be studied satisfactorily for sylvan between 170°C to 190°C, at similar temperatures a large amount of cleavage of the carbon chain and hydrogenation without hydrogenolysis occurred for furan. At 180°C less than 24% of the products from the hydrogenation of furan are due to rupture of C - O bonds only (resulting in n-butanol and n-butane).

4.3 Hydrogenations over 5% Pt/SiO_2 catalysts (C6 series)

Preliminary hydrogenation reactions of furan over Pt/SiO_2 catalysts showed that while the catalyst is highly active at as low a temperature as 40°C (which is advantageous since the temperature gradient along the reaction vessel becomes negligible at temperatures below 100°C see graph 2.3) the product distribution changes sharply with the reaction time, section 4.3.2. Furthermore the reaction vessel pressure drop predicted from the % reaction and the product distribution did not compare favourably with observed pressure drops, as is shown in the following section.

4.3.1. Mismatch of observed and calculated reaction vessel pressures.

Theoretical pressure drops in the reaction vessel were calculated using the method outlined in section 3.1.5. For all the reactions analysed using equation 3.32 (e.g. C6L1, C6E3, C6H1, C6D1) the calculated pressure drops were smaller than those observed as is illustrated by table 4.2 for runs C6E3 and C6H1, using 0.081g and 0.0182g Pt/SiO_2 catalyst respectively. For these furan hydrogenations the following reaction pathways (see section 3.1.5) were used:

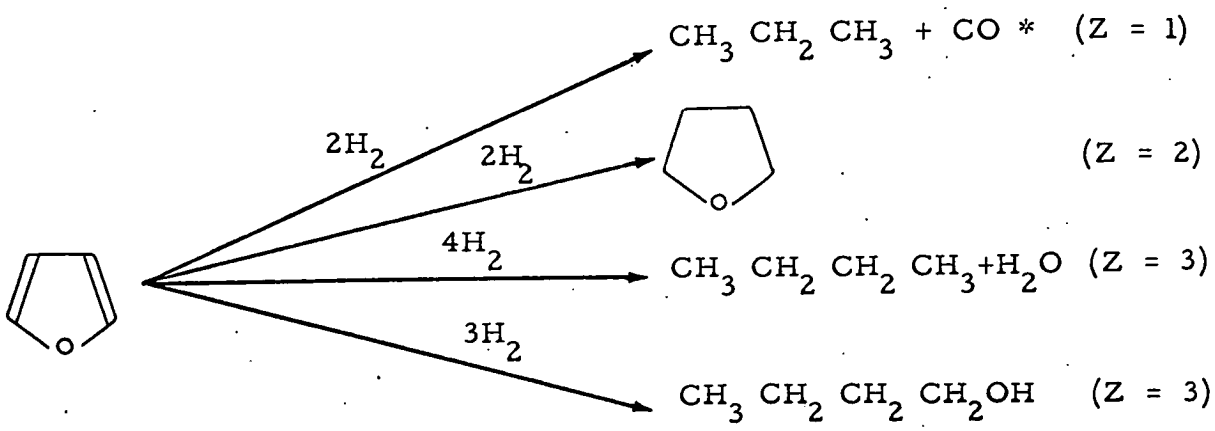

(Z is defined in section 3.1.5.)

* Since very little n-propane was formed the mechanism used is of little importance.

Table 4.2 Calculated and observed reaction vessel pressure changes for runs C6E3 and C6H1, (initial furan pressures are 23.6 mm. and 16.3 mm.)

Sample	Observed pressure drop, ΔP_{OBS}, mm. Hg.		Calculated pressure drop, ΔP_C, mm. Hg.		$\Delta P_{OBS} - \Delta P_C$, mm. Hg.	
	C6E3	C6H1	C6E3	C6H1	C6E3	C6H1
1	26	9.7	6.1	4.0	20	5.7
2	33.5	22.4	12	17.5	21.5	4.9
3	45	27.1	27	23	18	4
4	52	35.3	35	32.5	17	2.8
5	59	-	46	-	13	-

The errors in $\Delta P_{OBS} - \Delta P_C$ in table 4.2 are particularly severe for runs such as C6H1 where less than 0.03g of catalyst were used. For example the error in $\Delta P_{OBS} - \Delta P_C$ for C6H1 due only to a 5% error in the value of the initial furan pressure is 3% and 60% for the first and last samples respectively, while the errors possible in $\Delta P_{OBS} - \Delta P_C$ due to errors in the measurement of peak areas are 20% and 50% respectively. When $\Delta P_{OBS} - \Delta P_C$ is large, as for C6E3, the maximum combined error is 30% (for the last sample).

GRAPH 4.7

PRODUCT DISTRIBUTIONS FOR A FURAN HYDROGENATION OVER A 5% Pt/SiO_2 CATALYST [0.018g.]

RUN C6H1

Reaction temperature = 50.1°C
Initial furan and hydrogen pressures = 16.3 and 74.3 mm. Hg

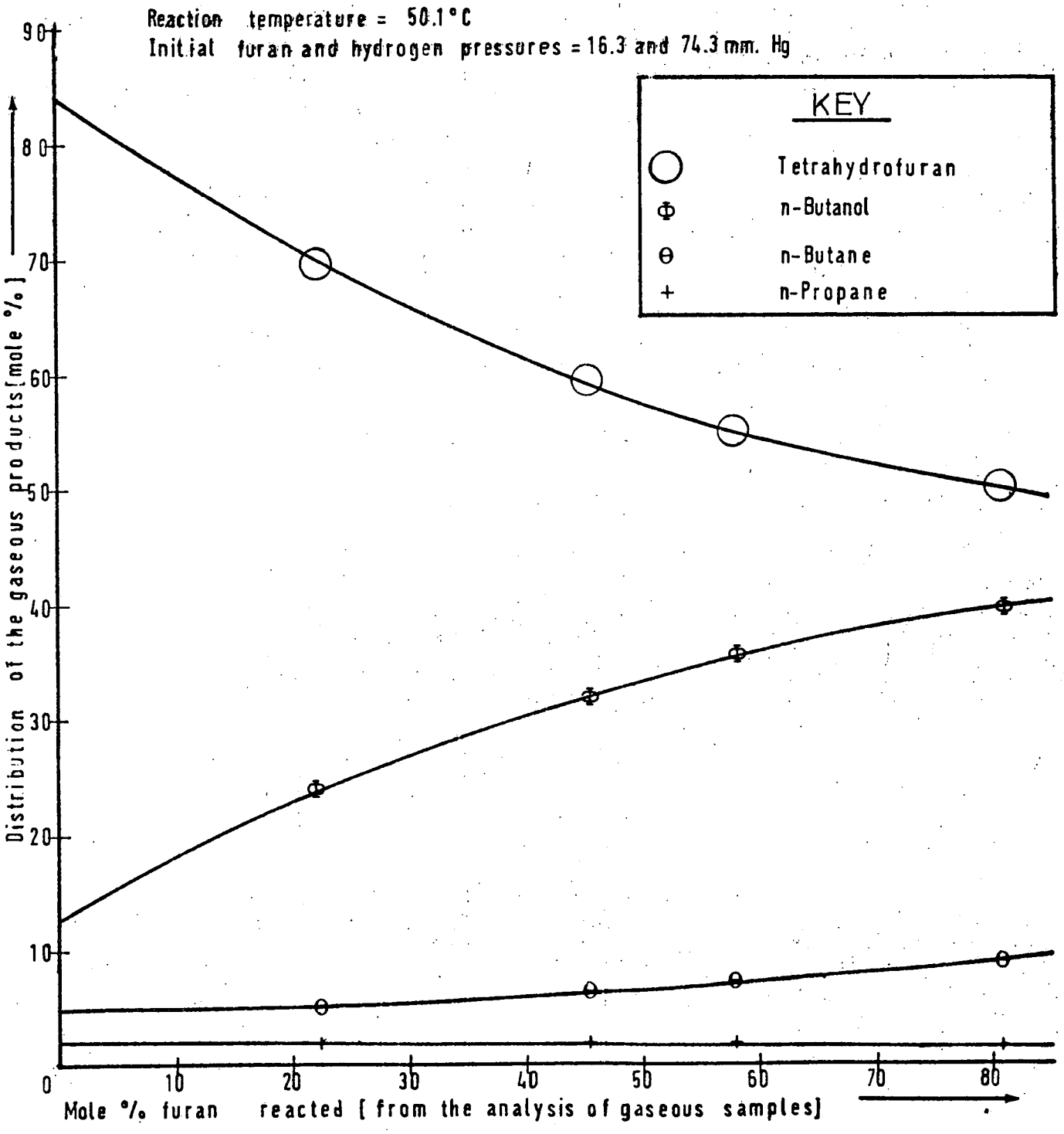

The data for run C6E3 given in table 4.2 shows that ΔP_C is smaller than ΔP_{OBS} even when ΔP_C is approximately twice as large as the initial furan pressure. Hence, as was shown in section 3.1.5, the reaction vessel pressure drop is not caused solely by furan adsorption, one or more of the products must be adsorbing on the catalyst.

As expected for a given value of ΔP_C $(\Delta P_{OBS} - \Delta P_C)$ is approximately proportional to the weight of catalyst (see table 4.2).

4.3.2. Product distributions

All percent reaction/product distribution graphs for furan hydrogenations over Pt/SiO_2 had the same characteristic form illustrated by graph 4.7 for run C6H1. The product distribution changes throughout the reaction, particularly sharply at the start of a hydrogenation. Table 4.3 compares the estimated initial product distribution with that for 70% reaction for run C6L1, reaction temperature is 48°C.

Table 4.3 Product distributions for the furan hydrogenation C6L1 at 48°C.

Product	Initial % product distribution	% Product distribution at 70% reaction
n-propane	2.5	2
n-butane	5	9
tetrahydrofuran	79	50.5
n-butanol	13	39.5

Some possible explanations for the skewed product distributions are :-

A. The reaction is diffusion controlled. Electronmicrographs show the silica to have an extensive fine pore structure (see figs. 2.5 and 2.6).

B. One or more of the products are adsorbing, from the shapes of the percent reaction/product distribution graphs it appears that n-butanol is being adsorbed. In section 4.3.1. it was shown that adsorption by products is occurring.

C. The electronic properties of the catalyst surface change during the reaction. This might take the form of selective poisoning of active sites on the catalyst surface, such a hypothesis presupposes that different products are produced at different types of sites.

Hypothesis A may be eliminated since the degree of distortion of the product distributions differs little with the speed of reaction. For example runs C6H1 and C6E3 both had severely distorted product distributions even though 50% reaction was reached after 17 and 162 minutes respectively.

Added weight was lent to hypothesis B by run C6I1 where a reaction mixture of n-butanol and hydrogen at 47°C was exposed to 0.0536g 5% Pt/SiO_2, initial n-butanol pressure was 4 mm.Hg. On taking a sample at 2.1 minutes no n-butanol was present in the gas phase, the adsorbed alcohol reacting slowly to form n-butane and a trace of n-propane. Hence the supported catalyst adsorbs n-butanol strongly which explains why the % of gaseous n-butanol formed increases with time on hydrogenating furan and the hydrogenation of n-butanol to n-butane explains why the percent of gaseous n-butane formed increases with time on hydrogenating furan.

In order to attempt to verify that adsorption of n-butanol causes the time dependent product distribution a further reaction, C6J1 was carried out at 50°C in which 0.0772g of 5% Pt/SiO_2 catalyst were saturated with n-propanol vapour, 6 mm.Hg. After 47 minutes 79.3 mm. Hg of a mixture of 20% furan and 80% hydrogen was admitted to the reaction vessel. As expected the hydrogenation reaction was badly poisoned, reacting at

approximately the same rate as run C6E3. However unlike run C6E3 the molar ratio of tetrahydrofuran to n-butanol remained almost constant at 1.5 ± 0.1 for the first hour (the same ratio for run C6E3 dropped from 5.0 to 1.7 in the first hour).

A more detailed examination of the product distributions for run C6J1 show that furan or its products slowly displace the adsorbed n-propanol. Since the molar ratios of (propanol and its hydrogenation products) / (furan and its hydrogenation products) increases with time, see table 4.4 , either n-propanol is being displaced from the catalyst's surface by furan and/or its products or furan itself is being adsorbed slowly. The former hypothesis is the more probable since the molar ratio of ethane (which is only formed when the catalyst was exposed to n-propanol and hence its concentration remains constant) to n-propanol drops initially with increasing reaction time until nearly all the furan has reacted when the n-propanol starts to be hydrogenated.

Table 4.4 Molar ratios from run C6J1, 50°C.

(n-propanol + products)/ (furan + furan products)	ethane / n-propanol	propane / n-propanol	time (mins.)	% furan reacted
0.380	0.0725	0.0481	6	2.5
0.471	0.0676	0.0492	30	11.8
0.493	0.0634	0.0505	56	17.3
0.751	0.0789	0.0908	1204	99

4.3.3 Conclusions from hydrogenations over 5% Pt/SiO_2 catalysts.

The catalyst has a high initial activity for furan hydrogenations, inducing a high percentage of hydrogenolysis of the furan ring to form n-butane and n-butanol at 50°C with less than 3% conjugative hydrogenolysis occurring. However the catalyst is rapidly poisoned by the reaction and more serious the product distribution is strongly time dependent. The latter factor seems to be caused by n-butanol adsorbing on the catalyst, in all probability on the SiO_2. (see refs. 68 and 73).

It is of interest that while the silica probably enters furan-hydrogen reactions as an adsorbant an attempt to hydrogenate furan over one gram of silica alone met with no success (run C5A1), even when the reaction mixture had been exposed to the oxide at 230°C for four hours. However, on removal of the silica sample a slight decolouration was detected.

Since adsorption occurs it is only possible to calculate the percent reaction from the gas phase reactants and products. Clearly since this would not yield the actual percent reaction this is unsatisfactory for any kinetic analysis. Reducing the amount of catalyst would reduce the adsorption effects but the distortion of the product distribution would remain a problem. Moreover if a very small weight of catalyst were used the reaction would be badly affected by poisoning.

Hence it was decided to try other supports for platinum in order to find a more satisfactory catalyst.

4.4 Hydrogenations over 5% Pt/Al_2O_3 catalysts (C9 catalysts)

On hydrogenating furan this catalyst was found to suffer from all the disadvantages of the silica supported catalyst namely the product distribution/percent reaction graphs were distorted, see Graph 4.8, adsorption of products occurred, see table 4.5, and the reaction was autopoisoned. In addition

GRAPH 4.8

Product distribution for the furan hydrogenation C9A1

(over 0.205 g. 5% Pt/Al_2O_3 at 49.5°C, initial furan and hydrogen pressures = 31.1 and 131.0 mm. Hg respectively)

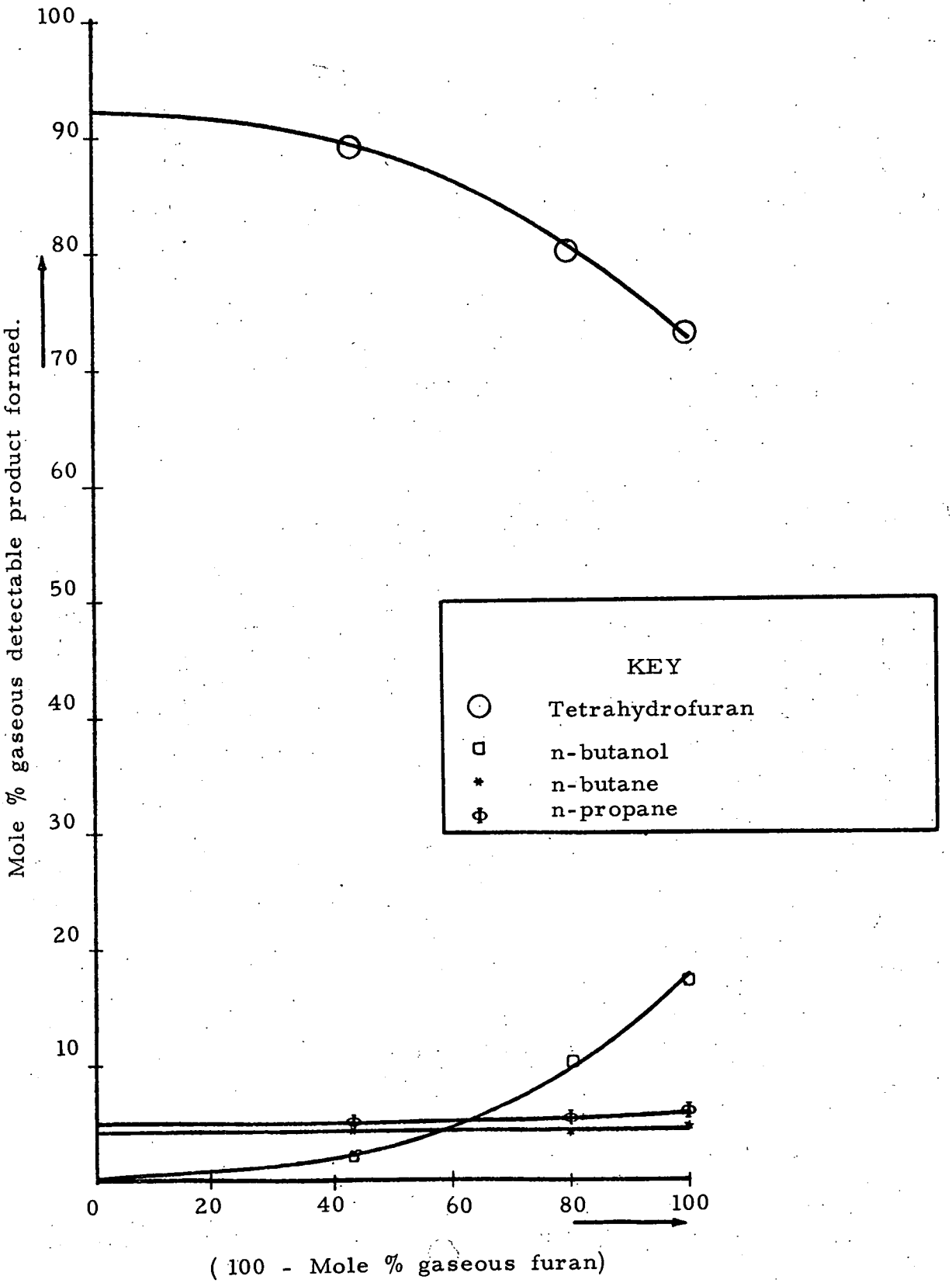

the amount of hydrogenolysis of the C - O bonds was reduced (the sum of the initial percent of n-butanol and n-butane formed was only 4.5%) which alone made the catalyst useless for the study of C - O bond cleavage. Furthermore in all the reactions examined the percent of n-propane was higher than the percent of n-butane formed.

Table 4.5 Comparison of calculated pressure drops, ΔP_C, assuming no adsorption and observed pressure drops ΔP_{OBS} for run C9A1. (Reaction temperature = 49.5°C, Weight of catalyst = 0.205g, initial furan pressure = 31.1 mm.Hg., initial hydrogen pressure = 131.0 mm.Hg.)

ΔP_C, mm.Hg.	ΔP_{OBS}, mm.Hg.	$\Delta P_{OBS} - \Delta P_C$, mm.Hg.	percent Furan reacted
28.1	41	13	43.5
48.5	61	12.5	70.2
75.0	80.5	5.5	99

Comparing the values for $\Delta P_{OBS} - \Delta P_C$ for run C9A1, table 4.5, with those for C6E3, table 4.2, shows that it is probable that the extent of adsorption on alumina supported platinum is about a third of that for a silica supported catalyst. 2.5 times as much catalyst was used for run C9A1 yet at 57% reaction $\Delta P_{OBS} - \Delta P_C$ is 1.4 times higher for reaction C6E3 than for C9A1, this could be attributed to the smaller amount on n-butanol produced over the Pt/Al_2O_3.

4.5 Hydrogenations over Pt/Pumice catalysts (C7, C8 and C10 series).

This catalyst system was finally adopted since the product distributions for the hydrogenations of furan and sylvan are constant over most of the reaction and the calculated and observed pressure drops correspond closely, hence little adsorption is occurring. Furthermore the initial yield of n-butanol on hydrogenating furan is greater than 60% for reaction temperatures between 22°C and 95.5°C while the yield of n-propane is less than 1.8% for reaction temperatures below 50°C.

The catalyst system has the disadvantage that it is two orders of magnitude less reactive than either Pt/Al_2O_3 or Pt/SiO_2 (weight for weight).

4.5.1 Reproducibility.

The initial product distributions from furan hydrogenations over different catalyst samples are reproducible to within $\pm$ 2% for reactions carried out at the same temperature as is illustrated by runs C10F1, C10H1, CS8H1 and C8G1 in table 4.6.

Table 4.6 Initial distributions of detectable products for furan hydrogenations over 5% Pt/pumice.

RUN	A	B	C	D	E	F	G
C10F1	0.8	20.5	17.6	61.0	22.0	9.9	44.7
CS8H1	0.7	20.4	18.5	60.0	23.2	13.7	95.0
C8G1	0.6	18.8	19.9	60.2	23.2	12.5	125.2
CR10C1	0.7	17.5	20.5	61.2	28.2	12.8	104.2
CS8E1	0.9	18.2	20.6	59.3	30.2	11.6	75.2
CS8G1	0.8	19.5	19.5	60.3	30.9	12.9	72.2
C10E1	0.9	20.1	17.5	61.8	42.6	11.3	51.0
CS8C1	1.1	14.9	22.1	62.2	45.1	11.6	151.6
C10H1	0.8	19.7	17.9	61.3	46.0	13.9	57.4
C7B1 *	0.9	11.6	25.5	62.0	46.1	24.5	106.4
C10B1	0.9	12.2	23.4	63.5	46.4	12.1	51.8
C8A1	1.2	13.2	23.1	62.5	46.4	18.8	82.0
C8D2 **	1.4	13.1	24.1	61.4	47.3	11.4	49.5
C8D3 **	1.8	7.5	27.2	61.4	48.5	9.6	41.8
CR10B1	1.5	12.7	22.9	62.5	53.5	20.4	201.6
C8H1	2.0	11.6	19.2	67.0	65.2	15.2	96.8
C8D1	4.9	7.5	14.0	74.5	95.5	13.5	68.5

* A 10% Pt/Pumice catalyst used

** Catalyst had been used before and regenerated by heating first in air (at 425°C) then in hydrogen (at 400°C).

A, B, C and D are the initial product distributions (mole %) of n-propane, n-butane, tetrahydrofuran and n-butanol respectively, E is the reaction temperature (°C), and F and G are the initial furan and hydrogen pressures respectively (mm. Hg.)

Addition of n-hexane, run C10A1 or n-propanol, run C10C1, or sylvan, runs C10J1, C10K1, C10N1, C10M1 and C1001 to a furan/hydrogen reaction mixture does not affect the product distribution appreciably, compare the following table of the initial product distributions with table 4.6.

Table 4.7 Initial distributions of the detectable products for furan hydrogenations, the reaction mixtures containing another reactant.

RUN	A	B	C	D	E	F	G	H	I
C10J1	0.5	20	20	60	26.1	8.8	77.7	10.5	Sylvan
C10H1	0.4	17	21	61	30.5	8.5	120.9	7.4	Sylvan
C10C1	0.9	14	22	63	47.2	13.8	61.8	12.0	n-propanol
C10K1	0.9	14	23.5	62	48.5	12.3	98.5	9.2	Sylvan
C10L1	0.9	18	19.5	62	48.5	14.5	91.5	7.3	Benzene
C10L2	0.9	11	22	63	49.5	8.2	51.7	4.1	Benzene
C10N1	1.1	13	22	64	49.5	14.2	96.1	10.6	Sylvan
C1001	2.5	11	20	66	60.2	10.1	80.2	8.4	Sylvan
C10A1	2.0	12	17.5	67.5	62.5	10.0	54.2	9.3	n-hexene

A, B, C and D are the initial product distribution in mole % of n-propane, n-butane, tetrahydrofuran and n-butanol respectively, E is the reaction temperature (^{o}C), F, G and H are the initial furan, hydrogen and additive pressures (mm. Hg.) respectively and I is the additive.

Run C10L2 shows that the addition of benzene to the reaction mixture has no effect on the initial product distribution for the hydrogenation of furan. It is thought that an error was made when recording the reaction temperature for run C10L1 and that the thermocouple reading should have been 0.94 mv. ($23^{o}C$) as opposed to 1.94 mv. ($48.5^{o}C$) since both the product

distributions and the poisoning constant (Table 5.42) correspond to 23°C.

The evidence for reproducibility of the initial distributions of the detectable products for sylvan hydrogenations is not as strong as for the furan hydrogenations since far fewer reactions of sylvan and hydrogen were carried out. The initial distributions for sylvan hydrogenations are given in table 4.8.

Table 4.8 Initial distributions of detectable products for sylvan hydrogenations over 5% Pt/Pumice catalysts.

RUN.	A	B	C	D	E	F	G	H	I	J
C10I1	16	31	24.5	25.5	3	23.2	11.0	53.2	0.0	none
C10J1	14	35	25	24	2	25.9	10.5	77.7	8.8	Furan
C10M1	15	32	24.5	24	3.5	30.5	7.4	120.9	8.5	Furan
C10P1	14	32	25	25	4	41.2	12.6	60.0	0.0	none
C10K1	11	31	25	28.5	5	48.5	9,2	98.5	12.3	Furan
C10N1	10	29	28	28	5	49.5	10.6	96.1	14.2	Furan
C8C1	9	28	27	31	5	49.5	18.3	91.0	0.0	none
C1001	6.5	29	21	36	7	60.2	8.4	80.2	10.1	Furan

A, B, C, D and E are the initial product distributions (mole %) of n-pentane, tetrahydrosylvan, pentan-2-one, pentan-2-ol and n-pentanol respectively, F is the reaction temperature (°C), G, H and I are the initial partial pressures (mm.Hg.) of sylvan, hydrogen and any additive present in the reaction mixture respectively and J is the additive to the reaction mixture.

Reproducibility of the rates of reaction of the furans will be dealt with in greater detail at the end of the following chapter, however an indication that a reasonable reproducibility was obtained is given by graph 4.9 which compares the rates of two pairs of reactions, C8A1 and C10B1 both at 47°C and C10F1 and C8G1 at 22.5°C.

GRAPH 4.9

Comparison of the rates of reaction of pairs of furan hydrogenations at the same temperature and over the same weights of Pt/pumice catalysts (runs C8A1 and C10B1 at 46.5°C over 0.524g. cat. and runs C10F1 and C8G1 at 23°C over 0.533g. cat.).

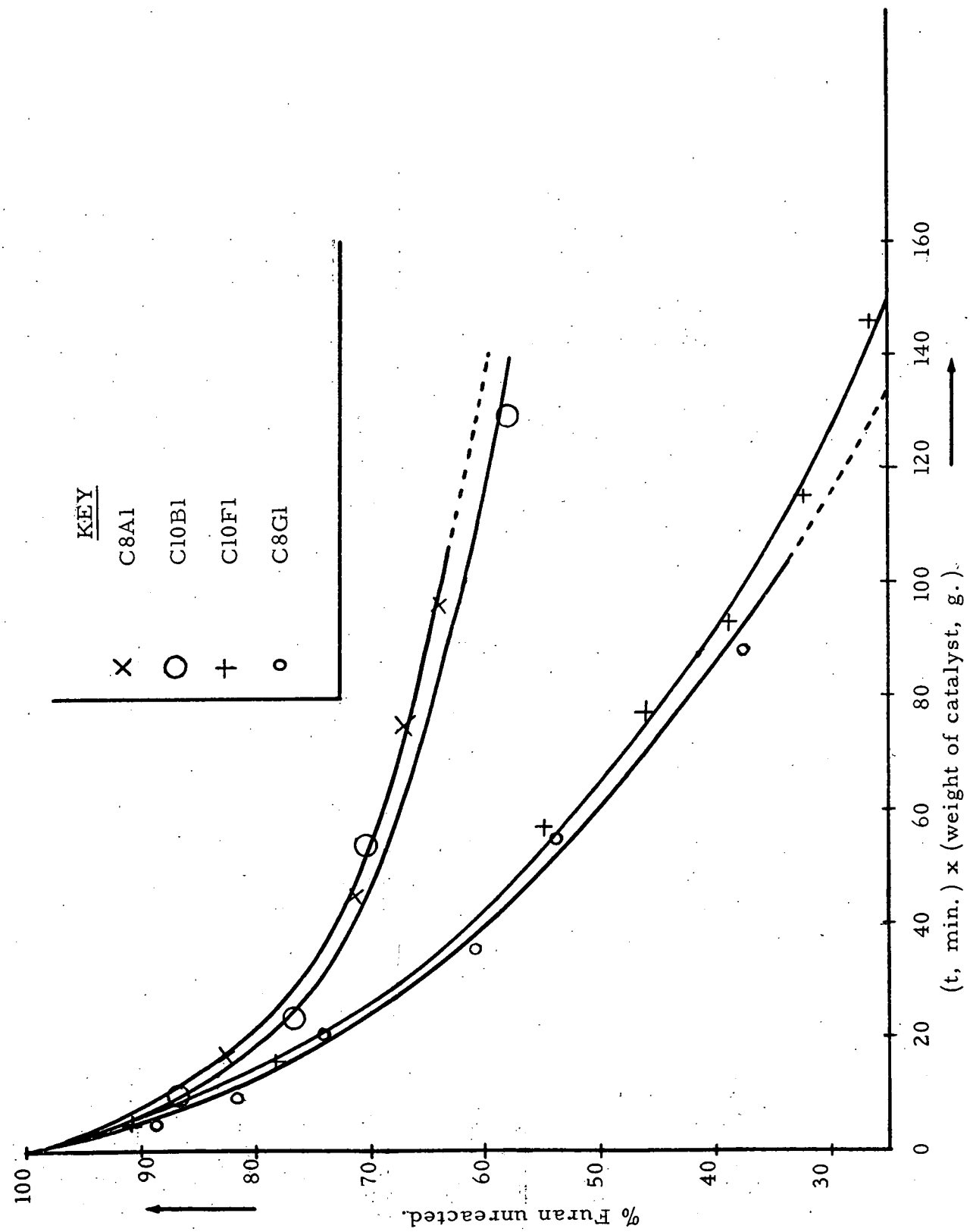

4.5.2 Adsorption of reactants or products.

As already mentioned very little adsorption occurs. Comparison of pressure drops calculated from analysis data assuming no adsorption (ΔP_C, using equation 3.32,) and pressure drops observed using a mercury manometer, ΔP_{OBS}, showed no significant difference either for 5 or 10% Pt/pumice catalysts. As an example the values for C7B1 (1.02g 10% Pt/pumice hydrogenating furan at 46°C) and C8A1 (0.382g 5% Pt/pumice hydrogenating furan at 47°C) are given in table 4.9

Table 4.9 Observed and calculated pressure drops, ΔP_{OBS} and ΔP_C respectively for furan hydrogenations C7B1 and C8A1.

ΔP_{OBS}, mm.Hg		ΔP_C, mm. Hg		$\Delta P_{OBS}-\Delta P_C$, mm. Hg		% reaction	
C7B1	C8A1	C7B1	C8A1	C7B1	C8A1	C7B1	C8A1
18.2	10.2	17.0	9.1	1 ± 3	1 ± 2	25.4	18.3
30.9	15.4	30.0	14.0	1 ± 3	1.5 ± 3	44.5	28.7
41.8	21.1	39.8	18.3	2 ± 4	3 ± 3	59.2	36.9
	31.5		29.2		2 ± 3.5		56.0

Initial furan pressures were 24.5 and 18.8 mm.Hg. and initial hydrogen pressures were 106.4 and 83 mm.Hg. for runs C7B1 and C8A1 respectively.

The errors in $\Delta P_{OBS} - \Delta P_C$ make the figures quoted in table 4.9 only interpretable in qualitative terms, namely one can only say little adsorption is occuring. In order to obtain more definite evidence as to the extent of adsorption it was necessary to devise a technique which not only gives an actual measure of the amount of adsorption but also has considerably lower inherent errors than the basically qualitative approach used for table 4.9. The method used, outlined in section 3.1.4, involves adding an inert gas, detectable by the

GRAPH 4.10

PRODUCT DISTRIBUTIONS FOR A FURAN HYDROGENATION OVER A 5 °/₀ Pt/PUMICE CATALYST [0.526 g.]

Initial furan and hydrogen pressures = 12.1 and 51.8 mm.Hg
Reaction temperature = 46.5 °C

RUN C10B1

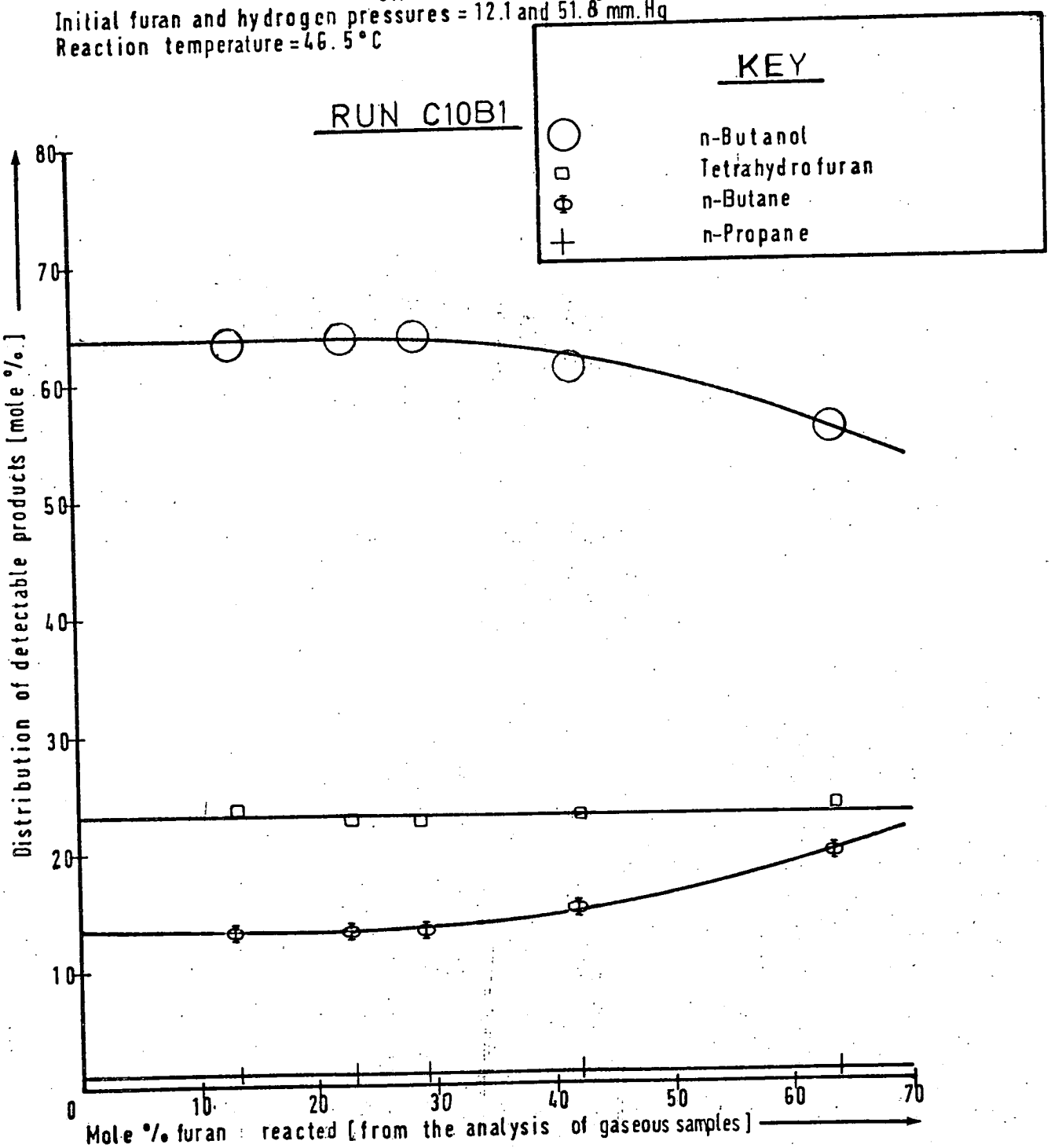

GRAPH 4.11

PRODUCT DISTRIBUTIONS FOR A SYLVAN HYDROGENATION OVER A 5% Pt/PUMICE CATALYST

RUN C1011

Reaction temperature = 23.2°C
Initial sylvan and hydrogen pressures = 11.0 and 52.2 mm. Hg respectively

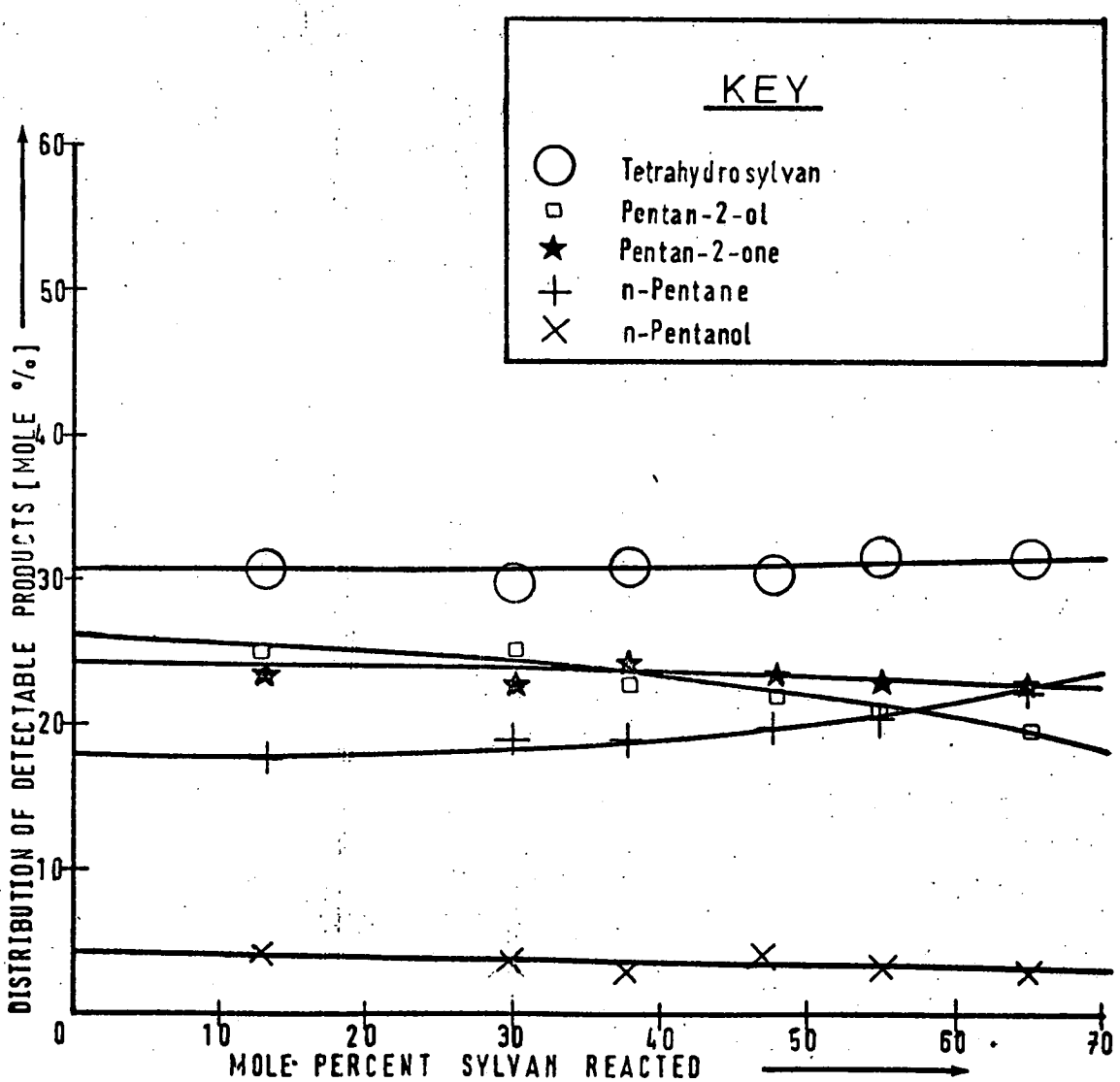

chromatograph, to the reaction mixture prior to its injection into the reaction vessel and treating the analysis data from the subsequent hydrogenation using equation 3.26. This equation is an expression for the fraction of the initial furan present as adsorbed species. The results from this method applied to run C10A1 are summarised in table 3.2, unfortunately the adsorption is so small that estimation of its extent is still hampered by experimental errors, the total amount of the initial furan present as adsorbed species is less than 10%, probably in the order of 5% (Weight of catalyst for C10A1 = 0.382g 5% Pt/pumice, initial furan, hexane and hydrogen pressures are 10.0, 9.3 and 54.2 mm.Hg. respectively) which amounts to a partial pressure of 0.5 mm.Hg. of reactants and products removed from the gas phase by adsorption.

4.5.3 Product distributions.

An interesting feature of all the furan and sylvan hydrogenations is that regardless of the reaction temperature (between 22°C and 95.5°C) the fraction of the tetrahydro derivatives formed remains constant throughout the entire reaction while the distribution of the other products, while remaining unchanged during the initial stages of the reaction, starts to alter slowly as the catalyst becomes increasingly poisoned. Typical product distributions for furan and sylvan hydrogenations are given in Graphs 4.10 (of run C10B1) and 4.11 (of run C10I1) respectively. It is worth pointing out that what changes in the product distributions which do occur are small compared with any of the other catalyst systems experimented with, compare graphs 4.3, 4.7 and 4.10.

These shifts in the product distributions are not thought to be due to changes in the electronic properties of the catalyst's surface such that the probability of an adsorbed furan or sylvan molecule reacting to form a given product changes but rather that one or more of the products react to form

GRAPH 4.12

TO SHOW THE RATE OF HYDROGENATION OF n-BUTANOL OVER A 5 % Pt/ PUMICE CATALYST AS A FUNCTION OF TIME FOR RUN C8E1.

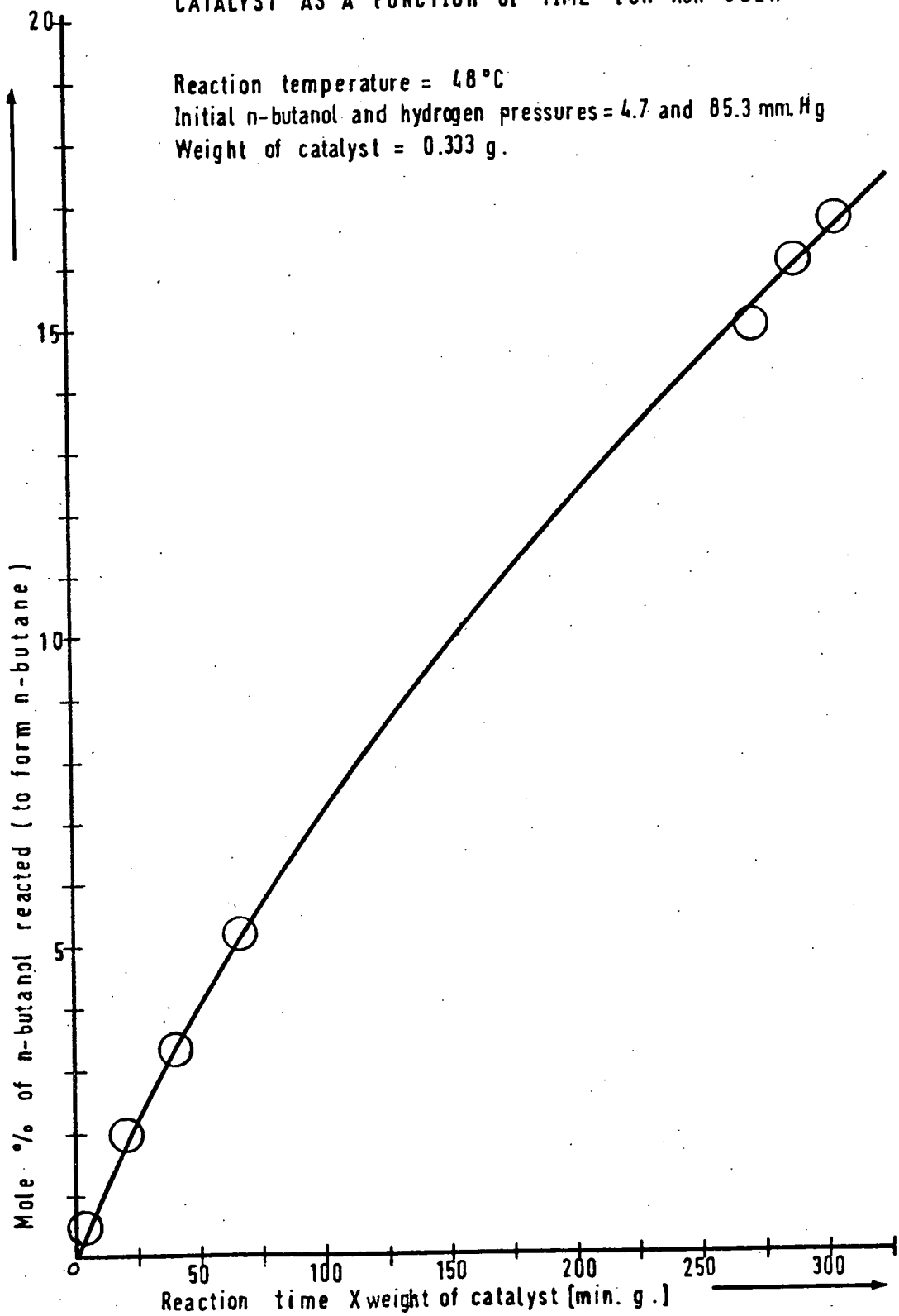

another product, this reaction being poisoned more slowly than the main reaction. For example in the furan/hydrogen reaction it is thought that the n-butanol produced slowly reacts to form n-butane and water. In the early stages of reaction this secondary reaction is too slow to have a noticeable effect until the furan hydrogenation becomes strongly poisoned. The effect is that in the beginning of the reaction the product distribution remains constant while in the later stages the fraction of n-butanol produced drops, while the fraction of n-butane produced rises by an equal and opposite amount, (see graph 4.10).

The above hypothesis is strengthened by four factors (apart from the unvarying fraction of the tetrahydro derivatives formed) for the furan hydrogenation.

First n-butanol reacts with hydrogen over Pt/pumice at 48°C to form n-butane as was shown by run C8E1, graph 4.12, (weight of catalyst = 0.333g, initial n-butanol and hydrogen pressures were 4.7 and 85.3 mm.Hg. respectively.) Furthermore the ratio of the initial rates for this reaction to that for a furan hydrogenation at the same temperature is approximately 1 : 15 (compare graph 4.12 of the rate of formation of n-butane during run C8E1 with graph 4.2, showing the rate of reaction of furan at three different temperatures; the time scales on both graphs are corrected for the weight of catalyst used).

Second, also from run C8E1, it was found that the rate of poisoning of the n-butanol/hydrogen reaction is insignificant compared with that for a furan hydrogenation at the same temperature (compare graphs 4.12 and 4.2). Provided the two reactions occur at different sites, an assumption implicit in the hypothesis, the hypothesis is proved. The evidence for this assumption is only indirect and is given in the following two paragraphs.

Third, the reduction in the percent of gas phase n-butanol produced, accompanied by an increase in the percent n-butane formed is not linked to the ratios of the partial pressures of n-butanol and furan, which would be the case if the n-butanol were competing with furan for the catalyst's surface. Evidence for this is found by comparing any fast furan hydrogenation where little poisoning occurs with a similar reaction where the rate of poisoning of the catalyst is high. For example, reaction C7B1 using 1g of catalyst at 50°C proceeded to 60% reaction without any detectable drop in the percentage of n-butanol produced. In contrast reaction C8D1 which used 1/3 of the weight of catalyst and was run at 95.5°C, hence was subject to strong poisoning of the furan hydrogenation, only proceeded to 22% before the fraction of n-butanol produced started to drop.

Fourth, further evidence that n-butanol is not competing with furan for the catalyst is obtained from run C10C1 carried out at 47.5°C. For this run the reaction mixture consisted of furan 15.9%, n-propanol 13.8% and hydrogen 70.2%. It was found that the furan/hydrogen reaction was not impeded by the presence of n-propanol, the alcohol should have an effect on the reaction not dissimilar to n-butanol. A rough indication of the validity of this statement is obtained by comparing the initial rates of reaction of run C10C1 with that for a furan hydrogenation reaction at the same temperature, e.g. C10B1, using 0.546g and 0.526g of catalyst respectively. The initial rate of run C10C1 was actually 1.2 times greater than that for run C10B1. A more complex treatment of the reaction kinetics, described in chapter 5, shows that the rate of poisoning of the catalyst C10C was equal to the expected value for this temperature within the range of experimental error (table 5.26).

GRAPH 4.13

THE INITIAL DISTRIBUTIONS OF THE DETECTABLE PRODUCTS FOR FURAN HYDROGENATIONS OVER 5 % Pt/ PUMICE CATALYSTS AS A FUNCTION OF REACTION TEMPERATURE

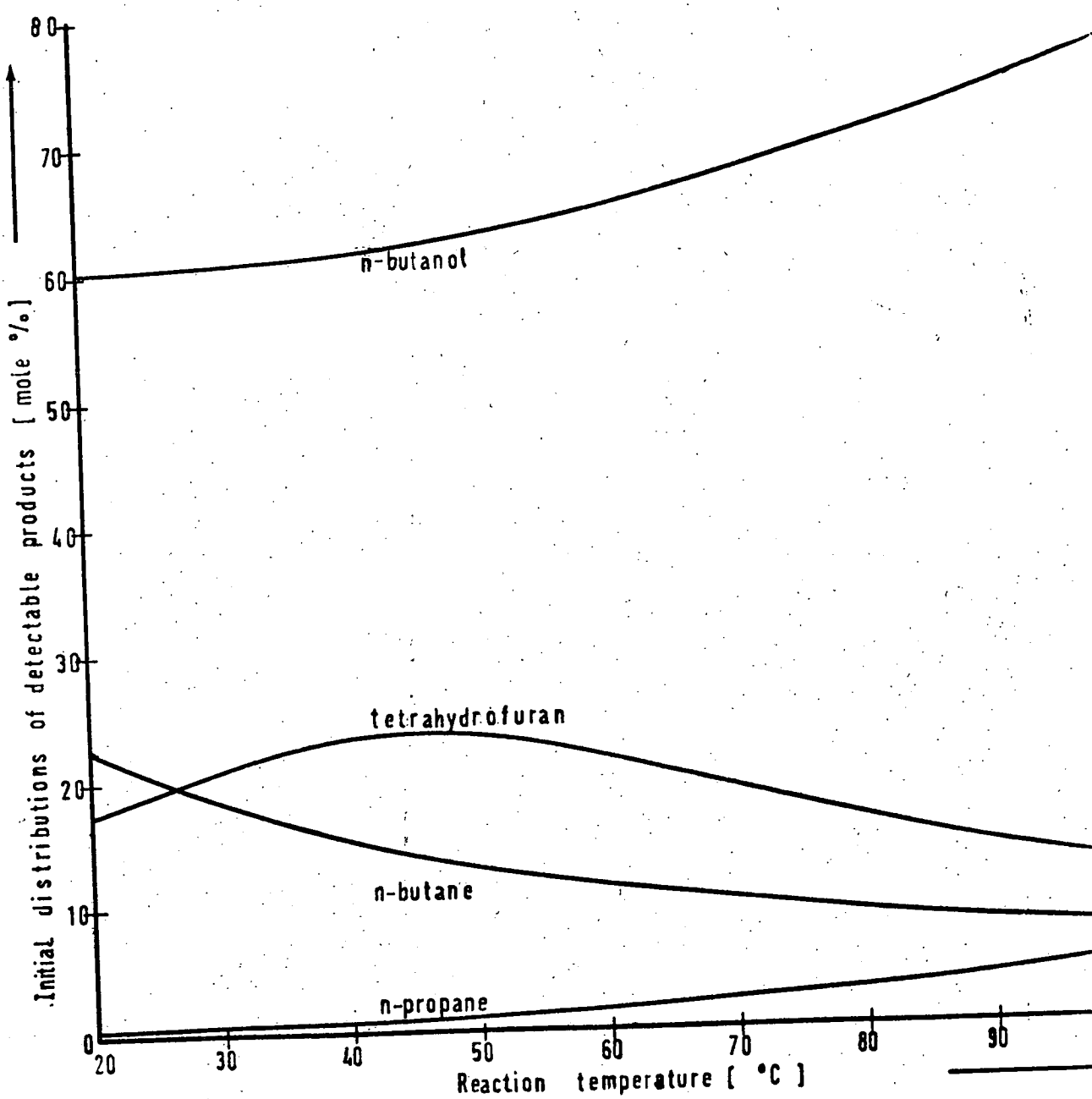

The temperature dependence of the initial product distributions for the hydrogenation of the furans is characterised by the increasing percentage of alcohols and decreasing percentage of alkane formed as the reaction temperature is raised. Graph 4.13, compiled from tables 4.6 and 4.7 shows furan's initial product distribution as a function of temperature.

4.5.4 Conclusions

The Pt/pumice catalysts are particularly suitable for kinetic analysis since they are free from complications arising from strong adsorption of reactants and products and they give product distributions which are stable for most of a reaction. Furthermore, at 50°C the ratios of C - O bond hydrogenolysis products to the 'hydrogenation only' product are 3 : 1 and 2.5 : 1 for the furan and sylvan hydrogenations respectively, hence the catalysts are particularly suitable for the study of C - O bond hydrogenolysis in furans.

The autopoisoning of the catalysts becomes increasingly severe for both furan and sylvan as the temperature is increased (Graph 4.2). The poisoning is not caused by the products of the reaction (runs C10A1, C8G1 and C10C1 showed that alkanes, tetrahydrofuran and alcohols respectively do not affect either the initial rates or the rates of poisoning of the furan/hydrogen reaction). In the following chapter it is shown that these three hydrogenations follow the same kinetics as ordinary furan reactions at this temperature and hence follow the same kinetics with respect to poisoning.

The poisoning which occurs is selective, affecting mainly the catalyst sites at which the furans are hydrogenated. As has been shown the n-butanol hydrogenation is not only poisoned at a very much slower rate (graph 4.12) than the furan hydrogenation but is also poisoned to a lesser degree when the

two compounds are reacting with hydrogen simultaneously (hence the distortion of product distributions from furan/hydrogen reactions in the later stages of a reaction). Similarly when a series of consecutive reactions, C10A1 to C10A5, were carried out where furan and n-hexene were hydrogenated simultaneously the n-hexene reaction did not appear to be severely poisoned even when the initial rate of the furan hydrogenation had been reduced by two orders of magnitude from C10A1 to C10A5. However it should be pointed out that since the hexene/hydrogen reaction was very fast it was not possible to obtain more than quantitative data (all the hexene reactions reached completion within one minute).

The reactions C10L1 and C10L2 where furan and benzene were hydrogenated simultaneously showed that the surface coverage of active catalyst by furan is high since no benzene (except 0.2% at the start of the reaction) was hydrogenated until practically all the furan had reacted, whereupon conversion of benzene to cyclohexane proceeded. This is particularly interesting since the gas phase hydrogenation of benzene is zero order with respect to benzene at low temperatures (ref. 69 ($50^{\circ}C$) and 70 ($17^{\circ}C$)), such an order is suggestive of a high surface coverage, hence if furan adsorbs more strongly than benzene it must be strongly adsorbed.

The low reactivity of the Pt/pumice catalysts as compared with their silica supported counterparts cannot be attributed to differences in surface area per gram of support alone. As was mentioned in section 2.3.2 the silica's surface area is approximately 500 to 600 $m^2\ g^{-1}$ as compared with $55 \pm 10\ m^2\ g^{-1}$ for the pumice, however, the ratio of the initial rates of reaction (per g of catalyst) of furan-hydrogen reactions carried out at the same temperature over 5% Pt/SiO_2 to that for 5% Pt/pumice is greater than 75.

This discrepancy in the activities/$m.^2$ of the two platinum catalysts is probably due, at least in part, to differences in the dispersion of the metal on the two supports (for excellent examples of the effect of supports on the catalytic properties and dispersions of platinum on various supports see references 23, 74 and 75). Since the product distributions obtained from hydrogenating furan over Pt/SiO_2 and Pt/pumice are similar, if one allows for adsorption effects, it is more probable that the differences in the specific activities of the two catalysts stem from different degrees of dispersion of the platinum, rather than from differences in the electronic interaction between the platinum and its supports (c.f. ref. 71).

The latter effect is more likely to have been the cause of the anomalous product distribution observed over Pt/Al_2O_3.

4.6 Hydrogenolysis.

When a furan molecule undergoes hydrogenolysis the fragments produced show that four types of cleavage reactions can occur, fission of a single C-O (n-butanol being produced), fission of both C-O bonds (n-butane being formed), fission of both C-O bonds and a C-C bond (forming n-propane), and severe cracking of the furan ring with the formation of methane.

As expected from the reports of furan hydrogenations in the literature (see Chapter 1), platinum catalysts were most effective for n-butanol production, this being the major product of a furan hydrogenation over Pt/pumice at temperatures as low as $22^{\circ}C$ (when it comprised 60% of the products). In order to illustrate the relative effectiveness of nickel and platinum as catalysts for this reaction compare the probability that a furan molecule undergoing hydrogenation at $95^{\circ}C$ will form n-butanol over Pt/pumice (0.73) with that for a similar reaction over

Ni/SiO_2, approximately 0.05. The probabilities were obtained from the product distributions after one hour's reaction for runs C8D1 and C4A1 respectively. The amount of this type of hydrogenolysis was found to increase with temperature, in the temperature ranges investigated for both platinum and nickel catalysts, hence the activation energy for the hydrogenolysis of a single furanic C-O bond is probably greater than for the hydrogenation of the furan ring.

The next most prevalent form of ring cleavage over the platinum catalysts is the fission of both C-O furanic bonds. Unlike the cleavage of a single C-O bond this form of multiple fission shows an inverse dependence on temperature, (graph 4.13). While the reason for this dependence is not known, it was shown in section 4.5.3 that some of the butane formed during the hydrogenation of furan was produced by the hydrogenation of the product n-butanol, hence the increased yield of the alkane at low temperatures may be due to a decrease in the equilibrium constant for the process $(\text{n-butanol})_{ads.} \rightleftharpoons (\text{n-butanol})_{g.}$. This hypothesis is made the more probable by butanol's low vapour pressure at low temperatures (5 mm. Hg at 20°C). Furthermore between 22 and 42°C the mole % of n-butanol produced remained almost constant while the mole % of n-butane formed at 22°C was 1.3 times that at 42°C, see Graph 4.13).

Since hydrogenations of furan over Ni/SiO_2 were carried out at higher temperatures than those over supported platinum it is difficult to make a meaningful comparison of the two metals' catalytic abilities, suffice it to say that at 180°C almost no butane (1.5%) was formed, some 2.5% being formed at 95°C (7.5% being formed over Pt/pumice at this temperature). The ratio of butane to butanol is five times greater for the nickel catalyst at 95°C, which suggests that the alcohol is desorbed less readily from the nickel than platinum or that the

adsorbed alcohol is hydrogenated more readily over nickel. It is interesting to compare this difference in the catalytic properties of the two metals for furan-hydrogen and diethyl ether-hydrogen reactions. It was found that only over platinum (ref. 41) was ethanol formed, nickel (ref. 42) inducing a more complete fragmentation of the ether molecule.

The ease with which nickel fragments the furan ring is demonstrated by examination of the product distribution for a furan hydrogenation at 180°C over Ni/SiO_2 (Graph 4.3) which shows that at 50% reaction the main product is n-propane (45%) while 12% methane is produced. n-Propane formation was also observed over the platinum catalysts, even at temperatures as low as 22°C (0.7%), the mole percent formed increasing with the reaction temperature, 4.9% being formed at 95°C. No methane was detected over platinum catalysts.

On hydrogenating sylvan the number of products is increased due to the sylvan molecule being unsymmetrical. The main types of hydrogenolysis products observed were n-pentanol (from the cleavage of the 1,2 C-O bond), pentan-2-one and pentan-2-ol (from the cleavage of the 1,5 C-O bond), n-pentane (from the cleavage of both C-O bonds), butan-2-one and butan-2-ol (from the cleavage of the 1,5 C-O and 4,5 C-C bonds) and finally methane from the severe cracking of the furan nucleus.

As was expected from previous work on the hydrogenation of sylvan (e.g. refs. 18 and 29) cleavage of the 1,5 bond occurs much more readily than 1,2 bond fission. Over Ni/SiO_2 at 180°C the 1,5 bond was cleaved approximately 25 times more readily than the other C-O bond (table 4.1), while over Pt/pumice this ratio was approximately 10 : 1 between 22°C and 60°C (table 4.8). In this temperature range over

platinum and over nickel between 170°C and 230°C (Graph 4.5), the major products of the hydrogenation of sylvan are the result of the cleavage of a single C-O bond.

However, although this constraint is operative for the sylvan-hydrogen reaction, it was found that sylvan reacts more quickly than furan at 180°C over Ni/SiO_2 (Graph 4.6). Of greater significance are the relative rates of reaction of the two furans over Pt/pumice between 22°C and 60° since under these conditions the proportions of single C-O bond hydrogenolysis which occur exceeds 50% for both the furans and are similar in magnitude (tables 4.6 and 4.8). From the results of the application of simulation computer programs to single furan and sylvan hydrogenations, Chapter 5, and to simultaneous reactions of the two furans with hydrogen, Chapter 6, it is clear that although the sylvan hydrogenation reaction has the larger activation energy, at approximately 50°C the rate constants for the two reactions are the same. Hence at this temperature the rate of cleavage of sylvan's 1,5 bond is twice that for a furan C-O bond.

As was pointed out in section 4.2 this effect cannot be caused solely by the shielding effect of the methyl group. A possible mechanism is given in the final chapter.

The temperature dependence of single C-O bond hydrogenolysis over supported nickel is complex (illustrated by graph 4.5), pentan-2-one being almost the only product, showing a well defined maximum at 200°C. It is thought that this is caused by multiple fission reactions, involving a C-C bond, having a higher activation energy than single C-O bond hydrogenolysis.

In passing it is interesting to note that although the fraction of tetrahydrosylvan in the products drops from approximately 0.9 to 0.1 between 140°C and 200°C, it remains fairly constant from 200°C to 245°C (Wilson, ref. 18, actually observed an increase in the percentage of tetrahydrosylvan produced in the latter temperature range over nickel). This anomalous effect is probably caused by the isomerisation reaction (pentan-2-one)⇌(tetrahydrosylvan) occurring. (tetrahydrosylvan isomerises over nickel at 250°C slowly to form pentan-2-one in a small yield, ref. 18).

In a similar manner to furan it was found that the product from the hydrogenolysis of both sylvan's C-O bonds increased with decreasing temperature, probably for the same reasons (the main alcohols formed over Pt/pumice, n-pentanol and pentan-2-ol, having even lower vapour pressures than n-butanol, 2.5 and 4.2 mm.Hg respectively at 20°C).

Over Pt/pumice, between 22°C and 60°C, sylvan showed little tendency to undergo the types of conjugative hydrogenolysis involving a C-C bond listed above, 1,5 C-O + 4,5 C-C bond cleavage products amounting to less than 0.6%. Similarly, the product formed by cleavage of both C-O bonds + the 4,5 C-C bond, which was produced during furan's hydrogenation to the extent of approximately 1.5% at 50°C, comprised only 0.1% of the reaction products for a sylvan hydrogenation at the same temperature. No methane was detected over this catalyst.

The salient features of furan and sylvan hydrogenolyses over Pt/pumice below 100°C may be summarised as follows:-

A When hydrogenolysis of the furan nucleus does take place, cleavage occurs almost exclusively at the C-O bonds.

B The major products of the hydrogenations of both furans result from cleavage of only one of the C-O bonds.

C For sylvan the C-O bond furthest from the methyl group is preferentially cleaved.

D C-C bond hydrogenolysis, which occurs only to a limited extent, takes place solely at C-C bonds adjacent to the C-O bonds. Furthermore C-C bond fission is always accompanied by C-O bond cleavage.

E For sylvan a further limitation to 'D' applies - only the 4,5 C-C bond is cleaved.

F The degree of hydrogenolysis increases with temperature for both compounds.

Over Ni/SiO_2, since the hydrogenolysis reactions are strongly temperature dependent, the above generalisations do not hold for the whole of the temperature range investigated ($100^{\circ}C$ to $245^{\circ}C$). However, for sylvan the above six points are applicable between $170^{\circ}C$ and $230^{\circ}C$ (above $230^{\circ}C$ conjugative hydrogenolysis accounts for the major products while below $170^{\circ}C$ hydrogenation of the furan nucleus is the dominant reaction).

A cursory examination of the furan hydrogenation over supported nickel showed that at $180^{\circ}C$ the bulk of the products are the result of conjugative hydrogenolysis, while at $100^{\circ}C$ hydrogenation occurs almost exclusively.

Finally, there is evidence to show that C-C bond fission occurs to a greater extent over Ni/SiO_2 than over Pt/pumice.

CHAPTER 5

Kinetics of the hydrogenation of single furans over 5% Pt/pumice catalysts.

The kinetics of the furan and sylvan hydrogenations are represented by a model of the form

$$dP/dt = - K f(P) . g(t) , \qquad 5.1$$

where f(P) is a function of the reactant pressure P, g(t) is a function of time only and K is the rate constant.

The method by which f(P) and g(t) are found is as follows:

A Evidence that the rate equation can be represented as in 5.1 (section 5.1).

B Determination of the function g(t) (section 5.2).

C Determination of the function f(P) (section 5.3).

D Having found the general form of g(t) and f(P) other experimental data from furan hydrogenations is processed to give a more accurate picture of g(t). (sections 5.4 and 5.5)

Of all the catalysts tried only the Pt/pumice was readily amenable to analysis by the above scheme since not only was adsorption of reactants and products slight but also the product distributions for hydrogenations over this catalyst were only slightly time dependent.

Throughout the bulk of this chapter furan/hydrogen reactions only will be considered since these have been dealt with in much greater detail than their sylvan counterparts. The sylvan reactions will be discussed at the end of the chapter where strong evidence is presented to show that their rate equation can be represented by a form almost identical to that for furan.

5.1 The General Form of the rate equation for furan hydrogenations.

From earlier runs furan hydrogenations were shown to be self poisoning over all the catalysts tried, the poisoning increasing in severity as the reaction temperature is increased (see Graph 4.2 which shows the extent of reaction as a function of time for three furan reactions, over 5% Pt/pumice, at different temperatures). Furthermore the results from numerous reactions show that the longer a catalyst has been exposed to a reaction mixture the more extreme is the poisoning (see Graphs 4.1 and 4.2) whereas short consecutive runs over the same catalyst sample at low temperatures reacted at approximately the same rate. An example of such a series of reactions is CS8A, the initial rate data (from manometric readings of the reaction vessel pressure) for which is presented in table 5.1.

Table 5.1 Initial rates of the change in the reaction vessel pressure found manometrically for the series of consecutive reactions CS8A. Reaction temperature = 25.3°C, weight of 5% Pt/pumice catalyst = 0.776g

Run	Initial rate (mm. Hg min)	Initial furan pressure(mm. Hg)	Initial hydrogen pressure(mm. Hg)	duration of reaction(min)
CS8A1	0.75	19.9	121.2	10
CS8A2	0.62	19.0	117.4	20
CS8A3	0.68	18.0	113.6	10
CS8A4	0.60	18.8	117.2	21
CS8A5	0.57	17.8	112.9	53

Evidence that the products of the reaction do not poison the hydrogenation of furan comes from two cources. First, direct evidence was found by carrying out furan hydrogenations with a compound added to the reaction mixture. It was shown that n-propanol (run C10C1), n-hexane (run C10A1), benzene (runs C10L1 and C10L2) and tetrahydrofuran (run C8G1) affect neither the rate constant nor

the rate of poisoning of the furan - hydrogen reaction. Quantitative data is given at the end of this chapter in tables 5.26 and 5.27. Second, comparison of a fast furan hydrogenation with a relatively slow one carried out at the same temperature shows poisoning to be independent of the concentration of the products, rather being a function of the reaction time. For example compare reaction CS8B1 with C10B1, both carried out at 46°C and both having similar initial furan and hydrogen pressures, 12 and 52 mm. Hg respectively, but using 0.988 and 0.526g of 5% Pt/pumice catalyst respectively. Graph 5.1 shows the percent conversion of furan as a function of time for both reactions. As the graph shows CS8B1 reached 60% reaction within an hour without showing signs of strong poisoning, however, run C10B1 had not reached 40% reaction in five hours, by which time the reaction was showing signs of strong poisoning. Clearly the time which the reaction mixture is in contact with the catalyst is of greater importance than the pressure of the products since their partial pressure was greater for run CS8B1 after an hour than for C10B1 after 5 hours yet the poisoning was much more severe for C10B1 at this time.

Furthermore the furan and hydrogen partial pressures themselves do not appear to affect the rate of poisoning as is illustrated qualitatively by comparing the rates of percent reaction of furan for runs carried out at the same temperature over approximately the same weight of catalyst but with different initial furan and hydrogen pressures. For example see graph 5.1 of the rates of reaction as a function of time for runs CS8B1 (reaction conditions given above) and run C7B1 also carried out at 46°C over 1.02 g of catalyst whose initial furan and hydrogen partial pressures were 24.5 and 106.4 mm. Hg respectively. Both hydrogenations react at approximately the same speed. (see Appendix 11).

GRAPH 5.1

Rates of reaction for three furan hydrogenations carried out at 46.5 ± 1°C over platinum pumice catalysts.

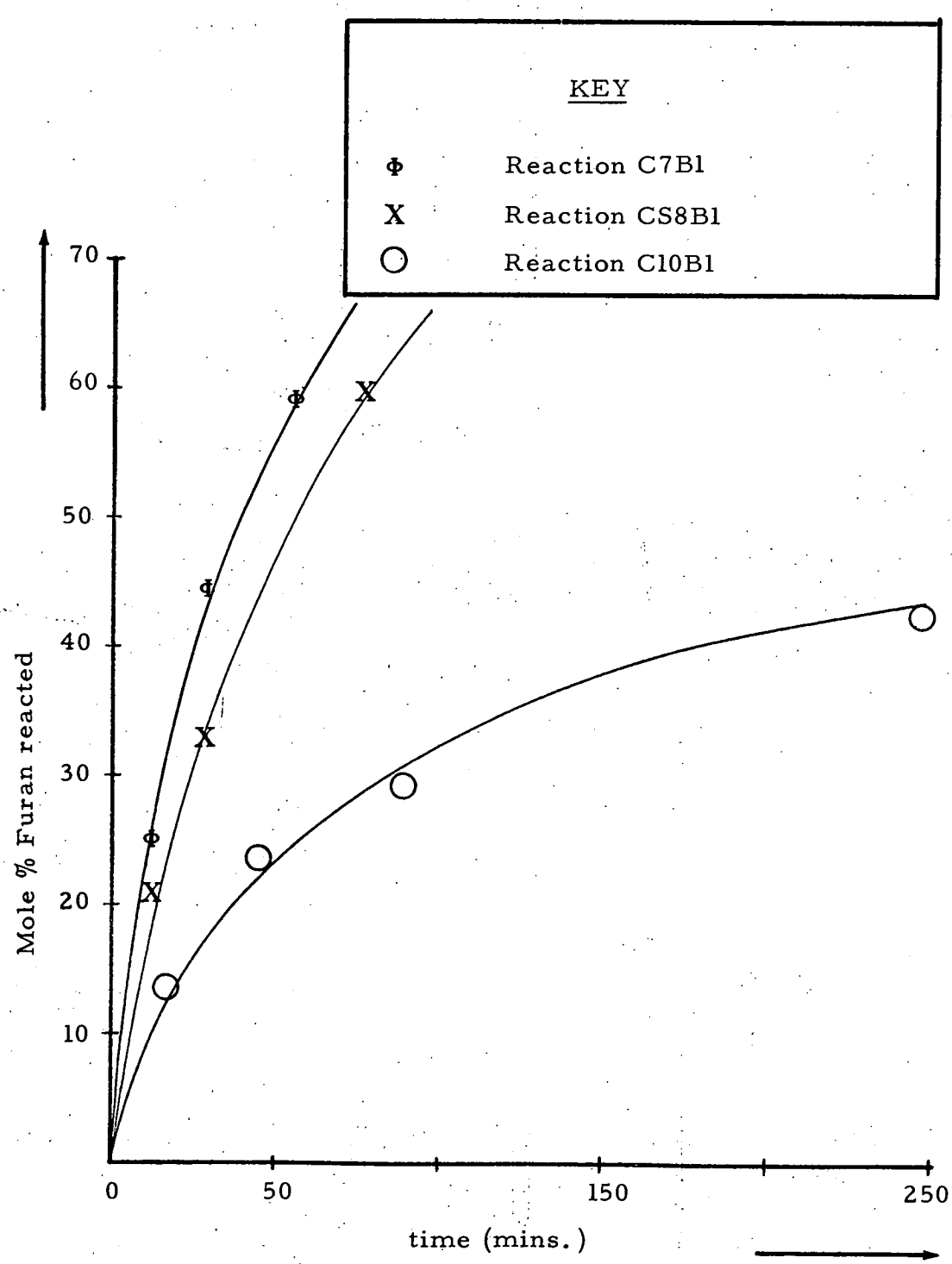

However exposure of a platinum catalyst to either furan alone (run C6L1, 12.2 mm. Hg) or n-propanol alone (run C6I1, 4.1 mm. Hg) leads to almost complete poisoning, hence the procedure adopted to protect catalysts between runs in the consecutive reactions (CS and CR series) as is outlined in Chapter 3.

Since the above evidence shows that poisoning is neither a function of the partial pressure of the products or of the reactants one is forced to conclude it is a function of time. Apparently the proportion of active catalyst surface is being reduced during a hydrogenation, e.g., by the formation of strongly adsorbed species or polymerisation of the furan (ref. 76), and that this process could be represented by some function of time. Since the rate of reaction is proportional to the amount of free surface available the rate equation for a furan hydrogenation may be represented as

$$\frac{d P_F}{dt} = - K_F \, g(t) \, f(P_F P_H \ldots), \qquad 5.2$$

where P_F and P_H are the furan and hydrogen partial pressures respectively, K_F is the rate constant, $g(t)$ is the fraction of the free surface (being a function of time only) and $f(P_F, P_H \ldots)$ is a function of the partial pressures of the gas phase components present during a reaction. In other words $f(P_F, P_H \ldots)$ describes the kinetics which the furan hydrogenation would follow if no poisoning occurred.

The evidence presented above suggests that $f(P_F, P_H \ldots)$ in equation 5.2 may be simplified to $f(P_F, P_H)$ since the products do not appear to affect the rate of reaction, hence 5.2 becomes :

$$\frac{dP_F}{dt} = - K_F \, g(t) . \, f(P_F, P_H) \qquad 5.3$$

But it is shown in Appendix 8 that the hydrogen pressure may be expressed in terms of the furan pressure if the initial furan and hydrogen pressures and the product distributions are known. Hence the function $f(P_F, P_H)$ will be rewritten as $f(P_F)$ for simplicity, equation 5.3 becoming

$$\frac{dP_F}{dt} = - K_F \cdot g(t) \cdot f(P_F) \qquad 5.4$$

In order to proceed further equation 5.4 must be examined more carefully. As yet no mention has been made of possible changes in K_F during a reaction. Because poisoning is occurring it is not unlikely that K_F will drop with increasing reaction time since it is probable that the most active catalytic sites will be poisoned first. In order to remove this complication it is worth noting that if K_F does change during the reaction then it will be a function of the extent of poisoning which has occurred, therefore g(t) is redefined as the product of the fraction of the active catalyst's surface remaining unpoisoned at time t and the ratio of the rate constant at time t to the rate constant at time t = zero, this new function will be referred to as the poisoning function. By this means equation 5.4 contains only two variable functions.

It is also possible that $f(P_F)$ might change during the course of a reaction however for simplicity it is assumed, for the time being, that $f(P_F)$ remains unchanged during a reaction.

By making use of consecutive reactions over the same catalyst sample it is possible to isolate g(t) and examine it without requiring any knowledge of the pressure function as is described in section 5.2. Experiments that would isolate $f(P_F)$ without any knowledge of the time dependent function in equation 5.4 suffer from the drawback that comparisons would have to be made of the kinetics of furan's hydrogenation over

different catalyst samples which would be inherently more prone to error than a series of experiments over the same catalyst sample (due to uncertainty over the reproducibility of catalyst samples). Furthermore while it is possible to put forward reasonable hypotheses for $f(P_F)$ one has no knowledge of the form g(t) will take.

5.2 The determination of the poisoning function g(t)

As mentioned previously in section 5.1 it is assumed that the catalyst surface is being poisoned by a time dependent process and that g(t) is the fraction of its original activity. Hence a function chosen for g(t) should decrease with increasing time (since poisoning becomes increasingly severe with increasing time) and should ideally be subject to the constraint

$$\lim_{t \to 0} g(t) = 1 \qquad 5.5$$

since at the start of the reaction none of the surface is poisoned. A further, more tentative, constraint might be applied :-

$$\lim_{t \to \infty} g(t) = 0 \qquad 5.6$$

since after long reaction times (in excess of 20 hrs.) furan hydrogenation becomes very slow for reaction temperatures in excess of 50°C, however, complete poisoning was never observed.

A final arbitrary constraint was applied in order to facilitate the elucidation of g(t), namely, only one disposable constant was used in each function tried for g(t) for an isothermal reaction.

On examining equation 5.4 two methods for isolating g(t) from $f(P_F)$ become apparent :-

A Elimination of $f(P_F)$ from equation 5.4

B Elimination of $f(P_F)$ from the integrated form of 5.4.

Method A suggests an initial rate approach while B indicates the use of a fractional life time method. Although the latter leads to more complex calculations it is preferable in view of the higher accuracy that can be achieved; the initial rate method has therefore been used mainly as a quick approximate test. (Both methods are discussed in detail in the remaining subsections of Section 5.2).

The general procedure adopted to find g(t) can be conveniently summarised in block diagram form :-

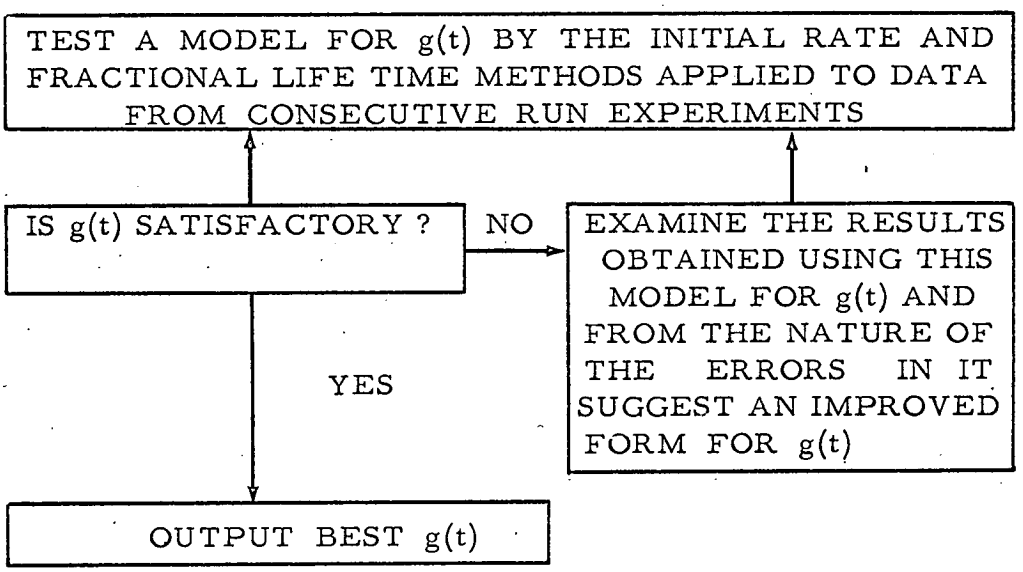

The above block diagram emphasises the empirical nature of g(t). Such a scheme can of course only work satisfactorily if a method can be found for eliminating f(P), in other words if g(t) can be found regardless of the nature of f(P). Methods which meet this requirement are discussed in the following sections.

5.2.1 The Initial rate method for determining g(t) for furan hydrogenations.

Let R_A and R_B be the initial rates of the consecutive reactions A and B, carried out at the same temperature (over the same catalyst sample). Then, using equation 5.2 or 5.3 these rates are given by :-

$$R_A = dP_F/dt = - K_F g(t_A) f({}_AP^\circ_F, {}_AP^\circ_H) \qquad 5.7$$

and $$R_B = dP_F/dt = - K_F g(t_B) f({}_BP^\circ_F, {}_AP^\circ_H) \qquad 5.8$$

where ${}_AP^\circ_F$, ${}_AP^\circ_H$, ${}_BP^\circ_F$ and ${}_AP^\circ_H$ are the initial furan and hydrogen pressures for runs A and B respectively while t_A and t_B are the times of the start of reactions A and B respectively measured from the time a reaction mixture was first exposed to the catalyst sample.

Then dividing 5.7 by 5.8 gives

$$R_A/R_B = g(t_A) f({}_AP^\circ_F, {}_AP^\circ_H) / (g(t_B) f({}_BP^\circ_F, {}_AP^\circ_H)) \qquad 5.9$$

Clearly the pressure dependent terms cancel out if the same initial partial pressures of the reactants are used for both reactions, equation 5.9 then reducing to

$$R_A / R_B = g(t_A) / g(t_B) \qquad 5.10$$

Hence, using equation 5.10, g(t) may be examined in isolation from $f(P_F, P_H)$. For such a method to operate successfully the reactions A and B must be carried out at the same temperature over the same catalyst sample and care must be taken not to poison the catalyst between the consecutive reactions. See chapter 2 section 2.5.3 for the experimental techniques used for these experiments. Indirect evidence that the catalyst's surface properties are not altered in between the consecutive runs comes from the product distributions which remain constant within $\pm$ 2.0% between any two consecutive reactions, this divergence being only slightly greater than the observed $\pm$ 1.5% variance for readings for a single reaction.

Since it is more convenient to express the initial rates in terms of mole % furan reacted/min. rather than the partial pressure of furan reacted/min., as in equations 5.7 and 5.8 ,

proof that the ratios in equation 5.10 are unaltered by this change of units is given as follows :-

Let Q_A be the rate of reaction A in mole % furan reacted/min.,

or

$$Q_A = \frac{d(\text{mole \% furan reacted})}{dt} = \frac{dP_F}{dt} \cdot \frac{d(\text{mole \% furan reacted})}{dP_F} \quad 5.11$$

but since,

$$\text{Mole \% furan reacted} = (1 - \frac{P_F}{{}_AP^o_F}) . 100, \quad 5.12$$

equation 5.11 may be rewritten as:

$$Q^o_A = - \frac{dP_F}{dt} \cdot \frac{d(100P_F / {}_AP^o_F)}{dP_F} = - \frac{dP_F}{dt} \cdot \frac{100}{{}_AP^o_F} = - \frac{R_A . 100}{{}_AP^o_F} . \quad 5.13$$

(Q^o_A is the initial rate for reaction A in mole percent/min)

A similar relationship is obtained for run B

$$Q^o_B = - \frac{R_B . 100}{{}_BP^o_F}, \quad 5.14$$

Q^o_B being the initial rate for run B in terms of mole percent furan reacted/min. Hence dividing equation 5.13 by 5.14 gives

$$Q^o_A / Q^o_B = (R_A / R_B) . ({}_BP^o_F / {}_AP^o_F) \quad 5.15$$

but since the initial pressures are equal (as above) 5.10 becomes

$$Q^o_A / Q^o_B = R_A / R_B = g(t_A) / g(t_B) \quad 5.16$$

Hence all initial rates used in the remainder of this chapter will have the units mole % furan reacted/min. and will be given the symbol R.

5.2.2 The fractional life time method for determining g(t) for furan hydrogenations.

Integration of equation 5.4 gives

$$\int_{P_F^o}^{(1 - Z)\, P_F^o} \frac{dP_F}{f(P_F)} = - K_F \int_{t_i}^{t_j} g(t).\, dt\,, \qquad 5.17$$

Where Z is the fraction of furan reacted at time t_j and t_i is the time at which the reaction mixture is admitted to the reaction vessel, both times being measured from the time when the catalyst sample was first exposed to a reaction mixture.

Similarly for a second reaction carried out consecutively over the same catalyst sample at the same temperature, starting at time t_i^*

$$\int_{P_F^o}^{(1 - Z)\, P_F^o} \frac{dP_F}{f(P_F)} = - K_F \int_{t_i^*}^{t_j^*} g(t).\, dt\,, \qquad 5.18$$

where t_j^* is the time at which a Z^{th} of the furan has reacted.

Clearly the left hand sides of equations 5.17 and 5.18 will be equal if, firstly, both t_j values are measured at the same fraction of furan reacted. Secondly, the initial pressures of the reactants are the same for both reactions. Thirdly, the product distributions remain fairly constant from run to run, and, fourthly, the catalyst's properties are not altered between reactions. All these conditions are met by the consecutive run experiments used in the initial rate method for determining g(t), section 5.2.1. (It is necessary that the product distributions do not change greatly from run to run since were they to, the hydrogen pressures at Z^{th} reaction of furan would differ, hence so would the

integrals of the pressure function in equations 5.17 and 5.18). Therefore, assuming the four above conditions have been met, combination of 5.17 and 5.18 gives

$$\int_{t_i}^{t_j} g(t).\,dt = \int_{t_i^*}^{t_j} g(t).\,dt \qquad 5.19$$

Hence, as with the initial rate technique, a means of isolating the poisoning function g(t) has been found.

In practice more than two consecutive runs were carried out over the same catalyst sample thus improving the resolution of g(t) (see Graph 5.2 of the four consecutive hydrogenations of furan at 23°C, CS8E1 to 4 (over 5% Pt/pumice)).

5.2.3 Models for g(t) tried.

The functions for g(t) that were tried, were

K'/t	I
$(1 - K't^{\frac{1}{2}})$ (c.f. Ref. 77)	II
$K'/t^{\frac{1}{2}}$	III
$1 - \exp(-K'/t)$	IV
$\exp(-K't)$	V
$\exp(-K't^{\frac{1}{2}})$	VI

Where K' is a constant which will be referred to as the poisoning constant. Of these models VI is most satisfactory.

On inserting the above functions into equations 5.10 and 5.19 it becomes apparent that they may be grouped into two distinct sets, class A and class B respectively. For class A models K' disappears on substitution into the two equations while this is not the case for the class B models. Hence the application and the interpretation of the results from the initial rate and fractional order techniques differ for the two sets.

Consecutive run experiment CS8E for finding g(t), the Z value=0.16

Reaction temperature = 23° C

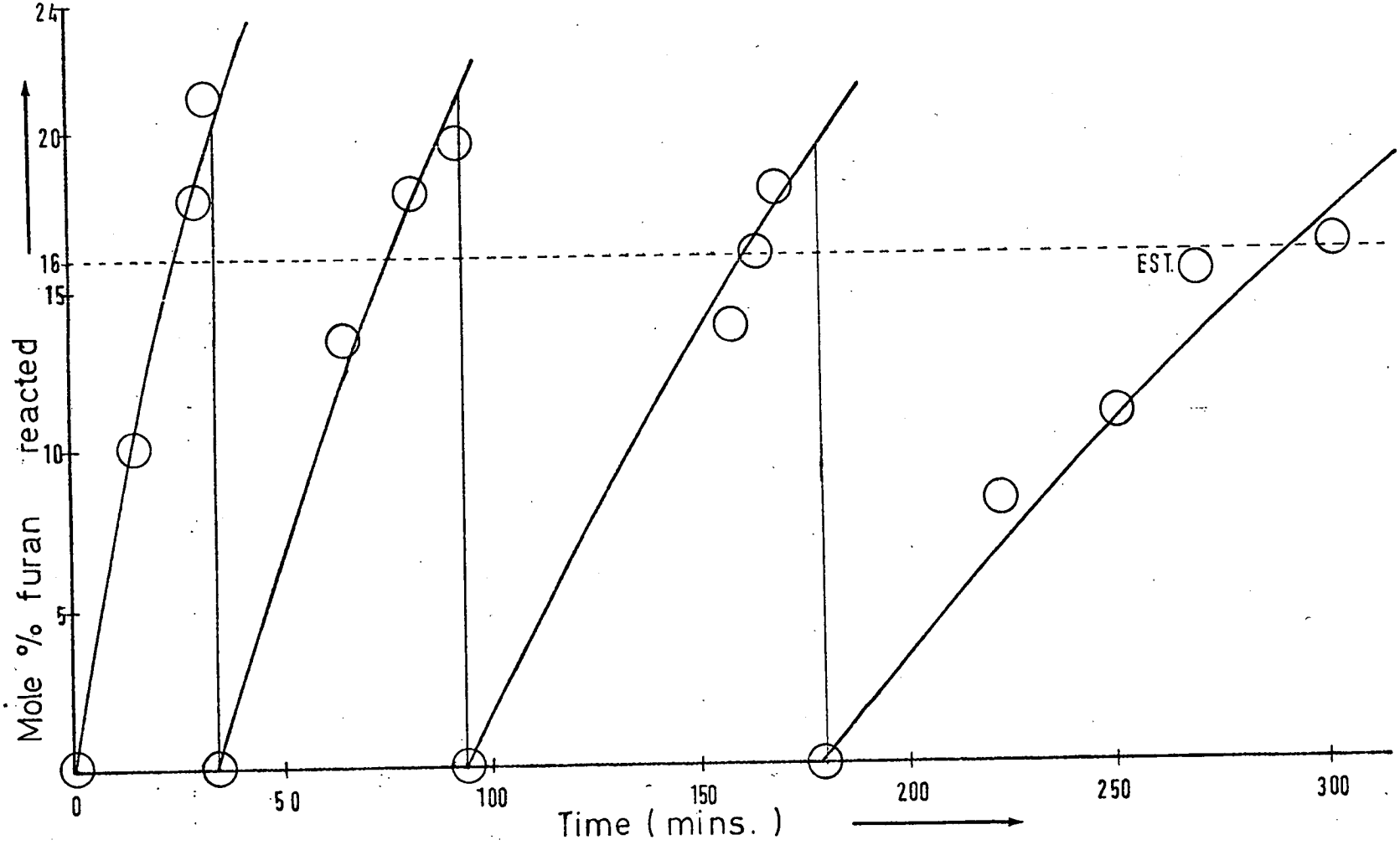

GRAPH 5.2

Class A comprises models I and III while class B models are II, IV, V and VI.

For example, on substituting model III into equation 5.19 and integrating :-

$$2K'\sqrt{t^*_i} - 2K'\sqrt{t^*_j} = 2K'\sqrt{t_i} - 2K'\sqrt{t_j}, \qquad 5.20$$

or, dividing through by 2K' ,

$$\sqrt{t^*_i} - \sqrt{t^*_j} = \sqrt{t_k} - \sqrt{t_j} \qquad 5.21$$

However on substitution of model V (class B) into equation 5.19, integrating and simplifying, the following expression is obtained.

$$\exp(-K' t^*_i) - \exp(-K' t^*_j) = \exp(-K' t_i) - \exp(-K' t_j) \qquad 5.22$$

In order to analyse 5.22 it is necessary to solve the equality for K' and examine the way in which it varies from run to run. If the correct form of g(t) has been chosen then K' will remain constant for a series of consecutive reactions, any deviation from constancy is used to postulate a new function which will minimise the deviations.

In contrast 5.21 will provide a set of equalities from a series of consecutive reactions only if Model III is correct. If it is not, one will be presented with a series of inequalities from which one deduces an improved form of g(t).

In the following three sections Models I and V will be used to illustrate the different techniques used for class A and B models respectively.

5.2.4 The Initial rate method applied to a class A model for g(t)

To illustrate the analysis of a class A model for g(t) model I will be processed using the data from the five consecutive reactions CS8H1 to CS8H5 given in table 5.2.

Table 5.2 The initial rate data from experiment CS8H, for the hydrogenation of furan at 22°C, over 0.4121g 5% Pt/pumice.

Run J	t_j min.	R_j	P_F^o mm. Hg	P_H^o mm. Hg	R_1 / R_j	R_{j-1} / R_j
1	0	1.11	13.7	95.0	1.0	-
2	35	0.645	13.3	91.3	1.72	1.72
3	91	0.407	14.0	94.8	2.73	1.58
4	150	0.245	13.5	93.2	4.54	1.37

t_j is the time at which run j starts, measured from t_1. R_j is the initial rate for the reaction of furan (for the j^{th} run) in mole percent of furan reacted/min. and P_F^o and P_H^o are the initial furan and hydrogen pressures respectively.

Substitution of $g(t) = K'/t$ into equation 5.16 gives

$$R_A / R_B = t_B / t_A \qquad 5.23$$

Table 5.3 lists the calculated initial rate ratios, using equation 5.23, and their experimentally determined counterparts.

Table 5.3 Comparison of calculated (equation 5.23) and experimentally determined initial rate ratios for experiment CS8H. ($g(t) = K'/t$)

Run J	R_{j-1} / R_j calculated	R_{j-1} / R_j experimental
1	-	-
2	∞	1.72
3	2.60	1.58
4	1.65	1.21
5	1.66	1.37

The nomenclature used in table 5.3 is the same as for table 5.2.

Comparison of the initial rate ratios in table 5.3 shows that K'/t is not a satisfactory function for g(t). Furthermore since all the calculated initial rate ratios are larger than their corresponding experimentally determined counterparts a less steeply decreasing function is required. This is most easily seen by selecting a value for K' such that K'/t_{j-1} equals the actual value of g(t) at time t_{j-1}. Therefore, since the experimentally determined value of $g(t_{j-1}) / g(t_j)$ is always smaller than its calculated counterpart, $g(t_j)$ is always too small. Since t_j is larger than t_{j-1} by definition, K'/t decreases too rapidly.

5.2.5 The initial rate method applied to a class B model for g(t) (model V).

Substituting model V, $\exp(-K't)$, into equation 5.10 gives

$$R_A / R_B = \exp(-K'(t_B - t_A)) \qquad 5.24$$

Since K' is unknown equation 5.24 is solved for K' by taking logarithms of both sides :

$$K' = \frac{2.303 \log (R_B / R_A)}{(t_B - t_A)} \qquad 5.25$$

Since one can apply 5.25 to numerous pairs of runs if a whole series of consecutive reactions is being studied, for example experiment CS8H, it is convenient to label K'. For reactions i and j the following notation is used

$$^{j}_{i}K' = \frac{2.303}{t_j - t_i} \log (R_j / R_i) \qquad 5.26$$

Table 5.4 summarises two series of $^{j}_{i}K'$ values for the consecutive run experiment CS8H calculated using equation 5.26.

Table 5.4 ${}^{j}_{i}K'$ values for model V for g(t) calculated by equation 5.26 for the consecutive run furan hydrogenation experiment CS8H (over Pt/Pumice).

Run	$t_j - t_1$ (min.)	${}^{1}_{j}K'$	$t_j - t_{j-1}$ (min.)	${}^{j-1}_{j}K'$
2	35	0.017	35	0.017
3	91	0.0094	56	0.0065
4	150	0.0082	59	0.0045
5	250	0.0063	100	0.0036

Average value of the poisoning constant = 0.008 ± 0.009,

$\sigma = 0.540$ (Normalised)

where t_j and t_{j-1} are the times at which the j^{th} and $(j-1)^{th}$ runs start respectively and ${}^{j}_{i}K'$ is described above.

Were $\exp(-K't)$ the correct model for g(t) then the ${}^{j}_{i}K'$ values in table 5.4 should all be equal, within the limits of experimental error. The $\pm$ 100% divergence from the mean of the K' 's shows that model V is unsatisfactory.

Interpretation of the divergences of the ${}^{1}_{j}K'$ values in table 5.4 is most effectively achieved graphically. If one plots time against $\exp(-{}^{1}_{j}K't)$ one obtains a family of curves passing through the origin, one for each value of ${}^{1}_{j}K'$, see Graph 5.3. Since each curve is the best fit to the actual poisoning function for time 6, (zero secs.) and t_j obtainable using $g(t) = \exp(-{}^{1}_{j}K't)$ one can conclude upon examining these curves (see Graph 5.3) that the actual poisoning function should decrease more rapidly than $\exp(-K't)$ in the initial stages of the reaction, the reverse being true for the later stages.

This conclusion is also obtained by examination of the ${}^{j-1}_{j}K'$ values. Since these show the best fit of adjacent data points

GRAPH 5.3

Testing $g(t) = \exp(K' t)$ by the initial rate method

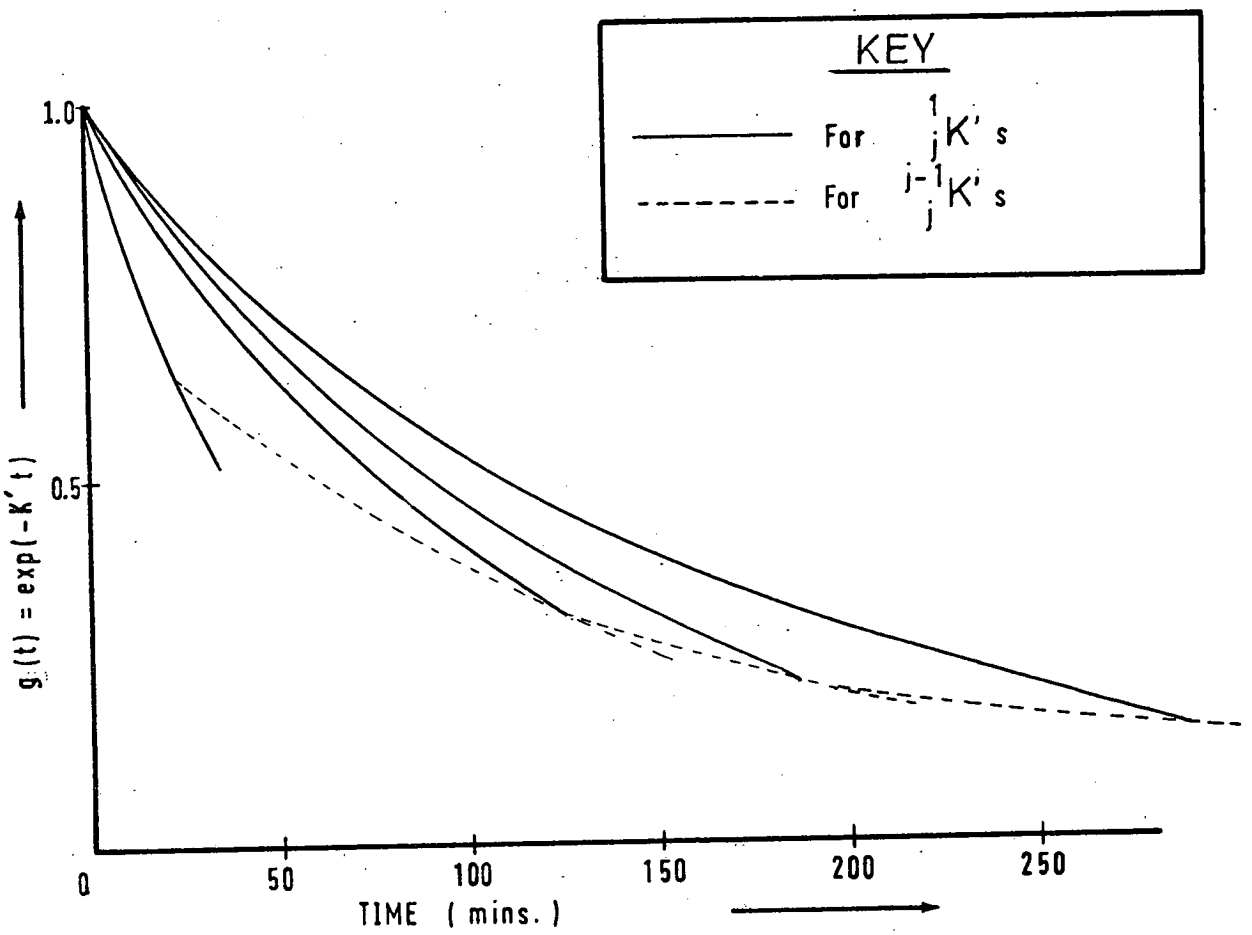

the gradients of the curves generated by $\exp(-{}^{j-1}_{j}K')$'s are a closer approximation to the actual gradients of g(t) than the $\exp(-{}^{1}_{j}K' t)$ curves. However, unlike the latter curves there is no point known through which they will pass. See Graph 5.3 for a diagrammatic representation of both families of curves. The required shape of the improved form of g(t) is illustrated diagrammatically in fig. 5.1.

Fig. 5.1 Diagrammatic representation of $g(t)=\exp(-K't)$ and the predicted shape of the improved function for g(t).

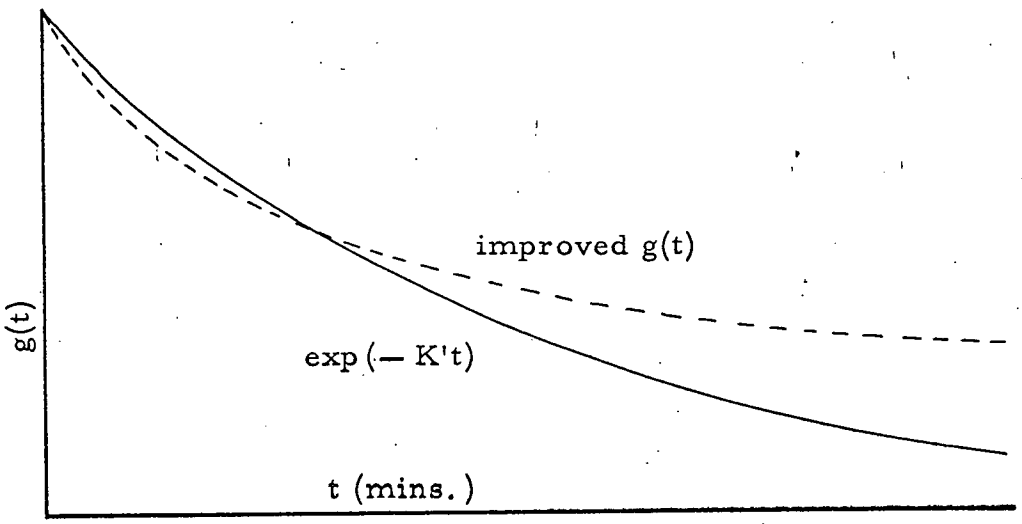

5.2.6 The application of the fractional life time method to class B model V for g(t).

As has been stated previously the fractional life time method is more accurate than the initial rate technique, however, the initial rate method is sufficiently accurate to rule out models which are grossly inaccurate. Since both models in Class A fall into this category the fractional life time method will only be applied to a class B model (model V) in this section, using the experimental data from the set of consecutive furan hydrogenations CS8G presented in table 5.5.

Table 5.5 Fractional life time data for the consecutive run furan hydrogenations experiment, CS8G, using 0.4016 g. 5% Pt/pumice catalyst at 25°C (fractional life of 0.20 was used).

RUN	i	j	t_i (min.)	t_j (min.)	P_F^o (mm. Hg)	P_H^o (mm. Hg)
1	1	2	0	25.6	12.9	72.2
2	3	4	32.2	74.6	12.4	69.5
3	5	6	80.0	146.2	13.1	74.2
4	7	8	160.0	265.3	12.6	71.3

t_i is the time at which the $(\frac{i+1}{2})^{th}$ run starts and t_j is the time at which 20% of the furan has reacted in the $(\frac{i-1}{2})^{th}$ run, the times measured from $t_1 = 0$ secs.

The nomenclature used in table 5.5 will be used in all the following sections dealing with fractional life time techniques.

Rearranging equation 5.19 and defining the new function so obtained as Q(K') :

$$Q(K') = \int_{t_i}^{t_j} g(t).dt - \int_{t_i^*}^{t_j^*} g(t).dt = 0 \qquad 5.27$$

For convenience in defining the pair of integrals in 5.27 equation 5.27 is re-expressed in terms of the two following variables:

$$I.(\frac{i+1}{2}) = \int_{t_i}^{t_j} g(t).dt , \qquad 5.28$$

and

$$I\left(\frac{i^{*}+1}{2}\right) = \int_{t_i^{*}}^{t_j^{*}} g(t).dt \qquad 5.29$$

Hence equation 5.27 becomes

$$Q(K') = I\left(\frac{i+1}{2}\right) - I\left(\frac{i^{*}+1}{2}\right) = O \qquad 5.30$$

Substituting the trial function $g(t) = \exp(-K't)$ into equation 5.27, integrating and dividing throughout by K' gives

$$O = \exp(-K't_i) - \exp(-K't_j) - \exp(-K't_j^{*}) + \exp(-K't_i^{*}) = Q(K) \qquad 5.31$$

As in equation 5.24, which was generated during the initial rate calculations applied to model V, information about g(t) and suggestions as to the form an improved model for g(t) will take is obtained by solving 5.31 for K'. Since Q(K) is a transcendental function it is necessary to use an approximate method to find the non trivial roots of Q(K). The Newton-Raphson method for the successive approximation to a root of a function was employed, taking the form, when applied to 5.31 of :

$$K'_{n+1} = K'_n - Q(K'_n) \Big/ \frac{\partial (Q(K'_n))}{\partial K'_n} . \qquad 5.32$$

Where K'_n and K'_{n+1} are the n^{th} and the $(n+1)^{th}$ approximations respectively to the value of K' which satisfies equation 5.31. A computer program (Appendix 9) was written to find the K 's for all the possible combinations of i 's and i^{*}'s where $i < i^{*}$ using equation 5.32. Use was made of arithmetic statement functions for Q(K') and Q'(K') so that the same program could be used to test many different models for g(t). The results from this program applied to the data

for experiment CS8G (see table 5.5) are given in table 5.6.

Table 5.6 Calculated K' values, from equation 5.32, for $g(t) = \exp(-K't)$ using the data for experiment CS8G given in table 5.5

K' from I(1)—I(2)=0.014	K' from I(1) —I(3)=0.011 K' from I(2) —I(3)=0.009	K'from I(1)—I(4)=0.008 K'from I(2)—I(4)=0.007 K' from I(3)—I(4)=0.005

The nomenclature used in this table is defined by equation 5.30

In passing if all the combinations of the integrals were used a 4 x 4 symmetric array would be obtained, the diagonal elements of which would be zero. Hence all the possible non-zero K' values are obtainable by examining only combinations of i and i^* in equation 5.30 where $i < i^*$.

Examination of the K' values in table 5.6 shows $\exp(-K't)$ to be unsatisfactory since there is a $\pm$ 60% divergence in the calculated K' values from their mean. To obtain information on an improved form of the poisoning function from the nature of these divergences one must return to equation 5.30 which shows that each K' found was obtained by equating two areas under a time against g(t) graph. Graphs 5.4 and 5.5 display the information from the first row and the diagonal elements in table 5.6 respectively.

The interpretation of Graphs 5.4 and 5.5 is similar to that for the results from the initial rate technique, see graph 5.3 and section 5.2.5, the only difference being that in the fractional life method areas are considered instead of gradients. Hence graph 5.5 shows the closest fit to the areas under the correct form of g(t) since consecutive points are considered, therefore from graph 5.5 it is clear that the type of function required for g(t) must decrease rapidly near t = O and slowly

A graphical interpretation of the fractional life time technique applied to the data in table 5.6 ($\exp(-K't)=g(t)$).

GRAPH 5.4

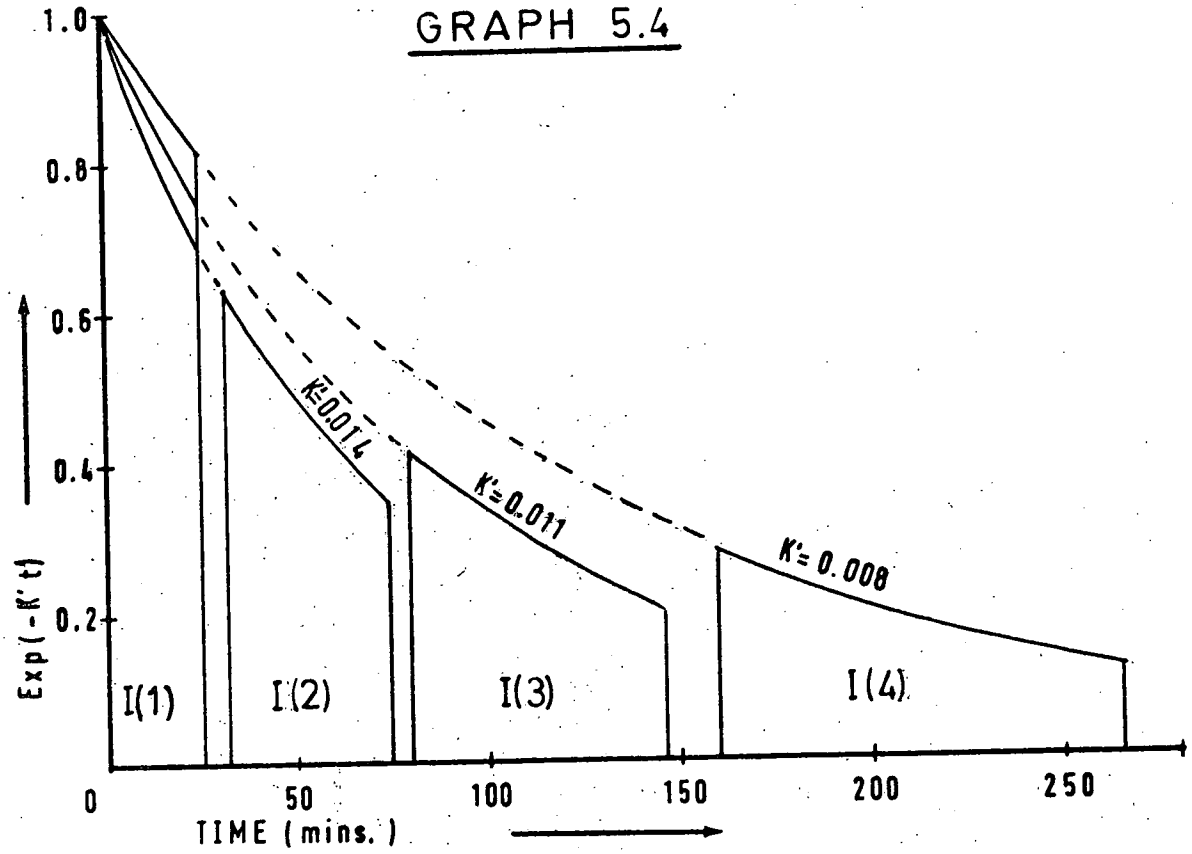

GRAPH 5.5

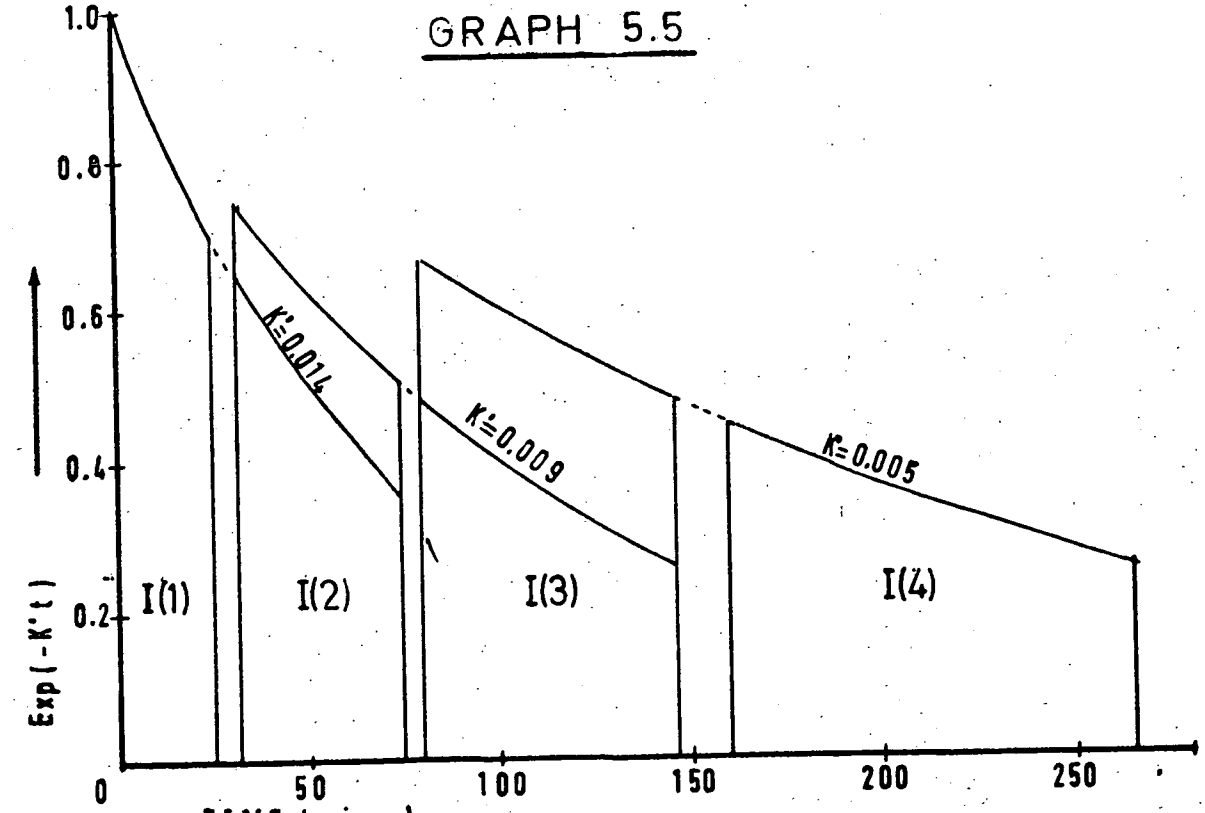

thereafter, which is in agreement with the conclusions from section 5.2.5, see Fig. 5.1.

5.2.7. The initial rate and fractional life time methods for $g(t) = \exp(-K' t^{\frac{1}{2}})$

From the conclusions reached in sections 5.2.5 and 5.2.6 the next model tried for g(t) was $\exp(-K' t^{\frac{1}{2}})$. Since this function was satisfactory it was adopted as the poisoning function in all later calculations. The application of both techniques to experimental data will be summarised in the following section.

In order to apply the initial rate method for isolating g(t), for the poisoning function $\exp(-K' t^{\frac{1}{2}})$, $\exp(-K' t^{\frac{1}{2}})$ is substituted into 5.10 whence:

$$R_A / R_B = \exp(-K'(t_B^{\frac{1}{2}} - t_A^{\frac{1}{2}})) \qquad 5.33$$

Solution of 5.33 for K' for runs i and j gives

$$^{i}_{j}K = \frac{2.303 \log (R_i / R_j)}{(t_j^{\frac{1}{2}} - t_i^{\frac{1}{2}})}, \qquad 5.34$$

the same nomenclature being used in 5.34 as in 5.26.
If $\exp(-K' t^{\frac{1}{2}})$ is satisfactory then all the $^{i}_{j}K$ values found for a series of consecutive runs will be identical.

The application of equation 5.34 to the experimental results will be dealt with in the following section.

To apply the fractional life time method to $g(t) = \exp(-K' t^{\frac{1}{2}})$ this function is substituted into equation 5.27 and integrated

$$Q(K')=O=\frac{2\exp(-K't^{\frac{1}{2}})}{K'}\left(t^{\frac{1}{2}}+\frac{1}{K'}\right)\Bigg|_{t_j}^{t_i} - \frac{2\exp(-K't^{\frac{1}{2}})}{K'}\left(t^{\frac{1}{2}}+\frac{1}{K'}\right)\Bigg|_{t_j^*}^{t_i^*}, \qquad 5.35$$

where the nomenclature used is identical to that in 5.19.

In order to complete the integration of 5.35 conveniently a new function, $Z(X, K)$ is defined:

$$Z(X, K') = \frac{2\exp(-K' X^{\frac{1}{2}})}{K'} \left(X^{\frac{1}{2}} + \frac{1}{K'} \right) \qquad 5.36$$

Hence expanding 5.35 in terms of 5.36 :-

$$Q(K') = Z(t_i, K') - Z(t_j, K') - Z(t_i^*, K') + Z(t_j^*, K') \qquad 5.37$$

(c.f. equation 5.31)

To solve the transcendental equation 5.37 use is made of the Newton-Raphson method for successive approximations to a root of an equation, hence K' is found, using the computer program outlined in Appendix 9, by equation 5.32 where,

$$\frac{\partial(Q(K'_n))}{\partial K'_n} = \frac{\partial(Z(t_i, K'_n))}{\partial K'_n} - \frac{\partial(Z(t_j, K'_n))}{\partial K'_n} - \frac{\partial(Z(t_i^*, K'_n))}{\partial K'_n} + \frac{\partial(Z(t_j^*, K'_n))}{\partial K'_n} \qquad 5.38$$

(K'_n being the n^{th} approximation to K')

and where

$$\frac{\partial Z(X, K'n)}{\partial K'_n} = - \frac{2\exp(-K'_n X^{\frac{1}{2}})}{K'_n} \left(X + \frac{X^{\frac{1}{2}}}{K'_n} + \frac{2}{K'^2_n} \right) \qquad 5.39$$

Hence to use equation 5.32, 5.39 is substituted into 5.38 for each of the four t values and 5.38 is in turn substituted into 5.32.

5.2.8. Application to the data from the consecutive run experiments of the initial rate and fractional life time techniques for the isolation of g(t) where $g(t)=\exp(-K't^{\frac{1}{2}})$.

The data for the consecutive run experiments for furan hydrogenations over 5% Pt/pumice catalysts is summarised in the following four tables. t_i and t_j are the times at which the $\frac{i+1}{2}^{th}$ reaction starts and when it reaches a Z^{th} reaction of the furan, Z being the fractional life used for that series of consecutive runs.

R_L is the initial rate of reaction of the furan in mole percent/min. and P_F^o and P_H^o are the initial furan and hydrogen pressures respectively.

Table 5.7 Data from the consecutive run experiment CS8C. Fractional life = 0.16. Reaction temperature = 45.1 °C, Weight of catalyst = 0.3601 g

RUN L	i	j	t_i(min.)	t_j(min.)	P_F^o(mm. Hg)	P_H^omm. Hg	R_L
1	1	2	0.0	13.9	11.6	151.6	3.84
2	3	4	30.0	55.1	11.4	148.8	1.18
3	5	6	91.1	154.5	11.2	149.1	0.38
4	7	8	160.0	308.0	10.9	148.0	0.22

Table 5.8 Data from the consecutive run experiment CS8E. Fractional life used = 0.16, reaction temperature = 30.2 °C, Weight of catalyst = 0.3211 g

RUN L	i	j	t_i(min.)	t_j(min.)	P_F^o(mm. Hg)	P_H^omm. Hg	R_L
1	1	2	0.0	26.0	8.1	52.6	0.79
2	3	4	35.0	77.6	7.8	50.6	0.46
3	5	6	95.0	164.5	8.4	52.4	0.27
4	7	8	180.0	293.0	8.1	50.3	0.147

Table 5.9 Data from the consecutive run experiment CS8G. Fractional life used = 0.20, reaction temperature = 30.9 °C, Weight of catalyst = 0.4016 g

RUN L	i	j	t_i(min.)	t_j(min.)	P_F^o(mm. Hg)	P_H^o(mm. Hg)	R_L
1	1	2	0.0	25.6	12.9	72.2	1.2
2	3	4	32.2	74.6	12.4	69.5	0.65
3	5	6	80.0	146.2	13.1	74.2	0.40
4	7	8	160.0	265.3	12.6	71.3	0.24

Table 5.10 Date from the consecutive run experiment CS8H. Fractional life used = 0.12. Reaction temperature = 23.2 °C, Weight of catalyst = 0.4121 g.

RUN L	i	j	t_i(min.)	t_j(min.)	P_F^o(mm. Hg)	P_H^o(mm. Hg)	R_L
1	1	2	0.0	16.0	13.7	95.0	1.11
2	3	4	35.0	61.0	13.3	91.3	0.645
3	5	6	91.0	129.0	14.0	94.8	0.407
4	7	8	150.0	202.0	13.4	91.7	0.336
5	9	10	250.0	306.0	13.5	93.2	0.245

The results from the application of the initial rate method for isolating g(t) to the data given above is summarised in the following four tables. The model used was $g(t) = \exp(-K' t^{\frac{1}{2}})$. The ${}^{i}_{j}K$'s calculated were found using equation 5.34.

Table 5.11 ${}^{i}_{j}K'$'s found for the i^{th} and j^{th} runs of experiment CS8C (see table 5.7) by the initial rate method.

j	${}^{1}_{j}K'$	${}^{2}_{j}K'$	${}^{3}_{j}K'$
2	0.22	-	-
3	0.24	0.28	-
4	0.23	0.24	0.18

Average value for the poisoning constant = 0.23 ± 0.06

Table 5.12 ${}^{i}_{j}K'$'s found for the i^{th} and j^{th} runs of experiment CS8E (see table 5.8) by the initial rate method.

j	${}^{1}_{j}K'$	${}^{2}_{j}K'$	${}^{3}_{j}K'$
2	0.092	-	-
3	0.11	0.14	-
4	0.11	0.13	0.12

Average value for the poisoning constant = 0.12 ± 0.03

Table 5.13 ${}^{i}_{j}K'$'s found for the i^{th} and j^{th} runs of experiment CS8G (see table 5.9) by the initial rate method.

j	${}^{1}_{j}K'$	${}^{2}_{j}K'$	${}^{3}_{j}K'$
2	0.11	-	-
3	0.13	0.15	-
4	0.12	0.14	0.13

Average value for the poisoning constant = 0.13 ± 0.02

Table 5.14 ${}^{i}_{j}K'$'s formed for the i^{th} and j^{th} runs in experiment CS8H (see table 5.10) by the initial rate method.

j	${}^{1}_{j}K'$	${}^{2}_{j}K'$	${}^{3}_{j}K'$	${}^{4}_{j}K'$
2	0.092	-	-	-
3	0.105	0.127	-	-
4	0.098	0.096	0.071	-
5	0.096	0.100	0.084	0.094

Average value of the poisoning constant = 0.096 ± 0.02

Examination of tables 5.11 to 5.14 shows that $\exp(-K' t^{\frac{1}{2}})$ is a satisfactory model for g(t) since the errors in the poisoning constants never exceed $\pm$ 30% for the temperatures at which the above consecutive reactions were carried out. Little would be gained by attempting to improve the model for g(t) further on the strength of the initial rate data since there was an uncertainty of approximately $\pm$ 15% in determining the individual initial rates.

It is interesting to contrast the percent divergences in the poisoning constants obtained using $g(t) = \exp(-K' t^{\frac{1}{2}})$ with those for the next best poisoning function obtained, $\exp(-K't)$, (see tables 5.14 and 5.4 respectively for the application of these two models to experiment CS8H). The divergences for the latter model are five times greater than for $\exp(-K' t^{\frac{1}{2}})$.

To examine model VI more closely the fractional life time method for isolating g(t) is applied to the experimental data in tables 5.7 to 5.10. The values of the poisoning constants, which were found using the computer program outlined in Appendix 9 applied to the equations in section 5.2.7, are listed in tables 5.15 to 5.18. The nomenclature used in the following four tables is the same as is used in equation 5.30.

Table 5.15 Poisoning constants for experiment CS8C (see table 5.7) found by the fractional life time technique.

I(1)-I(2) gives K'=0.146	I(1)-I(3) gives K'=0.177 I(2)-I(3) gives K'=0.205	I(1)-I(4) gives K'=0.187 I(2)-I(4) gives K'=0.207 I(3)-I(4) gives K'=0.210

Average value of the poisoning constant = 0.189 ± 0.043

Table 5.16 Poisoning constants for experiment CS8E (see table 5.8) found by the fractional life time technique.

I(1)-(2)gives K'=0.123	I(1)-I(3)gives K'=0.124 I(2)-I(3)gives K'=0.125	I(1)-I(4)gives K'=0.123 I(2)-I(4)gives K'=0.124 I(3)-I(4)gives K'=0.120

Average value of the poisoning constant = 0.123 ± 0.003

Table 5.17 Poisoning constants for experiment CS8G (see table 5.9) found by the fractional life time technique.

I(1)-I(2)gives K'=0.130	I(1)-I(3)gives K'=0.137 I(2)-I(3)gives K'=0.138	I(1)-I(4)gives K'=0.135 I(2)-I(4)gives K'=0.138 I(3)-I(4)gives K'=0.132

Average value of the poisoning constant = 0.135 ± 0.005

Table 5.18 Poisoning constants for experiment CS8H (see table 5.10) found by the fractional life time technique.

I(1)-I(2):- K'=0.114	I(1)-I(3):- K'=0.110 I(2)-I(3):- K'=0.106	I(1)-I(4):- K'=0.111 I(2)-I(4):- K'=0.109 I(3)-I(4):- K'=0.114	I(1)-I(5):-K'=0.106 I(2)-I(5):-K'=0.103 I(3)-I(5):-K'=0.102 I(4)-I(5):-K'=0.093

Average value of the poisoning constant = 0.107 ± 0.014

Tables 5.15 to 5.18 show that the divergence in K' from its average value for each set of consecutive runs to be less than 15% with the exception of run CS8C where the divergence is approximately 20%, these figures are only slightly larger than the errors expected due to experimental error. However, examination of the diagonal elements in the above four tables do show a consistent trend (again with the exception of CS8C, table 5.15) which suggests that an improved function for g(t) could be found. Using reasoning similar to that in sections 5.2.5 and 5.2.6 the results from both the initial rate and fractional life time methods for resolving K' suggest that $\exp(-K' t^{\frac{1}{2}})$ decreases too quickly at both high and very low values of t. However, since the deviations are small little would be gained by altering the function further.

The constancy of the values for K' obtained for each run, particularly using the fractional life technique, indicate that both techniques are feasible for the study of poisoning. Furthermore the values of the poisoning constants for a given consecutive run experiment found by the two techniques agree within 12% except for experiment CS8C where they differ by about 17%, both values lying within the individual percentage deviations for the respective experiments.

As expected from the results of preliminary hydrogenations of furan the size of the poisoning constant appears to increase with increasing temperature (the poisoning becomes more severe). This temperature dependence will be dealt with in greater detail in section 5.4.

It should be stressed that the expression $g(t) = \exp(-K' t^{\frac{1}{2}})$ is an empirical function and as such is only open to limited interpretation. Moreover, as has been mentioned in section 5.3.1, in finding g(t) it has been assumed that $f(P_F)$ remains unchanged throughout the reaction. Hence strictly speaking g(t) describes the decreasing activity of the catalyst and any change

that might be occurring in $f(P_F)$ with time. However, if one assumes an unchanging $f(P_F)$ and K_F it is interesting to note that the form of g(t) chosen implies an inhomogeneous surface since the probability of an adsorbed furan molecule poisoning an active site decreases with increasing poisoning. (In contrast $g(t) = \exp(-K' t)$ implies a homogeneous surface where the probability of an adsorbed molecule poisoning an active site is independent of time).

5.3 The determination of the pressure function, $f(P_F)$.

Having obtained an optimum expression for g(t) in section 5.2 which represents the reduction in catalytic activity of a Pt/pumice catalyst as a function of time it is now possible to study the underlying kinetics of the furan hydrogenation, represented by the function $f(P_F)$, with the masking effect of the poisoning removed. The rate equation used is

$$\frac{dP_F}{dt} = -K_F f(P_F). \exp(-K' t^{\frac{1}{2}}) \qquad 5.40$$

Since the products of the reaction do not appear to affect the kinetics (section 5.1) simple models which have only furan and hydrogen pressures as variables were tried. Furthermore it was assumed for simplicity, as in section 5.1, that $f(P_F)$ did not alter during the reaction.

The pressure function was studied using three techniques. First, by use of computer programs which simulated the reaction, see Appendix 10, the model for $f(P_F)$ which fulfilled equation 5.40 being adopted. Second, by an initial rate method applied to data from consecutive hydrogenations over the same catalyst sample and third by a fractional life time method also using data from consecutive reactions.

5.3.1 Models for $f(P_F)$ experimented with.

Since it has been shown that the detectable products of a furan hydrogenation do not affect the kinetics of the reaction the models tried used only the furan and hydrogen pressures as variables. The most successful model was of the form

$$f(P_F) = P_H^n \quad P_F^m \qquad 5.41$$

However a model based on a Langmuir-Hinshelwood adsorption isotherm (ref. 79) was examined briefly. The derivation of this model is as follows:-

The adsorption-desorption isotherms for furan and hydrogen are represented respectively by

$$K_1 P_F (1 - \theta_F - \theta_H) = K_2 \theta_F \qquad 5.42$$

and

$$K_3 P_H (1 - \theta_F - \theta_H) = K_4 \theta_H \qquad 5.43$$

(where θ_F and θ_H are the fractions of the catalyst's surface covered by adsorbed furan and hydrogen respectively and K_1, K_2, K_3 and K_4 are the rate constants for the adsorption and desorption of furan and hydrogen respectively).

Solution of equations 5.42 and 5.43 for θ_F and θ_H yields

$$\theta_F = K_A P_F/(1 + K_A P_F + K_B P_H) \qquad 5.44$$

and

$$\theta_H = K_B P_H/(1 + K_A P_F + K_B P_H) \qquad 5.45$$

(K_A and K_B are K_1 / K_2 and K_3 / K_4 respectively, these ratios being the equilibrium constants for the adsorption of the two gases).

But since the rate of reaction is proportional to the fraction of the surface covered by each species then the following expression is obtained for $f(P_F)$ from equations 5.44 and 5.45.

$$f(P_F) = \theta_F \theta_H = K_A K_B P_F P_H / (1 + K_A P_F + K_B P_H)^2 \qquad 5.46$$

Rather than test the model for $f(P_F)$ outlined by equation 5.46 it was decided to simplify the model further for a preliminary study. Since it has already been shown that furan adsorbs strongly (section 4.5.4) the equilibrium constant for its adsorption must be large, hence a reasonable approximation to 5.46 is

$$f(P_F) = \theta_F \theta_H = K_A K_B P_F P_H / (K_A P_F + K_B P_H)^2 \qquad 5.47$$

which becomes, on dividing the numerator and denominator of the right hand side throughout by K_A,

$$f(P_F) = K_B P_F P_H / (P_F + K_C P_H)^2 \qquad 5.48$$

(where $K_C = K_B / K_A$)

As is shown in the following section equation 5.48 was not sufficiently satisfactory to merit an investigation of the model outlined by equation 5.47. Both models for $f(P_F)$ were tested using a simulation program, the conclusion being that not only does the optimum form of 5.41 fit the experimental data more satisfactorily than of 5.48 but it also is more in keeping with a system where furan is strongly adsorbed relative to hydrogen.

5.3.2 The simulation technique for resolving $f(P_F)$

The experiments designed to be used for finding $f(P_F)$ by use of the rate simulation computer programs outlined in Appendix 10 consisted of pairs of consecutive reactions (e.g. experiments CR10A and CR10B). The poisoning constant K^1 was found first by applying the fractional life time technique given in section 5.2.7, to both reactions, in this way reducing the number of unknowns by one. The rate constant K_F and the

remaining unknowns in $f(P_F)$ were then found by applying the simulation technique to the second of the consecutive runs, using equation 5.40.

Both simulation programs operate by solving the differential equation 5.40 for the rate constant K_F, using a trial model for $f(P_F)$, at each pair of data points, i.e., when a sample is taken. The solution for K_F is achieved by rearranging 5.40 and integrating :

$$K_F = -\left(\int_{i^{P_F}}^{j^{P_F}} \frac{dP_F}{f(P_F)} \right) \Big/ \int_{t_i}^{t_j} \exp(-K' t^{\frac{1}{2}}).\, dt. \qquad 5.49$$

(where j^{P_F} and i^{P_F} are the furan pressures at times t_j and t_i respectively).

The denominator of the right hand side of equation 5.49 is found using the closed form of the integral;

$$\frac{2}{K'} \left((t_j^{\frac{1}{2}} + \frac{1}{K'}).\exp(-K' t_j^{\frac{1}{2}}) - (t_i^{\frac{1}{2}} + \frac{1}{K'}).\exp(-K' t_i^{\frac{1}{2}}) \right) \qquad 5.50$$

The numerator however is integrated numerically, hence increasing the flexibility of the programs. Clearly if the correct model has been chosen the K_F values calculated should be identical within experimental error since when g(t) was redefined in section 5.1 as the product of the fraction of active surface remaining unpoisoned at time t and the ratio of the rate constant at time t to the initial value of K_F, any changes which might occur during the reaction to K_F have been allowed for (providing the form of $f(P_F)$ is not time dependent). In other words the K_F in all the equations in this chapter is, strictly speaking, the initial value of the rate constant.

The programs make allowances for reaction vessel pressure drops caused by removal of samples for analysis and changes in the product distributions. The experimental data may either be read directly into the programs or approximated to by a least squares Chebyshev polynomial incorporated in one of the simulation programs, as subroutine CHEB (Appendix 6), the latter method being superior provided sufficient data points are available since the Chebyshev polynomial, see Appendix 6, smoothes out random errors.

The simulation technique has two advantages over the more conventional initial rate and fractional life time methods. First, a furan hydrogenation can be studied up to 100% reaction while the other two methods are limited to about 20% reaction unless a technique for storing large numbers of samples is available. Second, as has been mentioned, the integration performed on the pressure function is carried out using a general technique, hence many models for $f(P_F)$ may be examined within a relatively short space of time.

The major disadvantages of the simulation technique is that it assumes $f(P_F)$ and $g(t)$ are not affected by the extent of reaction. However it will be shown later that the values for the poisoning constant calculated from short consecutive reactions differ by only 10% from those calculated, using a simulation program, for long single runs. All three techniques for examining $f(P_F)$ have the disadvantage that they assume that the pressure function itself is not time dependent.

The experimental data used for the application of the simulation technique for the examination of $f(P_F)$ for furan hydrogenations over Pt/pumice catalysts is summarised below in table 5.19.

Table 5.19 Summary of the data from the consecutive run experiments CR10A and CR10B for use in the study of $f(P_F)$ by the simulation technique for furan hydrogenations over 5% Pt/pumice.

Experiment	CR10A		CR10B	
Reaction temperature, ^oC	47.2		46.3	
Catalyst weight, g	0.6101		0.6311	
Initial furan pressures, mm. Hg	17.2		13.6	
Initial hydrogen pressure, mm. Hg	101.2		60.9	
Poisoning constant, K'	0.21		0.22	
sample	run	CR10A2	run	CR10B2
i	t_i	MF_i	t_i	MF_i
o	25.5	1.000	22.3	1.000
1	40.2	0.889	44.2	0.861
2	65.3	0.785	62.5	0.825
3	100.4	0.682	78.1	0.766
4	130.3	0.606	135.2	0.690
5	151.3	0.586	180.2	0.645
6	197.3	0.548	211.4	0.629
7			271.4	0.601
8			985.5	0.421

t_i is the time at which the i^{th} sample is taken, at which time the mole fraction of furan remaining unreacted is MF_i.

On applying the simulation technique to the data summarised in the above table it was found that the simple model defined by equation 5.41 was the most satisfactory, see table 5.20. In investigating this form of $f(P_F)$ it was found convenient to vary only one order at a time, hence when investigating the furan order, n, the hydrogen order was kept constant at 1.0

(yielding an optimum furan order which lay between 0.1 and 0.3) while when examining the hydrogen order, n, the furan order was maintained at 0.0 (yielding an optimum hydrogen order of between 0.9 and 1.2). Hence the form of $f(P_F)$ finally adopted was

$$f(P_F) = K_F P_H^{1.0} P_F^{0.2} \qquad 5.51$$

(When integrating the reciprocal of the pressure function, $f(P_F)$ in the simulation programs, see equation 5.49, the hydrogen pressure was expressed in terms of the furan pressure using equation A8.10 in Appendix 8).

The above orders are in agreement with those expected for a system obeying the Rideal-Eley mechanism or one of its variants, for instance where the hydrogen is adsorbed in the interstices between a layer of strongly adsorbed furan, (see ref. 78), the situation originally envisaged by Rideal, that furan is strongly adsorbed on 5% Pt/pumice has already been shown, see section 4.5.4.

The optimal form of equation 5.48 was found to be

$$f(P_F) = K_B P_F P_H / (P_F + 0.5P_H)^2 \qquad 5.52$$

which suggests that the ratio of the equilibrium constants of hydrogen to furan is approximately 0.5. This is not in keeping with strong adsorption of furan.

Table 5.20 compares the results of the application of the simulation program RATESIM 6 (appendix 10) to the data for run CR10B2, see table 5.19. (The criterion by which the validity of a model is tested is the constancy of the calculated constants, the rate constant for model 5.51 and the product of the rate constant and the equilibrium constant for the adsorption of hydrogen for model 5.52)

Table 5.20 Rate constants for the furan hydrogenation over 5% Pt/pumice, run CR10B2, calculated using the simulation program RATESIM 6 (using subroutine CHEB) for

A $f(P_F) = P_H^{1.0} \; P_F^{0.2}$

Sample	$10^4 \times K_F$ found using 'segmented integrals'	$10^4 \times K_F$ found using 'weighted integrals'	$10^4 \times K_F$ found using 'normal integrals'
1	34.0	34.0	34.0
2	32.6	33.8	33.6
3	29.5	32.2	33.2
4	30.6	32.0	33.0
5	32.4	32.0	32.9
6	34.8	32.9	32.9
7	38.9	33.7	33.0
8	108.9	47.2	36.2
Normalised Standard deviation	1.086	0.138	0.023

B $f(P_F) = K_B P_F P_H / (P_F + 0.5 P_H)^2$

	$K_F \times K_B$ using 'segmented integrals'	$K_F \times K_B$ using 'weighted integrals'	$K_F \times K_B$ using 'normal integrals'
1	1.09	1.09	1.09
2	0.92	1.02	1.04
3	0.80	0.97	1.01
4	0.69	0.93	0.97
5	0.65	0.89	0.94
6	0.73	0.88	0.92
7	0.93	0.89	0.92
8	2.02	1.21	1.11
Normalised Standard deviation	0.426	0.111	0.070

Comparison of the calculated constants in table 5.20A with those in 5.20B shows that equation 5.51 fits the data better than the corresponding Langmuir-Hinshelwood model for the pressure function except at very long reaction times (the last sample was taken after the reaction had proceeded for over 19 hrs.) The difference between the two models is seen most clearly by examination of the constants calculated using segmented integrals which, as is pointed out in Appendix 10, provide the most delicate test. Since most of the reactions studied were only followed up to reaction times of less than 6 hrs. the breakdown of equation 5.53 at large values of t does not affect the bulk of the current research hence the following model was adopted to represent the rate equation.

$$-\frac{dP_F}{dt} = K_F P_H^{1.0} . P_F^{0.2} \exp(-K' t^{\frac{1}{2}}) \qquad 5.53$$

The cause of the failure of 5.53 at large t is thought to be caused by g(t) (which is only empirical in nature) only being applicable to reactions lasting for less than 5 to 6 hrs. rather than the pressure function collapsing due to the furan's pressure dropping to such a degree that a change in its order occurs. The rate equation 5.53 had already failed for run CR10B2 when the calculated furan partial pressure was 7 mm. Hg however, on applying the simulation programs to faster single reactions (section 5.4) it was shown that their kinetics could be adequately represented by 5.53 down to partial pressures of furan of 4 mm. Hg, provided this pressure were reached within 5 hrs. (e.g. runs C7B1, C10F, C10H1 and C10L1).

In the remainder of section 5.3 the furan and hydrogen orders are found by two other independent techniques.

5.3.3 Introduction to the determination of the order of reaction with respect to hydrogen pressure for the hydrogenation of furan.

Examination of $f(P_F)$ by the simulation technique shows that the pressure function is adequately represented by equation 5.41 and hence experiment CR10C, consisting of a set of five consecutive hydrogenations over the same catalyst sample, was designed to find the order of reaction, given the symbol n, with respect to hydrogen pressure. The first two runs of CR10C which had the same initial reactant pressures, were used to determine the poisoning constant K' by the fractional life time method outlined in section 5.2.7 while the remaining three reactions, which had identical initial furan pressures ($\pm$ 0.3mm.Hg) but differing initial hydrogen pressures, together with the first two reactions were processed by either the initial rate or fractional life time methods to yield n. The experimental data for experiment CR10C is summarised in table 5.21.

Table 5.21 Experimental data for the consecutive run experiment CR10C to find the order with respect to hydrogen for a furan hydrogenation over 5% Pt/Pumice.

RUN L	i	j	R_L	t_i(min.)	t_j(min.)	P_H^o (mm.Hg)	P_F^o(mm.Hg)	C
1	1	2	1.10	0.0	16.6	104.2	12.8	0.138
2	3	4	0.542	83.2	60.1	101.2	12.5	0.137
3	5	6	0.256	85.5	126.0	76.3	13.0	0.100
4	7	8	0.372	171.0	235.2	160.7	12.8	0.212
5	9	10	0.235	225.0	311.8	130.3	12.6	0.175

R_L is the initial rate of the L^{th} run (mole percent reaction of furan/min.), t_i is the time at which the $\left(\frac{i+1}{2}\right)^{th}$ run starts, t_j is the time at which 5% of the hydrogen has reacted in the $j/2^{th}$ run, at which time a C^{th} of the furan has been consumed and

P_H^o and P_F^o are the initial hydrogen and furan pressures respectively. The reaction was carried out at 28.2°C over 0.367 g catalyst.

5.3.4 Initial rate method to find the hydrogen order for experiment CR10C.

The rate of reaction of a furan hydrogenation is given by the expression obtained by substituting equation 5.41 into equation 5.40 :

$$\frac{dP_F}{dt} = -K_F P_H^n P_F^m \exp\left(-K' t^{\frac{1}{2}}\right) \qquad 5.54$$

or, by making use of equation 5.13

$$\frac{d(\%\ \text{furan reacted})}{dt} = \frac{100.K_F P_H^n P_F^m \exp(-K' t^{\frac{1}{2}})}{P_F^o} \qquad 5.55$$

Rewriting equation 5.55 for the initial conditions of the L^{th} reaction starting at time t_i minutes :

$$R_L = K_F \left(P_H^o\right)^n \left(P_F^o\right)^{m-1} \exp(-K' t_i^{\frac{1}{2}}) \qquad 5.56$$

But for all the runs making up experiment CR10C the initial furan pressure was constant to within $\pm$ 0.3 mm.Hg partial pressure and furthermore the value of K' was found to be 0.20 by applying the fractional order technique, outlined in section 5.2.7, to reactions CR10C1 and CR10C2. Hence equation 5.56 may be rewritten as a proportionality applicable to all the runs which comprise experiment CR10C :

$$R_L \propto \left(P_H^o\right)^n \exp\left(K' t_i^{\frac{1}{2}}\right) \qquad 5.57$$

Using the data in table 5.21 a graph of $(R_L / \exp(-0.2\, t_i^{\frac{1}{2}}))$ against the initial hydrogen pressure for the L^{th} run was plotted, graph 5.6. Since an approximately straight line was obtained the hydrogen order is approximately unity which is in agreement with the results from the stimulation technique (section 5.3.2.)

As a further check the poisoning constants were calculated assuming the hydrogen order to be unity by a method similar to that outlined in section 5.2.7. In brief the ratio of the initial rates for runs A and B is given by equation 5.58, derived from the proportionality 5.57.

$$R_A / R_B = ({}_AP^o_H / {}_BP^o_H) \exp(-{}^A_BK'(t_A^{\frac{1}{2}} - t_B^{\frac{1}{2}})) \qquad 5.58$$

(Where ${}_AP^o_H$ and ${}_BP^o_H$ are the initial partial pressures of hydrogen for runs A and B starting at times t_A and t_B respectively, ${}^A_BK'$ is the poisoning constant found from data for runs A and B).

Solution of 5.58 for ${}^A_BK'$ gives

$${}^A_BK' = \frac{2.303}{(t_B^{\frac{1}{2}} - t_A^{\frac{1}{2}})} \text{ Log } ({}_{A\,B}P^o_H / {}_{B\,A}P^o_H) \qquad 5.59$$

The ${}^A_BK'$ values for experiment CR10C are given in the following table.

Table 5.22 ${}^i_jK'$ values for experiment CR10C found using equation 5.59.

(a consecutive run hydrogenation of furan at 28.2°C over 5% Pt/pumice)

j	${}^1_jK'$	${}^2_jK'$	${}^3_jK'$	${}^4_jK'$
2	0.120			
3	0.124	0.123		
4	0.116		0.097	
5	0.112			0.130

Average K' from the above diagonal elements = 0.117 ± 0.020

GRAPH 5.6

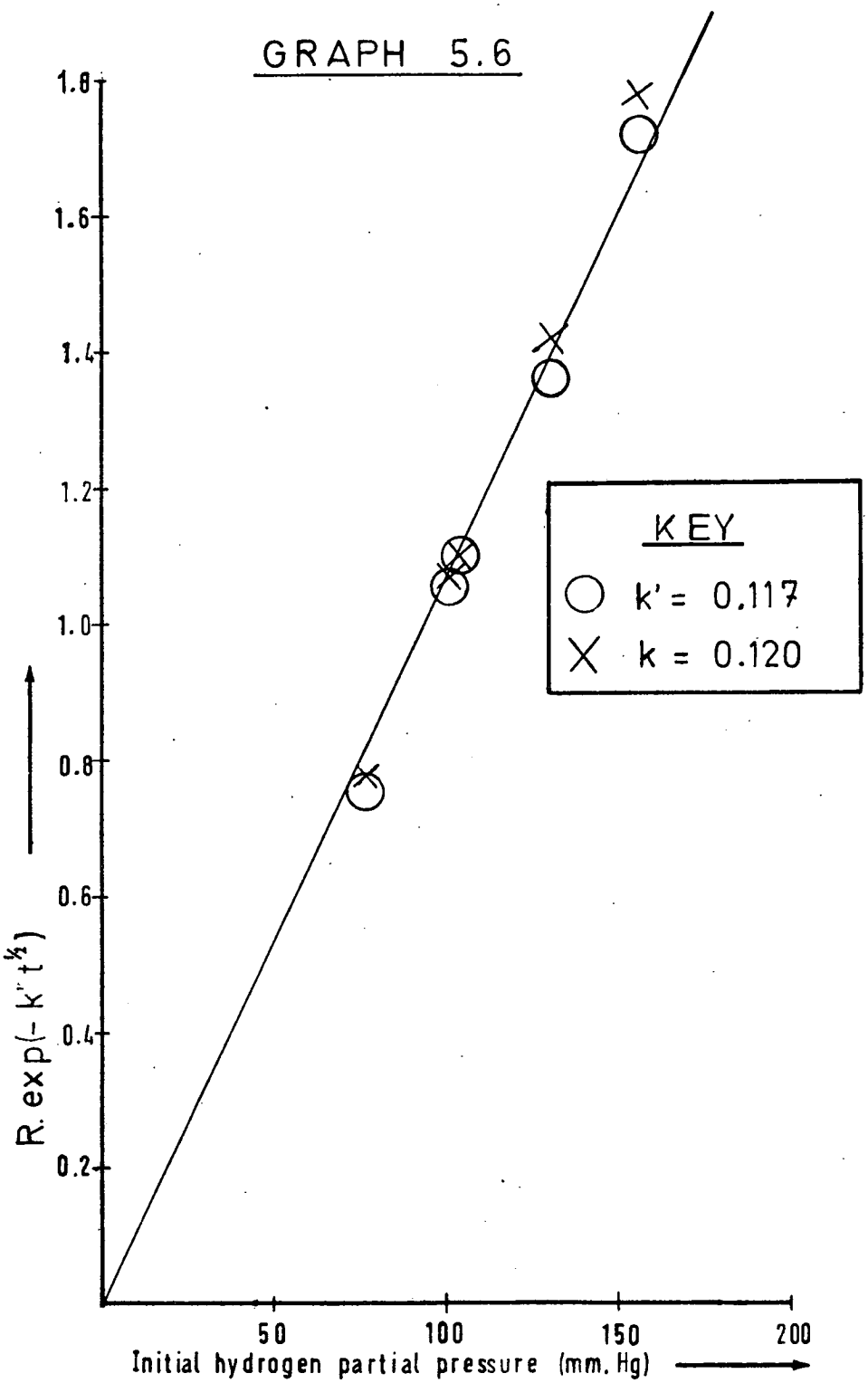
1.8
1.6
1.4
1.2
1.0
0.8
0.6
0.4
0.2
R. exp(- k' t½)
KEY
k' = 0.117
k = 0.120
50
100
150
200
Initial hydrogen partial pressure (mm. Hg)

The above results confirm that the order in hydrogen is one for the hydrogenation of furan. A further graph of $R_L / \exp(-K' t_i^{\frac{1}{2}})$ against the initial hydrogen pressure, where K' was 0.117, obtained above, was plotted (graph 5.6) giving a straight line.

5.3.5 Fractional life method for determining the order in hydrogen for experiment CR10C.

It is not feasible to apply the isolation technique (ref. 80), such as was originated by W. Ostwald, to experiment CR10C in order to simplify the determination of the order with respect to hydrogen since this method would require that the partial pressure of furan used would be sufficiently large in comparison with that of hydrogen such that the furan pressure could be taken as constant. Not only would such conditions diverge too far from the experimental conditions actually used in all the furan hydrogenations performed but more important it is experimentally unfeasible to find the percent reaction from analysis data with any accuracy unless between 10 to 15% reaction of furan has occurred, hence the furan pressure cannot be considered to be constant. (Furthermore, since on hydrogenation each mole of furan requires approximately 2.5 moles of hydrogen, the minimum initial ratio of the partial pressures of hydrogen to furan would be approximately 1 : 4, which is not small enough for the isolation technique to operate). Hence it is necessary to assume an order for furan, the results from the simulation programs (section 5.3.2) suggest an order of 0.2, an order of zero* was used for simplicity. Equation 5.54 becomes :

$$- \frac{dP_F}{dt} = K_F P_H^n \exp(-K' t^{\frac{1}{2}}) \qquad 5.60$$

* If the order with respect to furan, m, is close to zero P_F^m will to all intents and purposes remain constant, which is the condition required for the isolation technique.

Differentiating equation A8.10 with respect to furan pressure :

$$\frac{dP_H}{dP_F} = \text{constant} = B = 4 - F_2 - F_3 \quad , \qquad 5.61$$

where F_2 and F_3 are the product distributions (mole fractions) of tetrahydrofuran and n-butanol respectively.

Hence combining equations 5.60 and 5.61

$$-\frac{dP_H}{dt} = -\frac{dP_F}{dt} \cdot \frac{dP_H}{dP_F} = B\,K_F P_H^n \exp\left(-K' t^{\frac{1}{2}}\right) \qquad 5.62$$

Rearranging and integrating 5.62 :

$$-\int_{P_H^o}^{(1-Z)P_H^o} dP_H / P_H^n = B\,K_F \int_{t_k}^{t_j} \exp(-K' t^{\frac{1}{2}}).\,dt. \qquad 5.63$$

Where t_j is the time at which a Z^{th} of the hydrogen has reacted, t_i is the time at which the run started, P_H^o is the initial hydrogen pressure and Z is the fractional life time of hydrogen.

For n = 1 completion of the integration gives :

$$2.303 \log (1-Z) = -2BK_F \frac{\exp(-K' t^{\frac{1}{2}})}{K'} \left(t^{\frac{1}{2}} + \frac{1}{K} \right) \Bigg|_{t_i}^{t_j} \qquad 5.64$$

Since hydrogen pressures are not measured directly but are calculated from the furan partial pressures (Appendix 8) it is necessary to be able to find the fraction of furan reacted when a Z^{th} of the hydrogen has been consumed in order to find the t_j values needed for the solution of equation 5.64.

Rewriting equation A8.10 :

$$P_H = A + BP_F \qquad 5.65$$

(where A and B are $P^o_H - P^o_F B$ and $4 - 2F_2 - F_3$ respectively, F_2 and F_3 being the product distributions, / mole percent, of tetrahydrofuran and n-butanol respectively, see Appendix 8).

Solving 5.65 for P_F:

$$P_F = (P_H - A) / B \qquad 5.66$$

But since at a Z^{th} reaction of hydrogen its partial pressure is

$$P_H = (1 - Z)\, P^o_H , \qquad 5.67$$

therefore substituting for P_H in 5.66 using 5.67 and dividing by the initial furan pressure :

$$E = ((1 - z)\, P^o_H - A) / BP^o_F \qquad 5.68$$

(E is the fraction of unreacted furan at a Z^{th} reaction of the hydrogen).

Hence the time at which a Z^{th} of the hydrogen has reacted is the time at which an E^{th} of the furan remains unreacted (E being given by equation 5.68 and t_j found from a time/fraction of furan unreacted graph).

If the hydrogen and furan orders are one and approximately zero respectively then, from equation 5.64, $(t^{\frac{1}{2}} + 1/K')\exp(K' t^{\frac{1}{2}}) \Big|_{t_i}^{t_j}$ will be independent of the initial hydrogen pressure for the series of consecutive runs CR10C, table 5.23 shows this to be the case.

Table 5.23 Data from the application of the fractional life method to experiment CR10C (see table 5.21) for the determination of the hydrogen order.

(Furan hydrogenation over 5% Pt/pumice, fractional life used, Z, = 0.05, K' = 0.12, furan and hydrogen orders are approximately zero and 1.0 respectively)

t_i min.	t_j min.	P^o_H mm. Hg.	P^o_F mm. Hg	$\int_{t_i}^{t_j} \exp(-K't^{\frac{1}{2}})dt$
0.0	16.6	104.2	12.8	0.724
32.2	60.1	101.2	12.5	0.746
85.5	126.0	76.3	13.0	0.711
171.2	235.2	160.7	12.8	0.701
225.3	311.8	130.3	12.6	0.734

Average value of the above integrals = 0.723 ± 0.023
(normalised standard deviation = 0.022)

Table 5.23 confirms the order with respect to hydrogen is unity.

5.3.6 The order in furan for a furan hydrogenation

Experiment CR10D was designed to determine the order of furan with respect to the rate of hydrogenation of furan. The experiment consists of four consecutive reactions carried out over the same catalyst sample, 5% Pt/pumice, at the same reaction temperature, the first two runs having the same initial furan and hydrogen pressures ($\pm$ 1.5%) while the following two runs have the same initial hydrogen pressure but differing initial furan pressures, see table 5.42. The poisoning constant K' was found by applying the technique outlined in section 5.2.7 to the first two reactions while all four runs were studied by both the initial rate and fractional life time techniques.

The value of K', the poisoning constant, was found to be 0.26

Table 5.24 Experimental data for experiment CR10D, consecutive furan hydrogenations at 53.5°C over 0.301 g 5% Pt/pumice (K' = 0.26).

RUN L	i	j	t_i min.	t_j min.	P^o_H mm. Hg	P^o_F mm. Hg	R_L mole %/min
1	1	2	0.0	13.9	201.6	20.4	2.2
2	3	4	30.0	83.6	203.2	20.8	0.47
3	5	6	90.0	162.0	202.2	10.5	0.29
4	7	8	175.0	293.4	206.1	6.2	0.21

5.3.7 Initial rate and fractional life time techniques for the determination of the furan order for experiment CR10D.

Since the initial hydrogen pressures are constant to within $\pm$ 1.5% the initial rates of the four runs in CR10D obey the proportionality

$$R \quad \alpha \quad (P^o_F)^{m-1} \quad \exp(-K' t^{\frac{1}{2}}) \ , \qquad 5.69$$

derived from equation 5.54 (t is the time at which the reaction starts)

If the order with respect to furan, m, is approximately zero as is indicated by the simulation experiments (section 5.3.2) then 5.69 becomes

$$R \quad \alpha \quad \exp(-K' t^{\frac{1}{2}}) \ / \ P^o_F \qquad 5.70$$

Since Graph 5.7 of $K' t^{\frac{1}{2}}$ against the natural logarithm of $(R. P^o_F)$ is approximately linear, m is approximately zero.

As can be seen from table 5.24 the initial hydrogen pressures for all the runs in experiment CR10D are large in comparison with the initial furan pressure, hence it is possible to

GRAPH 5.7

For experiment CR10D

INITIAL RATE METHOD FOR FURAN'S ORDER

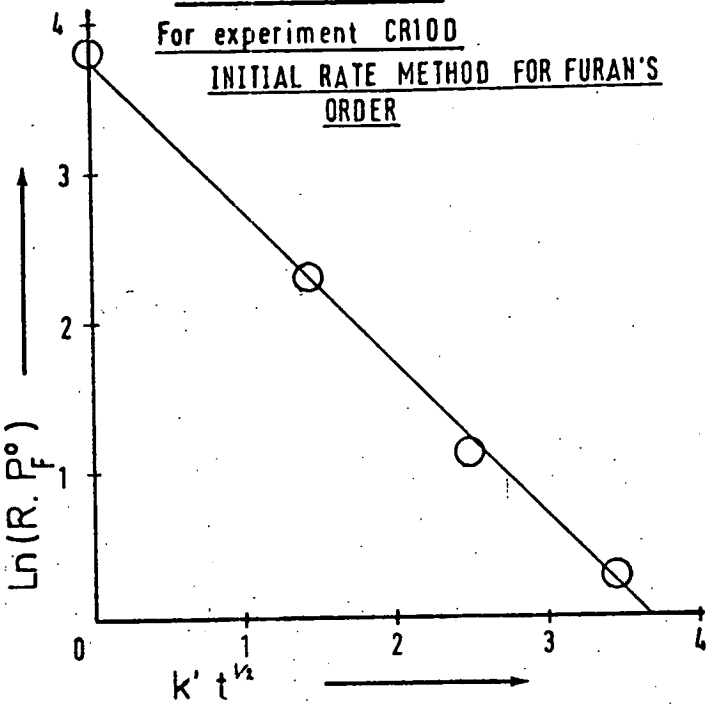

GRAPH 5.8

FRACTIONAL LIFE METHOD FOR FURAN ORDER

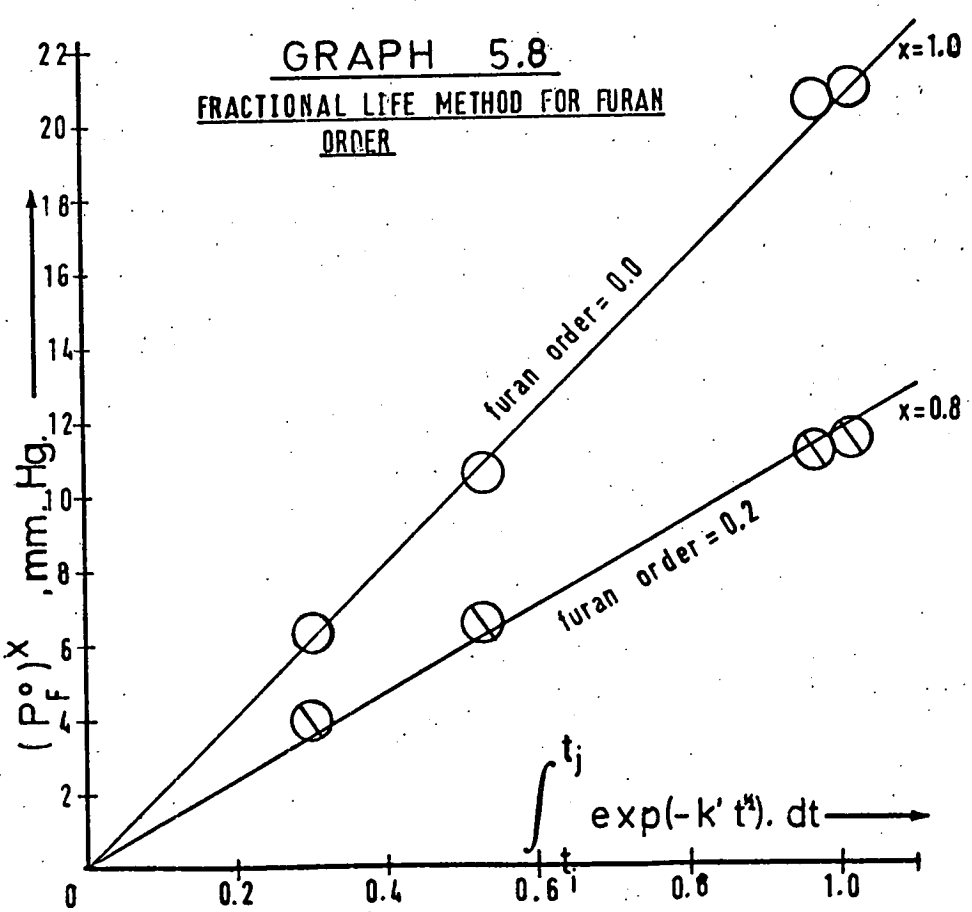

use the isolation technique (ref. 80) in order to reduce the number of variables when finding furan's order by the fractional life technique since the hydrogen pressure may be taken as being constant during a reaction. Hence rearrangement of equation 5.54 followed integration gives

$$\frac{1}{(P_H^o)^n} \int_{P_F^o}^{(1-Z)P_F^o} \frac{dP_F}{P_F^m} = -K_F \int_{t_i}^{t_j} \exp(-K' t^{\frac{1}{2}}).dt \quad , \qquad 5.71$$

where Z is the fraction of furan reacted at time t_j min.

If, as is indicated by the rate simulation programs, the furan order, m, is approximately zero then for m = zero equation 5.71 becomes

$$P_F^o \; Z/(P_H^o)^n = -\frac{2K_F}{K'} \left((t^{\frac{1}{2}} + \frac{1}{K'}) \exp(-K' t^{\frac{1}{2}}) \right) \Bigg|_{t_i}^{t_j} \qquad 5.72$$

Hence, since the initial hydrogen pressures are constant ($\pm$ 1.5%) the initial furan pressures will be proportional to the integral with respect to time, equation 5.72. Graph 5.8, using the data in table 5.25, shows this to be the case, therefore the order with respect to furan is confirmed to be approximately zero.

Table 5.25 Fractional life analysis using equation 5.72 to verify that the order with respect to furan is approximately zero, data from the furan hydrogenations CR10D (also see table 5.24)

($K' = 0.26$, $Z = 0.16$, reaction temperature = 53.5°C)

t_i min.	t_j min.	P_H^o mm. Hg	P_F^o mm. Hg	$\int_{t_i}^{t_j} \exp(-K' t^{\frac{1}{2}}).dt$
0.0	13.9	201.6	20.4	0.97
30.0	83.6	203.2	20.8	1.04
90.0	162.0	202.2	10.5	0.528
175.0	293.4	206.1	6.2	0.303

If the furan order were assumed to be 0.2 rather than zero equation 5.72 would have been

$$-0.8(P_F^o)^{0.8}\frac{(1-(1-Z)^{0.8})}{(P_H^o)^n} = K_F\int_{t_i}^{t_j}\exp(-K' t^{\frac{1}{2}}).dt. \qquad 5.73$$

If this order were correct $(P_F^o)^{0.8}$ would be proportional to the integral of the poisoning function. Graph 5.8 shows that the difference between an order of zero and of 0.2 is small, both graphs are linear within experimental error, hence the rate equation used in subsequent analyses is that given by equation 5.53.

5.4 Kinetic analysis of single furan hydrogenations.

Once the general form for the poisoning function had been determined in section 5.2 it was possible to proceed to the investigation of the pressure function $f(P_F)$ which was found by various independent techniques to be $P_F^{0.2}\ P_H^{1-0}$, section 5.3. If one assumes that the pressure function is independent of the reaction temperature, 22°C to 95.5°C was the range covered by hydrogenations over Pt/pumice catalysts, then a more detailed study of the reaction kinetics may now be achieved by applying the simulation programs (Appendix 10) already used in section 5.3.2 to the single furan-hydrogen reactions using the model for the rate equation given by equation 5.53. Examination of this equation shows that there are only two unknowns, the rate constant K_F and the poisoning constant K'. However, since the simulation programs calculate K_F from the data and the form of the rate equation under investigation, using the constancy of these calculated values as a criterion of the validity of the rate equation, the number of unknowns is effectively reduced to one, the poisoning constant.

The advantage of this form of analysis over the consecutive run experiments is that a large number of reactions may be processed in a short space of time, and furthermore one is not tied to the rather artificial conditions imposed by the consecutive run experiments which only investigate reactions up to about 20% reaction of the furan.

The following two tables summarise all the values of the poisoning constants and the rate constants respectively.

Table 5.26 Poisoning constants, K', for furan hydrogenations over Pt/pumice.

Experiment.	K'(initial rate method).	K'(fractional life method).	K'(simulation method).	Reaction temperature °C.	Additive to reaction mixture.
C10F1	-	-	0.090	22.0	-
CS8H	0.096	0.107	-	23.2	-
C8G1	-	-	0.128	23.2	THF
C10J1	-	-	0.122	26.0	SYLVAN
C8F1	-	-	0.130	27.5	-
CR10C	-	0.120	-	28.2	-
CS8E	0.117	0.123	-	30.2	-
C10M1	-	-	0.130	30.5	SYLVAN
CS8G	0.130	0.136	-	30.9	-
C10E1	-	-	0.195	42.6	-
CS8C	0.230	0.190	-	42.6	-
C10H1	-	-	0.190	46.0	-
C7B1	-	-	0.220	46.2	-
CR10A	-	0.22	-	46.3	-
C10B1	-	-	0.230	46.4	-
C8A1	-	-	0.245	46.4	-
C10C1	-	-	0.255	47.2	n-PROPANOL
CR10B	-	0.21	-	47.2	-
C10L1 *	-	-	0.105	48.5	BENZENE
CR10D	0.230	0.260	-	53.5	-
C1001	-	-	0.315	60.2	SYLVAN
C10A1	-	-	0.320	62.5	n-HEXENE
C8H1	-	-	0.320	65.2	-
C8D1	-	-	0.645	95.5	-

* As mentioned previously it is thought that an error was made in recording this reaction temperature (it was probably 23°C).

Table 5.27 Rate constants, K_F's, for furan hydrogenations over 5% Pt/pumice.

Experiment	$10^3 . K_F$, $(mm.Hg)^{-0.2}$ g^{-1} catalyst	Reaction temperature (^oC)	additive to reaction mixture
C10F1	2.82	22.0	-
C8G1	2.51	23.2	THF
C8F1	2.99	27.5	-
C10E1	5.66	42.6	-
C10H1	6.13	46.0	-
C7B1 **	4.98	46.2	-
C10B1	5.61	46.4	-
C8A1	4.13	46.4	-
C10C1	5.57	47.2	n-PROPANOL
C10L1 *	2.47	48.5	BENZENE
C10A1	9.02	62.5	n-HEXENE
C8H1	8.91	65.2	-
C8D1	44.0	95.5	-

* As mentioned previously it is thought that the reaction temperature for this run was actually 23^oC.

** 10% Pt/pumice catalyst.

5.4.1 The poisoning constants, K'.

Graph 5.9 of reaction temperature against the poisoning constant (data taken from table 5.27) shows clearly that the poisoning constant increases with the reaction temperature, this relationship being implied by the increasingly severe poisoning observed with increasing temperature (shown qualitatively by graph 4.2). Graph 5.9 shows this relationship to be linear to a first approximation, or to be more specific the poisoning constant is given by

$$K' = 2.47 \times 10^{-2} + T \times 2.87 \times 10^{-3} + T^2 \times 2.82 \times 10^{-5} \qquad 5.74$$

GRAPH 5.9

Furan's poisoning constant as a function of the reaction temperature

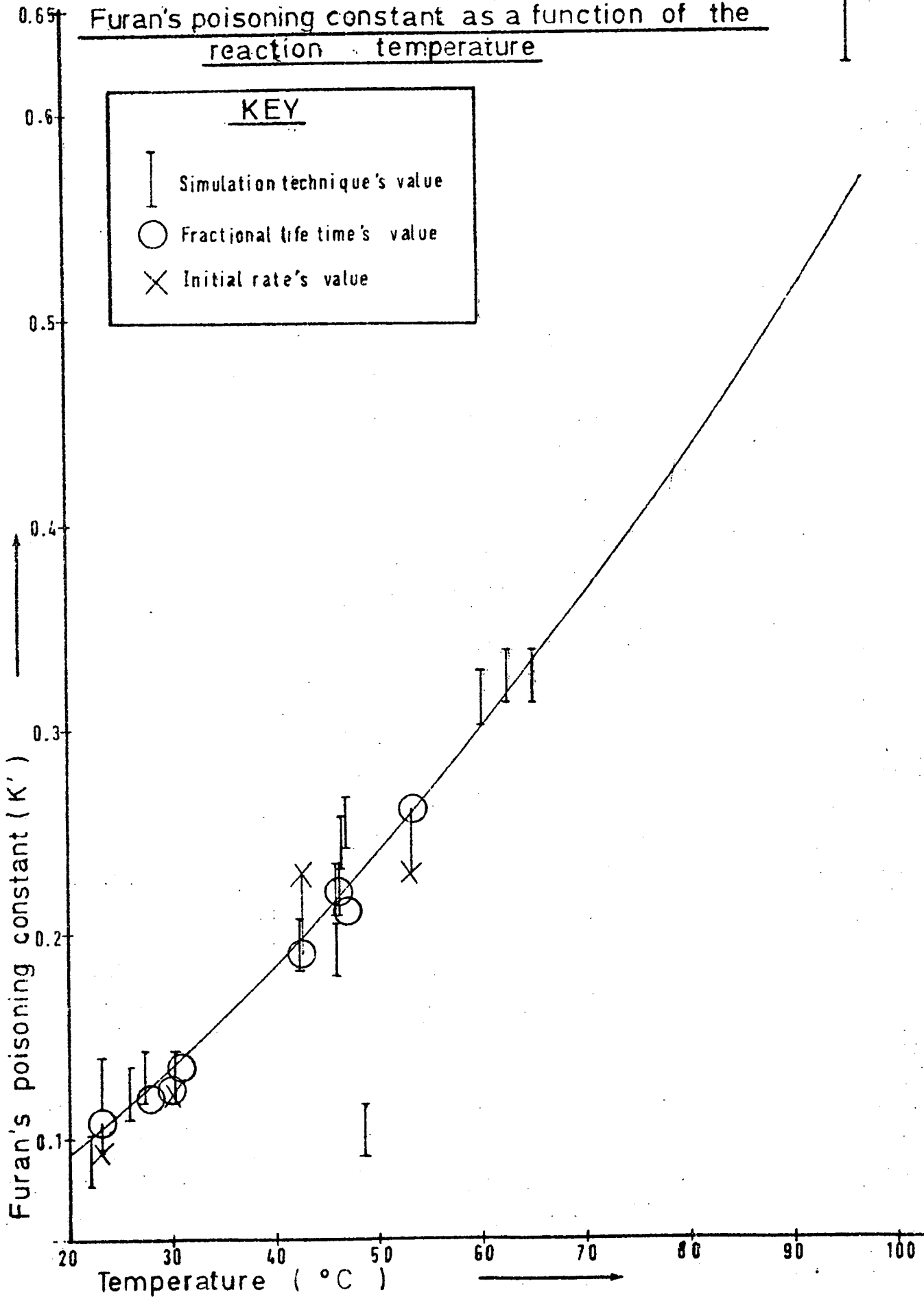

where T is the reaction temperature in ^{o}C. Relationship 5.74 was found using the Chebyshev curve fitting program described in appendix 6 applied to the data in table 5.26.

It is interesting to note that nearly all the values of K' can be predicted, within the limits of the experimental accuracy, by equation 5.74 regardless of whether there is any additive to the reaction mixture. Hence addition of n-hexene, n-propanol, tetrahydrofuran or sylvan to a furan-hydrogen mixture does not affect the rate of poisoning. The anomalous furan hydrogenation C10L1, where benzene had been added to the reaction mixture, has already been shown in chapter 4 (using evidence from the observed product distributions) to have been probably carried out at $23^{o}C$, not as recorded, at $48.5^{o}C$. This supposition is strengthened by the value of K' of 0.105, found using the simulation program, since this corresponds closely to the expected value at $23^{o}C$. Since the poisoning constant does not appear to be affected by additives to the reaction mixture one may conclude that the gaseous detectable products of a furan hydrogenation are not the cause of the observed poisoning.

The similarity of the values of the poisoning constants obtained by the simulation technique applied to single runs and those from the consecutive run experiments, as is illustrated by graph 5.9, shows the latter experiments to be suitable for the study of both $f(P_F)$ and $g(t)$ for furan hydrogenations. However it is worth pointing out that the K' 's obtained from the consecutive run experiments tend, on average, to be about 10% lower than their counterparts obtained by the simulation technique.

5.4.2 The furan rate constant K_F.

As with the poisoning constants table 5.27 shows that the rate constants increase with the reaction temperature and that they do not appear to be affected by additives to the reaction mixture. The anomalous behaviour of benzene as an additive in reaction C10L1 has already been explained as being due to the reaction temperature being probably recorded incorrectly as 48.5°C (the correct value should be 23°C), the evidence coming not only from a second hydrogenation, C10L2, of furan with benzene as an additive, but also from the product distributions, poisoning constant and rate constant, all corresponding to a reaction temperature of 23°C.

The activation energy for the furan-hydrogen reaction was calculated by making use of the Arrhenius equation (ref. 81),

$$K_F = Z \exp (- E_A / RT) , \qquad 5.75$$

Z is the pre-exponential factor, E_A the activation energy (cals.) and T the reaction temperature (K).

Taking natural logarithms of 5.75 :

$$\mathrm{Ln}K_F = - E_A / RT + M Z \qquad 5.76$$

A least squares best straight line library program was applied to the points on graph 5.10 whereby the activation energy (7.5 K.cals. $mole^{-1}$, standard deviation = 1.1 K.cals. $mole^{-1}$) and the natural logarithm of the pre-exponential factor Z (6.6 sec^{-1}, standard deviation = 0.9 sec^{-1}) were computed from the gradient and the point at which the line crosses the Y axis respectively, see equation 5.76. The value for the activation energy is similar to the literature value of 8.0 K.cals. $mole^{-1}$ (ref. 82) for the hydrogenation of furan in acetic acid over PtO_2 but clearly since these reaction conditions differ so greatly

GRAPH 5.10

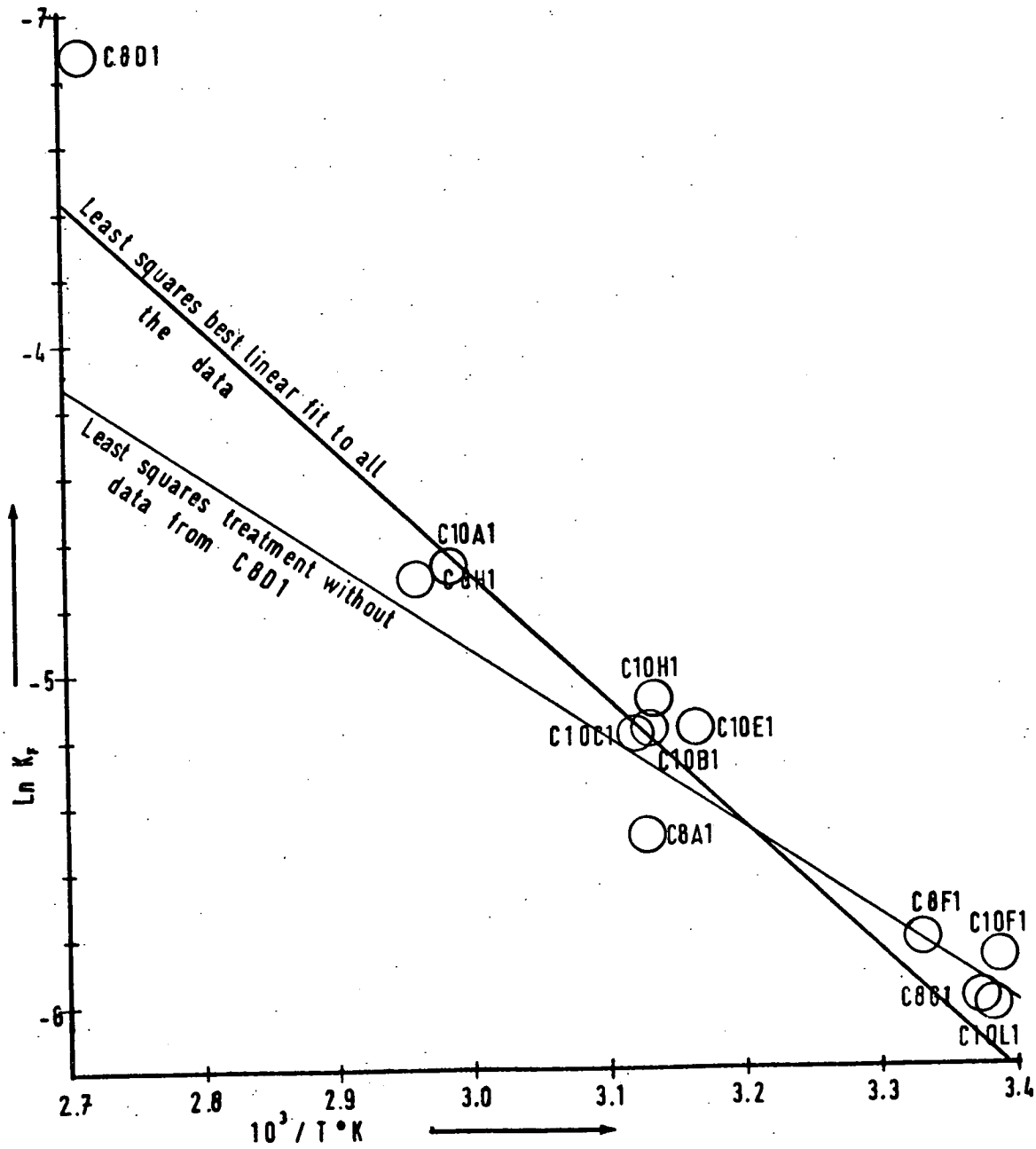
-7
-4
-5
-6
Ln K_r
C8D1
Least squares best linear fit to all the data
Least squares treatment without data from C8D1
C10A1
C8H1
C10H1
C10C1
C10E1
C10B1
C8A1
C8F1
C10F1
C8G1
C10L1
2.7
2.8
2.9
3.0
3.1
3.2
3.3
3.4
10^3 / T °K

from those used in the present work this agreement of the values for the activation energies is coincidental.

On examining graph 5.10 it might at first sight be advantageous to ignore the point corresponding to a reaction temperature of 95.5°C since this appears to be anomalous. However, on recalculating the activation energy from the data for the remaining eleven points it was found to be 5.4 K.Cals. $mole^{-1}$ with a standard deviation of 1.3 K.Cals.$mole^{-1}$. Hence by omitting the one apparently anomalous data point the percentage uncertainty in the activation energy is almost doubled (which stresses the importance of using as large a temperature range as possible when attempting to find activation energies).

5.5 Analysis of single sylvan hydrogenations.

Rather than repeat the process outlined in the sections 5.2 to 5.4 for sylvan hydrogenations the form of both the pressure and poisoning functions were assumed to be the same as for furan since furan and sylvan are so similar chemically. Hence the rate equation used for sylvan was

$$\frac{dP_S}{dt} = - K_S P_S^{0.2} P_H^{1.0} \exp (- K'' t^{\frac{1}{2}}) \qquad 5.77$$

P_S is the sylvan partial pressure, mm.Hg, K_S the rate constant for a sylvan hydrogenation and K'' is the poisoning constant for the sylvan reaction (notice the similarity of 5.77 and 5.53). If 5.77 is satisfactory one may immediately apply the simulation programs to the single sylvan hydrogenations thus determining K_S and K''. Should 5.77 not represent the kinetics of a furan-hydrogen reaction no value of K'' inserted into the simulation program will give constant values for the rate constant K_S (see Appendix 10), fortunately, as is illustrated by table 5.28 model 5.77 is satisfactory.

Table 5.28 K_S values (rate constants) for single sylvan hydrogenations over 5% Pt/pumice calculated by the simulation program 'RATESIM 6' (Appendix 10) applied to equation 5.77.

	C10I1		C10P1		C10C1	
reaction temperature, °C	23.2		41.2		49.5	
weight of catalyst, g.	0.3916		0.4211		0.5008	
initial sylvan pressure (mm.Hg)	11.0		12.6		18.3	
initial hydrogen pressure (mm.Hg)	53.2		60.0		91.0	
optimum poisoning constant	0.083		0.235		0.280	
sample	A	B	A	B	A	B
1	2.02	10.3	5.26	15.2	6.11	20.2
2	2.09	31.3	5.16	40.3	6.03	45.2
3	2.19	97.3	5.19	51.3	5.92	86.3
4	2.08	127.3	5.17	65.3	6.01	130.4
5	2.09	180.3	5.19	120.8	5.97	180.4
6	2.12	215.4	5.21	150.4	6.06	222.4
7	2.16	275.4	5.28	200.4	8.02	386.4
8	-	-	30.15	891.5	-	-
standard deviation of K_S values (normalised)	0.021		0.856 (0.01 without last reading)		0.112 (0.01 without last reading)	

A = 10^3. K_S /g. of catalyst, $(mm.Hg)^{-0.2}$. $min.^{-1}$ (found using 'normal' integrals)

B = Time at which the sample was taken, min.

Comparison of table 5.28 with tables 5.27 and 5.26 shows that the poisoning and rate constants for the sylvan-hydrogen reactions increase more sharply with increasing reaction temperature than their counterparts for the analagous furan reactions. This is confirmed in the following chapter where

simultaneous hydrogenations of these two furans are discussed.

The stronger temperature dependence of the sylvan hydrogenations' rate constant implies that the activation energy for these reactions is greater than for furan hydrogenations (as was found to be the case for hydrogenations over PtO_2 in acetic acid, ref. 82).

5.6 Summary and Conclusions.

The kinetics of a furan or sylvan hydrogenation are described by a rate equation consisting of the product of two functions, one, a function of time only (g(t)), representing the decrease in the catalyst's activity due to poisoning occurring, the other (f(P)) representing the underlying kinetics of the reaction governed by the partial pressures of the reactants. It has been shown in this chapter that both g(t) and f(P) may be determined and that the resulting rate equation takes the form

$$\frac{dP_R}{dt} = K_R P_H^{1.0} P_R^{0.2} \exp(-K' t^{\frac{1}{2}}), \qquad 5.78$$

P_R is the partial pressure of the furan which has a poisoning constant K' and a rate constant K_R. Equation 5.78 being applicable for reaction times of up to five hours and for furan partial pressures exceeding 2 mm. Hg. for hydrogen partial pressures in the order of 50 mm. Hg. The rate equation 5.78 is characteristic of a system where a furan is adsorbed much more strongly than the hydrogen.

In order to achieve the separation and elucidation of f(P) and g(t) a series of experiments and techniques were developed, falling into two categories, the consecutive run experiments and the simulation techniques. The consecutive run experiments and their ancilliary techniques for processing the data which they provide may be divided into two sets, the CS series (section 5.2) which enable g(t) to be studied without

requiring any knowledge of the nature of f(P) and the CR series (section 5.3) which make it possible to examine f(P) once the general form of g(t) has been found. The simulation techniques are not only used to find an optimum form of f(P) (section 5.3) but also to study large numbers of hydrogenations in a short space of time (sections 5.4 and 5.5) once the general form of the rate equation has been found.

The two best proofs that the above techniques, which are based on widely differing principles, do work satisfactorily is that they yield complimentary results and that the activation energy may be calculated for the furan hydrogenations from 22°C to 95.5°C over 5% Pt/pumice, comparing well with the literature value (section 5.4.2) even though heavy poisoning is occurring in most of the reactions used for its determination.

A further indication that furan-hydrogen reactions are first order in hydrogen and approximately zero order in furan is that the mole percent reaction of furan against time graphs for two furan hydrogenations carried out at the same temperature using differing initial reactant pressures are almost identical, a correction being made for any differences in the weights of catalyst used. For an example see graph 4.9 of two pairs of furan hydrogenations, C10B1 and C10A1 and C10F1 and C8G1 , carried out at 46°C and approximately 23°C respectively. In Appendix 11 it is shown that this is indicative of the kinetics used.

To recap, g(t) is defined as a function which relates the dependence on time of the combination of the fraction of active surface remaining unpoisoned and the change, if any, in the rate constant. That this function is not dependent upon the partial pressures of the reactants is illustrated by the fact that reactions carried out at the same temperature but having differing initial partial pressures of reactants have similar poisoning

constants (for example the CRC and CRD series). That g(t) is purely empirical in nature is stressed by the method by which it was found, outlined in the block diagram in the beginning of section 5.2. Hence, that it provides a fit for the true poisoning function only over a limited range of reaction times is not surprising (it is satisfactory from t = O to about five hours after which it appears to decrease faster than the actual poisoning function). Furthermore, it is the very empirical nature of g(t) which makes its interpretation meaningless, except in general terms. However, it is perhaps worth pointing out that if one assumes that the rate constant remains unchanged throughout a reaction then the probability of an adsorbed furan molecule poisoning the catalyst's active surface is a function of time for $g(t) = \exp (- K' t^{\frac{1}{2}})$, implying an inhomogeneous surface ($g(t) = \exp (- K' t)$ would imply a homogeneous surface).

In section 5.4.1 and 5.4.2 it was shown that addition of n-hexene, tetrahydrofuran, benzene or n-propanol to a reaction mixture of furan and hydrogen does not affect either the poisoning constant (and hence the rate of poisoning) or the rate constant (and hence the rate of reaction of an adsorbed furan molecule). It is hence deduced that none of the gaseous detectable products of a furan-hydrogen reaction are the cause of the poisoning and therefore these products do not adsorb strongly on the platinum surface of the catalyst. However, furan hydrogenations over 5% Pt/SiO_2 show that considerable adsorption of the product does occur over these catalysts (section 4.3.2) which substantiates the hypothesis put forward in chapter 4 that the bulk of the adsorption of the products, in particular the n-butanol, occurs on the silica support rather than on the platinum itself. A further piece of evidence to support this theory is that little adsorption per unit area of catalyst occurs over the Pt/pumice catalysts (section 4.5.2) compared with that for Pt/SiO_2 catalyst (contrast the adsorption

observed for furan hydrogenations over approximately 50 m^2 of Pt/pumice catalyst, run C7B1, with that for 12 m^2 of Pt/SiO_2, run C6H1). The conclusion is that adsorption occurring over Pt/SiO_2 occurs on the support and further that pumice is not an efficient adsorbant for the products of furan hydrogenations.

While the cause of the observed poisoning is not known it is thought to be caused in part by the polymerisation of the furan at acid sites on the pumice support (which explains why the pumice catalysts are the most prone to poisoning) and on to some degree over the platinum, the latter reaction being catalysed by traces of HCl (ref. 76) formed during the reduction of the catalyst. The acid catalysed polymerisation of furan is known to be accelerated by increasing the reaction temperature (ref. 76) which is in agreement with the temperature dependence of the poisoning observed for furan hydrogenations (section 5.4.1).

Whatever the cause of the poisoning the techniques outlined in this chapter make it feasible to study the kinetics of poisoned reactions in depth.

Chapter 6

Simultaneous hydrogenations of furan and sylvan over 5% Pt/pumice

Theoretically the most effective method for finding the relative rates of hydrogenation of two compounds is to carry out both reactions simultaneously over the same catalyst sample. By this means possible errors introduced by differences in the properties of catalyst samples and, of lesser importance, by differences in the reaction temperatures and displacement of the catalyst in the reaction vessel are eliminated. Clearly such a technique is most readily applicable to the hydrogenation of two compounds whose surface coverage is small since in such a case neither compound will have a measurable effect on the other's kinetics (providing they are mutually inert).

Furan-sylvan hydrogenations suffer from the drawback that both these reactants adsorb strongly (section 5.6) and hence compete for the catalyst surface, therefore it is necessary to separate the relative strengths of adsorption of the two furans from their relative rates in order to obtain useful information about their relative reactivities. A second difficulty presented by the system investigated is that the hydrogenation of either reactant poisons the catalyst, both compounds poisoning at different rates.

6.1 The calculation of the relative rates of hydrogenation of furan and sylvan.

Nomenclature :-

θ_F Fraction of the active catalyst surface covered by furan

θ_S Fraction of the active catalyst surface covered by sylvan

α Fraction of the active catalyst surface poisoned by furan

β Fraction of the active catalyst surface poisoned by sylvan

P_F Furan pressure (mm. Hg)

P_S Sylvan pressure, mm. Hg

P_H Hydrogen pressure, mm. Hg

K_1 Rate constant for furan adsorption

K_2 Rate constant for furan desorption

K_3 Rate constant for sylvan adsorption

K_4 Rate constant for sylvan desorption

K' Furan's poisoning constant

K'' Sylvan's poisoning constant

6.1.1 General form of the rate equations used.

Before proceeding with the mathematical analysis of simultaneous hydrogenations of furan and sylvan it is necessary to examine the implications of the high surface coverage of a catalyst by a furan during its hydrogenation (section 5.6). Furan itself will be used as an example though the following arguments also apply to sylvan.

At the start of a reaction

$$\theta_F = 1 , \qquad 6.1$$

since the proportion of the surface covered by hydrogen or the products of the reaction is negligible compared with furan (section 5.6). However, as the reaction proceeds an increasing proportion of the catalyst's active surface is poisoned by the hydrogenation, hence 6.1 becomes

$$\theta_F = 1 - \alpha \qquad 6.2$$

(In other words the furan covers all the catalyst surface which remains unpoisoned). But in chapter 5 g(t) was defined as the fraction of the catalyst's surface remaining unpoisoned (the

dependence of g(t) on K_F is ignored here since it neither affects nor is germain to the argument) which is shown by 6.2 to equal θ_F. Hence the general form of the rate equation 5.4 may be re-written as

$$\frac{dP_F}{dt} = - K_F \theta_F f(P_F) . \qquad 6.3$$

But $f(P_F)$ was shown (section 5.3) to be $P_F^{0.2} P_H^{1.0}$, hence 6.3 may be expressed as

$$\frac{dP_F}{dt} = - K_F \theta_F P_F^{0.2} P_H^{1.0} \qquad 6.4$$

If both furan and sylvan adsorb strongly, react at similar sites and do not interfere with each other's hydrogenations when both are reacting at the same time with hydrogen then one may assume that equation 6.4 applies equally to single and simultaneous hydrogenations. That they both adsorb strongly was shown in Chapters 4 and 5 while that they react on similar sites seems probable since they are structurally and chemically very similar. The assumption that they do not interfere with each other's hydrogenations when reacting simultaneously is shown to probably be the case by the fact that the product distributions for either compound's hydrogenation is the same, for a given reaction temperature, whether the other furan is present or not (section 4.5.1). Therefore the two rate equations used for the simultaneous hydrogenation of furan and sylvan over the same catalyst sample are 6.4 and its analog for the consumption of sylvan :-

$$\frac{dP_S}{dt} = - K_S \theta_S P_S^{0.2} P_H^{1.0} \qquad 6.5$$

θ_S and θ_F are found by applying the Langmuir isotherm (ref. 79) to the adsorption and desorption of furan and sylvan. Equating the rates of adsorption and desorption for the two compounds yields 6.6 and 6.7 respectively :-

$$K_1 (1 - \theta_F - \theta_S - \alpha - \beta) P_F = K_2 \theta_F \qquad 6.6$$

$$K_3 (1 - \theta_F - \theta_S - \alpha - \beta) P_S = K_4 \theta_S \qquad 6.7$$

(In the derivation of the above two equations the coverage by hydrogen or the products is assumed to be neglibible, c.f. equation 6.2 for the hydrogenation of a single furan).

Solving 6.1 and 6.2 for θ_F and θ_S respectively :-

$$\theta_F = \frac{K_1}{K_2} P_F(1 - \theta_S - \alpha - \beta)/(1 + \frac{K_1}{K_2} P_F) \qquad 6.8$$

$$\theta_S = \frac{K_3}{K_4} P_S(1 - \theta_F - \alpha - \beta)/(1 + \frac{K_3}{K_4} P_S) \qquad 6.9$$

To obtain the coverage θ_S in terms of α , β , P_F and P_S, 6.8 is substituted into 6.9, K_1/K_2 and K_3/K_4 being replaced by K_A and K_B for simplicity ,

$$\theta_S = K_B P_S(1 - \alpha - \beta - \frac{(K_A P_F(1 - \theta_S - \alpha - \beta))}{1 + K_A P_F})/(1 + K_B P_S), \qquad 6.10$$

which on rearrangement becomes ,

$$\theta_S = K_B P_S(1 - \alpha - \beta)/(1 + K_A P_F + K_B P_S) \qquad 6.11$$

Similarly θ_F is given by

$$\theta_F = K_A P_F(1 - \alpha - \beta)/(1 + K_A P_F + K_B P_S) \qquad 6.12$$

Hence by substituting 6.12 and 6.11 into 6.4 and 6.5 respectively, the rate equations for the hydrogenation of a mixture of furan and sylvan are :-

$$-\frac{dP_F}{dt} = K_F \Theta_F P_F^{0.2} P_H = \frac{K_F K_A P_F^{1.2} P_H (1-\alpha-\beta)}{(1 + K_A P_F + K_B P_S)} \qquad 6.13$$

$$-\frac{dP_S}{dt} = K_S \Theta_S P_S^{0.2} P_H = \frac{K_S K_B P_S^{1.2} P_H (1-\alpha-\beta)}{(1 + K_A P_F + K_B P_S)} \qquad 6.14$$

Without making any further assumptions it is possible to extract some useful information out of equations 6.13 and 6.14. Dividing 6.14 by 6.13 :

$$\frac{dP_S}{dP_F} = \frac{K_S K_B P_S^{1.2}}{K_F K_A P_F^{1.2}} \qquad 6.15$$

which on rearranging and integrating becomes

$$\int_{P_S^O}^{P_S} \frac{dP_S}{P_S^{1.2}} = \frac{K_S K_B}{K_F K_A} \int_{P_F^O}^{P_F} \frac{dP_F}{P_F^{1.2}} \qquad 6.16$$

where P_S^O and P_F^O are the initial sylvan and furan pressures respectively. Completing the integration and rearranging, 6.16 becomes

$$\frac{(P_F^{-0.2} - (P_F^O)^{-0.2})}{(P_S^{-0.2} - (P_S^O)^{-0.2})} = \frac{K_F K_A}{K_S K_B} \qquad 6.17$$

But since P_F/P_F^O = the mole fraction of furan unreacted = M_F 6.18

and P_S/P_S^O = the mole fraction of sylvan unreacted = M_S 6.19

By use of equations 6.18 and 6.19 equation 6.17 may be expressed, for convenience in terms of mole fractions and initial pressures :

$$\frac{(M_F^{-.2} - 1)}{(M_S^{-.2} - 1)} \left(\frac{P_F^O}{P_S^O}\right)^{-.2} = \frac{K_F K_A}{K_S K_B} \qquad 6.20$$

The uses of equation 6.20 are threefold. First, if the assumptions made so far are correct then on substituting experimental data into the left hand side of equation 6.20 for any simultaneous hydrogenation of furan and sylvan a constant value should be obtained, within experimental error, hence 6.20 is a simple test for the validity of the theoretical model being used. Table 6.1 of the $K_F K_A/K_S K_B$ values computed using equation 6.20 show that the model is satisfactory.

Second, were one to assume $K_A = K_B$, which is not unreasonable considering the similarity of furan and sylvan, a quick method for finding the relative rates of reaction, K_F/K_S, would be provided by the above relationship. It was decided not to make this assumption but to attempt to separate the ratio of the rate constants from the ratio of the equilibrium constants (K_A/K_B). Since this process is very time consuming if one wished to examine the relative rates of reaction of a large number of closely related compounds equation 6.20 would have to be used in conjunction with the assumption that the ratio K_A/K_B was approximately unity.

Third, use will be made later in this chapter of relation 6.20 in order to reduce the number of variables when attempting to separate K_F/K_S from K_A/K_B.

Table 6.1 $K_F K_A$ / $K_S K_B$ values found using equation 6.20 applied to simultaneous hydrogenations of furan and sylvan over 5% Pt/pumice catalysts.

sample	C10J1	C10K1	C10N1	C10M1	C10O1
1	1.13	1.04	0.90	0.99	0.89
2	1.29	0.81	1.05	1.16	0.79
3	1.33	0.94	0.97	0.85	(1.05)
4	1.35	0.95	1.02	1.29	0.90
5	1.37	0.93	0.97	1.27	(0.78)
6	1.33	0.99	0.96	1.28	0.89
7		1.05	1.01	1.28	0.90
8		1.00	0.99	(1.35)	0.88
9		0.99	1.01	1.30	0.91
10				1.27	0.87
11				1.28	0.89
reaction temperature					
°C	26.0	48.5	49.5	30.5	60.0

It should be noted that the errors in equation 6.20 are large at low percent reaction because both the numerator and denominator of the left hand side of the relationship tend to zero as M_F and M_S tend to one. As an example the first figure for run C10J1 in table 6.1 was found as follows :

$$\left(\frac{8.80}{10.50}\right)^{-0.2} \frac{((0.9592)^{-0.2}-1)}{((0.9623)^{-0.2}-1)} = 1.0361 \frac{(1.000837-1)}{(1.000770-1)} = 1.0361 \frac{(0.000837)}{(0.000770)} = 1.13$$

Hence an error of $\pm$ 0.005 in the determination of M_F and M_S would lead to a $\pm$35% error in $K_F K_A / K_S K_B$ (for the first reading for C10J1).

6.1.2 Separation of K_F/K_S from K_A/K_B

One of the main difficulties encountered in the separation of the ratio of the rate constants, K_F/K_S, from the ratio of the equilibrium constants for the adsorption-desorption processes, K_A/K_B, is that both reactants are poisoning the reaction at differing rates. Therefore the differential equations 6.13 and 6.14 cannot be solved unless α and β, the degrees of poisoning by furan and sylvan respectively, can be expressed in terms of the other variables, P_F, P_S and t (P_H has been omitted since it may be expressed in terms of P_F and P_H, Appendix 8). To proceed further it is necessary to re-examine the kinetics for the hydrogenation of a single furan, as an example furan itself is chosen.

In the previous section it was shown that Θ_F equal g(t) (equations 6.2 and 6.3). However, in the previous chapter it was shown that $g(t) = \exp(-K' t^{\frac{1}{2}})$ for reaction times smaller than five hours, therefore,

$$\Theta_F = \exp(-K' t^{\frac{1}{2}}) = 1 - \alpha , \qquad 6.21$$

and hence, by differentiating 6.21 with respect to time:-

$$\frac{d\Theta_F}{dt} = - \frac{K' \exp(-K' t^{\frac{1}{2}})}{2 t^{\frac{1}{2}}} = - \frac{d\alpha}{dt} , \qquad 6.22$$

or, by substituting for $\exp(-K'_F t^{\frac{1}{2}})$ in 6.22 by 6.21:

$$\frac{d\Theta_F}{dt} = - \frac{K' \Theta_F}{2 t^{\frac{1}{2}}} = - \frac{d\alpha}{dt} \qquad 6.23$$

To proceed to hydrogenations of mixtures of two furans a final assumption is required: equation 6.23 is equally applicable to either the hydrogenation of a single furan or a mixture of two furans, the poisoning constants being the same for both systems providing both types of reactions are carried out at the same temperature. This assumption is merely an extension of the three assumptions made in the previous section which resulted in equations 6.4 and 6.5 applying both to the hydrogenation of furan and sylvan respectively separately or simultaneously. Expressed in words equation 6.23 states that the probability of an adsorbed furan molecule poisoning the catalyst surface, at a given value of t, is the same whether sylvan is present or not, the same being true for sylvan whose poisoning is described by the following equation, analagous to equation 6.23.

$$\frac{d\,\Theta_S}{dt} = -\frac{K''\,\Theta_S}{2\,t^{\frac{1}{2}}} = -\frac{d\beta}{dt} \qquad 6.24$$

Hence, substituting for Θ_F in 6.23 by 6.13,

$$\frac{d\alpha}{dt} = \frac{dP_F}{dt} \cdot \frac{K'}{2 P_F^{0.2} P_H K_F t^{\frac{1}{2}}}, \qquad 6.25$$

and, by substituting for $_S$ in 6.24 by 6.14

$$\frac{d\beta}{dt} = \frac{dP_S}{dt} \cdot \frac{K''}{2 P_S^{0.2} P_H K_S t^{\frac{1}{2}}} \qquad 6.26$$

Equations 6.13, 6.14, 6.25 and 6.26 form a set of four simultaneous differential equations in four dependent variables, P_F, P_S, α and β, and one independent variable, t, and hence are soluble (as before it is assumed that P_H is expressible in terms of P_F and P_S, see Appendix 8, equation A8.15).

However, the four differential equations contain six constants, K_F, K_S, K_A, K_B, K' and K''. Of these only the last two, the furan and sylvan poisoning constants, are known since, if the assumption that 5.23 and 5.24 are equally applicable to single or mixed reactions, then the poisoning constants may be predicted from kinetic analysis of single furan hydrogenations (equations 5.74 and table 5.28).

The remaining four unknown constants may be reduced by one since it has already been shown that both furan and sylvan adsorb strongly, hence their equilibrium constants for the adsorption-desorption process, K_A and K_B, must be large and therefore equation 6.12 reduces to

$$\Theta_F = K_A P_F (1 - \alpha - \beta)/(K_A P_F + K_B P_S) \qquad 6.27$$

Dividing the numerator and denominator of the right hand side of 6.27 by K_A :-

$$\Theta_F = P_F (1 - \alpha - \beta)/(P_F + \frac{K_B}{K_A} P_S) \qquad 6.28$$

The analagous expression for the surface coverage by sylvan (from equation 6.11) is

$$\Theta_S = P_S (1 - \alpha - \beta)/(P_S + \frac{K_A}{K_B} P_F) \qquad 6.29$$

Hence the rate equations for furan and sylvan consumption respectively are

$$-\frac{dP_F}{dt} = K_F \Theta_F P_F^{0.2} P_H = \frac{K_F P_F^{1.2} P_H (1 - \alpha - \beta)}{(P_F + \frac{K_B}{K_A} P_S)} , \qquad 6.30$$

(by substitution of 6.28 into 6.4) and

$$-\frac{dP_S}{dt} = K_S \Theta_S P_S^{0.2} P_H = \frac{K_S P_S^{1.2} P_H (1 - \alpha - \beta)}{(P_S + \frac{K_A}{K_B} P_F)} \quad , 6.31$$

(by substitution of 6.29 into 6.5).

The three remaining unknown constants, K_F, K_S and K_A/K_B, may be reduced to two by making use of equation 6.20. Clearly which constant is eliminated is purely arbitrary, however, since the value of K_A/K_B is probably close to one it is more convenient to eliminate either of the rate constants, in practice the two remaining unknowns were K_A/K_B and K_F.

Before proceeding further it is necessary to show that K_F and K_A/K_B are theoretically resolvable. Using a method based on the theory underlying the least squares technique for finding the optimum fit to data, it is shown in Appendix 7 that the two constants are separable.

In order to find the relative rates of reaction (K_F/K_S) the four simultaneous differential equations 6.25, 6.26, 6.30 and 6.31 are solved by the Runge-Kutta numerical integration technique, using Runge's coefficients, (ref. 83) making use of the computer program 'MTRUNGE' (Appendix 5). This program employs a curve fitting technique to find the optimum values for K_F and K_A/K_B, the latter value being substituted into equation 6.20 which is solved for the ratio of the rate constants while the value of sylvan's rate constant is found by substituting both K_F and K_A/K_B into equation 6.20 and solving for K_S.

Briefly 'MTRUNGE' operates by solving the four differential equations given above for some value of K_F and of K_A/K_B. It then compares the resultimg time against furan pressure curve with a similar curve, generated by a Chebyshev curve fitting computer program (Appendix 6), which represents the best fit to the experimentally determined data points. Using the same value of K_A/K_B 'MTRUNGE' selects a new K_F which is likely to give an improved fit to the data and solves the four differential equations again using this new K_F. The process of solving, matching the theoretical with the experimentally determined time against furan pressure curves and selection of a K_F which is likely to give an improved fit of the two curves is continued until an optimum value of K_F has been found. The whole process is then repeated for a new K_A/K_B until the optimum values of both constants have been found. The procedure is tedious but would be greatly aided by the use of a high speed computer (an IBM 1620 was used). To complicate matters the values of K' and K'' were usually altered slightly to further optimise the curve fitting. Graph 6.1 shows the fraction of furan unreacted as a function of time for run C10M1 together with the curve synthesised by the curve fitting program.

The above curve fitting procedure is only applied to the furan pressure/time curve even though the sylvan pressure/time curve is of course synthesised as well during the solution of the four differential equations. At first sight it may appear that useful information is being discarded, however, since equation 6.20 is utilised to reduce the number of unknowns the relative positions of the two curves are fixed, therefore, to attempt to fit both the theoretical furan pressure/time and sylvan pressure/time curves to their experimentally determined counterparts would not yield additional information.

GRAPH 6.1

A graphical representation of the application of the curve fitting program (appendix 5) to the simultaneous hydrogenation of furan and sylvan for run C10M1

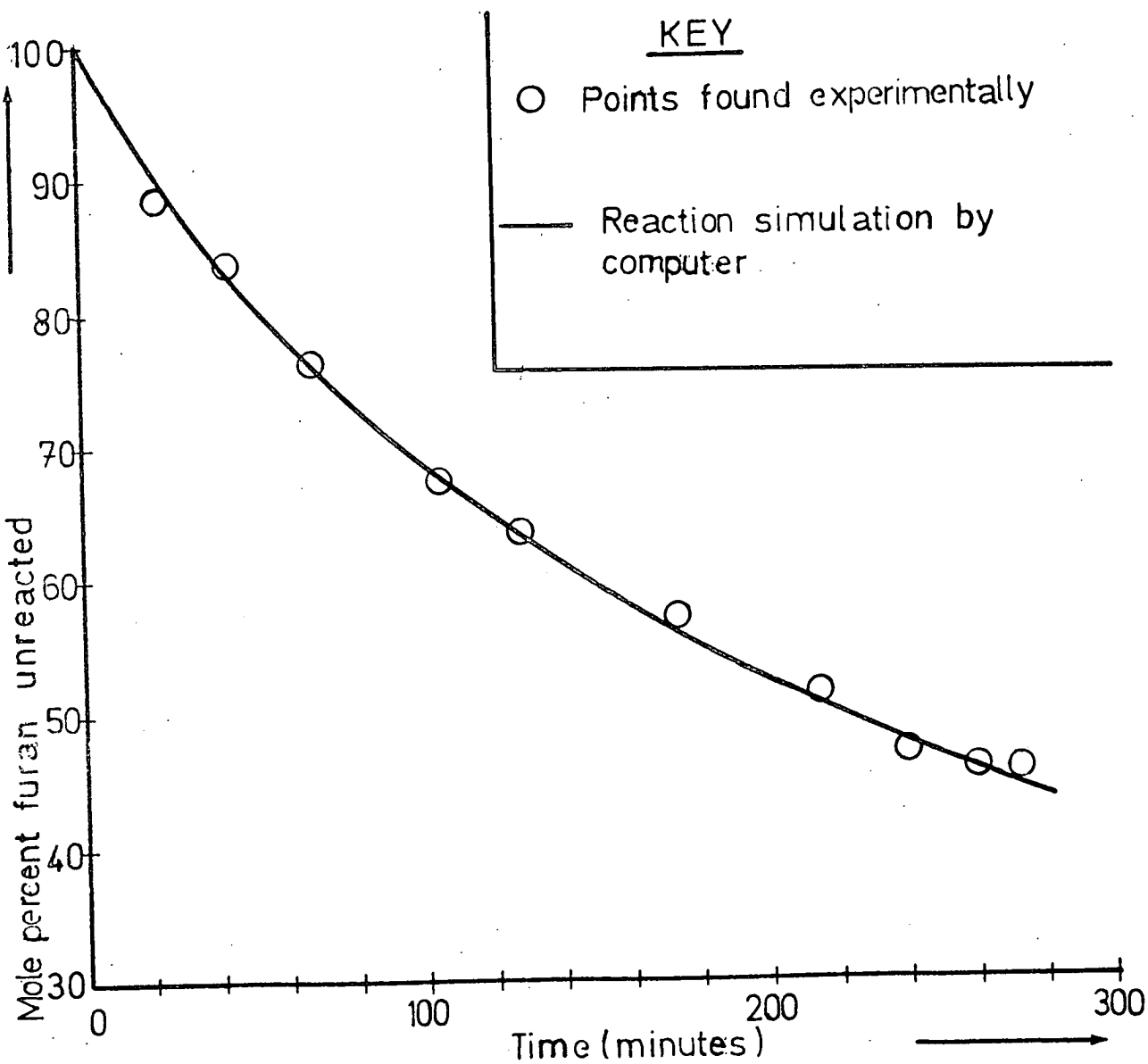

Although it was shown in Appendix 7 that K_F and K_A/K_B are theoretically resolvable using the curve fitting, procedure, in practice considerable difficulty was encountered since the standard deviation between the theoretical and experimental time/furan pressure curves was more than an order of magnitude more sensitive to change in the furan rate constant than to similar changes in the ratio of the equilibrium constants K_A/K_B. Hence in order to be able to achieve a high degree of accuracy it would be necessary either to increase the number of readings by a factor greater than four (which would lead to large inaccuracies in calculated pressures) or to improve the accuracy of the analysis technique.

The results of the analysis by program 'MTRUNGE' of the simultaneous hydrogenations of furan and sylvan over 5% Pt/pumice catalysts are summarised in the following table. The 'least squares deviations' quoted in table 6.2 were calculated using formula 6.32 :

$$S = \frac{\sum_{i=1}^{n} (Y_i - y_i)^2}{n} \qquad 6.32$$

S is the least squares deviation, n is the number of data points used, Y_i and y_i are the mole fractions of furan remaining unreacted, calculated by the simulation program and found experimentally respectively. A difference of 0.01 between the calculated and observed mole fractions of furan unreacted for each data point would result in a least squares deviation of approximately 0.003.

Table 6.2 Results of analysis by the curve fitting program 'MTRUNGE' of the data from the simultaneous hydrogenations of furan and sylvan over 5% Pt/pumice.

RUN	A	B	C	D	E	F	G	H	I	J	K	L	M	N
C10J1	26.0	0.0038	0.7	1.33	0.122	0.096	77.7	8.8	10.5	0.5111	1.28	2.50	1.9	1.3
C10M1	30.5	0.0040	0.9	1.29	0.130	0.110	120.9	8.5	7.4	0.4636	1.15	2.49	1.4	1.8
C10K1	48.5	0.0020	0.8	0.99	0.245	0.280	89.3	12.2	9.2	0.4406	2.21	5.02	1.2	4.2
C10N1	49.5	0.0019	1.0	0.99	0.250	0.280	96.1	14.2	10.6	0.6212	3.09	4.99	1.0	5.0
C10O1	60.0	0.0040	1.2	0.89	0.315	0.368	80.2	10.1	8.4	0.4712	3.76	7.98	0.7	10.8

A = Reaction temperature (^{o}C), B = least squares deviation between the calculated and experimental mole fraction furan unreacted/time curves, C = K_A/K_B, D = K_AK_F/K_BK_S (from table 6.1), E = K', F = K'', G, H and I are the initial furan, sylvan and hydrogen pressures respectively (mm.Hg), J = weight of 5% Pt/pumice catalyst, K and L are the furan rate constants found by the program 'MTRUNGE' and per gram respectively, $(mm.Hg)^{-0.2}.min.^{-1}$, M = K_F/K_S, N = the sylvan rate constant / g , $(mm.Hg)^{-0.2}.min.^{-1}$, all rate constants have been multiplied by 10^3.

6.2 Discussion

As is shown by the least squares deviations in table 6.2 the agreement between the experimentally determined mole fraction furan unreacted/time curve and its counterpart synthesised by the simulation program 'MTRUNGE' is within the limits of experimental error for all the five simultaneous hydrogenations. It is worth remembering that the effect of random experimental errors has been greatly reduced by the use of the smoothing technique which has been applied to the data points (using the Chebyshev curve fitting program, Appendix 6).

Furthermore, since these close fits between the two curves were obtained using values for the furan and sylvan poisoning constants which compare well with those found from the analysis of single reactions, see tables 5.27 and 5.28, the model adopted to represent the hydrogenation of a mixture of the furans (given by the four simultaneous differential equations 6.25, 6.26, 6.30 and 6.31) is satisfactory.

However, since the least squares deviations are relatively insensitive to small changes in the ratio K_A/K_B compared with changes of a similar magnitude in the furan rate constant, K_F, the figures quoted for the ratios of furan to sylvan's adsorption equilibrium constants are only approximate ($\pm$ 25%) and hence so are the rate constants and their ratios. While the errors in the rate constants K_F and K_S are about twice those for values obtained from hydrogenations of single furans the simultaneous reactions were carried out in order to find the relative rates of reaction of the two furans, the error in this ratio being in the order of $\pm$ 25 to $\pm$ 30%. Since relative rates of reaction found from hydrogenations of furan and sylvan separately are

subject to an error equal to the sum of the possible errors in the rate constants for each of these reactions (amounting to approximately $\pm$ 20%), the two techniques give values for K_F/K_S to approximately the same accuracy. Graph 6.2 shows the dependance of K_F/K_S on the reaction temperature for the five simultaneous hydrogenations, data from table 6.2, and the three single sylvan hydrogenations, C10C1, C10I1 and C10N1, the value of the rate constants for the furan hydrogenations at the same temperature being found from Graph 5.10. As Graph 6.2 shows the two techniques yield similar values (at the same temperatures) for K_F/K_S.

Although the information which may be extracted from the simultaneous reactions is only semi-quantative in nature it is interesting to note that sylvan's rate constant increases more sharply with increasing reaction temperature than furan's, see Graph 6.2, hence the activation energy for the sylvan-hydrogen reaction is greater than for furan's hydrogenation (equation 5.76). This is in agreement with the results obtained for the hydrogenations of the two furans separately, contrast tables 5.27 and 5.28, and with the activation energies quoted for furan and sylvan hydrogenations over PtO_2 in acetic acid (ref. 82) of 8 and 8.6 K. cals. respectively.

While the change in the K_A/K_B values with reaction temperature is just within the limits of the experimental accuracy the figures for this ratio in table 6.2 suggest that at room temperature sylvan adsorbs more strongly than furan while at 60°C the reverse is true. The slightly stronger adsorption of sylvan at low temperatures could be attributed to its higher boiling point (63°C as opposed to furan's boiling point of 32°C), while the stronger adsorption of furan at 60°C could either be caused by a difference in the electronic

GRAPH 6.2

The ratio of the rate constants for the hydrogenations of furan and sylvan as a function of temperature.

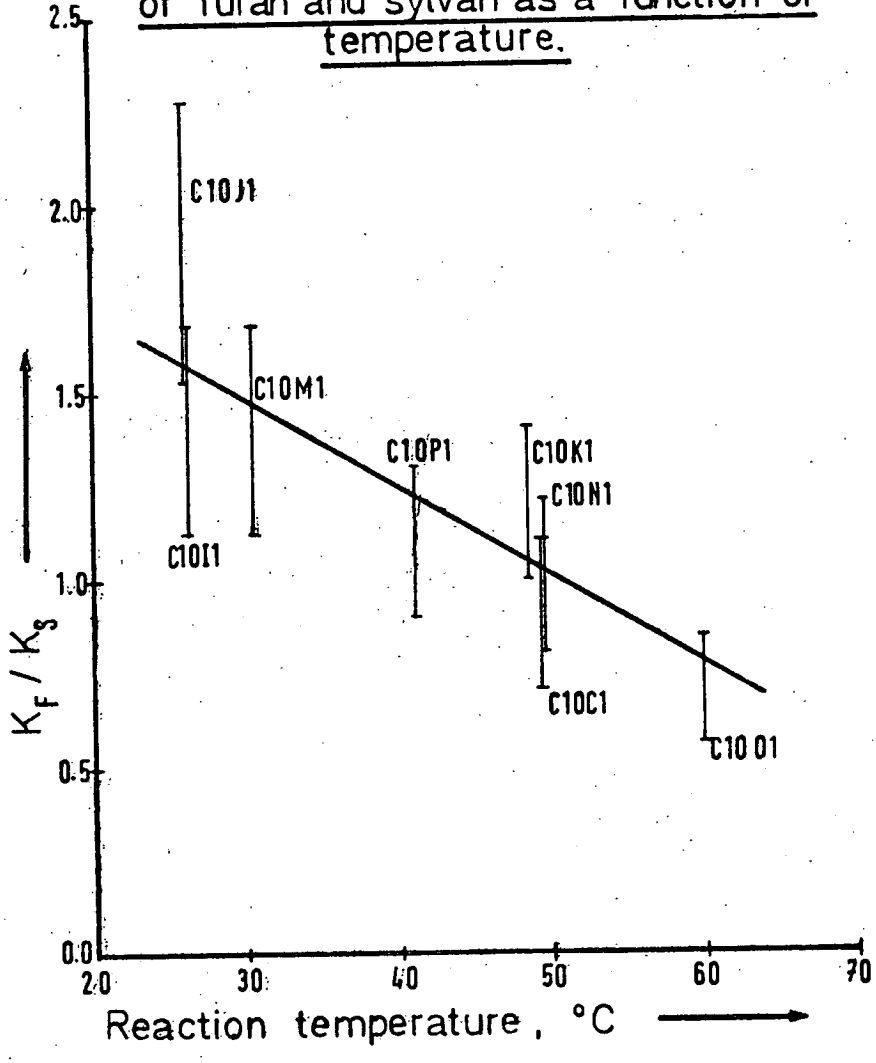

properties between the two compounds or simply by the greater ease with which furan molecules may be packed on the catalyst's surface.

A by-product of the mathematical analysis of the simultaneous hydrogenations of furan and sylvan is that it provides additional evidence to show that the models adopted to represent the kinetics of the hydrogenations of these compounds singly (equations 5.53 and 5.77 respectively) are satisfactory since these basic models were used to construct the model used to describe the kinetics of the simultaneous hydrogenations of these two compounds. Since this latter model is shown above to be satisfactory so must its precursors, equations 5.53 and 5.77.

A large amount of time was devoted to the examination of the simultaneous reactions since the rate constants obtained using the early simulation programs for the hydrogenation of a single compound showed only a general correlation with increasing reaction temperatures, the errors being as high as $\pm$ 50% for furan hydrogenations, hence the ratios of the rate constants for the two furans' hydrogenations were liable to errors of up to $\pm$ 100%. Hence it was thought to be profitable to examine these compounds' competitive hydrogenations where the errors in the ratio of the rate constants is in the order of $\pm$ 25% to $\pm$ 30%. However, re-examination of the data from single hydrogenations using an improved simulation program ('RATESIM 6', Appendix 10), which has a subroutine included to smooth out random errors (Appendix 6) in the data, showed that, with only a few exceptions, values for the poisoning and rate constants for reactions at the same temperatures were reproducible to within $\pm$ 10% as is shown by graphs 5.9 and 5.10. Hence the errors in the ratio of the rate constants for furan and

sylvan hydrogenations carried out at the same temperature would be approximately the same size as those found from simultaneous hydrogenations. Since a complete analysis of the latter type of reaction can take a matter of weeks as opposed to about 15 minutes for each single reaction the simultaneous reactions are only of limited use. A method whereby the analysis of competitive reactions may be speeded up is given at the end of Appendix 5, this had not been perfected at the time of writing this thesis.

CHAPTER 7

Mechanism.

Relatively little work has been carried out on furan hydrogenations with a view to gaining some insight into the mechanism of the reaction. However as was stressed in section 1.4, because the benzene-hydrogen and furan-hydrogen systems show many similarities, it is possible to draw upon the large body of research carried out on the former reactions. To recap on the most important similarities :-

First, both compounds have a large resonance energy.

Second, the rates of reactions of the two compounds differ by less than a factor of two.

Third, redistribution of deuterium does not occur during deuteration of the two compounds' nuclei.

Fourth, there is evidence to show that the dihydro-derivatives of the two compounds act as intermediates in their hydrogenations.

Fifth, both compounds are strongly adsorbed on the catalyst's surface.

The mechanisms put forward will deal principally with furan and sylvan reactions over Pt/pumice since most of the research has been concerned with these systems. The salient features of these reactions are :-

A Both furans are strongly adsorbed.

B Hydrogen exchange occurs predominantly at the 2 and 5 positions.

C Hydrogenolysis occurs nearly exclusively at the C-O bonds.

D Sylvan's 1, 5 C-O bond is cleaved more than ten times as readily as its 1, 2 C-O bond.

E Sylvan's 1, 5 C-O bond is cleaved twice as readily as either of furan's C-O bonds.

F The rate at which the furan nucleus is hydrogenated is affected to a negligible extent by the presence of a methyl group at the 2 position.

G C-C bond fission occurs more readily for furan than sylvan, the only C-C bond to be cleaved being the 4, 5 one.

H 4, 5 C-C bond fission only occurs in conjunction with cleavage of both C-O bonds.

I Neither dihydro- nor tetrahydro- furans are intermediates in the hydrogenolysis reactions.

J The dihydro- furans are probably short lived intermediates in the hydrogenation of the furan ring which results in the formation of tetrahydrofurans.

Initial adsorbed species.

The adsorption of furans probably occurs in a manner similar to that thought to occur for benzene, Ref. 53, namely by the overlap of the furan ring's delocalised π electrons with vacant metallic d orbitals. In addition, partial donation from a furanic oxygen's lone pair will probably also occur, forming the adsorbed complex I.

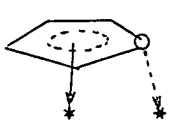

I

Evidence for the strong adsorption of furan comes not only from the calculated furan order of approximately zero (chapter 5, confirmed in chapter 6) but also from the simultaneous reaction of furan and benzene (reported in chapter 4), which showed furan to adsorb preferentially. However, the hydrogenations of n-hexene and n-butanol in the presence of furan suggests that, like benzene, either the furans adsorb strongly on relatively few sites (c.f. benzene, ref. 70) or furan does not pack efficiently on the catalyst's surface, leaving the metal atoms in the interstices between the adsorbed furan free to react (c.f. benzene, ref. 78). Evidence for gaps in an adsorbed monolayer of benzene comes from the ease with which o - p hydrogen interconversions and D_2 - H_2, D_2O - H_2 and DCl - H_2 exchange reactions occur over catalysts in the presence of benzene).

Hydrogenation:

In chapter 1 section 3 evidence, gathered by other workers, was presented to show that dihydrofurans are probably intermediates in the formation of tetrahydrofurans from furans, the rate determining step being the first addition of hydrogen to the furan nucleus. Therefore the hydrogenation reaction probably proceeds as follows :

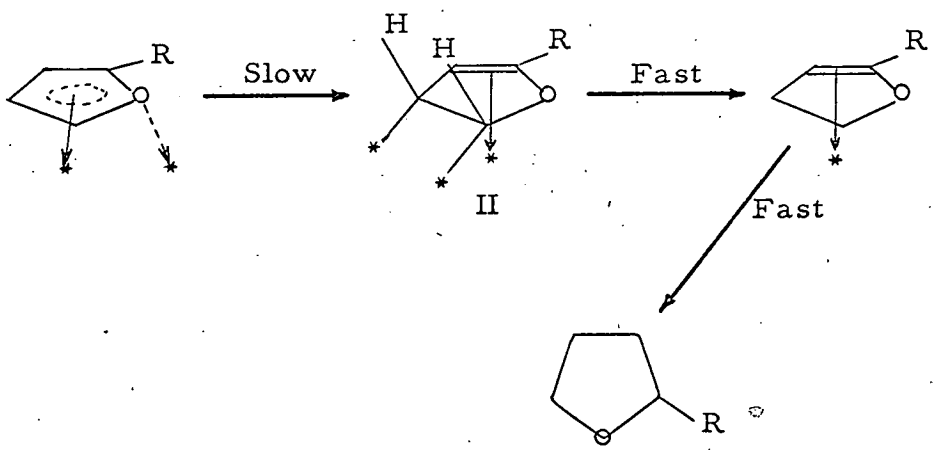

Such a mechanism, which is similar to that proposed by Anderson and Kemball (ref. 53) for the hydrogenation of benzene, is consistent with the above conditions A and F and with the lack of exchange during hydrogenation (ref. 51).

C-O bond hydrogenolysis.

Hydrogenolysis products have been shown to be formed by a pathway which involves neither the dihydrofuran (ref. 49) nor the tetrahydrofuran (ref. 18). Furthermore it is unlikely that the reaction will proceed by the adsorbed complex II since hydrogen addition to this species is much more feasible than bond cleavage (from the product distributions of furan and sylvan, hydrogenolyses of the C-O bond in II would have to occur twice as fast as addition of hydrogen).

A possible reaction mechanism involves the adsorbed 5-furyl radical (which, by analogy with the benzene-hydrogen exchange intermediate (ref. 53), is probably an intermediate in the hydrogen exchange reaction of furans) :-

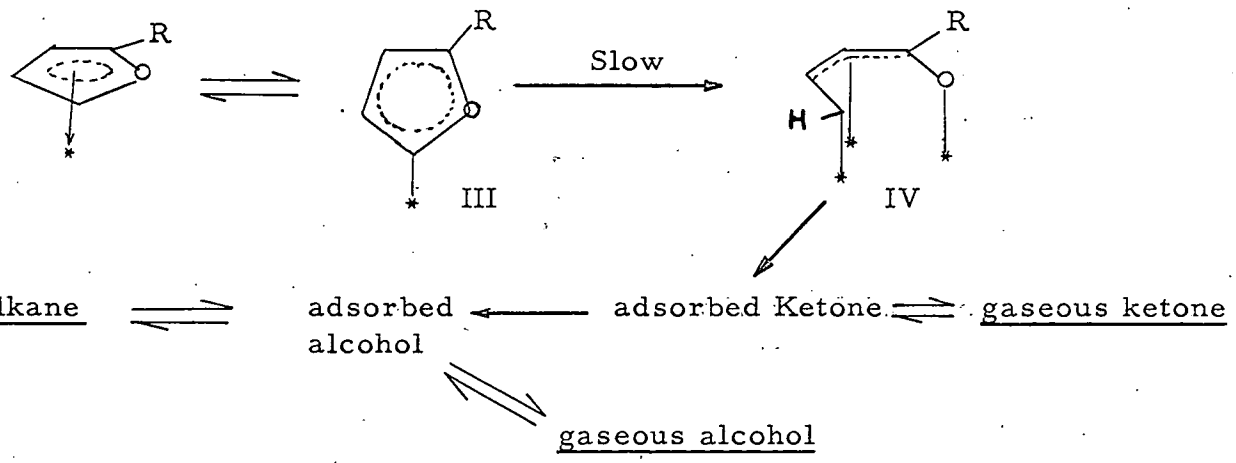

The above scheme represents the hydrogenolysis of a 2-alkyl furan, for furan itself species IV would be converted straight to the adsorbed alcohol.

C-C bond hydrogenolysis.

Even at 95.5°C no n-propanol was detected in the products from the furan-hydrogen reaction over Pt/pumice although 4.9% n-propane was formed. However, at this temperature the ratio of n-butanol to n-butane formed was approximately 10 : 1. Therefore, it seems unlikely adsorbed n-propanol or one of its adsorbed analogs is the intermediate in the formation of n-propane, this probably being formed by fission of the C-C bond adjacent to the C-O bond in IV (R = H) or adsorbed n-butanol.

If one postulates that C-C cleavage only occurs by cleavage of the C-C bond adjacent to a primary OH group (C-C bonds adjacent to C-O bonds are more prone to cleavage over platinum than unsubstituted aliphatic C-C bonds, ref. 41) then the stability of the C-C bonds in the sylvan molecule is explained - primary alcohols are formed from furan and sylvan in a ratio which exceeds 10 : 1. Furthermore, such a mechanism explains why only sylvan's 4, 5 C-C bonds are prone to cleavage.

APPENDIX 1.

Nomenclature :-

r	Internal radius of the capillary (cm.)
l	Capillary length (cm.)
η	Approximate viscosity of the reaction mixture (poise)
$\frac{dV^o}{dt}$	Flow rate of gas into the capillary ($cm^3 . sec.^{-1}$)
P_1	Pressure in the sampling system (dynes $cm.^{-2}$)
P_2	Pressure in the reaction vessel (dyne $cm.^{-2}$)
$\frac{dn}{dt}$	Flow rate of gas through the capillary (mole $sec.^{-1}$)
R	Ideal gas constant (erg. $mole^{-1}$ K^{-1})
T	Temperature (K)

Using Poiseuille's equation A1.1 (ref. 67) for the laminar flow of a gas through a capillary an expression is derived which relates the pressure in a sampling system to the time taken in sampling, and the reaction vessel pressure assuming laminar flow, no slip effect, the reaction vessel pressure remains constant during sampling, the expansion is isothermal and that at t = O, P_1 = O. The relationship is only intended to be correct to a first approximation.

Poiseuille's equation applied to the sampling system outlined in fig. 2.3 is

$$P_2 \frac{dV^o}{dt} = \frac{\pi r^4 (P_2^2 - P_1^2)}{16 l \eta} \qquad \text{A1.1}$$

Differentiating the ideal gas law,

$$PV = n R T, \qquad \text{A1.2}$$

with respect to time gives

$$P_2 \frac{dV^o}{dt} = \frac{R T dn}{dt} \qquad \text{A1.3}$$

Where equation A1.3 applies to gases entering the capillary. Similarly applying A1.2 to the sampling system and differentiating with respect to time, gives ,

$$V_1 \frac{dP_1}{dt} = R\,T \frac{dn}{dt} \qquad \text{A1.4}$$

Combining A1.3 and A1.4 :

$$\frac{dV^o}{dt} = \frac{V_1}{P_2} \frac{dP_1}{dt} \qquad \text{A1.5}$$

and substituting A1.5 into A1.1 :

$$V_1 \frac{dP_1}{dt} = \frac{\pi r^4 (P_2^2 - P_1^2)}{16 l \eta} \qquad \text{A1.6}$$

Poiseuille's equation is now in a form where all the variables are either known or are easily measurable with the exception of P_1.

Rearranging A1.6 and integrating :

$$\int_o^{P_1} \frac{dP_1}{(P_2^2 - P_1^2)} = \int_o^t \frac{\pi r^4}{V_1 16 l \eta} dt \qquad \text{A1.7}$$

(Where the integration limit P_1 is the pressure in the sampling system at time t secs.), which gives

$$\frac{1}{2 P_2} \ln \left(\frac{P_2 + P_1}{P_2 - P_1} \right) = \frac{\pi r^4 t}{V_1 16 l \eta} \qquad \text{A1.8}$$

Solving for time:-

$$t = \frac{V_1 8 l \eta}{P_2 \pi r^4} \ln \left(\frac{P_2 + P_1}{P_2 - P_1} \right) \qquad \text{A1.9}$$

For the sampling system outlined in fig. 2.3 $r = 0.01$ cms., $l = 20$ cms. and $V_1 \simeq 5$ cm^3. Comparison of the literature value for the viscosity of hydrogen, 88 micropoise (Ref. 83) and for various organic molecules, e.g., isopentane vapour, 69.5 micropoise (Ref. 84), benzene vapour 85 micropoise (Ref. 85) n-butanol vapour, 105 micropoise, (Ref. 86), all at 25°C, suggests that a value of the viscosity of the reaction mixture of 88 micropoise is a fair approximation. Graph A1.1 of the time taken sampling, t, against the pressure in the sampling system, P_1, was found by using the above data in equation A1.9 using a typical reaction pressure of 100 mm.

GRAPH A1.1

Sampling time/pressure in the sampling system, illustrated in Fig. 2.3, calculated using Equation A1.9

(Reaction vessel pressure = 100 mm.)

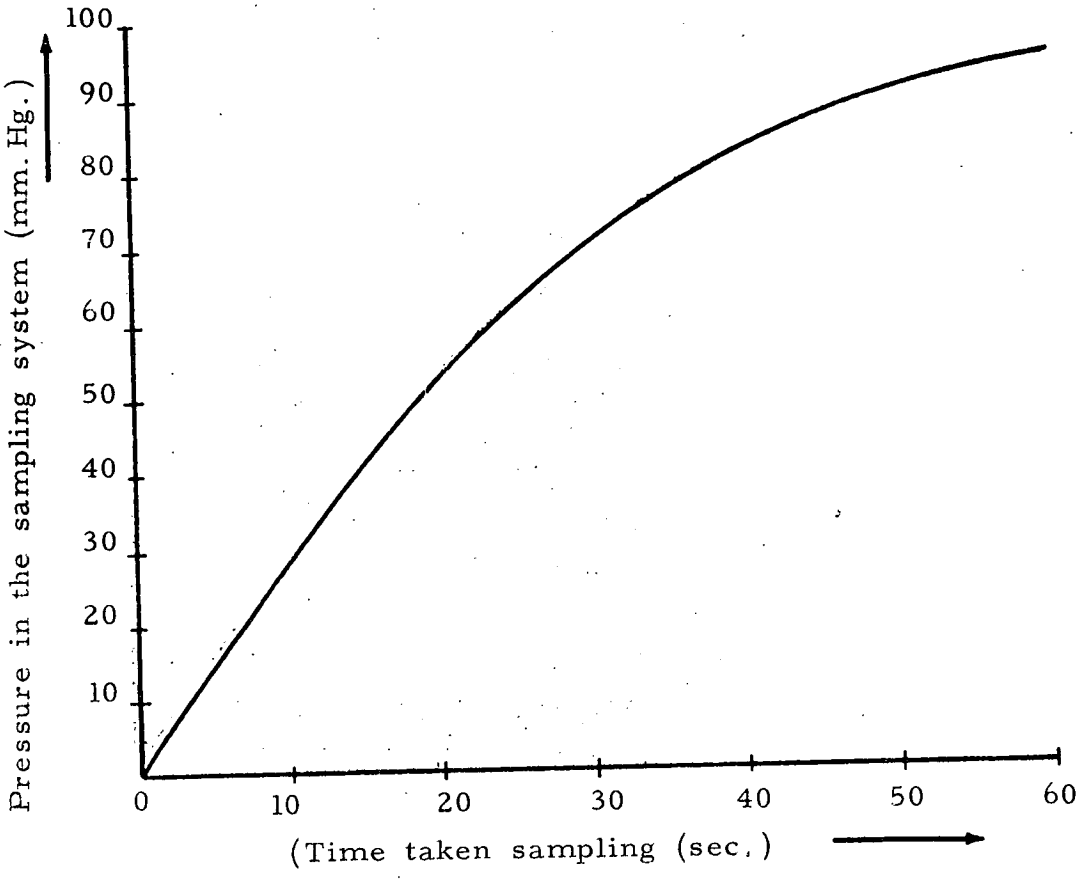

APPENDIX 2

Alterations to equation 3.20 to allow for possible cleavage of a furan's carbon skeleton resulting in the formation of two detectable products.

Nomenclature :- The same as that used in chapter 3, section 3.1.4.

This appendix has been included in order to show that the techniques developed in section 3.1.4 are applicable to a more general class of reaction than those considered in chapter 3.

Let $\zeta(J)$ be the fraction of furan reacted, for the J^{th} sample, which has been formed by cleavage of the carbon chain to form two detectable products, product distributions of each being $\xi(J)$, the rest of the furan reacted forming one mole of products per mole of furan reacted.

Then equation 3.17 (for sample '1') becomes :-

$$\sigma(1) = M_F(1) \,/\, M_F^O \,(1 + \zeta(1)\,\xi(1)) \,, \qquad \text{A2.1}$$

and therefore 3.20, on expression for the ratio of the mole fraction of furan present for samples '1' and '2', becomes :

$$\frac{\sigma(2)}{\sigma(1)} = \frac{A_X(1)A_F(2)}{A_X(2)A_F(1)} \quad \frac{(1 + \zeta(1)\ \xi(1))}{(1 + \zeta(2)\ \xi(2))} \qquad \text{A2.2}$$

To simplify the following expressions let

$$R = A_X(1)\ A_F(2) \,/\, A_X(2)\ A_F(1) \qquad \text{A2.3}$$

If, for simplicity, sample '1' is a blank on the reaction mixture, A2.2 in conjunction with A2.3 yields the following expression for O (2) :-

$$\sigma(2) = \sigma(1) \quad R \;/\; (1 + \zeta(2) \quad \xi(2)) \qquad \text{A2.4}$$

$$\text{but} \quad \zeta(2) = 1 - R \qquad \text{A2.5}$$

Therefore by substituting A2.5 into A2.4 an expression is obtained for $\sigma(2)$ in terms of $\sigma(1)$ and peak areas only (the analog of equation 3.20) :-

$$\sigma(2) = \sigma(1)\, R \;/\; (1 + \quad \xi(1 - R)) \qquad \text{A2.6}$$

APPENDIX 3

The three computer programs, in Fortran, which were used most frequently for the conversion of G L C analysis data into molar percentages

A3.1 The computer program to process visually measured data (program DATA3)

The mole percent of detectable reactant and the product distributions in terms of mole percents are calculated by using equations A3.1 and A3.2 respectively, both of which were derived from equation 3.8. Both types of mole percents apply only to detectable reactants and products.

$$R = 100 \Big/ \sum_{j=1}^{n} (C_B^j \; A_j/A_B) \quad , \qquad \text{A3.1}$$

where R is the mole percent detectable reactant of the detectable reactant and products. If no adsorption and little cleavage of the carbon skeleton of the reactant or its products occurs (as is to all intends and purposes the case for the reactions over Pt/pumice catalysts) then R is the mole percent of the reactant which has not reacted when the sample for analysis was removed.

$$P_i = \frac{100\, A_i}{A_B} \; C_B^i \Big/ \left(\left(\sum_{j=1}^{n} C_B^j \frac{A_j}{A_B} \right) - 1 \right) \qquad \text{A3.2}$$

where P_i is the mole percent of product i of the detectable products ($A_i \neq A_B$), in other words the product distribution of i.

Program DATA3 also calculates the maximum errors in R and P_i assuming an error of $\pm$ 0.2 mm. in the measurement of peak heights and peak widths at half height on a chromatogram as follows:-

The expressions for the minimum values of R (R_{MIN}) and P_i(P_{iMIN}) assuming all the peak area measurements are subject to the maximum error are derived from equations A3.1 and A3.2 respectively:

$$R_{MIN} = \frac{100(A_B - \delta_B)}{(A_B + \delta_B)} \Big/ \sum_{j=1}^{n} \frac{(A_j + \delta_j)}{(A_B + \delta_B)} \; C_B^j \;, \qquad \text{A3.3}$$

(where δ_j is the maximum error in mm.^{2} in the area of the $_j$th peak) and

$$P_{iMIN} = \frac{100(A_i - \delta_i)}{(A_B + \delta_B)} \; C_B^i \Big/ \left(\sum_{j=1}^{n} \left(\frac{(A_j + \delta_j)}{(A_B + \delta_B)} \; C_B^j \right) - 1 \right) \qquad \text{A3.4}$$

The maximum errors in R and P_i are respectively

$$\pm (R - R_{MIN}) \qquad \text{A3.5}$$

and

$$\pm (R - P_{iMIN}) \qquad \text{A3.6}$$

PROGRAM DATA3

```
C    ANALYSIS DATA TREATMENT , AREAS MEASURED VISUALLY
C    N=NUMBER OF PEAKS/CHROMATOGRAM ,  M=NUMBER OF
C    CHROMATOGRAMS.  CONV(J)=CONVERSION FACTOR FOR J TH.
C    COMPOUND, NAME STORED IN NAME(1,J) TO NAME(15,J)
C    ARED(1)=PEAK HT.,ARED(2)=PEAK WIDTH AT 1/2 HT.,
C    ARED(3)=AMPLIFIER SENSITIVITY
C*************************************************************************
     DIMENSION CONV(10),AREA(3,10,8),OLFN(2,10,8),ARED(3),PR(2,10)
     DIMENSION OLP(2,10,8),NAME(15,10)
  1  FORMAT(F5.3,15A1)
  2  FORMAT(3F8.4)
  3  FORMAT(2I2)
     READ 3,N,M
     DO 4 J=1,N
     READ 1,CONV(J),(NAME(K,J),K=1,15)
  4  CONTINUE
     IF(1.0-CONV(1)) 5,6,5
```

```
5     DO 7 J=1, N
      CONV(J)=CONV(J)/CONV(1)
7     CONTINUE
6     DO 16 L=1, M
      SUM=0.0
      ESUM=0.0
      DO 17 K=1, N
      READ 2, ARED
      AREA(1, K, L)=ARED(1)*ARED(2)*ARED(3)/100.
      AREA(2, K, L)=(ARED(1)-0.2)*(ARED(2)-0.2)*ARED(3)/100.
      AREA(3, K, L)=(ARED(1)+0.2)*(ARED(2)+0.2)*ARED(3)/100.
      OLFN(1, K, L)=AREA(1, K, L)*CONV(K)/AREA(1, 1, L)
      OLFN(2, K, L)=AREA(2, K, L)*CONV(K)/AREA(3, 1, L)
      ESUM=AREA(3, K, L)*CONV(K)/AREA(3, 1, L)+ESUM
      SUM=SUM+OLFN(1, K, L)
17    CONTINUE
      DO 100 I=2, N
      OLP(1, I, L)=OLFN(1, I, L)*100./(SUM-1.0)
      OLP(2, I, L)=(OLP(1, I, L)-OLFN(2, I, L)*100./(ESUM-1.0))/2.0
100   CONTINUE
      PR(1, L)=100./SUM
      PR(2, L)=(PR(1, L)-OLFN(2, 1, L)*100./ESUM  )/2.0
16    CONTINUE
11    FORMAT(16X, 19HPEAK AREAS (SQ. CM.), /)
12    FORMAT(16X, 15HMOLAR FUNCTIONS, /)
13    FORMAT(16X, 32HMOLE PERCENT PRODUCT OF PRODUCTS, /)
14    FORMAT(16X, 21HMOLE PERCENT STANDARD, /)
15    FORMAT(2X, 15A1, 5F16.4)
      PRINT 11
      DO 115 K=1, N
      PRINT 15, (NAME(I, K), I=1, 15), (AREA(1, K, L), L=1, M)
115   CONTINUE
      PRINT 12
      DO 118 K=1, N
      PRINT 15, (NAME(I, K), I=1, 15), (OLFN(1, K, L), L=1, M)
118   CONTINUE
      PRINT 13
      DO 119 K=2, N
      PRINT 200, (NAME(I, K), I=1, 15), ((OLP(M1, K, L), M1=1, 2), L=1, M)
119   CONTINUE
200   FORMAT(2X, 15A1, 7X, 10F8.3)
      PRINT 14
      PRINT 200, (NAME(I, 1), I=1, 15), ((PR(M1, L), M1=1, 2), L=1, M)
      CALL EXIT
      END
```

A3.2 Computer program to process peak areas measured using an Integrator

DATA 4

DATA 4 finds the same mole fractions as those found by DATA 3 using equations A3.1 and A3.2 together with the mole fraction of each of the detectable constituents relative to all the detectable gaseous constituents using equation A3.7, derived from equation 3.8,

$$Qi = \frac{100A_i}{A_B} \Big/ \sum_{j=1}^{n} C_B^j \frac{A_j}{A_B} \quad , \qquad \text{A3.7}$$

Qi being the required mole fraction for the i^{th} constituent.

PROGRAM DATA 4

```
C    ANALYSIS DATA TREATMENT , AREAS MEASURED BY
C    INTEGRATOR.  N=NO. OF PEAKS/CHROMATOGRAM,
C    M=NO. OF CHROMATOGRAMS.  CONV(J)=CONVERSION
C    FACTOR FOR J TH. COMPOUND, NAME STORED IN
C    NAME(1,J) TO NAME(15,J).  ARED(1)=PEAK AREA ,
C    ARED(2)=INTEGRATOR SENSITIVITY.
     **********************************************************
     DIMENSION  CONV(10),AREA(10,8),ARED(2),OLFN(10,8),OLP(2,10,9),
    1NAME(15,10)
   1 FORMAT(F5.3,15A1)
   2 FORMAT(2F6.1)
   3 FORMAT(2I2)
     READ 3,N,M
     DO 4 J=1,N
     READ 1,CONV(J),(NAME(K,J),K=1,15)
   4 CONTINUE
     DO 310 J=1,N
     DO 310 K=1,8
     AREA(J,K)=0.0
     OLFN(J,K)=0.0
     OLP(1,J,K)=0.0
 310 OLP(2,J,K)=0.0
     IF(1.0-CONV(1))5,6,5
   5 DO 7 J=1,N
     CONV(J)=CONV(J)/CONV(1)
```

```
  7  CONTINUE
  6  DO 16 L=1, M
     SUM=0. 0
     DO 17 K=1, N
     READ 2, ARED
     AREA(K, L)=ARED(1)*ARED(2)/100.
     OLFN(K, L)=AREA(K, L)*CONV(K)/AREA(1, L)
     SUM=SUM+OLFN(K, L)
 17  CONTINUE
     DO 100 I=2, N
     OLP(1, I, L)=OLFN(I, L)*100. /(SUM-1. 0)
     OLP(2, I, L)=OLFN(I, L)*100. /SUM
100  CONTINUE
     OLP(2, 1, L)=100. /SUM
 16  CONTINUE
 11  FORMAT(16X, 50HPEAK AREAS (INTEGRATOR AT SENS. 1, AMPL.
    1  AT 1**-8) , /)
 12  FORMAT(16X, 15HMOLAR FUNCTIONS, /)
 13  FORMAT(16X, 32HMOLE PERCENT PRODUCT OF PRODUCTS, /)
 14  FORMAT(16X, 21HMOLE PERCENT STANDARD, /)
 18  FORMAT(16X, 37HMOLE PERCENT OF PRODUCTS AND REACTANT, /)
 15  FORMAT(2X, 15A1, 8F15. 4)
     PRINT 11
     PRINT 15, ((NAME(I, K), I=1, 15), (AREA(K, L), L=1, 8), K=1, N)
     PRINT 12
     PRINT 15, ((NAME(I, K), I=1, 15), (OLFN(K, L), L=1, 8), K=1, N)
     PRINT 13
     PRINT 15, ((NAME(I, K), I=1, 15), (OLP(1, K, L), L=1, 8), K=2, N)
     PRINT 18
     PRINT 15, ((NAME(I, K), I=1, 15), (OLP(2, K, L), L=1, 8), K=1, N)
     PRINT 14
     PRINT 15, (NAME(I, 1), I=1, 15), (OLP(2, 1, L), L=1, 8)
     CALL EXIT
     END
```

A3.3 Computer program to process peak areas measured using an integrator for a reaction where two reactants are hydrogenated simultaneously, DATA 6.

The program finds the Qi's, P_i's and R's defined above first for all the detectable gaseous constituents, then for one of the reactants and its products and finally for the other reactant and its products. Equation 3.13 is used to calculate the conversion factors for the second reactant, hence only one set of conversion factors are required.

PROGRAM DATA 6

```
C     PROCESSING OF DATA FROM THE ANALYSIS OF A MIXED
C     REACTION (DATA FROM VPC WITH INTEGRATOR)
C     NM=NO. OF PEAKS ASSOCIATED WITH PRINCIPLE REACTANT
C     N=NO. PEAKS/CHROMATOGRAM  M=NO. OF CHROMATOGRAMS
C     ARED(j, K, 1)=PEAK AREA   ARED(J, K, 2)=UNTEG. SENS.
C     **********************************************************
      DIMENSION CONV(10, 3), AREA(10, 10, 3), ARED(10, 10, 2), OLFN(10, 10,
     1 3), NAME(15, 10, 3), PMOLEA(10, 10, 3), PMOLEB(10, 10, 3), NN(3)
    1 FORMAT(F5. 3, 15A1)
    2 FORMAT(10F6. 1)
    3 FORMAT(3I3)
      READ 3, N, M, NM
      READ 1, (CONV(J, 1), (NAME(K, J, 1), K=1, 15), J=1, N)
      DO 310 J=1, 8
      DO 310 K=1, N
      DO 310 JJ=1, 3
      AREA(J, K, JJ)=0. 0
      OLFN(J, K, JJ)=0. 0
      PMOLEA(J, K, JJ)=0. 0
      PNOLEB(J, K, JJ)=0. 0
  310 CONTINUE
      READ 2, (((ARED(J, K, L), L=1, 2), K=1, N), J=1, M)
      NN(1)=N
      NN(2)=NM
      NN(3)=N-NM
      DO 185 JJ=1, 3
      NFN=NN(JJ)
      DO 85 K=1, NFN
      IF(JJ-3)30, 31, 31
   31 KK=K+NM
      GO TO 32
   30 KK=K
   32 DO 80 J=1, M
      IF(JJ-2)82, 82, 83
```

```
 82   AREA(J, K, JJ)=ARED(J, K, 1)*ARED(J, K, 2)/100. 0
      GO TO 80
 83   AREA(J, K, JJ)=ARED(J, KK, 1)*ARED(J, KK, 2)/100. 0
 80   CONTINUE
      IF(2-JJ)86, 87, 87
 87   CONV(K, JJ)=CONV(K, 1)
      DO 89 LT=1, 15
      NAME(LT, K, JJ)=NAME(LT, K, 1)
 89   CONTINUE
 86   CONV(K, 3)=CONV(KK, 1)
      DO 85 LTT=1, 15
      NAME(LTT, K, 3)=NAME(LTT, KK, 1)
 85   CONTINUE
      IF(1. 0-CONV(1, JJ))5, 6, 5
  5   DO 7 J=1, NFN
      CONV(J, JJ)=CONV(J, JJ)/CONV(1, JJ)
  7   CONTINUE
  6   DO 16 L=1, M
      SUM=0. 0
      DO 17 K=1, NFN
      OLFN(L, K, JJ)=AREA(L, K, JJ)*CONV(K, JJ)/AREA(L, 1, JJ)
      SUM=SUM+OLFN(L, K, JJ)
 17   CONTINUE
      DO 100 I=2, NFN
      PMOLEA(L, I, JJ)=OLFN(L, I, JJ)*100. 0/(SUM-1. 0)
      PMOLEB(L, I, JJ)=OLFN(L, I, JJ)*100. 0/SUM
100   CONTINUE
      PMOLEB(L, 1, JJ)=100. 0/SUM
 16   CONTINUE
 11   FORMAT(26X50HPEAK AREAS (INTEGRATOR AT SENS. 1, AMPL. AT 10**-8)
 12   FORMAT(16X15HMOLAR FUNCTIONS)
 13   FORMAT(16X32HMOLE PERCENT PRODUCT OF PRODUCTS)
 14   FORMAT(16X21HMOLE PERCENT STANDARD)
 18   FORMAT(16X37HMOLE PERCENT OF PRODUCTS AND REACTANT)
 15   FORMAT(2X, 15A1, 8F15. 4)
 19   FORMAT(1H030X17HS T A N D A R D =, 15A1, /)
      PRINT 19, (NAME(LT, 1, JJ), LT=1, 15)
      IF(2-JJ)92, 94, 93
 93   PRINT 11
      PRINT 15, ((NAME(I, K, JJ), I=1, 15), (AREA(L, K, JJ), L=1, 8), K=1, NFN)
 92   PRINT 12
      PRINT 15, ((NAME(I, K, JJ), I=1, 15), (OLFN(L, K, JJ), L=1, 8), K=1, NFN)
 94   PRINT 18
      PRINT 15, ((NAME(I, K, JJ), I=1, 15), (PMOLEB(L, K, JJ), L=1, 8), K=1, NFN)
      IF(JJ)91, 185, 91
 91   PRINT 13
      PRINT 15, ((NAME(I, K, JJ), I=1, 15), (PMOLEA(L, K, JJ), L=1, 8), K=2, NFN)
      PRINT 14
      PRINT 15, (NAME(I, 1, JJ), I=1, 15), (PMOLEB(L, 1, JJ), L=1, 8)
185   CONTINUE
      CALL EXIT
      END
```

APPENDIX 4.

Theoretical pressure drop in the reaction vessel assuming adsorption of products occur.

The reaction produces n detectable products and all sumations in this appendix are over the n products only. A single molecule of reactant R produces only one molecule of a detectable product.

Nomenclature

G_i Fraction of reactant R reacting to form product i, the product may be either in the gaseous or adsorbed state.

Z_i Pressure drop associated with a partial pressure of one mm. Hg. R reacting to form product i, mm. Hg.

$^{O}P_R$ Initial reactant R pressure, mm. Hg.

X Partial pressure of products removed from the gas phase by adsorption, mm. Hg.

M_i Number of moles of the i^{th} product in the gas phase.

M_{iADS} Number of moles of the i^{th} product adsorbed on the catalyst.

M_R Number of moles of the reactant R present.

ΔP_C Reaction vessel pressure drop, due to reaction, calculated assuming no adsorption occurs, mm. Hg.

ΔP_{OBS} Observed reaction vessel pressure drop, mm. Hg, from mercury manometer readings.

The total pressure drop, L, in the reaction vessel due to the reaction of a partial pressure of one mm. Hg. of R is

$$L = X + \sum_{i=1}^{n} G_i Z_i \quad \text{mm. Hg}, \qquad \text{A4.1}$$

(c.f. equation 3.27 and G_i is given by equation A4.2, derived from 3.9 :-

$$G_i = (M_i + M_{iADS}) \; / \; (\sum_{i=1}^{n} (M_i + M_{iADS})). \qquad \text{A4.2}$$

Substituting A4.2 into A4.1 gives

$$L = X + \frac{\sum_{i=1}^{n} Z_i \, (M_i + M_{iADS})}{\sum_{i=1}^{n} (M_i + M_{iADS})} \text{ mm. Hg} \qquad \text{A4.3}$$

But if the fraction of reactant R which has reacted is D then the partial pressure of R which has reacted is

$$^{O}P_R \; D \text{ mm. Hg} \qquad \text{A4.4}$$

Hence the total pressure drop in the reaction vessel, ΔP_{OBS}, is

$$\Delta P_{OBS} = {}^{O}P_R \; D \; (L - X) + X \text{ mm. Hg}, \qquad \text{A4.5}$$

Where D is given by A4.6 derived from A3.1 ,

$$D = \sum_{i=1}^{n} (M_i + M_{iADS}) \; / (M_R + \sum_{i=1}^{n} (M_i + M_{iADS})) \qquad \text{A4.6}$$

Substituting equations A4.3 and A4.6 into A4.5 and cancelling gives

$$\Delta P_{OBS} = \frac{{}^{O}P_R \sum_{i=1}^{n} Z_i (M_i + M_{iADS})}{M_R + \sum_{i=1}^{n} (M_i + M_{iADS})} + X \text{ mm. Hg} \qquad \text{A4.7}$$

Since there are too many unknowns in equation A4.7 it does not yield useful information on its own. However, if it is used in conjunction with an expression for ΔP_C (the calculated pressure drop in the reaction vessel assuming no adsorption occurs) it is found that $\Delta P_{OBS} - \Delta P_C$ varies with percent reaction in a distinctive fashion.

An expression for ΔP_C in terms of moles of reactant R and its products is found from equation A4.7 by omitting any terms involving adsorption,

$$\Delta P_C = \frac{{}^{O}P_R \sum_{i=1}^{n} Z_i M_i}{M_R + \sum_{i=1}^{n} M_i} \qquad \text{A4.8}$$

Then clearly $\Delta P_{OBS} > \Delta P_C$ for all % reaction since

$$\frac{\sum_{i=1}^{n} Z_i (M_i + M_{iADS})}{M_R + \sum_{i=1}^{n} (M_i + M_{iADS})} \geq \frac{\sum_{i=1}^{n} Z_i M_i}{M_R + \sum_{i=1}^{n} M_i} \qquad \text{A4.9}$$

Two simple cases of the above expressions are obtained for the percent reaction tending to zero and to 100% respectively :-

A Percent reaction tending to zero

Expression A4.9 becomes

$$\frac{\sum_{i=1}^{n} Z_i (M_i + M_{iADS})}{M_R} > \frac{\sum_{i=1}^{n} Z_i M_i}{M_R} \qquad \text{A4.10}$$

therefore $\Delta P_{OBS} - \Delta P_C = \sum_{i=1}^{n} M_{iADS}/M_R + X$ A4.11

B Percent reaction tending to 100%

Expression A4.9 becomes

$$\frac{\sum_{i=1}^{n} Z_i(M_i + M_{iADS})}{\sum_{i=1}^{n} (M_i + M_{iADS})} = \frac{\sum_{i=1}^{n} Z_i M_i}{\sum_{i=1}^{n} M_i} \qquad \text{A4.12}$$

Hence for a reaction which has run to completion

$$\Delta P_{OBS} - \Delta P_C = X \qquad \text{A4.13}$$

This dependance of $\Delta P_{OBS} - \Delta P_C$ (always positive) makes it possible to distinguish between adsorption of the reactant alone and adsorption of products since as shown by equation 3.34 $\Delta P_{OBS} - \Delta P_C$ becomes negative at high percent reaction.

Appendix 5

A curve fitting program to find the relative rates of reaction of furan and sylvan when both these compounds are being hydrogenated simultaneously.

Of the various programs which were written to find the relative rate constants only the final and most successful will be described. This program used the Runge-Kulta approximate technique using Runge's coefficients (ref. 87) to solve the four simultaneous differential equations 6.22, 6.23, 6.27 and 6.28 finding the standard deviation of this synthetic curve from the experimental results and changing the rate constant automatically in a way likely to reduce the standard deviation. When an optimum value for the furan rate constant is obtained the process is repeated with another value of $\frac{K_A}{K_B}$, the ratio of the equilibrium constants for the adsorption of furan and sylvan. The cycle is continued until both constants are optimised. The sylvan rate constant is then found using relationship 6.18 and hence the ratio of the furan and sylvan rate constants is obtained.

The program consists of a subroutine RUNGE (ref. 87) which carries out the integration in conjunction with another subroutine TRUNGE. The main functions of TRUNGE are controlling RUNGE, calculating the hydrogen pressures adjusting the partial pressures of the reactants for each sample taken and calculating the standard deviation for the pair of constants used. TRUNGE in turn is controlled by the main program which in practice incorporates a Chebyshev polynomial subprogram but which has for simplicity's sake been described separately (Appendix 6). The main program's other functions

are arranging the data in a suitable form and selecting the next value of the furan rate constant to be tried.

A5.1 The Main Program.

The Runge Kutta method is an approximate technique which operates by increasing the independent variable, time in this case, in discrete steps, predicting the values of the dependent variables from their values and gradients during the transition of a step, for a fuller explanation of the technique see (ref. 88). Because of this step nature values of the dependent variables are only obtainable at set intervals of the independent variables and hence the main program must first find the steps which lie as close as possible to the times at which the samples were taken. For example if the time scale used ranges from 0 to 300 minutes increasing in steps of ten minutes and if a sample were taken at 73 minutes then the nearest calculated value obtained by the integration is 70 minutes.

Having selected the best approximations to the sample times used the corresponding mole fractions of furan are calculated by simply substituting into a Chebyshev polynomial (Appendix 6) which has previously been synthesised representing the best fit to the mole fraction furan reacted/time graph.

The main program then starts calling the subroutine TRUNGE, each time with a different value for the furan rate constant. At first the rate constant is changed by an arbitrary amount, then the last three standard deviations obtained together with their corresponding rate constants are used to construct a Lagrange polynomial (ref. 89) which may take one of the six forms illustrated in fig. A5.1.

Fig. A5.1 The six possible forms of the Lagrange polynomial.

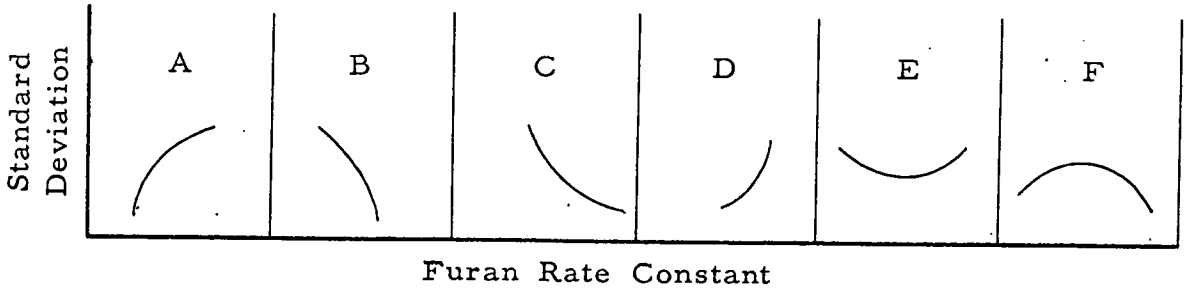

Of the above six possible shapes of the Lagrange polynomial only five occur in practice, F was never observed and hence it was ignored.

For types A and B the rate constant is simply varied by an arbitrary amount (the rate constant is decreased below the lowest value for a type A curve and increased above the highest value for a type B curve). For the other three possible types the minimum value of the curve is calculated by finding where the derivative is zero. The highest of the three standard deviations is then discarded and the new estimate of the furan rate constant is used when subroutine TRUNGE is recalled.

Main Program 'MTRUNGE'

```
C OPTIMISATION OF FURAN RATE CONSTANT
C IF SENCE SWITCH 2....ON TO RECORD, OFF TO RUN NORMALLY
C IF SENCE SWITCH 1.... ON TO FETCH, OFF TO RUN NORMALLY
C **** IF SENCE SWITCH 3 OFF...NORMAL, ON... TO CHANGE
C BK1 **** RECORD AND FETCH HOLD SD(J), RCF(J), J=1, 3 AND RC
C P3=HYDR, PRESSURE INITIAL, P4=FURAN PRESS. INITIAL,
C P5=SYLVAN PRESS, INITIAL, T3=FURAN POIS. CONST., T4=SYLVAN
C POIS. CONST., BK1=RADIO OF ADS. EQUIL. CONSTS., RCF=GUESSED
C RATE CONST. FURAN.
**********************************************************************
DIMENSION DY(4), Y(4), F(28), SD(3), FURG(10, 2), RCF(3) , R3(10)
DIMENSION SRCF(3), SSD(3)
DEFINE DISK(10, 000)
YL=10.0
XL=10.0
YD=0.05
YMIN=0.4
YMAX=1.0
XD=10.0
```

```
      XMAX=300.0
      XMIN=0.0
      READ 235, T3, T4, P4, P5, P3
      IC=1
      READ 236, BK1, RC      , RATIO, F1, F2, S1, S2, S3, S5
      PRINT 2001, RATIO, BK1, T3, T4
      PRINT 2000, P3, P4, P5
2000  FORMAT(9X, 22HINITIAL HYDR. PRESS. =  , F7.2, 9X, 22HINITIAL
     1 FURAN PRESS. = , F6.2, 9X, 23HINITIAL SYLVAN PRESS. =  , F6.2//)
2001  FORMAT(1H1, 9X, 7HRATIO=  , F8.4, 9X, 26HADSORPTION EQUIL.
     1 CONST. = , F8.5, 9X, 20HPOIS. CONST. FURAN=  , F8.5, 9X, 21HPOIS
     2. CONST. SYLVAN=  , F8.5)
      READ238 , ((FURG(K, J), J=1, 2), K=1, 9 )
      TU=RC/5.0
 235  FORMAT(2F9.6, 3F7.2)
 236  FORMAT(9F8.6)
 238  FORMAT(8F9.4)
      TIME SELECTOR
      PRINT 778
 778  FORMAT(5X, 17HTIME SAMPLE TAKEN)
      T=0.1
      K=0
 220  K=K+1
      PRINT 777, FURG(K, 1)
      T=T+5.0
      IF( FURG(K, 2))221, 221, 222
 222  IF( FURG(K, 1)-T)223, 225, 224
 224  T=T+5.0
      GO TO 222
 223  IF(FURG(K, 1)-T+2.5)226, 225, 225
 225  FURG(K, 1)=T
      GO TO 220
 226  FURG(K, 1)=T-5.0
      GO TO 220
C     MOLE FRACTION ADJUSTMENT
 221  READ99, M, (R3(I), I=1, M)
  99  FORMAT(I2, 5E13.7)
 777  FORMAT(F10.5)
      PRINT 779
 779  FORMAT(1H0, 5X, 46HCALCULATED MOLE FRACTION , FROM
     1 CHEBYCHEV POLN.)
      J=1
 107  IF(FURG(J, 2))94, 59, 94
  94  X=R3(1)
      DO 93 K=2, M
      X=X+R3(K)*FURG(J, 1)**(K-1)
  93  CONTINUE
      FURG(J, 2)=X
      PRINT 777, FURG(J, 2)
      J=J+1
```

A refinement to the process whereby a prediction is made of the value of K_F which will give the best fit of the experimental and theoretical furan reacted/time curves which was not completed at the time when this thesis was written up is to store all the standard deviations between the two curves obtained together with their corresponding furan rate constants in large dimensioned array, the program proceeding as before until a 'type E' curve (fig. A5.1) is located. At this point the old optimum rate constant prediction part of the program is discarded and all the n standard deviations found so far together with their corresponding rate constants are used to construct a best fit polynomial of order n - 1 (using subroutine "CHEB", Appendix 6). The minimum possible standard deviation is found by the Newton-Raphson approximation technique applied to the differentiated form of the polynomial, the value of K_F which corresponds to this minimum being used as the next approximation to the rate constant.

Such a technique should speed the determination of the rate constant yielding a result of superior accuracy.

pp 211 to 216 inclusive are in the reverse order, viz.

read p 216 for p 211

" " 215 " " 212

" " 214 " " 213

" " 213 " " 214

" " 212 " " 215

" " 211 " " 216.

A5.3 Subroutine RUNGE (Ref. 87).

```
      SUBROUTINE RUNGE (T, DT, N, Y, DY, F, L, M, J)
      DIMENSION DY(4), Y(4), F(28)
      GO TO (100, 110, 300), L
100   GO TO (101, 110), IG
101   J=1
      L=2
      DO 106 K=1, N
      K1=K+3*N
      K2=K1+N
      K3=N+K
      F(K1)=Y(K)
      F(K3)=F(k1)
106   F(K2)=DY(K)
      GO TO 406
110   DO 140 K=1, N
      K1=K
      K2=K+5*N
      K3=K2+N
      K4=K+N
      GO TO (111, 112, 113, 114), J
111   F(K1)=DY(K)*DT
      Y(K)=F(K4)+.5*(K1)
      GO TO 140
112   F(K2)=DY(K)*DT
      GO TO 124
113   F(K3)=DY(K)*DT
      GO TO 134
114   Y(K)=F(K4)+(F(K1)+2.*(F(K2)+F(K3))+DY(K)*DT)/6.
      GO TO 140
124   Y(K)=.5*F(K2)
      Y(K)=Y(K)+F(K4)
      GO TO 140
134   Y(K)=F(K4)+F(K3)
140   CONTINUE
      GO TO (170, 180, 170, 180), J
170   T=T+.5*DT
180   J=J+1
      IF(J-4)404, 404, 299
299   M=1
      GO TO 406
300   IG=1
      GO TO 405
404   IG=2
405   L=1
406   RETURN
      END
```

```
      RCF(NN)=RC+NN*TU
      RCS=BK1*RCF(NN)/RATIO
      LMN=1
      SUE=0.0
      LJ=0
      Y(1)=PF
      Y(2)=PS
      Y(3)=0.0
      Y(4)=0.0
 10   L=3
      M=O
 50   CALL RUNGE (T, DT, N, Y, DY, F, L, M, J)
      IF(M-1)75, 10, 75
 75   GO TO (100, 200, 999), L
100   DY(1)=-RCF(NN)*Y(1)*HPF(PH, Y(1), Y(2))*(1.0-Y(3)-Y(4))/(Y(1)+Y(2)/BK1)
      DY(2)=-RCS*Y(2)*HPF(PH, Y(1), Y(2))*(1.0-Y(3)-Y(4))/(Y(1)*BK1+Y(2))
      DY(3)=-DY(1)*T3/(2.0*SQRTF(T)*RCF(NN)*HPF(PH, Y(1), Y(2)))
      DY(4)=-DY(2)*T4/(2.0*SQRTF(T)*RCS*HPF(PH, Y(1), Y(2)))
      GO TO 50
200   LJ=LJ+1
      IF(LJ-2 )250, 241, 250
241   A=Y(1)/(PPFS+PF)
      IC=9
      LJ=O
      B=Y(2)/(PPSS+PS)
      PRINT 1111, T, A, B, Y(3), Y(4)
1111  FORMAT(7X, 5F20.4)
250   IF(FURG(LMN, 2))999, 999, 260
      ADJUST PRESSURES IF SAMPLE IS TAKEN
260   C=1.0-A
      IF(T-FURG(LMN, 1))50, 49, 49
 49   SUE=SUE+(A-FURG(LMN, 2))**2
      LMN=LMN+1
      PPFS=PPFS+PF-Y(1)
      PPSS=PPSS+PS-Y(2)
      PPS=PPS+PPFS+PPSS
      PPS=PRESSURE OF PRODUCTS
      TOTP=Y(1)+Y(2)+HPF(PH, Y(1), Y(2))+PPS
      D=(1.0-1.5/TOTP)
      PPS=PPS*D
      PH=HPF(PH, Y(1), Y(2))*D
      Y(1)=Y(1)*D
      Y(2)=Y(2)*D
      PF=Y(1)
      PS=Y(2)
      PPFS=PPFS*D
      PPSS=PPSS*D
      GO TO 10
999   RMN=LMN
      SD(NN)=SQRTF(SUE)/RMN
      PRINT 998, SD(NN), RCF(NN)
998   FORMAT(4X, 14HSTANDARD DEV. =, F10.6, 10X, 17HRATE CONST.
     1 FURAN=, F10.6)
      RETURN
      END
```

A5.2 Subroutine TRUNGE

TRUNGE calculates the hydrogen pressure for each step using equation A8.15. For the sake of increased flexibility the hydrogen pressure is described by an arithmetic statement function (HPF) this in turn being defined using two other arithmetic statement functions, FHDELF and SHDELF, describing the contributions of the furan and sylvan reactions respectively to the change in the hydrogen pressure. In this way were another pair of compounds to be hydrogenated simultaneously it would only be necessary to redefine FHDELF and SHDELF.

The drops in the partial pressures of furan, sylvan and hydrogen caused by the removal of a sample from the reaction vessel are calculated by assuming a total pressure drop of 1.2 mm.Hg. The individual pressure drops are then simply calculated knowing the relative pressures of the three reactants and the products of the reactions.

Subroutine TRUNGE is as follows:-

```
      SUBROUTINE TRUNGE(DY, Y, F, NN, TU, RCF, SD, FURG, T3, T4, P3,
     1 P4, P5, BK1, RATIO, F1, F2, S1, S2, S3, S5, XMIN, XMAX, XD, YMAX,
     2 YMIN, YD, XL, YL, RC)
      FHDELF(Z)=(PF-Z)*(4.0-2.0*F1-F2)
      SHDELF(V)=(PS-V)*(4.0-2.0*S1-2.5*S2-S3-S5)
      HPF(P8, Z, V)=P8-FHDELF(Z)-SHDELF(V)
      DIMENSION DY(4), Y(4), F(28), SD(3), FURG(10, 2), RCF(3)
      PH=P3
      PF=P4
      PS=P5
      PPS=0.0
      PPFS=0.0
      PPSS=0.0
      N=4
  800 FORMAT(10XF20.2, 4F20.4)
  237 FORMAT(23X92HTIME(MIN.) FURAN UNREACTED. SYLVAN REACTED.
     1 FURAN COVERAGE. SYLVAN COVERAGE)
      PRINT 237
      DT=5.0
      T=0.1
      RNR=NN
```

```
      SSD(1)=SD(L1)
      IF(RCF(L2)-RCF(L3))1005,1005,1006
1006  L4=L2
      L2=L3
      L3=L4
1005  SRCF(2)=RCF(L2)
      SRCF(3)=RCF(L3)
      SSD(2)=SD(L2)
      SSD(3)=SD(L3 )
      DO 1007 J=1,3
      SD(J)=SSD(J)
1007  RCF(J)=SRCF(J)
      END OF SORT
      PRINT 969,(RCF(J),SD(J),J=1,3)
      QO=      SD(1)/((RCF(1)-RCF(2))*(RCF(1)-RCF(3)))
      Q1=      SD(2)/((RCF(2)-RCF(1))*(RCF(2)-RCF(3)))
      Q2=      SD(3)/((RCF(3)-RCF(1))*(RCF(3)-RCF(2)))
      DDL=2.0*(QO+Q1+Q2)
      IF(DDL)229,228,228
 229  TU=ABSF(TU)
      IF(SD(3)-SD(1))230,231,231
 230  SD(1)=SD(3)
      RCF(1)=RCF(3)
      GO TO 240
 231  TU=-TU
 240  RC=RCF(1)-2.0*TU
      GO TO 3
 228  RO=(RCF(2)+RCF(3))*SD(1)/((RCF(1)-RCF(2))*(RCF(1)-RCF(3)) )
      R1 =(RCF(1)+RCF(3))*SD(2)/((RCF(2)-RCF(1))*(RCF(2)-RCF(3)))
      R2=(RCF(1) +RCF(2))*SD(3)/((RCF(3)-RCF(1))*(RCF(3)-RCF(2)) )
      RC=(RO+R1+R2)/DDL
      PRINT 969,DDL,RC
 969  FORMAT( E12.4)
      IF(RC)251,251,260
 251  RC=0.0-3.0*TU
      GO TO 3
 260  DO 242 J=1,3
      IF(RC-RCF(J))241,242
 242  CONTINUE
      SD(1)=SD(3)
      RCF(1)=RCF(3)
      GO TO 243
 241  DO 247 J=1,3
      IF(RC-RCF(J))247,246,246
 247  CONTINUE
      GO TO 243
 246  IF(SD(1)-SD(3))249,249,248
 248  SD(1)=SD(3)
      RCF(1)=RCF(3)
 249  TU=TU/4.0
 243  RC=RC-3.0*TU
 671  CONTINUE
  28  CALL EXIT
      END
```

```
      GO TO 107
   59 DO 671 K=1, 5
      GO TO (98, 3, 3, 3, 3), K
   98 IF(SENSE SWITCH 1)4, 96
    4 FETCH (II)(SD(JJ), RCF(JJ), JJ=1, 3), RC
      GO TO 5
   96 NN=1
      CALL TRUNGE(DY, Y, F, NN, TU, RCF, SD, FURG, T3, T4, P3, P4, P5,
     1 BK1, RATIO, F1, F2, S1, S2, S3, S5, XMIN, XMAX, XD, YMAX, YMIN, YD,
     2 KL, YL, RC)
      IC=99
   30 NN=2
      CALL TRUNGE(DY, Y, F, NN, TU, RCF, SD, FURG, T3, T4, P3, P4, P5,
     1 BK1, RATIO, F1, F2, S1, S2, S3, S5, XMIN, XMAX, XD, YMAX, YMIN, YD,
     2 XL, YL, RC)
      IF(SD(1)-SD(2))269, 3, 3
  269 TU=-TU
      RC=RC-1.0*TU
    3 IF(SENSE SWITCH 3)2400, 33
 2400 ACCEPT 2200, BK1
 2200 FORMAT(F7.4)
 2300 FORMAT(1H1, 20X, 38HRATIO OF ADSORPTION EQUIL. CONSTANTS= ,
     1 F7.4)
      PRINT 2300, BK1
      TU=RC/3.0
      K=2.0
      GO TO 96
   33 IF(SENSE SWITCH 2)7, 5
    7 RECORD(II)(SD(JJ), RCF(JJ), JJ=1, 3
      GO TO 28
    5 IC=99
      NN=3
      CALL TRUNGE(DY, Y, F, NN, TU, RCF, SD, FURG, T3, T4, P3, P4, P5,
     1 BK1, RADIO, F1, F2, S1, S2, S3, S5, XMIN, XMAX, XD, YMAX, YMIN, YD,
     2 XL, YL, RC)
      IC=99
      L1=1.0
      L2=2.0
      L3=3.0
 1004 IF(RCF(L1)-RCF(L2))1001, 1001, 1002
 1001 IF(RCF(L1)-RCF(L3))1003, 1003, 1002
 1002 GO TO(1, 2), L1
    1 L1=2.0
      L2=1.0
      L3=3.0
      GO TO 1004
    2 L1=3.0
      L2=1.0
      L3=2.0
 1003 SRCF(1)=RCF(L1)
```

Appendix 6

Chebyshev polynomial curve fitting computer program.

The Chebyshev polynomial curve fitting method is a high speed technique relying on the least squares principle for the optimum approximation of a function to data points. The principle states that the partial derivatives of S, the sum of the squares of the 'residuals' (the difference in the Y coordinate of each data point and the value calculated using a trial function), with respect to each unknown constant in the trial function is zero when the function giving the optimum fit to the data points is used.

Using this principle a polynomial of degree m which approximates to the data can be found by solution of the m + 1 'normal' or simultaneous linear equations generated by the partial differentiation of S with respect to each of the m + 1 unknown constants in turn. This is the method most usually adopted for least squares approximations to data.

The Chebyshev polynomial approach is superior in that it is inherently faster and requires less storage space. Both advantages arise because the data is processed in such a way that rather than solve m + 1 linear simultaneous equations in m + 1 unknowns, simple expressions can be derived for each of the unknown constants. The simplification relies on the following property of Chebyshev polynomials :-

$$\sum_{i=1}^{m+1} T_K(\bar{x}_i).\ T_l(\bar{x}_i) = \begin{cases} 0 & \text{for } K \neq l \\ (m+1)/2 & \text{for } K = l \neq 0 \\ m+1 & \text{for } K = l = 0 \end{cases} \qquad \text{A6.1}$$

where $T_j(\bar{x})$ is the Chebyshev polynomial of degree j, m is an integer and $\bar{x}_i = \cos \frac{(2i-1)\pi}{2(m+1)}$ A6.2

In brief, a linear transform is applied to the data so that the x coordinates lie in the interval $(-1,1)$. By using Lagrangian interpolation the altered data is used to find the Y coordinates ($\bar{y}_i$) which correspond to the $\bar{x}_i$ values generated by equation A6.2 and these new data points, $(\bar{x}_1, \bar{y}_1)$, $(\bar{x}_2, \bar{y}_2)$.... $(\bar{x}_{m+1}, \bar{y}_{m+1})$, are approximated to by the polynomial,

$$Y_M(\bar{x}) = \sum_{j=0}^{m} A_j T_j(\bar{x}) \quad , \qquad \text{A6.3}$$

where A_j is the polynomial's j^{th} constant and m is the polynomial's order. Then, applying the least squares criterion to A6.3 and making use of A6.1 :

$$A_j = \frac{2}{m+1} \sum_{i=1}^{m+1} \bar{y}_i T_j(\bar{x}_j) \quad , \; j \neq 0 \qquad \text{A6.4}$$

$$A_j = \frac{2}{m+1} \sum_{i=1}^{m} \bar{y}_i T_j(\bar{x}_j) \quad , \; j = 0 \qquad \text{A6.5}$$

Finally, equation A6.3 is re-expressed as a polynomial in X and a linear transform is applied to change the data back to its original interval, the A_j's being used to find the new constants, C_j's, in this final equation ,

$$Y(x) = \sum_{j=1}^{m} C_j x^j \qquad \text{A6.6}$$

A more detailed description of the technique is given in ref. 90.

The Chebyshev polynomial curve fitting program was used to smooth out random errors in the data for the final simulation programs used for single reactions (RATESIM6, Appendix 10) and simultaneous hydrogenations of furan and sylvan ('MTRUNGE', Appendix 5). For single reactions it was found that the incorporation of the smoothing sub-program increased the reliability of the values found for the rate constant by a factor of approximately three.

The Chebyshev smoothing was carried out by subroutine 'CHEB', which was incorporated in 'RATESIM6', being called by a short main program 'MCHEB' whenever else it was used (e.g. 'MTRUNGE')

Program 'MCHEB'

```
      DIMENSION R(25), V(20 ), Y(20 ), C(25), F(25), G(10.10)
      CALL CHEB(N, M, Y)
      CALL EXIT
      END
```

SUBROUTINE CHEB

```
      SUBROUTINE CHEB(N, M, Y)
      CHEBYSHEV POLYNOMIAL CURVE FITTING - NON EQUIDISTANT
      DATA,  M=ORDER OF POLYNOMIAL,  N=NUMBER OF DATA
      POINTS USED,  Y(I) AND V(I) ARE Y AND X COORDS.RESP. OF
      ITH DATA POINT.
      ************************************************************
      DIMENSION R(25), V(20 ), Y(20 ), C(25), F(25), G(10.10)
      READ 5, M, N
      READ 2, (Y(I), V(I), I=1, N)
      PAUSE
      VM=V(1)
      IF(VM)30, 31, 30
   30 DO 32 I=1, N
   32 V( I ) = V( I )-VM
   31 M=M+1
    5 FORMAT(I2, I4)
    2 FORMAT(8F9.4)
 1234 FORMAT(8F9.4)
      M=M+1
      COMPUTE ROOTS
```

```
      X2=M
      DO 1000 I=1, M
      X1=I
      ARG=1.5707963268*(2.0*X1-1.0)/X2
      MSUB=M+1-I
      R(MSUB)=COSF(ARG)
1000  CONTINUE
      SUM1= (V(N)-V(1))/2.0
      SUM2=(V(N)+V(1))/2.0
      NORMALIZE VECTORS
      DO 1003 I=1, N
      V(I)=(V(I)-SUM2)/SUM1
1003  CONTINUE
      LAGRANGE INTERPOLATION, UNEQUALLY SPACED DATA
      I=1.0
      DO 150 L=1, N
 160  SS=0.0
      IF    (R(I)-V(L))151, 151, 150
 151  IF(L-2)154, 154, 155
 155  IF(N-L)156, 156, 157
 154  DO 13 K=1, 3
      PI=1.0
      LL=0.0
   4  LL=LL+1
      IF(LL-K)12, 4, 12
  12  IF(LL-3)10, 10, 7
  10  PI=PI*(R(I)-V(LL))/(V(K)-V(LL))
      GO TO 4
   7  SS=SS+PI*Y(K)
  13  CONTINUE
      GO TO 19
 156  L5=3.0
      GO TO 158
 157  L5=4
 158  DO 14 K=1, L5
      PI=1.0
      LL=L-3
  16  LL=LL+1
      IF(LL-L-K+3)15, 16, 15
  15  IF(LL-L-L5+3)18, 18, 17
  18  LLL=L-3+K
      PI=PI*(R(I)-V(LL))/(V(LLL)-V(LL))
      GO TO 16
  17  LLL=1-3+K
      SS=SS+PI*Y(LLL)
  14  CONTINUE
  19  F(I)=SS
      I=I+1
      IF(M+1-I)153, 153, 160
 150  CONTINUE
```

```
      COMPUTE COEFFICIENTS
  153 ZM=M
  992 FORMAT(5E16.6)
      PRINT 992,(F(I),I=1,M)
      DO 280 I=1,M
      SUM=0.0
      IF(I-2)260,265,270
  260 DO 261 J=1,M
  261 SUM=SUM+F(J)
      GO TO 275
  265 DO 266 J=1,M
  266 SUM=SUM+R(J)*F(J)
      GO TO 275
  270 V(1)=1.0
      DO 272 J=1,M
      V(2)=R(J)
      DO 271 K=3,I
  271 V(K)=2.*R(J)*V(K-1)-V(K-2)
  272 SUM=SUM+F(J)*V(I)
  275 C(I)=2.0*SUM/ZM
  280 CONTINUE
      C(1)=C(1)/2.0
      PRINT 992,(C(I),I=1,M)
      NN=M-1
      PRINT 305,NN
  305 FORMAT(2X,33HPOLYNOMIAL COEFFICIENTS - DEGREE ,I2,//)
C     CONVERT CHEBYSHEV SERIES TO ITS EQUIVALENT POWER SERIES
      DO 888 L6=1,5
      DO 888 L7=1,2
      G(L7,L6)=0
  888 CONTINUE
      G(1,2)=1.0
      G(2,3)=1.0
      F(1)=C(1)
      F(2)=C(2)
      DO 886 L=3,M
      F(L)=0
      J6=L+1
      DO 884 N=2,J6
      G(L,N)=G(L-2,N)+2.0*G(L-1,N-1)
      F(N-1)=F(N-1)+G(L)*G(L,N)
  884 CONTINUE
      G(L,1)=0.0
      G(L,L+2)=0.0
      G(L,L+3)=0.0
  886 CONTINUE
C     COEF OF POWER SERIES IN F(N)
C     GO BACK TO ORIGINAL INTERVAL
      PRINT 992,(F(I),I=1,M)
  597 Y(1)=F(1)
```

```
      DO 580 K=2, M
580   Y(K)=0. 0
      DO 583 K=2, M
      L=K-1
      Y(K)=Y(K)+F(K)/SUM2**L
      SUM3=1, 0
      ZIP=1. 0
      X2=K
      DO 582 J=1, L
      X1=J
      SUM3=SUM3*X1
      DV=SUM3*SUM2**L
      ZIP=ZIP*(X2-X1)
      LLL=K-J
582   Y(LLL)=Y(LLL)+(ZIP*SUM1**J*(-1. )**J*F(K))/DV
583   CONTINUE
      IF(VM)20, 21, 20
 20   DO 22 K=1, M
 22   V(K)=Y(K)
      Y(1)=0. 0
      DO 26 I=1, M
 26   Y(1)=Y(1)+(-VM)**(I-1)
      DO 27 M2=2, M
      K2=M2-1
      Y(M2)=0
      DO 27 I=M2, M
      RI=I
      PR=1. 0
      DO 28 K=1, K2
      RK=K
 28   PR=PR*(RI-RK)/RK
 27   Y(M2)=Y(M2)+PR*A(I)*(-VM)**(I-M2)
      COEFFICIENTS STORES IN Y(K)
 21   DO 584 K=1, M
      I=K-1
584   PRINT 585, I, Y(K)
585   FORMAT(30X, 2HA(, I2, 3H)=, E16. 8)
      RETURN
      END
```

APPENDIX 7.

Theoretical proof that $\frac{K_A}{K_B}$ and K_F are resolvable using a curve fitting procedure.

Nomenclature :-

^iP_F		The furan partial pressure (mm. Hg.) in the reaction vessel on taking the i^{th} sample.
^iP_S		The sylvan partial pressure (mm. Hg.) in the reaction vessel on taking the i^{th} sample.
R		K_A / K_B
t		Time (sec.)
D_i	=	$d\,^iP_F/dt = K_F\,{}^iP_F\,{}^iP_H(1-\alpha-\beta)\,/\,(^iP_F+{}^iP_S/R)$, from equation 6.27.
d_i	=	$d\,^iP_F/dt$, found from experimental results.
J_i	=	D_i/K_F, note that this function is independant of K_F.
S	=	$\sum_{i=1}^{n} (D_i - d_i)^2$, summed over all n readings.

The conditions for a best fit between the experimental and theoretical curves is the same as those involved in a least squares approximation, i.e.,

$$\frac{\partial S}{\partial K_F} = 0 \qquad \text{A7.1}$$

and

$$\frac{\partial S}{\partial R} = 0 \qquad \text{A7.2}$$

Using the definition of S, A7.1 and A7.2 expand to A7.3 and A7.4 respectively :-

$$\frac{\partial S}{\partial K_F} = \sum_{i=1}^{n} \frac{\partial (D_i - d_i)^2}{\partial K_F} = \sum_{i=1}^{n} 2(D_i - d_i)g_i = O \qquad \text{A.73}$$

$$\frac{\partial S}{\partial R} = \sum_{i=1}^{n} \frac{\partial (D_i - d_i)^2}{\partial R} = \sum_{i=1}^{n} \frac{2(D_i - d_i)\,{}^{i}P_S\, Di}{R\,({}^{i}P_F + {}^{i}P_S/R)} = O \qquad \text{A7.4}$$

Expanding A7.3 and dividing by two gives

$$\sum_{i=1}^{n} D_i g_i - \sum_{i=1}^{n} d_i g_i = O \qquad \text{A7.5}$$

and substitution for D_i (see nomenclature) into A7.5 gives

$$K_F \sum_{i=1}^{n} g_i^2 - \sum_{i=1}^{n} d_i g_i = O \qquad \text{A7.6}$$

Expanding the sum in A7.4 and dividing by two gives

$$\frac{1}{R} \sum_{i=1}^{n} \frac{D_i^2\, {}^{i}P_S}{({}^{i}P_F + {}^{i}P_S/R)} - \frac{1}{R} \sum_{i=1}^{n} \frac{d_i\, {}^{i}P_S\, D_i}{({}^{i}P_F + {}^{i}P_S/R)} = O \qquad \text{A7.7}$$

Substitution for D_i (see nomenclature) into A7.7 and removing $1/R$ terms gives

$$K_F \sum_{i=1}^{n} \frac{g_i^2\, {}^{i}P_S}{({}^{i}P_F + {}^{i}P_S/R)} - \sum_{i=1}^{n} \frac{d_i\, {}^{i}P_S\, g_i}{({}^{i}P_F + {}^{i}P_S/R)} = O \qquad \text{A7.8}$$

Equations A7.6 and A7.8 form a pair of simultaneous equations from which K_F may be conveniently eliminated (remembering that g_i and d_i are not functions of K_F) i.e.,

$$\sum_{i=1}^{n} \frac{d_i \, {}^iP_S \, g_i}{({}^iP_F + {}^iP_S/R)} = \left\{ \frac{\sum_{i=1}^{n} d_i g_i}{\sum_{i=1}^{n} g_i^2} \right\} \cdot \sum_{i=1}^{n} \frac{g_i^2 \, {}^iP_S}{({}^iP_F + {}^iP_S/R)} \qquad \text{A7.9}$$

A7.9 is an equation which involves R, and variables which are independant of K_F, hence K_F and R are theoretically seperable. In practice it was found that changes in K_F had a much larger effect on the shape of the theoretical curve generated by solution of the four simultaneous differential equations 6.27, 6.28, 6.22 and 6.23 then changes of a similar magnitude in R.

APPENDIX 8.

Calculation of the hydrogen pressure in the reaction vessel.

For a system where a reactant R is hydrogenated to n products:-

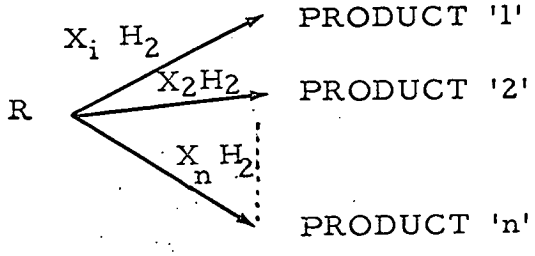

(Where X_i is the number of molecules of hydrogen required to hydrogenate one molecule of R to product 'i'.)

Let R_i be the fraction of product 'i' formed (e.g. section 3.1.5. In other words when one molecule of R is hydrogenated the probability of it forming product i is R_i (R_i is found from the product distribution, see equation A3.2). Then if a partial pressure of one mm. Hg of R reacts the drop in the partial pressure of hydrogen is

$$\sum_{i=1}^{n} X_i R_i \quad \text{mm. Hg.} \qquad \text{A8.1}$$

Therefore if a partial pressure of Z mm. Hg of R reacts the drop in the hydrogen's partial pressure is

$$Z \sum_{i=1}^{n} X_i R_i \quad \text{mm. Hg} \qquad \text{A8.2}$$

But the hydrogen pressure, P_H, in the reaction vessel during the hydrogenation of R is given by

$$P_H = P_H^o - \text{(the drop in the partial pressure of hydrogen)} \qquad \text{A8.3}$$

(where P_H^o is the initial partial pressure of hydrogen)

Combination of A8.3 and A8.2 gives

$$P_H = P_H^O - Z \sum_{i=1}^{n} X_i R_i \qquad \text{A8.4}$$

But Z is given by

$$Z = P_R^O - R_R \quad \text{mm. Hg} \qquad \text{A8.5}$$

where P_R^O is the initial reactant pressure and P_R is the reactant pressure at the time at which the hydrogen pressure is required. Therefore substituting A8.5 into A8.4 leads to an expression for the hydrogen pressure in terms of the partial pressure of the reactant:

$$P_H = P_H^O - (P_R^O - P_R) \sum_{i=1}^{n} X_i R_i \text{ mm. Hg.} \qquad \text{A8.6}$$

This expression was not usually used since, in order to minimise the number of bits of information used to calculate P_H one of the R_i values was expressed in terms of all the other R_i's making use of the following relationship

$$\sum_{i=1}^{n} R_i \equiv 1 \qquad \text{A8.7}$$

The application of A8.6 and A8.7 is best illustrated by the following examples of the furan and sylvan hydrogenations.

The Furan hydrogenation over Pt/Pumice

R = F in all the relationships used in this example. Since at low temperatures the fraction of n-propane formed is less than 2% this product will be omitted for simplicities sake.

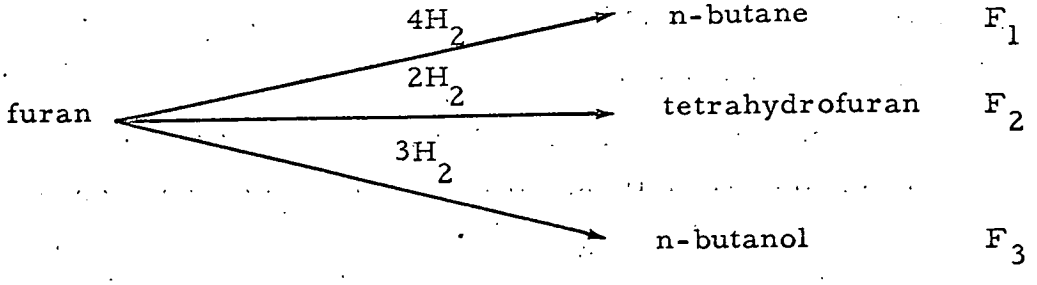

(Where F_1, F_2 and F_3 are the product distributions for the three products in terms of mole fractions). The hydrogen pressure when the furan partial pressure has dropped from an initial value of P_F^O to P_F mm. Hg is given by applying A8.6 to the furan hydrogenation:

$$P_H' = P_H^O - (P_F^O - P_F)(4F_1 + 2F_2 + 3F_3) \qquad \text{A8.8}$$

But by using the relationship A8.7;

$$F_1 = 1 - F_2 - F_3 , \qquad \text{A8.9}$$

Substitution of A8.9 into A8.8 gives

$$P_H = P_H^O - (P_F^O - P_F)(4 - F_3 - 2F_2) \qquad \text{A8.10}$$

The sylvan hydrogenation over Pt/pumice

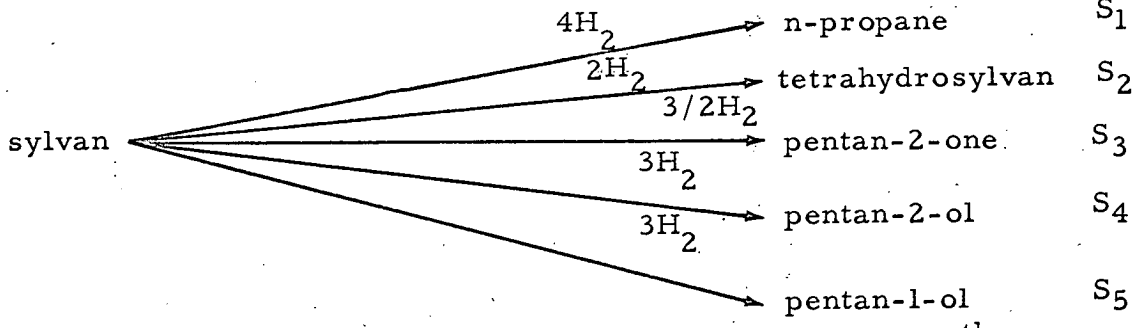

(where the S_i values are the product distributions for the i^{th} product in terms of mole fractions). The hydrogen pressure when the furan partial pressure has dropped from an initial value of P_S^O to P_S is given by equation A8.6 i.e.,

$$P_H = P_H^O - (P_S^O - P_S)(4S_1 + 2S_2 + \tfrac{3}{2}S_3 + 3S_4 + 3S_5) \qquad \text{A8.11}$$

but by using the relationship A8.7

$$S_1 = 1 - S_2 - S_3 - S_4 - S_5 \qquad \text{A8.12}$$

then substituting A.12 into A8.11 gives

$$P_H = P_H^O - (P_S^O - P_S)(4 - 2S_2 - 5/2S_3 - S_4 - S_5) \qquad \text{A8.13}$$

Hydrogenation of furan and sylvan simultaneously

For a simultaneous reaction the hydrogen pressure is given by $P_H = P_H^O$ - (drop in the hydrogen's partial pressure due to the furan reacting) - (drop in the hydrogen's partial pressure due to the sylvan reacting) A8.14

Clearly A8.14 may be re-expressed by substituting for the pressure drops by A8.10 and A8.13 giving

$$P_H = P_H^O - (P_F^O - P_F)(4-F_3-2F_2)-(P_S^O - P_S)(4-2S_2-2{\cdot}5S_3-S_4-S_5) \qquad \text{A8.15}$$

Appendix 9

Computer Program to solve equation 5.30 for the poisoning constant.

The program finds K' by solving equation 5.30 by the Newton-Raphson technique for successive approximations to the root of an equation (ref. 91).

By this technique a recursive procedure is used to find successively more accurate approximations to the solution of an equation in the form $f(x) = 0$ using the iterative sequence

$$X_{n+1} = X_n - f(X_n) / f'(X_n) \quad , \qquad \text{A9.1}$$

where X_n and X_{n+1} are the n^{th} and $(n+1)^{th}$ approximations.

The computer program written, using equation 5.32 (which is the form A9.1 takes if $f(x) = Q(K')$), finds K' for all the combinations of different runs in a consecutive run experiment. To increase the program's flexibility $Q(K')$ and $Q'(K')$ are defined in terms of the 'Arithmetic Statement Functions' TF(T) and DF(T) respectively. Since all the models for g(t) tried can be conveniently expressed in terms of $Z(X, K')$, c.f. equation 5.37, and $\partial(Z(X, K')) / \partial K'$, c.f. equation 5.38, TF(T) and DF(T) define these two variables rather than the more complex expressions for $Q(K')$ and $Q'(K')$. To use the program for a different model for g(t) it is only necessary to redefine TF(T) and DF(T), which are the first cards in the program.

In passing, all the models analysed using the program have trivial roots, for instance, for $g(t) = \exp(-K' t)$ one solution of equation 5.30 is for K'=0 while for $g(t) = \exp(-K' t^{\frac{1}{2}})$, $Q(K')$ tends to zero as K' tends to infinity. These trivial values of K'

were avoided by a suitable choice for the first approximation to the root of Q(K').

In the following program $g(t) = \exp(-K' t^{\frac{1}{2}})$.

Program to find K'

```
      TIMES OF START OF RUN IN T(1, J), OF XTH REACTION IN T(2, J)
      TF(T)=2. 0*EXPF(-CONST*SQRTF(T))*(SQRTF(T)+1. 0/CONST)/CONST*(-1. 0)
      DF(T)=2. 0*EXPF(-CONST*SQRTF(T))*(T+2. 0*SQRTF(T)/CONST+2. 0/
     1 CONST** 2)/CONST
      DIMENSION T(2, 4), SCONST(3, 3)
      READ 2, T
    2 FORMAT(8F6. 2)
      K=1
      N=1. 0
   55 N=N+1
      DO 50 J=N, 4
      S=99. 9
      CONST = 0. 001
      JM1=J-1
   51 DEN=DF(T(2, K))-DF(T(1, K))-DF(T(2, J ))+DF(T(1, J ))
      CONST=CONST-(TF(T(2, K))-TF(T(1, K))-TF(T(2, J ))+TF(T(1, J )))/DEN
      IF(0. 00001-ABSF((S-CONST)/CONST))19, 52, 52
   19 S=CONST
      GO TO 51
   52 SCONST(K, JM1)=CONST
   50 CONTINUE
      K=K+1
      IF(K-4)55, 56, 56
   56 PRINT 90, (SCONST(1, J), J=1, 3)
   90 FORMAT(20X, 18HI(1)-I(2) GIVES K=, F6. 4, 5X, 18HI(1)-I(3) GIVES K=,
     1 F6. 4, 5X, 18HI(1)-I(4) GIVES K=, F6. 4//)
      PRINT 91, (SCONST(2, J), J=2, 3)
   91 FORMAT(20X, 18HI(2)-I(3) GIVES K=, F6. 4, 5X, 18HI(2)-I(4) GIVES K=,
     1 F6. 4//)
      PRINT 92, SCONST(3, 3)
   92 FORMAT(20X, 18HI(3)-I(4) GIVES K=, F6. 4 )
      CALL EXIT
      END
```

APPENDIX 10

Two computer programs for the simulation of the kinetics of the hydrogenation of a single reactant.

The two programs used both solve equation 5.49 to find what K_F would be if the model for $f(P_F)$ and the poisoning constant K' under investigation are correct, clearly if they are satisfactory all the computed K_F's will have the same value within the limits of experimental error. The two programs therefore differ only in their means of operation rather than in their possible applications.

As has been mentioned in section 5.3.2 the integration of $\exp(-K' t^{\frac{1}{2}})$ is performed by solution of the closed form of its integral, equation 5.50, while the integral with respect to the reactant's partial pressure in equation 5.49 is carried out by an approximate numerical technique, wherein lies the major difference in the two programs. In the first program, RATESIM3, the numerical integration is performed by Simpson's method which splits the function to be integrated into short sections ranging between the required limits, approximates to each arc so obtained by a parabola, finds the area under each parabola by substitution into the closed form of the integral for a parabola and finally sums these areas to give the required integral (for further details see ref.(92)). Clearly the smaller the sections into which the function is partitioned the better is the approximation to the integral but this improved accuracy increases the calculation time.

The second more powerful program, RATESIM6, uses Gaussian quadrature to perform the numerical integration. Briefly the technique may be summed up by equation A10.1.

$$\int_{-1}^{1} f(x).\, dx = \sum_{i=1}^{n} w_i\, f(x_i) \qquad \text{A10.1}$$

Where f(x) is any continuous function in x, x_i is the i^{th} root of the Lagrange polynomial, $P_{n+1}(x)$, of degree n + 1, n is an arbitrary integer depending on the accuracy required, six was usually used, and w_i is the weighting coefficient which is found using equation A10.2

$$w_i = \frac{1}{P^1_{n+1}(x_i)} \int_{-1}^{+1} \frac{P_{n+1}(x)\, dx}{x - x_i} \qquad \text{A10.2}$$

An excellent explanation of this form of Gaussian quadrature is given by Kuo (ref. 87).

Clearly the second program is much faster than RATESIM3 and hence was used to process all the data from the later furan and sylvan hydrogenations.

Both computer programs allow for pressure changes in the reaction vessel due to sampling and both express all hydrogen pressures in terms of furan pressures, see Appendix 8. The furan pressures themselves are calculated from the initial furan pressure, P_F^O, and the mole fraction of furan unreacted, R, (found for each sample analysed using equation A3.1):-

$$P_F = RP_F^O \qquad \text{A10.3}$$

where P_F is the furan pressure, mm. Hg.

Both programs find the K_F values by using two types of integrals of the pressure function (see equation 5.49), these will be referred to as segmented and normal integrals respectively. These different methods for finding K_F were used since first, the pressures of the reactants change when a sample

is taken, hence $f(P_F)$ is not a continuous function, and second, because it is of interest to examine small divergences in the rate constant from its mean. The second factor increases in importance with increasing percent reaction since a small change in the reaction kinetics at high percent reaction will be masked by the bulk of the reaction which has already occurred. This is demonstrated diagrammatically in fig. A10.1 for a hypothetical reaction which proceeds under one type of kinetics until a reactant pressure of P_1 mm. Hg. is reached at time t_1 minutes when the kinetics changes slightly and the reaction continues up to time t_2 minutes when the reaction pressure is P_2 mm. Hg.

Fig. A10.1 Hypothetical dependance of 1/f(P) on pressure (diagrammatic)

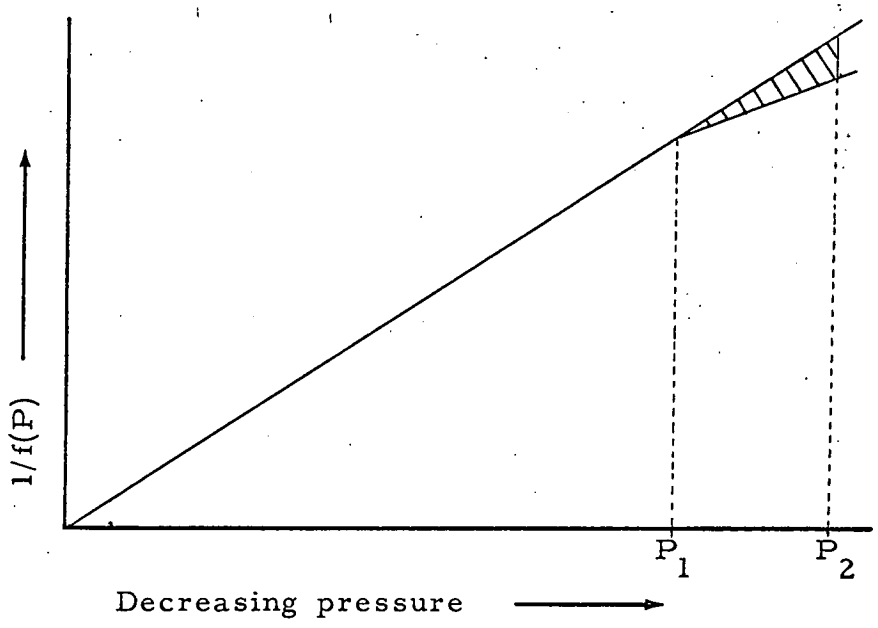

If one is calculating K_F in a similar manner to that summarised in equation 5.49 by using the integration limits of the initial conditions and those at reactant pressure P_2 the difference between the integral of the actual pressure function and that of the pressure function which describes the bulk of the reaction is the shaded area in fig. A10.1. As is apparent from the above figure this difference is only a small fraction of the total area under the straight line and hence would be difficult to detect.

Clearly both the above difficulties are overcome by changing the integration limits to the time and pressures for adjacent pairs of data points (i.e., when a sample is taken). These integrals will be referred to as segmented integrals.

Since there was an error of approximately $\pm$ 1.5% in the values of the reactant pressures found by analysis of samples of the reaction mixture taken, the fluctuations in the equilibrium constants found using segmented integrals was as high as 60%, hence another inherently more stable type of integral was used to find K_F: The 'normal integrals' are the equivalent of integrating from the start of the reaction to when a sample is taken, the reason for the stability in the K_F's found using them has been outlined above. The expression for K_F, derived from 5.49, for the n^{th} sample found using normal integrals is

$$K = - \sum_{i=1}^{n} \int_{i-1 P_F}^{i P_F} \frac{dP_F}{f(P_F)} \Big/ \int_{t_1}^{t_n} \exp(-K' t^{\frac{1}{2}}).dt \,, \qquad \text{A10.4}$$

where t_1 and t_n are the time at which the reaction starts and when the n^{th} sample is taken respectively, ${}_iP_F$ is the furan partial pressure in the reaction vessel when the i^{th} sample is withdrawn and the solution for the integral with respect to time is given by equation 5.50.

Program RATESIM 3

Smoothing out the random fluctuations in the calculated values of K_F, caused by experimental error, is achieved by plotting a graph of time against the mole fraction of furan unreacted, using analysis data. A best fit curve is then drawn through the points and the mole fraction of furan unreacted and time data which is fed into RATESIM 3 is found from the best fit curve. An additional feature of this program is that extra

data points, from the best fit curve, can be fed in as data to give a less disjointed picture of how K_F varies with time. (A provision is made so that the no pressure drops are calculated for such points).

The normalised standard deviations of both sets of equilibrium constants are calculated using a modification of the usual equation used to find standard deviations :

$$\sigma = \frac{\sqrt{N \sum_{i=1}^{n} {}_iK_F^2 - \left(\sum_{i=1}^{n} {}_iK_F\right)^2}}{\sum_{i=1}^{n} {}_iK_F} \qquad \text{A10.5}$$

where σ is the standard deviation, n is the number of data points used and ${}_iK_F$ is the rate constant found for the i^{th} data point. Equation A10.5 is the normal expression for the standard deviation divided by the mean value of the ${}_iK_F$'s. The advantage of expression A10.5 for σ is that all the standard deviations are on an absolute scale.

PROGRAM RATESIM3

```
C SIMULATION OF A FURAN HYDROGENATION USING SIMPSON
C INTEGRATION.
C N=THE NUMBER OF READINGS USED, TFF(J) IS THE MOLE
C FRACTION OF FURAN UNREACTED FOR THE JTH SAMPLE
C TAKEN AT TIME (J), PH AND PF ARE THE INITIAL HYDROGEN
C AND FURAN PRESSURES (MM.HG.) RESPECTIVELY, ALF AND
C BET = THE PROBABILITIES THAT A FURAN MOLECULE
C UNDERGOING HYDROGENATION FORMS THF AND N-BUTANE
C RESPECTIVELY, MM(J)=1 IF A PRESSURE DROP MUST BE
C ALLOWED FOR THE J TH. READING, ZERO IF NO PRESSURE
C DROP IS REQUIRED, T3= THE POISONING CONSTANT, B4= THE
C FURAN ORDER.
C **********************************************************
  DIMENSION TIME(26), TFF(26), MM(26), CONS(26,2), SIM(27), S(27),
 1XLAMDA(26), XX(26), TOT(2), TOTSQ(2), STDEV(2)
  READ 2, N, PH, PF, ALF, BET
  READ 1, (MM(J), J=I, N)
1 FORMAT(26I2)
2 FORMAT(I2, 4F9.4)
```

```
      DO 3 J=1,26
      TIME(J)=0
      TFF(J)=0
    3 CONTINUE
      T3=0.04
      PRINT 100,PF,PH
      A=PH-PF*(3.0-ALF+BET)
      B=3.0-ALF+BET
      XLAMDA(J)=0
      READ 101,(TFF(J),TIME(J),J=1,N)
  101 FORMAT(8F9.4)
  100 FORMAT(5X,24HINITIAL FURAN PRESSURE= ,F6.2,32HMM.,
     1INITIAL HYDROGEN PRESSURE= ,F6.2,4HMM. )
      DO 60 K=3,5
      S(1)=2.0/(T3*T3)
      SIM(1)=0
      PRINT 900,K
  900 FORMAT(I2)
      B6=4*K-10
      B4=B6/10.
      MC1=1
      X=PF
      JJ=1
      DO 500 J=1,26
      XX(J)=0
      XLAMDA(J)=0
      CONS(J,1)=0
      CONS(J,2)=0
  500 CONTINUE
      SIMINT=0
   51 L=0
      GO TO 10
   31 L=1
    4 IF(X-TFF(JJ)*PF)9,6,6
    6 X=X-0.02
   10 L=L+1
      GO TO (8,11,12),L
    8 SIMINT=SIMINT+0.02/(X**B4*(A+B*X)*3.)
      GO TO 4
   11 SIMINT=SIMINT+4.*0.02/(X**B4*(A+B*X)*3.)
      GO TO 4
   12 SIMINT=SIMINT+2.*0.02/(X**B4*(A+B*X)*3.)
      GO TO 31
    9 IF(L-2)40,41,40
   40 SIMINT=SIMINT-0.02/(X**B4*(A+B*X)*3.)
      GO TO 42
   41 X=X-0.02
      SIMINT=SIMINT+0.02/(X**B4*(A+B*X)*3.)
   42 IF(2-MM(JJ)401,400,400
  400 MC1=MC1+1
```

```
      SIM(MC1)=SIMINT
      S(MC1)=(TIME(JJ)**0.5+1.0/T3)*EXPF(-T3*TIME(JJ)**0.5)*2.0/T3
      CONS(JJ,1)=10.**4*SIMINT/(-S(MC1)+2.0/(T3*T3))
      CONS(JJ,2)=10.**4*(SIM(MC1)-SIM(MC1-1))/(S(MC1-1)-S(MC1))
      PRINT 899,(CONS(JJ,J6),J6-1,2)
  899 FORMAT(2F12.8)
      IF(1-MM(JJ)402,401,401
  401 XLAMDA(JJ)=TFF(JJ)*PF*0.7/(PH+PF+PF*(1.0-TFF(JJ))*(ALF-3.0))
      X=TFF(JJ)*PF-XLAMDA(JJ)
  402 XX(JJ)=X
      XGAMMA=(PH-(PF-PF*TFF(JJ)*B)*0.7/(PH+PF+PF*(1.0-TFF(JJ))*
     1(ALF-3.))
      PF=PF-XLAMDA(JJ)
      PH=PH-XGAMMA
      JJ=JJ+1
      IF(TFF(JJ))51,52,51
   52 TOT(1)=0
      TOTSQ(1)=0
      TOT(2)=0
      TOTSQ(2)=0
      DO 550 NN=1,2
      DO 450 J=1,N
      TOT(NN)=TOT(NN)+CONS(J,NN)
      TOTSQ(NN)=TOTSQ(NN)+CONS(J,NN)**2.
  450 CONTINUE
      TC1=MC1-1
      STDEV(NN)=ABSF((TC1**2*TOTSQ(NN)-TC1*TOT(NN)**2)/TOT(NN)
     1**2)**0.5/TC1**0.5
  550 CONTINUE
      JJ=JJ-1
      IF(13-JJ)999,998,998
  998 JJ=13
      GO TO 997
  999 JJ=26
  997 PRINT 5,B4,STDEV(1),STDEV(2)
    5 FORMAT(5X,12HFURAN ORDER= ,F4.1,2X,69HCORR.STAND.DEVS.
     1OF RATE CONSTS.,NORMAL AND SEGMENTED INTGRALS RESR.
     2 =        ,2F9.4)
  102 FORMAT(2X,22HNORMAL RATE CONSTANTS,13F9.4)
  103 FORMAT(2X,23HRATE CONST.VIA SEG.INT., 13F9.4)
  104 FORMAT(14X,11HTIMES,MINS., 13F9.3)
  105 FORMAT(2X,23HFURAN PRESSURES,MM.HG., 13F9.4 )
  106 FORMAT(5X,20HFURAN P.DROPS,MM.HG., 13F9.5)
      PRINT 102,(CONS(J,1),J=1,JJ)
      PRINT 103,(CONS(J,2),J=1,JJ)
      PRINT 104,(TIME(J),J=1,JJ)
      PRINT 105,(XX(J),J=1,JJ)
      PRINT 106,(XLAMDA(J),J=1,JJ)
   60 CONTINUE
      CALL EXIT
      END
```

PROGRAM RATESIM6

Not only is this program about an order of magnitude faster than RATESIM3 but it is also much more flexible due to extensive use of IF SENSE SWITCHES in conjunction with the typewriter for inputing information. One of the major differences in this program, over and above those already mentioned, is the inclusion of the subroutines CHEB and SP. Subroutine CHEB can be called, if required, to approximate to the data points using a Chebyshev curve fitting program discussed in Appendix 6. Having automatically found the best fit curve (which had to be done graphically for the previous program) ten data points are generated using subroutine SP, the points being spaced at intervals of 30 minutes from 30 minutes to 300 minutes.

The actual integration is performed by subroutine QUADR which is a modified version of that given by Kuo (ref. 87).

A further difference between the two programs is that a third set of equilibrium constants are calculated using 'weighted integrals', the expression for K_F being

$$K_F = -\frac{\sum_{i=1}^{n}\left(\left(\int_{i-1P_F}^{iP_F}\frac{dP_F}{f(P_F)}\right)^2 \Big/ \int_{t_{i=1}}^{t_i}\exp(-K^1 t^{\frac{1}{2}})dt\right)}{\sum_{i=1}^{n}\int_{i-1P_F}^{iP_F}\frac{dP_F}{f(P_F)}} \qquad \text{A10.6}$$

expression A10.6 was chosen because it exhibits properties which lie between A10.4 and that for K_F found using segmented integrals.

An additional feature of the program is that the number of statistical tests carried out on the output is increased to four (normalised standard deviation (A10.5), correlation

coefficient and the gradient and its standard deviation for the least squares straight line for the time against rate constant graph).

MAIN PROGRAM RATESIM6

```
C  RATE SIMULATION FOR A SINGLE REACTION USING GAUSSIAN
C  QUADRATURE *** SWITCH 1....ON - IMPUT NEW FURAN ORDER,
C  OFF - GO TO SWITCH 2******** SWITCH 2 ...ON - IMPUT NEW
C  POISONING CONSTANT, OFF - STOP     *******SWITCH 3 ...ON -
C  IMPUT HYDROGEN ORDER,  OFF - GO TO SWITCH 1 *******
C  SWITCH 4 ...ON - USE CHEBYSHEV APPROX. TO DATA, OFF -
C  USE DATA ****
C  **********************************************************************
C  W(I,K) AND T(I,K) =THE WEIGHTING COEF. AND THE LEGENDRE
C  ROOTS FOR THE INTEGRATION BY GAUSSIAN QUADRATURE OF
C  THE INVERSE OF THE PRESSURE FUNCTION
C  RUN = NAME OF RUN,  N = NUMBER OF READINGS USED,
C  TFF(J) IS THE MOLE FRACTION REACTANT UNREACTED FOR
C  THE J TH. SAMPLE TAKEN AT TIME(J), PH AND PF ARE THE
C  INITIAL HYDROGEN AND REACTANT PRESSURES (MM. HG.)
C  RESPECTIVELY,    ALF AND BET = THE PROBABILITIES THAT
C  A FURAN MOLECULE UNDERGOING HYDROGENATION FORMS
C  THF AND N-BUTANE RESPECTIVELY,     M = REQUIRED ORDER
C  OF CHEBYSHEV POLYNOMIAL.  B4 AND B5 = ORDERS WITH
C  RESPECT TO THE FURAN AND HYDROGEN PRESS.
C  T3 = THE POISONING CONSTANT
      HF(X)= ((PH-PF*(3.0-ALF+BET)-PHD+(3.0-ALF+BET)*X))
      DIMENSION TFF(26), TIME(26), CONS(26, 3), S(27), BS(26)
      DIMENSION R(25), V(20 ), Y(20 ), C(25), F(25), G(10, 10)
      DIMENSION W(4, 6),  T(4, 6)
      COMMON ANS.   TEMP. KOUNT, X, IPM2, IPOINT, EPS
      DO 8 I=1, 4
      IP2=I+2
    8 READ 9, (W(I, K), K=1, IP2), (T(I, K), K=1, IP2 )
    9 FORMAT(5F13.10)
      READ 40, RUN
   40 FORMAT(1A6)
      PRINT 41, RUN
   41 FORMAT(20X, 4HRUN , 1A6//, 20X, 10H**********//)
      READ 300, N, PH, PF, ALF, BET
      IF(SENSE SWITCH4)987, 887
  987 CALL CHEB(N, M, Y)
      CALL SP(N, TFF, TIME, M, Y)
      GO TO 772
  887 READ 301, (TFF(J), TIME(J), J=1, N)
  772 B4=0.2
      T3=0.12
      B5=1.0
```

```
2009  SUM2=0.0
      S(1)=2.0*EXPF (-T3*SQRTF(TIME(1)))*(SQRTF(TIME(1))+1.0/T3)/T3
      SUM3=0.0
      SUM4=0.0
      PFD=0.0
      PHD=0.0
 300  FORMAT(I2,4F9.4      )
 301  FORMAT(8F9.4)
      B=PF
      DO 302 J=2,N
   1  A=B-PFD
   2  B=TFF(J)*PF-PFD
      KOUNT=0.0
      X=9.999
   5  IF(B4) 200,201,200
 201  Q=1.0/((PH-PF*(3.0-ALF+BET)-PHD+(3.0-ALF+BET)*X))
      GO TO 6
 200  Q=1.0/(X**B4*(PH-PF*(3.0-ALF+BET)-PHD+(3.0-ALF+BET)*))
   6  CALL QUADR (A,B,Q,W,T,D)
  14  GO TO(5,5,5,5,5,5,17),KOUNT
  17  BS(J)=B
      SUM2=SUM2+ANS
      DJ=J-1
      FDD=(PH+PF+PF*(1.0-TFF(J))*(ALF-3,0)-DJ)
      FD=B/FDD
      PFD=PFD+FD
      HD=(PH-PF*(3.0-ALF+BET)-PHD+(3.0-ALF+BET)*B)/FDD
      PHD=PHD+HD
      S(J)   =(SQRTF(TIME(J))+1.0/T3)*2.0/(T3*EXPF(T3*SQRTF(TIME(J))))
      SUM4=SUM4+S(J)
      CONS(J,3)=10000.0*SUM2/(S(J)   -S(1))
      CONS(J,1)=-10.0**4*ANS/(S(J-1)-S(J))
      SUM3=CONS(J,1)*ANS+SUM3
      CONS(J,2)=SUM3/SUM2
      PRINT 899,CONS(J,1),CONS(J,2),CONS(J,3)
 899  FORMAT(3F12.4)
 302  CONTINUE
      PRINT 1000
      PRINT 1005,T3,B4,B5
      PRINT 1001,(CONS(J,1),J=2,N)
      PRINT 1002,(CONS(J,2),J=2,N)
      PRINT 1003,(CONS(J,3),J=2,N)
      PRINT 1004,(TIME(J),J=2,N)
      PRINT 1006,(BS(J),J=2,N)
      RN=N-1
      A=0.0
      B=0.0
      U=0.0
      D=0.0
      E=0.0
```

```
      DEV=0.0
      DO 500J=2,N
      A=A+TIME(J)
      B=B+CONS(J,3)
      U=U+TIME(J)**2
      D=D+TIME(J)*CONS(J,3)
  500 E=E+CONS(J,3)**2
      X=(RN*D-A*B)/(RN*U-A*A )
      DO 501 J=2,N
      YP=(B-X*A) /RN
  501 DEV=DEV+(CONS(J,3)-X*TIME(J)+YP)**2
      DEV=SQRTF(RN*DEV/((RN-2.0)*(RN*U-A*A)))
      SDEV=SQRTF(RN*E-B*B)/B
      CC=(RN*D-A*B)/SQRTF((RN*U-A*A)*(RN*E-B*B))
      PRINT 503,CC,SDEV
      PRINT 504,X,DEV
  503 FORMAT(15X74HCORRELATION COEF. AND STANDARD DEV. FOR
     1RATE CONSTS. FROM THE NORMAL INT. =,2F12.4)
  504 FORMAT( 15X,97HTHE GRADIENT AND ITS STAN. DEV. FOR THE
     1LEAST SQUARE  S STRAIGHT LINE FOR TIME/RATE CONST. ARE
     2RESP.,2F12.4/////)
 1000 FORMAT(20X,50HA L L   R A T E   C O N S T A N T S  X
     1 1 0 0 0 0)
 1001 FORMAT(1X,29HRATE CONST. VIA SEGMENTED INT.,6X,12F9.4)
 1002 FORMAT(1X,28HRATE CONST. VIA WEIGHTED INT.,6X,12F9.4)
 1003 FORMAT(1X,26HRATE CONST. VIA NORMAL INT.,8X,12F9.4)
 1004 FORMAT(1X,24HTIME SAMPLE TAKEN (MIN.),10X,12F9.4)
 1005 FORMAT(1X,17HPOISONING CONST. =,F9.5,5X,12HFURAN ORDER
     1 =,F6.3,5X,15HHYDROGEN ORDER=,F6.3)
 1006 FORMAT(1X,23HREACTION PRESSURE (MM.),11X,12F9.4)
      IF(SENSE SWITCH 3) 4000,4001
 4000 ACCEPT 2008,B5
 4001 IF(SENSE SWITCH 1) 2000,2001
 2000 ACCEPT 2008,B4
 2008 FORMAT(F5.3 )
 2001 IF (SENSE SWITCH 2)3000,3001
 3000 ACCEPT 2008,T3
      GO TO 2009
 3001 CALL EXIT
      END
```

SUBROUTINE QUADR (Ref. 87).

```
      SUBROUTINE QUADR (A, B, F, W, T, C)
      DIMENSION W(4, 6), T(4, 6)
      COMMON ANS, TEMP, KOUNT, X, IPM2, IPOINT, EPS
      IF(KOUNT) 8, 10, 8
    8 GO TO 30
   10 ANS=1.0
      IPOINT=2
      EPS=0.00
      C=(B-A)/2.
   18 IPOINT=IPOINT+1
      TEMP=ANS
      ANS=0.0
      IPM2=IPOINT-2
      KOUNT=1
   20 X=C*T( IPM2, KOUNT)+(B+A)/2.0
      RETURN
   30 ANS=ANS+C*W(IPM2, KOUNT)*F
      KOUNT=KOUNT+1
      IF(KOUNT-IPOINT)20, 20, 40
   40 IF(IPOINT-3)18, 18, 50
   50 DELT=ABSF(ANS-TEMP)
      RATIO=DELT/ABSF(TEMP)
    7 IF(RATIO-EPS)70, 70, 80
   70 PRINT 72, IPOINT, ANS
   72 FORMAT(///5X, 16HBY CONVERGENCE, , I2, 24H POINT GAUSS.
     1 QUADRATURE, 15H GIVES ANSWER =, E14.8//)
      KOUNT=7
      RETURN
   80 IF(IPOINT-6)18, 100, 100
  100 KOUNT=7
      RETURN
      END
```

SUBROUTINE SP

```
      SUBROUTINE SP(N, TFF, TIME, M, Y)
      DIMENSION TFF(26), TIME(26), Y(20)
      N=10
      DO 5J=2, 11
      TIME(J)=30*(J-1)
      TFF(J)=Y(1)
      DO 5 K=2, M
    5 TFF(J)=TFF(J)+Y(K)*TIME(J)**(K-1)
      RETURN
      END
```

APPENDIX 11

Proof that furan hydrogenations carried out at the same temperatures with the same ratio of initial furan and hydrogen pressures will yield identical % reacted/time graphs (if the same weight of catalyst is used for both reactions).

Restating equation 5.68 :-

$$E = ((1 - Z)P_H^O - A)/B\ P_F^O \qquad \text{All.1}$$

where E is the fraction of furan unreacted when a Z^{th} of the hydrogen has been consumed, A and B are constants defined in equation 5.65. On expressing A in terms of B (see equation 5.65 and the paragraph following it), All.1 becomes :

$$E = (\ (1 - Z)\ P_H^O - P_H^O + B\ P_F^O)/B\ P_F^O \qquad \text{All.2}$$

$$= (\ B\ P_F^O - Z\ P_H^O)/B\ P_F^O \qquad \text{All.3}$$

Solving 11.3 for Z :

$$Z = (1 - E)\ B\ \frac{P_F^O}{P_H^O} \qquad \text{All.4}$$

But an expression, 5.64, was derived in section 5.3.6 relating Z and t for a furan hydrogen reaction which is zero order in furan and first order in hydrogen. For a reaction starting at t = 0 secs. (i.e. t_i = 0 secs.) 5.64 becomes:

$$\ln (1 - Z) = -\frac{2BK_F}{K'}\ (\exp (-K't^{\frac{1}{2}})(t^{\frac{1}{2}}+1/k') - 1/K') \qquad \text{All.5}$$

Substituting All. 4 into All. 5 gives

$$\ln\left(1-(1-E)\frac{P_F^O}{P_H^O}\right) = -\frac{2\,B\,K_F}{K'}\left(\exp(-K't^{\frac{1}{2}})(t^{\frac{1}{2}}+1/K')-1/K'\right) \qquad \text{All. 6}$$

Clearly from equation All. 6, providing $\frac{P_F^O}{P_H^O}$ is the same for any two reactions carried out at the same temperature, graphs of E against time will be identical. This is demonstrated to be the case for reactions C8A1 and C10B1, 47°C, and C8G1 and C10F1, 23°C, by graph 4. 9.

A similar result would not have been obtained if the reaction had been first order in furan, zero in hydrogen.

REFERENCES

1 - J.W. Beach, J. Chem. Phys., 9, 54(1940).

2 - V. Schomaker and L. Pauling, J. Am. Chem. Soc., 61, 1769(1939).

3 - M.J.S. Dewar, "The Electronic Theory of Organic Chemistry", 1 st. Ed., Oxford University Press, (1952), p. 35.

4 - G.B. Kistiakowsky, J. Am. Chem. Soc., 57, 876 (1935).

5 - M.A. Dolliver, T.L. Gresham, G.B. Kistiakowsky, E.A. Smith and W.E. Vaughan, J. Am. Chem. Soc., 60, 440(1938).

6 - L. Pauling, "The nature of the Chemical Bond and the Structure of Molecules and Crystals", 2nd. Ed., Ithaca, Cornell University Press (1940).

7 - R. Truchet and J. Chapron, Compt. Rend., 198, 1934 (1934).

8 - A.W. Reitz, Z. Physik. Chem., B, 33, 179 (1936); B, 38, 275 (1937).

9 - H.B. Thomson and R.B. Temple, Trans. Far. Soc., 41, 27 (1945)

10 - C.R. Kanekar, G. Govil, C.L. Khetrapal and M.M. Dhingra, Proc. Ind. Acad. Sci., A, 64, 315 (1966).

11 - B. Zurawski, Acta Phys. Polon., 31, 1079 (1967)

12 - A.R. Katritzky and J.M. Lagowski, "Heterocyclic Chemistry", J. Wiley and Sons, N.Y., (1960).

13 - G.E. Calf and J.L. Garnett, Austr. J. Chem., 21, 1221 (1968)

14 - M. Padoa and U. Ponti, Atti R. Accad. dei Lincea Roma(5), 15, 610 (1906)

15 - P.A. LeFrancois, Iowa State Coll. J. Sci., 19, 41 (1944).

16 - R. Paul, Bull. Soc. Chim. France, 1946, 208.

17 - H. Adkins, "Reactions of Hydrogen with Organic Compounds over Copper-Chromium Oxide and Nickel Catalysts", Madison, University of Wisconsin Press, (1937).

18 - C.L. Wilson, J. Am. Chem. Soc., 70, 1313 (1948).

19 - A.S. Sultanov. Ya.Ya. Aliev, N.V. Vasip'eva, I.B. Romanova and M.I. Monakov, Dokl. Acad. Nauk Uzbek, SSSR, 12, 27 (1957).

20 - Jin Wang, Chih-Tsin Li and Chih-Knang Yen, K'o Hsuch T'ung Pao, 1958, 434; C.A., 53, 11333

21 - W. Kaufmann and H. Adkins, J.Am. Chem. Soc., 45, 3029 (1923).

22 - N.V. Williams, Compt. Rend. Acad. Sci. SSSR, A, 1930, 523.

23 - J.H. Sinfelt, Kinetics and Catalysis, 63, 16 (1967); E.B. Maxted and S. Aktar, J. Chem. Soc., 1960, 1995.

24 - I.F. Bel'skii and N.I. Shuikin, Russ. Chem. Rev., 32, 307 (1963).

25 - A.A. Ponomarev and V.V. Zelenkova, Prog. Chem., 20, 589 (1951).

26 - A.P. Dunlop and F.N. Peters, "The Furans", Reinholt, (1953), Ch, 15.

27 - R. Paul, Bull. Soc. Chim. France, 1947, 158

28 - B.H. Wojcik, Ind. Eng. Chem., 40, 210 (1948)

29 - H. Smith and J. Fuzek, J. Am. Chem. Soc., 71, 415 (1949).

30 - N.I. Shuikin and V.V. Daiber, Izv. Akad. Nauk SSSR, Otd. Khim. Nauk, 1941, 121.

31 - Yu. K. Yur'ev and I.P. Gragerov, Zhur. Obshch. Khim., 21, 264 (1951).

32 - N.I. Shuikin and I.F. Bel'skii, Dokl. Akad. Nauk SSSR, 125, 345, (1959).

33 - N.I. Shuikin and I.F. Bel'skii, Bull. Soc. Chim. France, 1956, 1556.

34 - G. Boles, Hungarian P. 132763 (1944); 42, 7286.

35 - N.I. Shuikin and I.F. Bel'skii, Actes Congr. Intern. Catalyse, Paris, 2, 2625 (1961).

36 - N.I. Shuikin and I.F. Bel'skii, Dokl. Akad. Nauk SSSR, 116, 621 (1957).

37 - N.I. Shuikin and I.F. Bel'skii, Zhur. Obshch. Khim., 29, 3627 (1959).

38 - C.W. Bradley, Iowa State Coll. J. Sci., 12, 108 (1937).

39 - N.I. Shuikin and E.M. Chilikina, J. Gen. Chem. SSSR, 6, 279 (1936).

40 - N.D. Zelinsky and N.I. Shuikin, Proc. Acad. Sci. SSSR, 2, 60 (1933).

41 - D.A. Whan and C. Kemball, Trans. Far. Soc., 61, 294 (1965).

42 - D.A. Whan and C. Kemball, Trans. Far. Soc., 64, 1102 (1968).

43 - N.I. Shuikin, V.A. Tulupov and I.F. Bel'skii, Zhur. Obshch. Khim., 25, 1125 (1955).

44 - C.L. Wilson, J. Chem. Soc., 1945, 48.

45 - S. Swadesh, S. Smith and A.P. Dunlop, J. Org. Chem., 16, 476 (1951).

46 - K.S. Topchiev, Compt. Rend. Acad. Sci. SSSR, 19, 497 (1938).

47 - L. Schniepp, H. Geller and R. Von Korff, J. Am. Chem. Soc., 69, 672 (1947).

48 - S. Swadesh and A.P. Dunlop, J. Org. Chem., 14, 692 (1949).

49 - N.I. Shuikin, I.F. Bel'skii and R.A. Karakhanov, Dokl. Akad. Nauk SSSR, 122, 625 (1958).

50 - A.A. Balandin and A.A. Ponomarev, Zhur. Obshch. Khim., 26, 1146, (1956).

51 - E.R. Bissell and M. Finger, J. Org. Chem., 24, 1259 (1959).

52 - P. Kieran and C. Kemball, J. Cat., 4, 394 (1965).

53 - J.R. Anderson and C. Kemball, Advances in Catalysis, 9, 51 (1957).

54 - A. Burger and G.H. Harnest, J. Am. Chem. Soc., 65, 2382 (1943).

55 - R. Paul, Bull. Soc. Chim. (5), 5, 1053 (1938).

56 - S. Mitui, Y. Ishikawa and Y. Takeuchi, Nippon Kagaku Zasshi, 81, 286 (1960).

57 - R.K. Greenhalgh and M. Polany, Trans. Far. Soc., 35, 520 (1939).

58 - S. Siegel and M. Dunkel, Advances in Catalysis, 9, 5 (1957).

59 - H. Gilman and A.P. Hewlett, Rec. Trav. Chim., 51, 93 (1932).

60 - F. Hartog and P. Zwietering, J. Cat., 2, 29 (1963).

61 - J.L. Garnett and W.A. Solich, J. Cat., 2, 350 (1963).

62 - W.F. Madden and C. Kemball, J. Chem. Soc., 1961, 302.

63 - J.L. Garnett and W.A. Sollich, Austr. J. Chem., 15, 62 (1962).

64 - R. Fitcher, Helv. Chim. Acta, 30, 2010 (1947).

65 - J.W. Mellor, "A Comprehensive Treatise on Inorganic and Theoretical Chemistry", Part 5, Longmans, (1960), p. 253.

66 - J. Ray, J. Appl. Chem., 4, 21 (1954).

67 - J.L.M. Poiseuille, Compt. Rend., 15, 1167 (1842).

68 - E. Borello, A. Zecchina and C. Morterra, J. Phys. Chem., 71, 2938 (1967).

69 - W.F. Taylor and H.K. Staffin, J. Phys. Chem., 71, 3314 (1967).

70 - A. Farkas and L. Farkas, Trans. Far. Soc., 33, 827 (1937).

71 - R. P. Eischens and W. A. Pliskin, Advances in Catalysis, 10, 1 (1958).

72 - R. A. Dewar and I. G. McWilliams, Nature, 181, 760 (1958).

73 - K. V. Topchieva, K. Yun-Pin and I. V. Smirnova, Advances in Catalysis, 9, 799 (1957).

74 - J. A. Cusumano, G. W. Dembinski, and J. H. Sinfelt, J. Cat., 5, 471 (1966).

75 - M. Boudart, A. Aldag, J. E. Benson, N. A. Dougharty and C. G. Harkins, J. Cat., 6, 92 (1966).

76 - U. V. Korshak, A. S. Sultaniv and A. A. Ubduvalier, Uzbek. Khim. Zh., 1959, 39.

77 - A. Voorhies, Ind. Engng. Chem., 37, 318 (1945).

78 - G. C. Bond, "Catalysis by Metals", Academic Press, (1962), p. 128-9.

79 - C. N. Hinshelwood, "The Kinetics of Chemical Change", Oxford University Press, Oxford (1940).

80 - A. A. Frost and R. G. Pearson, "Kinetics and Mechanism", John Wiley and Sons, (1961), p. 44.

81 - S. Arrhenius, Z. Physic. Chem., 1, 110 (1887).

82 - T. Kariyone, J. Pharm. Soc. Japan, 515, 1 (1925).

83 - M. Traute and F. Kurtz, Ann. Physik., 9, 981 (1931); C. A., 28, 387.

84 - W. M. Bleakney, Physics, 3, 123 (1932); C. A., 26, 5465.

85 - T. Titani, Bull. Chem. Soc. Japan, 8, 255 (1933); C. A., 28, 387.

86 - H. W. Thomson and R. B. Temple, Trans. Far. Soc., 41, 22 (1945).

87 - S.S. Kuo, "Numerical methods and computers", Addison-Wesley, (1966).

88 - A.H. Lightstone, "Concepts of calculus II", Harper and Row, (1966), p.408.

89 - L. Bers, "Calculus", Holt, Rinehart and Winston Inc., (1969).

90 - C. Lanczos, "Approximations by Orthogonal Polynomials", University of California, 1952.

91 - D.W. Martin, Comput. J., 1, 118 (1958).

92 - F.B. Hildebrand, "Introduction to numerical analysis", McGraw-Hill, (1956).